eZine for meteor observers emeteornews.net

MeteorNews

VOL 9 / ISSUE 2 / MARCH 2024

A stunning fireball recorded from Sevilla on 2024 January 21, at 20h03m07s UT. This is a sporadic event that overflew the south of Spain and Portugal (credit: José Madiedo).

- Iota-Centaurids 2024
- GMN report 2023
- CAMS reports
- Quadrantids 2024
- Radio meteor work
- Fireballs

Contents

Enhanced iota-Centaurids (ICN#919) activity in 2024

Peter Jenniskens

SETI Institute, 339 Bernardo Ave, Mountain View, CA 94043, USA
pjenniskens@seti.org

The iota-Centaurids (ICN#919) meteor shower, in other years a minor shower, displayed enhanced activity in 2024 of relatively long duration. The outburst was observed by both the southern hemisphere CAMS networks and the Global Meteor Network. The parent body is unknown. The orbital elements suggest the source is a Halley-type or long-period comet, with the meteoroids hitting Earth now in a relatively short semi-major axis of 4.8 AU. That makes it possible that the unusual activity is due to dust trapped in mean-motion resonance with Jupiter.

1 Introduction

The iota-Centaurids (ICN#919) were first identified as a minor shower by Jenniskens et al. (2018) in southern hemisphere CAMS data from the years 2011 to 2016, mostly based on CAMS New Zealand results. In some years, the shower was detected also from California and by the SonotaCo network in Japan, where the radiant elevation remained low. This meteor shower in the southern apex source was found active during the period January 16–25 ($\lambda_\odot$ 296° to 305°), radiating from a radiant α_g = 199° and δ_g = –38.9° with v_g = 63.9 km/s at about $\lambda_\odot$ = 301.1°. Based on more expansive 2020–2023 data, Jenniskens (2023) put the radiant at α_g = 197.4° and δ_g = –37.8° with v_g = 64.4 km/s, peaking at about $\lambda_\odot$ = 299.5°. That speed translates to a relatively short orbit with median semi-major axis a = 4.78 AU.

In the years 2022 and 2023, the shower remained unassuming, but not so in 2024. *T. Cooper* of CAMS South Africa first pointed out that this shower appeared to be unusually strong in early CAMS data. When all results had come in, including observations from the Global Meteor Network, the shower was clearly much stronger than in previous years (*Figure 1*).

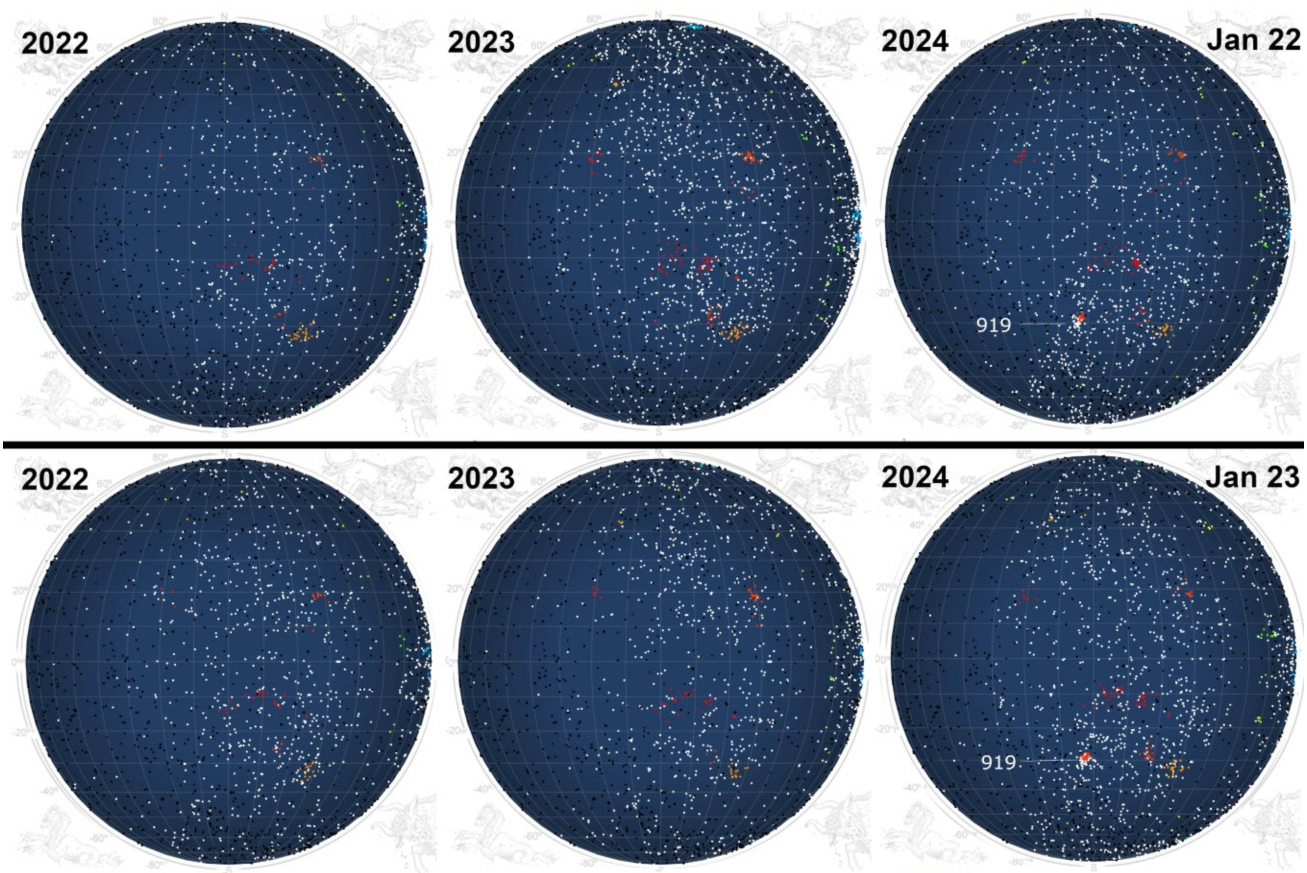

Figure 1 – The dense concentration of shower 919 radiants can be seen on the combined video-derived radiant maps from CAMS and GMN data for 2024 January 21–22 (top) and January 22–23 (bottom), compared to the same map at the same date in the previous two years (from near-real-time map)[1].

[1] http://cams.seti.org/FDL/

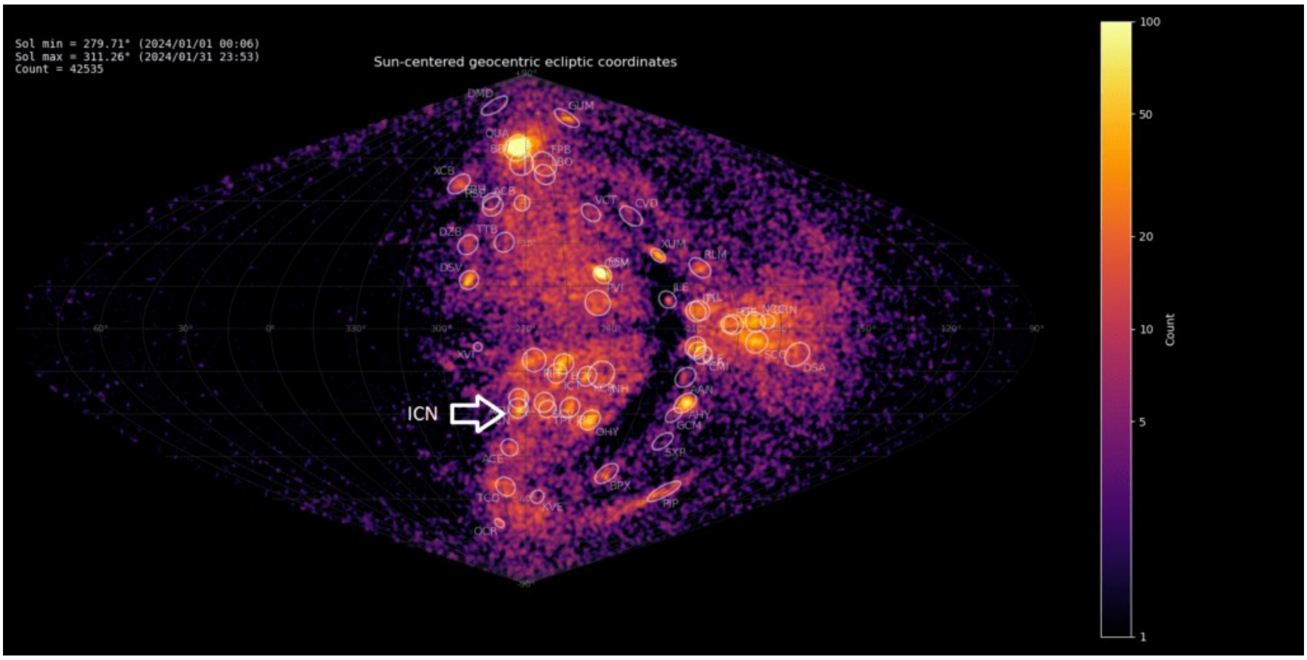

Figure 2 – Radiant plot of the Global Meteor Network[2] for 2024 January in Sun-centered geocentric ecliptic coordinates.

2 Enhanced activity in 2024

In 2024, this meteor shower showed stronger than usual activity (Jenniskens et al., 2024) during 2024 January 21–26, corresponding to $\lambda_{\odot}$ = 301.0 to 306.0 deg (equinox J2000.0). Forty-eight iota Centaurids were triangulated by CAMS New Zealand, coordinated by *J. Baggaley* (University of Canterbury) and *J. Scott* (University of Otago); 34 shower meteors by CAMS Australia, via *H. Devillepoix* (Curtin University) and *D. Rollinson*; 16 shower meteors by CAMS Chile, via *S. Heathcote* and *T. Abbott* (NOIRLAB/Cerro Tololo) and *E. Jehin* (University of Liège), two shower meteors by a mostly clouded CAMS Namibia, via *T. Hanke* (H.E.S.S. Collaboration), and 1 shower meteor by the northern-hemisphere United Arab Emirates Astronomical Camera Network, via *M. Odeh* (International Astronomical Center).

The dense radiant concentration in 2024 is obvious in *Figure 1*, where the radiant maps for January 21–22 and 22–23, 2024 are compared to previous years at the same date. To quantify the increase in activity, the annual ratio of triangulated iota-Centaurids to all sporadic meteors for these networks for the past 5 years was calculated as follows:

- 2020: 0.0037 ± 0.0009
- 2021: 0.0038 ± 0.0010
- 2022: 0.0018 ± 0.0007
- 2023: 0.0034 ± 0.0009
- 2024: 0.0145 ± 0.0015

In 2024 rates were above normal, peaking at $\lambda_{\odot}$ = 302.4 ± 0.1 deg. The time of the peak is later than in normal years, and also the activity period extended a little longer (cf., Jenniskens 2023). After plotting the detected number of meteors and comparing those to the total number detected iota-Centaurids in prior years, it showed that activity was normal prior to January 21, but then increased above normal activity, increasing exponentially to a peak and then decreasing exponentially with a full-width-at-half maximum duration of about 1.6 deg.

Table 1 – The 2024 orbital elements (Equinox J2000.0) compared to the median 2013–2023 orbit from Jenniskens (2023).

	2013–2023	2024
$\lambda_{\odot}$ (°)	299.5	302.4
α_g (°)	197.4	200.6
δ_g (°)	–37.8	–40.3
v_g (km/s)	64.4	63.7
$\lambda - \lambda_{\odot}$ (°)	271.9	272.8 ± 1.0
β (°)	–28	–29.1 ± 0.9
a (AU)	4.78	4.7
q (AU)	0.981	0.979 ± 0.005
e	0.795	0.790 ± 0.086
ω (°)	353.6	350.8 ± 3.4
Ω (°)	119.6	122.4 ± 1.7
i (°)	131.4	129.4 ± 1.5
Π (°)	113.2	113.2
T_j	0.3	0.39
N	113	101

The median orbital elements are shown in *Table 1* and are compared to the orbit for the iota-Centaurids in Jenniskens (2023). This identifies the outburst as due to this previously

[2] https://globalmeteornetwork.org/data/

known minor shower. The 2024 observations nearly double the number of known orbits for this shower.

These results include the CAMS-derived orbits from Global Meteor Network (Vida et al., 2020; 2021) stations in Australia (*D. Rollinson*) and New Zealand (*J. Scott*). These and other southern hemisphere stations participating in GMN confirm the detection independently from the CAMS observations in Chile. The iota-Centaurids (ICN) this year were found so strong that the shower is recognized even in the combined GMN data for January 2024 (*Figure 2*).

3 Discussion

The parent body is unknown. The short semi-major axis and long-duration activity suggest that the 2024 activity might be dust from a Halley-type comet trapped in the 1:1 mean-motion resonance with Jupiter. Indeed, the shower was also detected by northern-hemisphere CAMS and SonotaCo stations, with a low radiant elevation, in 2013 during solar longitudes 300.6–302.5 deg.

References

Jenniskens P., Baggaley J., Crumpton I., Aldous P., Pokorny P., Janches D., Gural P. S., Samuels D., Albers J., Howell A., Johannink C., Breukers M., Odeh M., Moskovitz N., Collison J. and Ganjuag S. (2018). "A survey of southern hemisphere meteor showers". *Planetary Space Science*, **154**, 21–29.

Jenniskens P. (2023). Atlas of Earth's Meteor Showers. Elsevier, USA. page 525.

Jenniskens P., Baggaley J., Scott J., Devillepoix H., Rollinson D., Heathcote S., Abbott T., Jehin E., Hanke T., Odeh M. (2024). "Iota Centaurid meteor shower". CBET 5347. D.W.E. Green (ed.), IAU Central Bureau for Astronomical Telegrams, 1 pp.

Vida D., Gural P.S., Brown P.G., Campbell-Brown M. and Wiegert P. (2020). "Estimating trajectories of meteors: an observational Monte Carlo approach–I. Theory". *Monthly Notices of the Royal Astronomical Society*, **491**, 2688–2705.

Vida D., Šegon D., Gural P. S., Brown P. G., McIntyre M. J. M., Dijkema T. J., Pavletić L., Kukić P., Mazur M. J., Eschman P., Roggemans P., Merlak A., Zubrović D. (2021). "The Global Meteor Network – Methodology and first results". *Monthly Notices of the Royal Astronomical Society*, **506**, 5046–5074.

Global Meteor Network report 2023

Paul Roggemans[1], Peter Campbell-Burns[2], Milan Kalina[3], Mark McIntyre[4], James M. Scott[5], Damir Šegon[6], Radim Stano[7], and Denis Vida[8]

[1] **Pijnboomstraat 25, 2800 Mechelen, Belgium**
paul.roggemans@gmail.com

[2] **UK Meteor Observation Network, Cavendish Gardens, Fleet, Hampshire, United Kingdom**
peter@campbell-burns.com

[3] **Czech Astronomical Society, Ondrejov, Czech Republic**
milank2010@gmail.com

[4] **UK Meteor Observation Network and Tackley Observatory, United Kingdom**
mark.jm.mcintyre@cesmail.net

[5] **University of Otago, Department of Geology, Dunedin, New Zealand**
james.scott@otago.ac.nz

[6] **Astronomical Society Istra Pula, Park Monte Zaro 2, 52100 Pula, Croatia**
damir@astro.hr

[7] **The Astronomical Society of Edinburgh, Scotland, United Kingdom**
radim.stano@outlook.com

[8] **Department of Physics and Astronomy, University of Western Ontario, London, Ontario, N6A 3K7, Canada**
dvida@uwo.ca

A status report is presented for the Global Meteor Network. Since the start of the network, 1174205 orbits have been collected until end of 2023, 425 different meteor showers have been identified among these orbits. During 2023 more than 430 new GMN cameras started contributing successfully paired meteors. 451895 orbits were collected in 2023. The development of the Global Meteor Network in different regions is described. The coverage of the camera fields of view is shown on maps.

1 Introduction

Over the past 15 years many video camera networks were created, both regional and national, with the aim of obtaining meteor trajectories through multi-station registrations. Most of these networks specialise in fireballs and meteorite droppers, others are dedicated to a fainter magnitude range comparable to what visual observers used to cover. The orbit data obtained by these networks brought a tremendous progress in our knowledge of meteoroid streams.

The Global Meteor Network is the most recent development in this domain. Its success builds on the many years of expertise of the Croatian Meteor Network, one of the pioneers in the field of video meteor observations and the origin of GMN (Gural and Šegon, 2009). Based on RMS, the significantly improved Raspberry Pi solution introduced by Zubović et al. (2015) and Vida et al. (2016), the Global Meteor Network began its operation at the end of 2018; its first six cameras located in New Mexico used IP cameras controlled by a Raspberry running its own dedicated software and reduction pipeline (Vida et al., 2021). GMN became the fastest growing meteor video network with 73 operational cameras at the end of 2019, 155 at the end of 2020, 341 at the end of 2021, 700 at the end of 2022 and 1066 in 2023. The analog cameras of the EDMOND network are being replaced gradually by RMS cameras and many new volunteers got involved worldwide with many amateur networks now building and installing RMS cameras.

2 Joining the Global Meteor Network

More information about this project can be found in Vida et al. (2020a; 2020b; 2021; 2022) and on the GMN website[3]. An informative video presentation about the Global Meteor Network project can be watched online[4]. Many sites and participants are still waiting to find partners to improve the coverage on their cameras. New participants are welcome to expand the network.

To obtain a camera for participation you can either buy it plug&play from Istream[5], or you buy the components and build your own camera for about 250 US$ or ~200 €. The RMS cameras are easy to build and operate. If you are interested in building your own camera you can find detailed instructions online[6].

[3] https://globalmeteornetwork.org/
[4] https://www.youtube.com/watch?v=MAGq-XqD5Po
[5] https://globalmeteornetwork.org/?page_id=136
[6] https://globalmeteornetwork.org/wiki/index.php?title=Build_A_Camera

The daily status of most (not all) meteor stations can be followed on a webpage[7]. The GMN results and data are publicly available and daily updated online[8]. The UK meteor network maintains a comprehensive archive[9] and daily update[10] which may inspire others. Their Wiki-page[11] may be helpful to people outside the UK as well as their github repos[12,13].

The meteor map[14] is an online tool for visualizing meteor cameras and ground tracks of observed meteors. Each participant can check the results obtained with each camera, check the location of the meteor trajectories and combinations with other camera stations. The tool has been described in an article (Dijkema, 2022).

As the static maps of camera FoVs presented in this report sometimes become overcrowded, the aggregated kml files valid for end of 2023 can be downloaded[15]. The individual up-to-date kml-files for all GMN cameras can be downloaded from the GMN website[16]. Camera operators are encouraged to point new cameras in function of optimal coverage with other cameras. Opening the kml files in Google Earth allows to toggle cameras on and off to get a better view on the actual coverage. Make sure to compare kml files at the same elevation (e.g. 100km) and prevent 3D perspective by changing the properties in the Google Earth graphical interface to "clamped to ground" instead of the default setting "absolute". A handy tool to check overlap between two cameras is available online[17].

If you have a dark site with a free view and if you are looking to make a scientifically useful contribution, with just five RMS cameras with 3.6 mm lenses (FoV 88° × 47°) pointed at azimuths 0° (North), 70°, 140°, 220° and 290°, between 35° and 40° elevation, you cover all the sky except your zenith. Avoid pointing a camera at the meridian (180° azimuth) as the transit of the Full Moon will take full effect in this position. Also do not point lower than 35° elevation: there are no meteors in the local scenery, trees or buildings. If you use 6 mm lenses, recommended where light pollution is an issue, you need six RMS to cover the sky with a royal overlap between the camera edges. Six cameras with 6 mm lenses (FoV 54° × 30°) pointed at azimuths 30°, 90°, 150°, 210°, 270° and 330°, between 35° and 40° elevation, would make you a key video meteor hub in the network. Building the cameras at the cost of the purchased components, or bought plug & play, both remain a low-cost project, affordable to many amateurs, observatories and societies.

The unavailability of Raspberry Pi because of production limitations due to Covid in former years has been meanwhile solved, but inspired people to explore alternative systems for unavailable RPi's. A cheap Linux PC can handle multiple cameras and a system has been developed to operate multiple GMN cameras using a single PC. Read the article written by Harman et al. (2023) and check the Wiki pages for the latest updates.

3 Annual GMN meeting 2023 (online)

The annual meeting of the Global Meteor Network got more than 100 people participating online from around the globe. The meeting took place in two sessions on February 25–26, 2023 in order to allow people from all time zones to participate. 12 presentations were given with enough time for questions and discussions, each session ended with a Q&A workshop session. Both sessions can be viewed online:

- Session 1 – February 25, 16^h00^m – 21^h00^m UTC[18]
- Session 2 – February 26, 00^h00^m – 03^h00^m UTC[19]

4 The GMN Outreach project

The GMN identified a great educational potential of the GMN cameras and a small team formed in 2022. After the initial discussion, it was decided that the Outreach project would focus on the high school level in the beginning with the potential to adapt the project for younger pupils and also university students, with different levels maintained. The team started to discuss and form the outlines of the curriculum and started to work on the materials. *Denis Vida* was able to secure funding and we are grateful to the anonymous donor who sponsored 15 GMN cameras for high schools around the world, plug-and-play and kits included. The team was working on preparations, project plan, demand for cameras from team members, hardware sourcing and distribution included.

Table 1 – The schools which are part of the project with their locations.

School name	Country
Bundesrealgymnasium Kepler Graz	Austria
Friedrich-Schiller-Gymnasium Preetz	Germany
Gymnasium Untergriesbach	Germany
Peebles High School	Scotland, UK
Inverclyde Academy	Scotland, UK
Wick High School	Scotland, UK
Laingsburg High School	South Africa
Touwsrivier Primary School	South Africa

The cameras were distributed in the spring of 2023 to the team members who later identified the schools and distributed them locally. In parallel the preparation of

[7] https://globalmeteornetwork.org/weblog/
[8] https://globalmeteornetwork.org/data/
[9] https://www.ukmeteornetwork.org
[10] https://www.ukmeteors.co.uk/live/index.html
[11] https://github.com/markmac99/ukmon-pitools/wiki
[12] https://github.com/markmac99/ukmon-pitools
[13] https://github.com/markmac99/UKmon-shared
[14] https://tammojan.github.io/meteormap/
[15] https://www.emeteornews.net/wp-content/uploads/2024/01/All_2023.zip
[16] https://globalmeteornetwork.org/data/kml_fov/
[17] http://www.davesamuels.com/cams/camspointing/scripts/latlong.html
[18] https://www.youtube.com/watch?v=IfUyCHjMATc
[19] https://youtu.be/I78KwF5-1GE

materials continued and the website was created to inform the general public about our project and to announce that the project will be made freely available for everybody interested via the website[20].

Figure 1 – Locations of European schools participating in the GMN-outreach project.

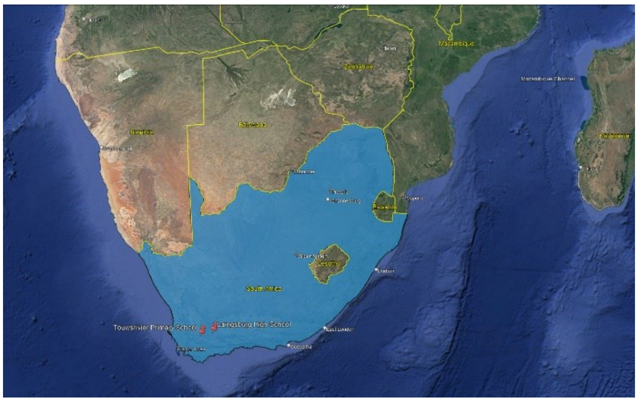

Figure 2 – Locations of South African schools participating in the GMN-outreach project.

In the summer of 2023, three cameras were successfully installed in Washington state during a summer camp. The official start of the project was set for September 2023 when the school year in Europe starts (*Figure 1*). The cameras were distributed to the schools in Austria (where it will be the first GMN camera), Germany, Scotland, Wales and South Africa (*Table 1*). We are grateful to The Astronomical Society of Edinburgh[21] which decided to fund three more cameras to the schools in Scotland and whose two members are also part of the Outreach team. In 2023 the first materials were published on the website. South African schools are starting later in January 2024 with the start of the school year (*Figure 2*). Austrian, German and Scottish schools started to assemble the camera from parts and install them, and good progress has been made. The project continues in 2024 where we expect all the cameras to be installed, operational and the end project presentations held.

Last but not least, the GMN outreach project team members[22] are: *Radim Stano, Denis Vida, Tim Cooper, Paul Roche, Laurie Stanton, Mirjana Malarić, Rob Steele, Mary McIntyre* and *Horst Meyerdierks*.

5 GMN camera coverage

The aim of the GMN is to cover all latitudes and longitudes to assure a global coverage of meteor activity in order to let no unexpected meteor event pass unnoticed. This is an ambitious goal especially for a project that depends for most efforts entirely on volunteers' work. In this report we describe the progress that was made by GMN during 2023 in different regions of the world. The status of the camera coverage is illustrated with maps showing the fields of view intersected at an elevation of 100 km in the atmosphere, projected and clamped to the ground. This way the actual overlap between the camera fields is shown without any effects of 3D perspectives. Where possible the camera ID has been mentioned on the plots. The status at the end of 2023 can be compared to the 2022 annual report (Roggemans et al., 2023).

Many RMS cameras with 4 mm optics have the horizon at the bottom of their field of view what results in a huge camera field at 100 km elevation. Rather few meteors will be bright enough to get registered near the horizon. The large distance between the camera station and the meteor also reduces the chances to obtain a useable triangulation. The number of paired meteors at the outskirts of these large camera fields is very small. However, cameras pointing so low towards the horizon turn out to be very useful regarding obtaining coverage at lower heights where meteorite dropping fireballs end their visible path. When looking for camera overlap, it is strongly recommended to look for an optimized overlap between cameras. An interesting study on this topic for the New Mexico Meteor Array has been published by Mroz (2021). Camera operators are encouraged to optimize their camera overlap.

The number of multi-station events mentioned per country corresponds to the number of orbits, unless an orbit was based on camera data from different countries, then it was counted once for each country. This can also be visualized on the MeteorMap[23] (Dijkema, 2022). The current camera coverage is presented per country or per region for reason of readability. To consider the real overlap for most European countries it is necessary to look at the camera coverage of neighboring countries. In several regions the camera coverage is too dense to visualize it in a single map. We strongly recommend to view the camera FoVs in Google Earth. The required kml-files have been grouped per country and can be downloaded for: Asia, Europe, North America and Southern hemisphere.

[20] https://globalmeteornetwork.org/outreach/
[21] https://www.astronomyedinburgh.org/2023/10/30/free-meteor-cameras-for-high-schools-stem-project/
[22] https://globalmeteornetwork.org/outreach/team/
[23] https://tammojan.github.io/meteormap/

5.1 Australia

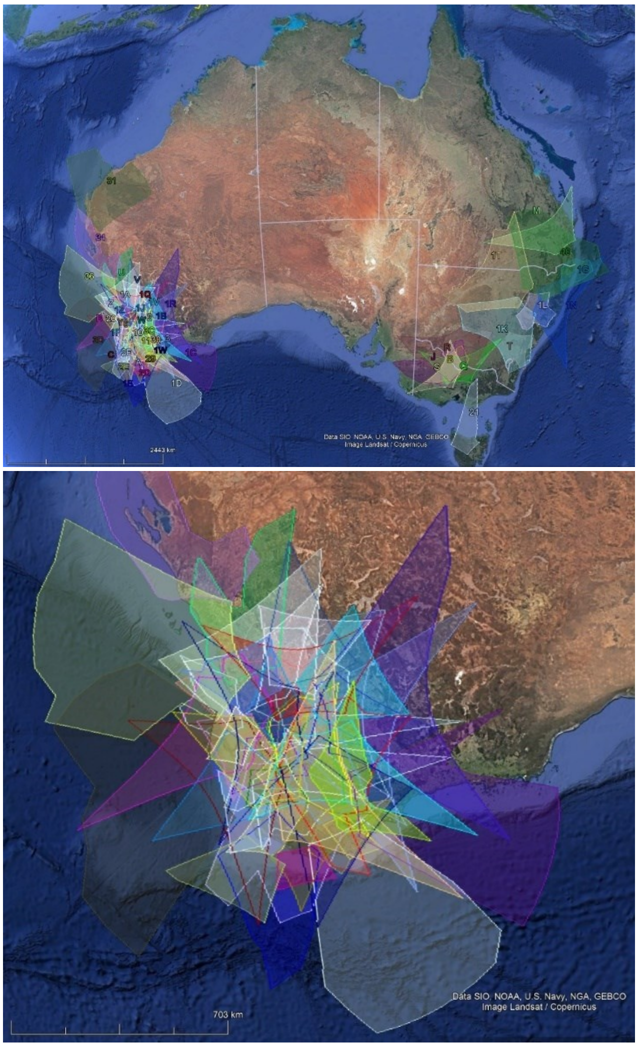

Figure 3 – GMN camera fields in 2023 intersected at 100 km elevation, for cameras active in Australia, global view on top and a close up for Western Australia at bottom.

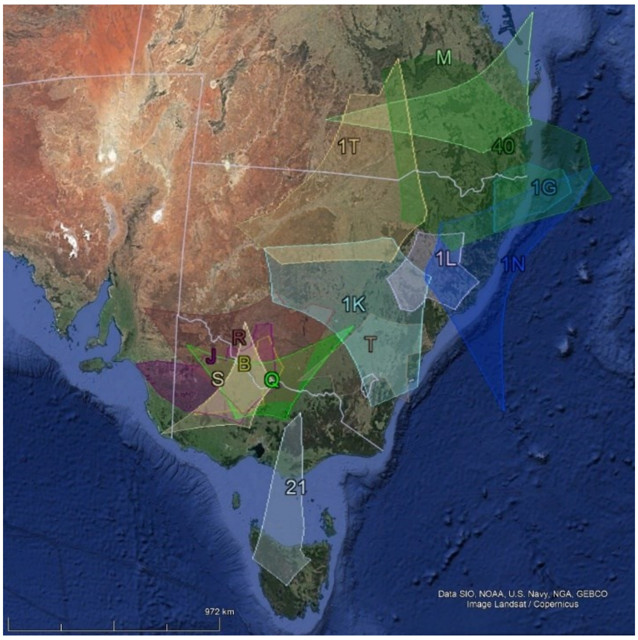

Figure 4 – GMN camera fields in 2023 intersected at 100 km elevation, for cameras active in Australia (eastern states).

The first 31 meteor orbits by Australian RMS cameras were registered in September 2021 when the first five cameras got ready to harvest meteors. By the end of 2021, 12 cameras managed to obtain 1871 orbits in the final 4 months of 2021. A real breakthrough was achieved in 2022 as the number of RMS cameras in Australia increased to 29, good for 12460 orbits in 2022. The expansion of the network accelerated even more in 2023 which ended with 67 operational cameras which contributed 41887 orbits making Australia one of the major contributors to GMN (see *Table 5*). Most cameras were installed in Western Australia (*Figure 3*) but a significant progress was made in the eastern states of Australia with more cameras in Victoria, Queensland and New South Wales (*Figure 4*). Australia being a very large country, describing its camera networks as a single network is a bit unfair as it is like considering all European countries as a single EU network.

5.2 Belgium

Belgium had its first RMS cameras operational in early 2019. *Figure 5* shows the GMN coverage at the end of 2023 for Belgium. The map can be compared with the situation end of 2022 in the previous GMN annual report (Roggemans et al., 2023).

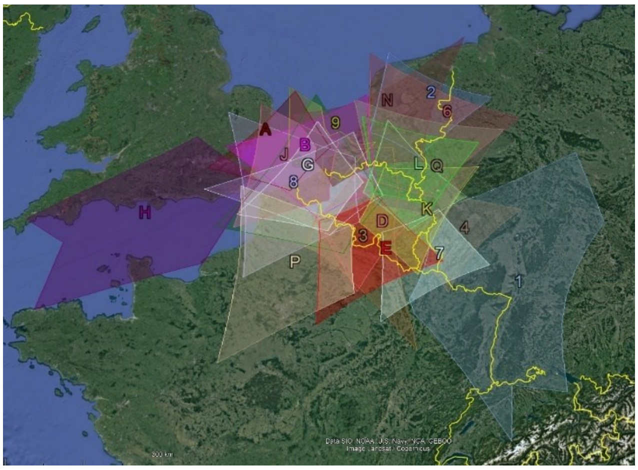

Figure 5 – GMN camera fields intersected at 100 km elevation, for 24 cameras installed in Belgium, status 2023.

Most of the Belgian RMS cameras are being installed for the reinforcement of the CAMS-BeNeLux network. For this purpose, the 6 mm lenses are preferred which have less distortion than the 3.6 mm and detect more fainter meteors. The weather in 2023 was significantly less favorable than during the exceptional year 2022, but Belgian cameras still contributed to 25720 orbits in 2023 compared to 23174 a year before. The number of cameras increased from 20 in 2022 to 24 in 2023. Belgian cameras have many paired meteors with those in neighboring countries, France, Germany, Netherlands and the UK.

5.3 Brazil

The BRAMON network had its first two RMS cameras getting paired meteors in October 2020 good for 40 orbits with two cameras in the last quarter of 2020. The network expanded to 13 operational cameras, good for 1645 orbits in 2021. In 2022 the number of cameras increased to 20 and 2760 orbits were obtained. In 2023 the number of cameras increased to 34 but the number of paired meteors dropped to 2331, it is not clear why but many cameras had several months without paired meteors. Brazil is a huge country and most RMS cameras are installed in the southern part (*Figure 6*).

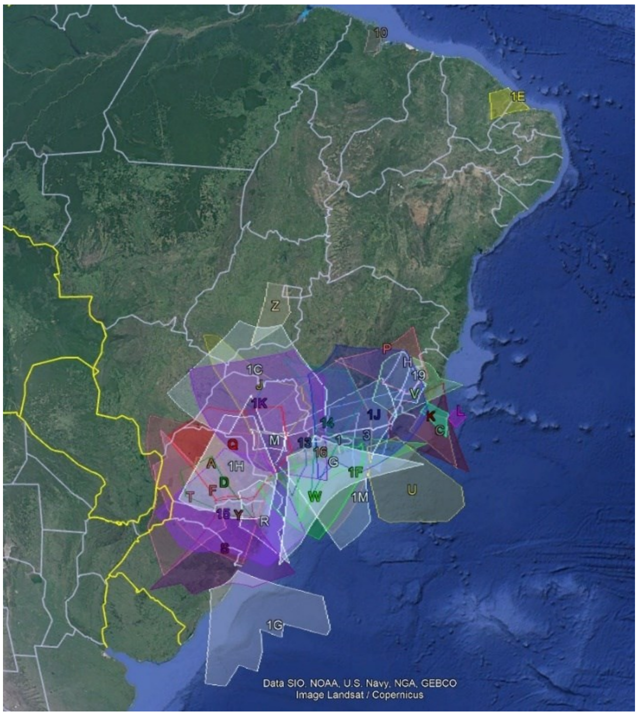

Figure 6 – GMN camera fields in 2023 intersected at 100 km elevation, for 34 cameras active in Brazil.

5.4 Bulgaria

Bulgaria got its first RMS camera operational in June 2021 and got three cameras installed by the end of 2021 of which two had 419 multi-station events. In April 2022 a 4th RMS and in July 2022, two extra cameras were installed. With 6 cameras in 2022, 3877 orbits could be collected. In 2023 three more cameras became operational, but BG0005 and BG0006 didn't have paired meteors in 2023. Seven operational cameras had 3530 orbits in 2023 (*Figure 7*). The new cameras were added in the last months of 2023 when the weather was less favorable. The Bulgarian RMS cameras also get paired meteors with cameras in Greece and in Romania.

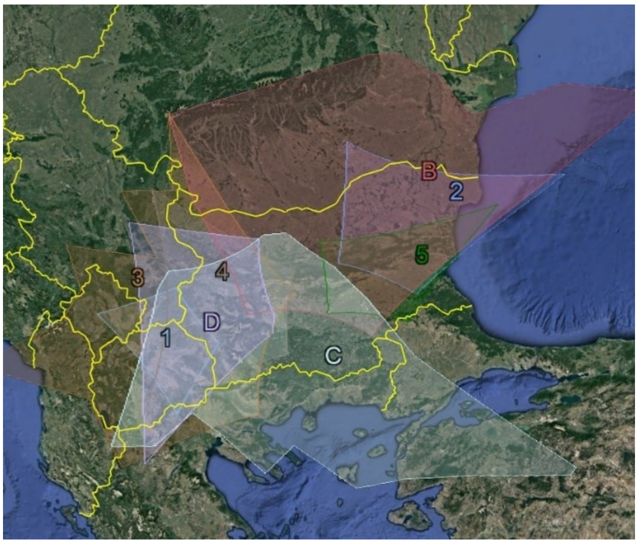

Figure 7 – GMN camera fields in 2023 intersected at 100 km elevation, for 7 cameras active in Bulgaria.

5.5 Canada

The Canadian GMN network got its first five operational RMS cameras providing orbits in June 2019 and expanded to 11 cameras by the end of 2019, good for 3599 orbits. The number of cameras increased to 18 by the end of 2020 with 10815 orbits registered. During 2021, 15 new camera IDs appeared in the list and 8809 orbits were recorded with 29 cameras in 2021, less than the year before despite the extra cameras. The number of cameras doubled from 29 to 58 in 2022 resulting in 16232 orbits. Some cameras in New Found Land still wait for a multi-station partner (*Figure 8*).

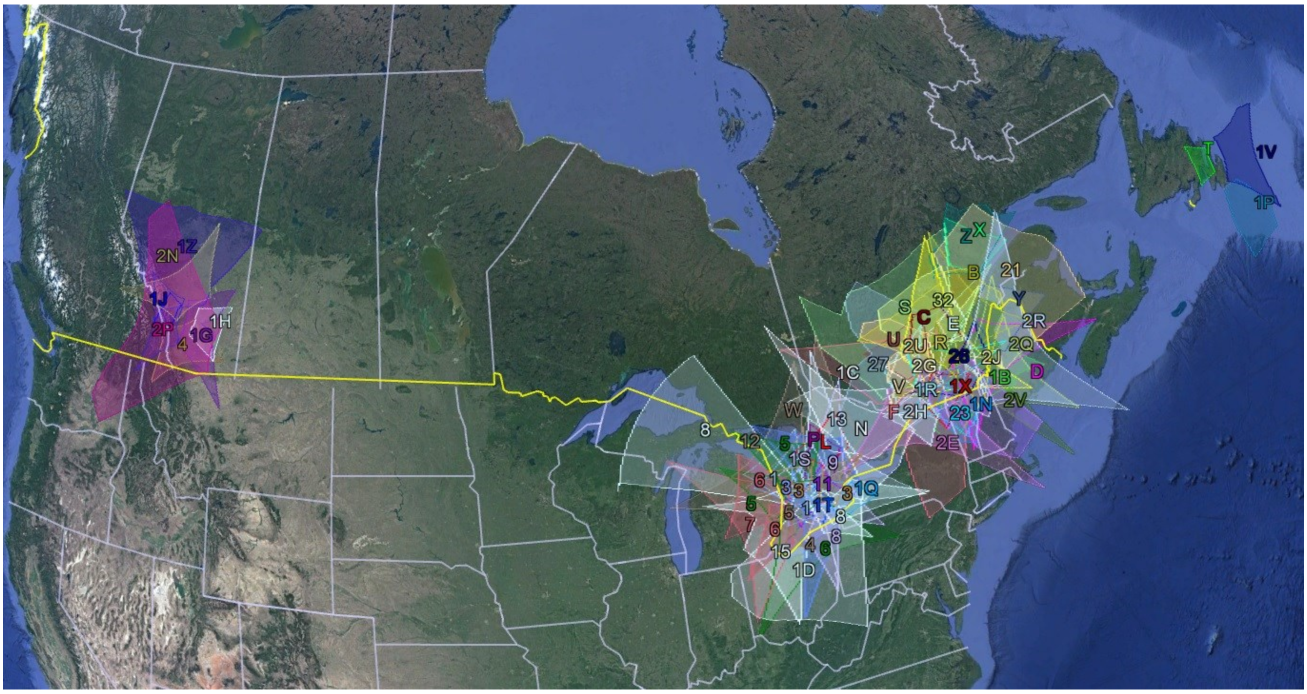

Figure 8 – GMN camera fields in 2023 intersected at 100 km elevation, for cameras active in Canada, overview.

Most cameras are installed in Quebec and Southern Ontario, ideal for volunteers south of the Canadian border in the US (*Figure 9*). In 2023 the number of contributing cameras increased to 67 resulting in 15023 orbits. As many as 16 Camera IDs that worked in previous years have disappeared from the list in 2023. Two smaller sub-networks exist, CAWE (Elginifield) which had 425 orbits and CAWT (Tavistock) which had 193 orbits in 2023, both networks being composed of eight cameras. A small network in the Calgary region of Alberta had its first orbits in 2022 (*Figure 10*) and improved coverage in 2023.

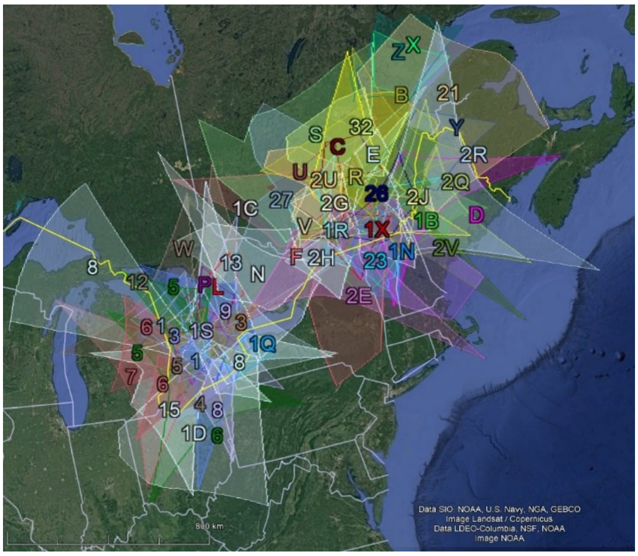

Figure 9 – GMN camera fields intersected at 100 km elevation, for cameras active in Canada, Quebec and Ontario in 2023.

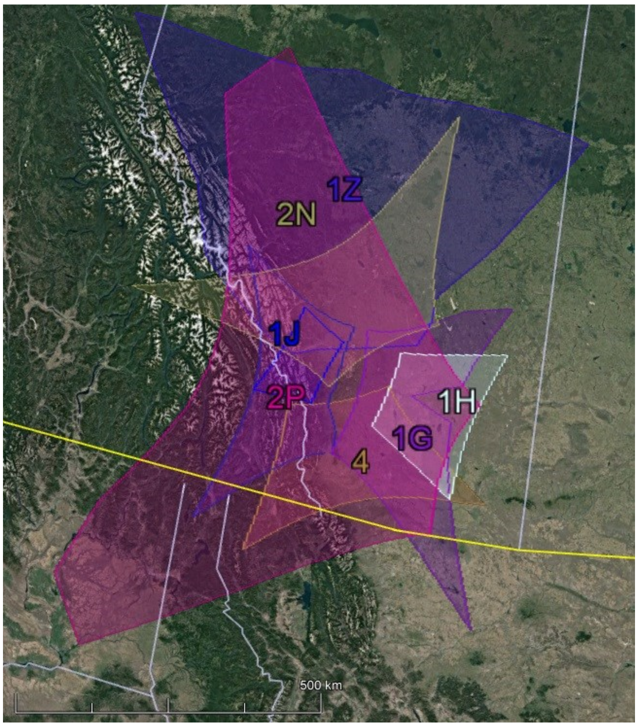

Figure 10 – GMN camera fields intersected at 100 km elevation, for cameras active in Canada, Alberta in 2023.

5.6 Croatia

Croatia was the first European country in May 2019 to harvest orbits with three RMS cameras. By the end of 2019 Croatia had already 23 cameras successfully contributing in triangulations, good for 12221 multi-station events. The number of cameras increased to 32 in 2020 resulting in 35099 orbits that year. 38370 multi-station events were recorded in 2021 with 48 cameras. 2022 was slightly less successful with 31329 orbits and 45 operational cameras. In 2023 the number of cameras slightly decreased at 41 which contributed to 27721 orbits. 14 camera IDs from previous years didn't appear in the 2023 data anymore. Lots of cameras were running on RPi3, for years - and the time has come for them to be replaced; some of those couldn't be replaced due to the huge workload that IstraStream guys had supplying the rest of the world with new cameras. One camera operator passed away and a number of cameras couldn't be reached anymore. The problems should be solved in 2024.

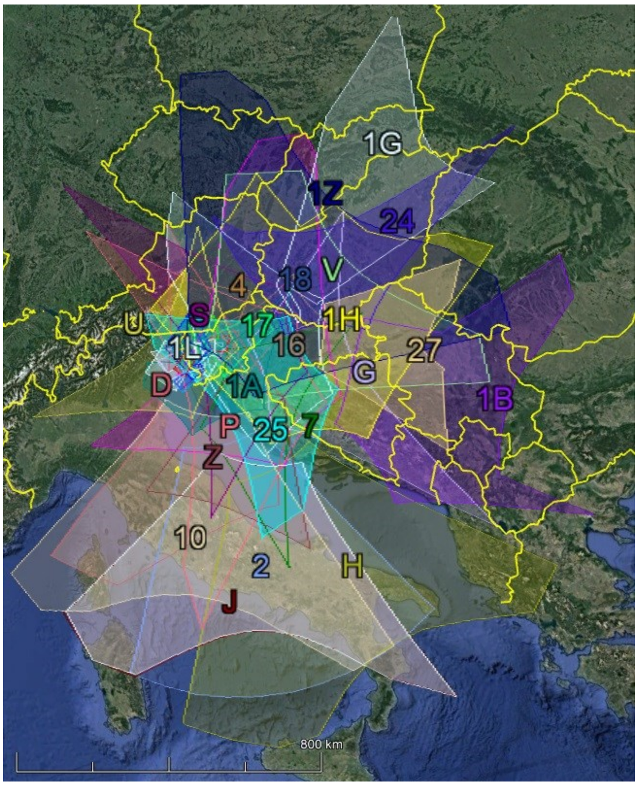

Figure 11 – GMN camera fields intersected at 100 km elevation, for cameras installed in Croatia, status 2023.

Croatia plays a major role in the coordination of GMN, maintaining the IstraStream service to produce and deliver new cameras for many countries and providing technical assistance to participants in the GMN project worldwide. The Croatian cameras provide a huge overlap on the neighboring countries (*Figure 11*). A number of Croatian cameras have a very small FoV to register fainter meteors with higher positional accuracy. To view these camera fields in detail we refer to the online KML files for consultation in Google Earth.

5.7 Czech Republic

The number of operational RMS cameras in the Czech Republic increased a lot in 2023 from six in 2022 to 20 in 2023. In total 11269 orbits were obtained in 2023 against 2490 in 2022 and 464 in 2021. The central location of the country in Europe and the increasing number of cameras installed in neighboring countries determine to a large extent the number of paired meteors (*Figure 12*).

Since the end of 2022, the Czech and Slovak GMN camera operators are grouped in the CSMON (Czech & Slovak Meteor Observation Network), which helps the new and current meteor enthusiasts to get on board. Started by skilled individuals, the network has recently grown thanks to several observatories located across the region.

In addition to GMN, the CEMeNt network has resumed the trajectory calculation from the past recordings, after a five years long break. It is hoped that many former analog cameras in this network will upgrade to RMS in the near future.

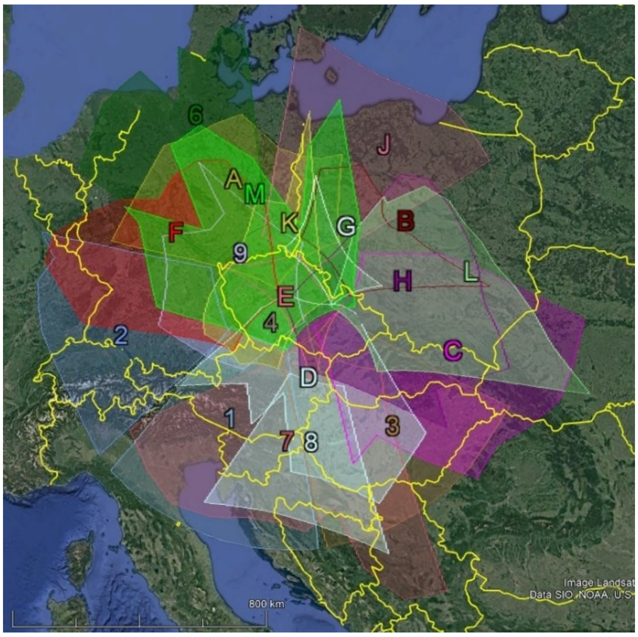

Figure 12 – GMN camera fields in 2023, intersected at 100 km elevation, for cameras active in the Czech Republic.

5.8 Denmark

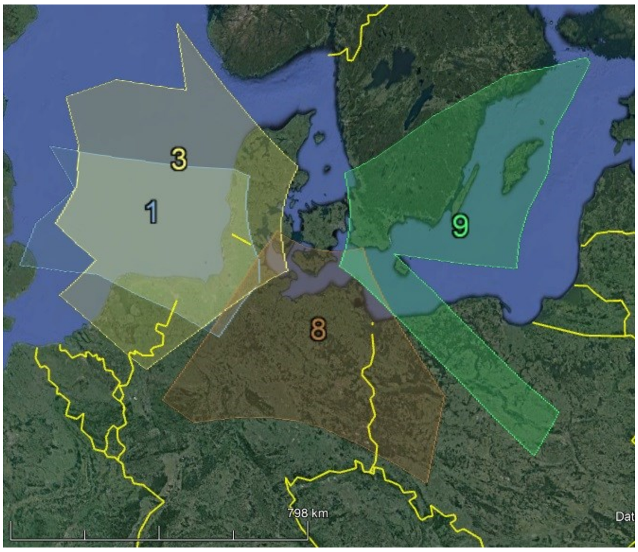

Figure 13 – GMN camera field in 2023 intersected at 100 km elevation, for cameras active in Denmark.

In October 2022 a first GMN camera got operational in Denmark, good for 55 orbits in 2022. In 2023 four cameras were active in Denmark which obtained 1386 orbits (*Figure 13*). These northern cameras create possibilities for further camera coverage in southern Norway and Sweden.

5.9 Finland

In October 2022 the first GMN cameras became operational at two sites in Finland, with 41 orbits as a first result (*Figure 14*). In 2023 there were five cameras active which resulted in 90 orbits.

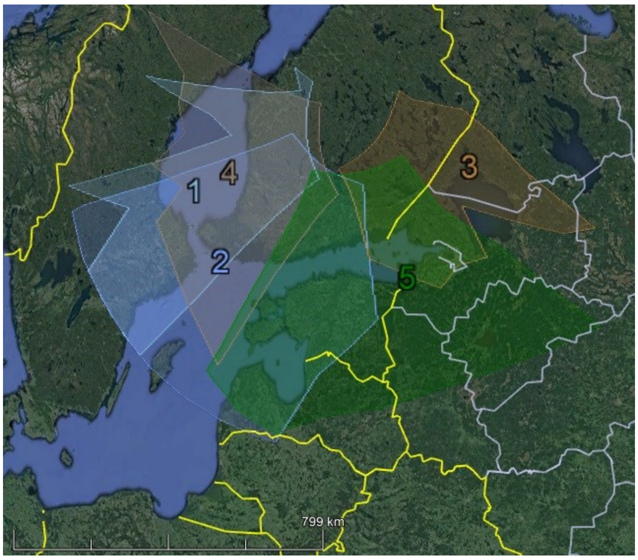

Figure 14 – GMN camera fields in 2023 intersected at 100 km elevation, for cameras active in Finland.

5.10 France

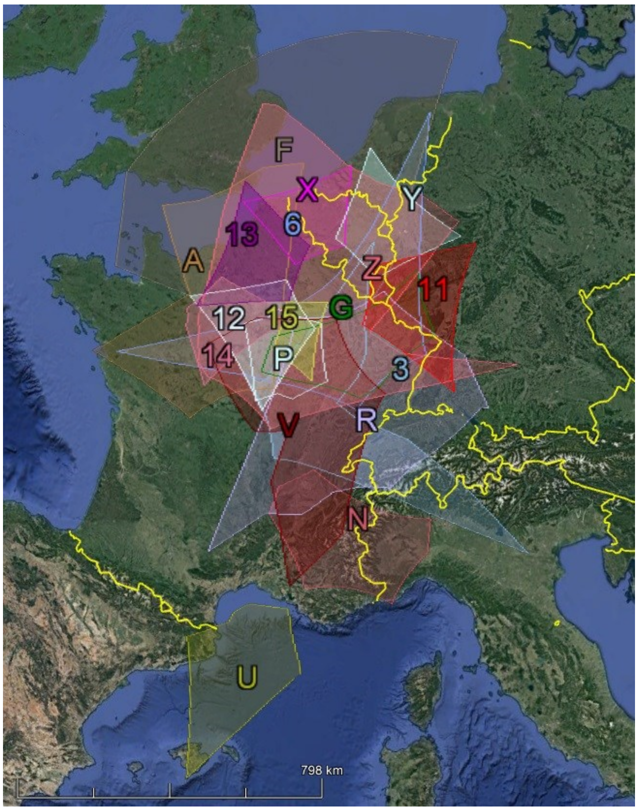

Figure 15 – GMN camera fields in 2023 intersected at 100 km elevation, for cameras active in France.

The number of RMS cameras in France increased gradually from 10 in 2020 to 14 devices in 2021 and 16 in 2022. More new cameras were installed in 2023 and 16682 orbits were obtained with 18 cameras, a much better result than in 2022 when 11990 orbits were obtained. In total 25 RMS cameras were installed since March 2020, but seven of them did not function anymore in 2023. A large part of France is still without GMN coverage (*Figure 15*).

5.11 Germany

The first GMN camera in Germany had its first orbits in August 2019 with Belgian GMN cameras. By the end of 2019 there were four GMN cameras in Germany, good for 200 orbits. The number of cameras increased to 10 and the numbers of orbits to 3963 in 2020. With 12 cameras in 2021, 7009 orbits were collected, in 2022, with 18 cameras 9128 orbits were collected. In 2023 as many as 12194 orbits were recorded with 19 cameras. Some GMN cameras in the North-Western part of Germany also participate in the CAMS-BeNeLux network, supporting both GMN and CAMS (*Figure 16*).

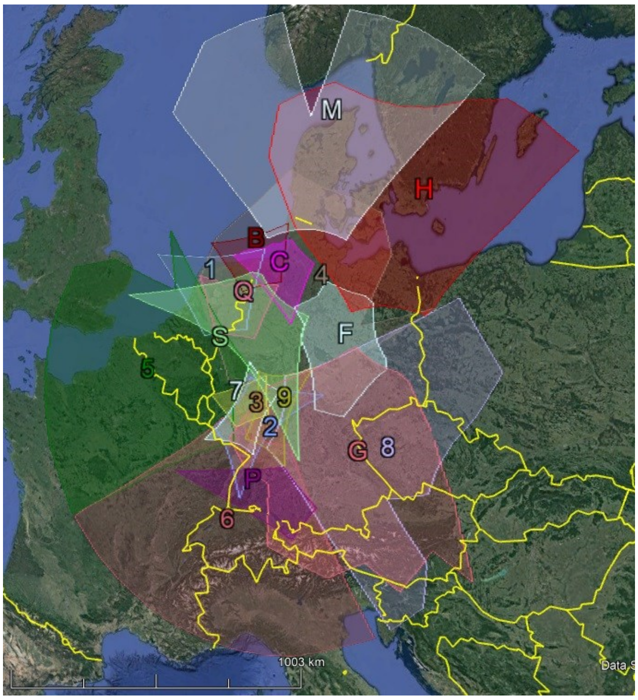

Figure 16 – GMN camera fields in 2023 intersected at 100 km elevation, for cameras active in Germany.

5.12 Greece

Figure 17 – GMN camera fields in 2023 intersected at 100 km elevation, for cameras active in Greece.

In September 2022 the first GMN camera got operational in Greece, ideally pointed to overlap with some Bulgarian GMN cameras, good for 977 paired meteors in the four last months of 2022. Three extra cameras were installed and with four cameras 3375 orbits were obtained in 2023 (*Figure 17*).

5.13 Hungary

A first GMN camera got operational in March 2022 in Hungary and by end of 2022, two Hungarian cameras had obtained 2114 orbits. One new camera was added in 2023 and last year, Hungarian cameras contributed to 7872 orbits, mainly paired meteors with Croatian and Czech cameras. Hungary has a long tradition in meteor astronomy and hopefully more GMN camera sites will get installed (*Figure 18*).

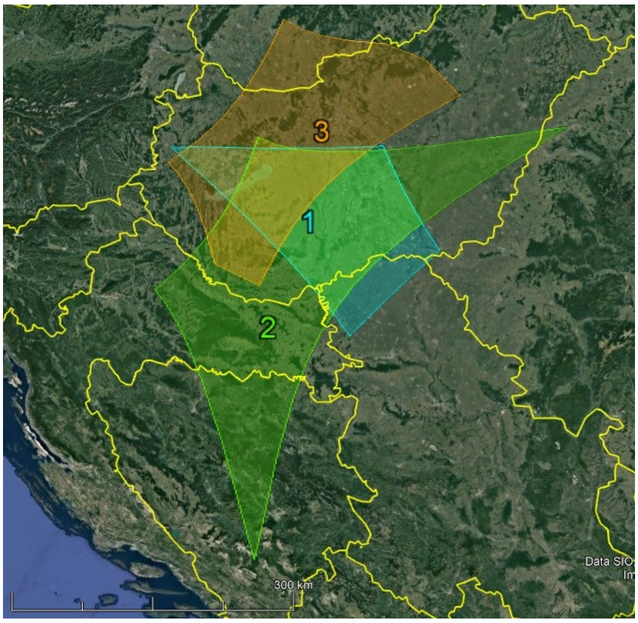

Figure 18 – GMN camera fields in 2023 intersected at 100 km elevation, for cameras active in Hungary.

5.14 Ireland

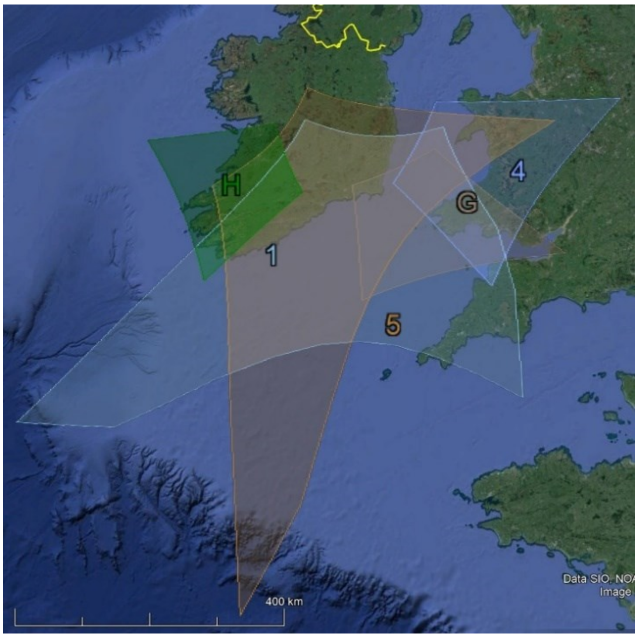

Figure 19 – GMN camera fields in 2023 intersected at 100 km elevation, for cameras active in Ireland.

Ireland got a first GMN operational in October 2020 and a second one a month later, good for 120 orbits in 2020. With three cameras in 2021 the number of orbits increased to 424. 3490 orbits were recorded in 2022 with five GMN cameras. In 2023 the number of cameras remained unchanged (*Figure 19*) but the number of orbits dropped to 1954. Most of the paired meteors were obtained thanks to the overlap provided by GMN cameras in the UK. Many attributed GMN camera IDs don't show up on the map.

5.15 Israel

Israel got its first three GMN cameras installed in November 2020, good for 553 orbits that year. In 2021 with three extra cameras 2009 orbits were obtained. In 2022 the cameras did not provide orbits during some time and one camera was discontinued, resulting in 975 orbits. In 2023, 1096 orbits were collected using six cameras (*Figure 20*).

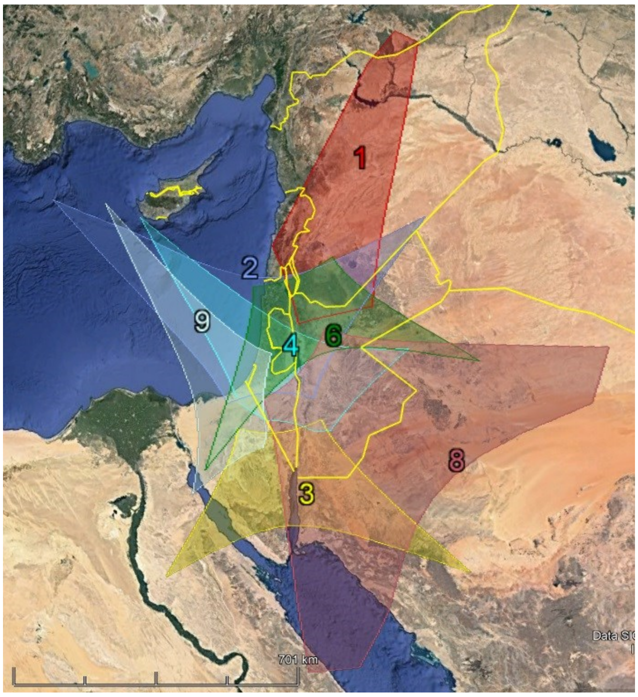

Figure 20 – GMN camera fields in 2023 intersected at 100 km elevation, for cameras active in Israel.

5.16 Italy

Italy got its first GMN camera installed and contributing to orbits in October 2019, good for 862 orbits in 2019. Italy remained with one GMN camera in 2020, which had as many as 5384 paired meteors with Croatian and Slovenian cameras. Italy increased its number of cameras from one to five and these cameras were involved in 5447 multi-station events in 2021. An extra camera was added in Bologna in 2022 when 4943 orbits were collected. With seven cameras in 2023, 5064 orbits were obtained (*Figure 21*).

5.17 Japan

A first GMN camera got installed in Japan in 2022, waiting for some multi-station partners at suitable distance for triangulation. In 2023 a second camera was installed which allowed to obtain 629 orbits (*Figure 22*). Japan has the very active SonotaCo network which uses analog Watec cameras. RMS cameras deliver UFO capture output which may offer opportunities for the SonotaCo network.

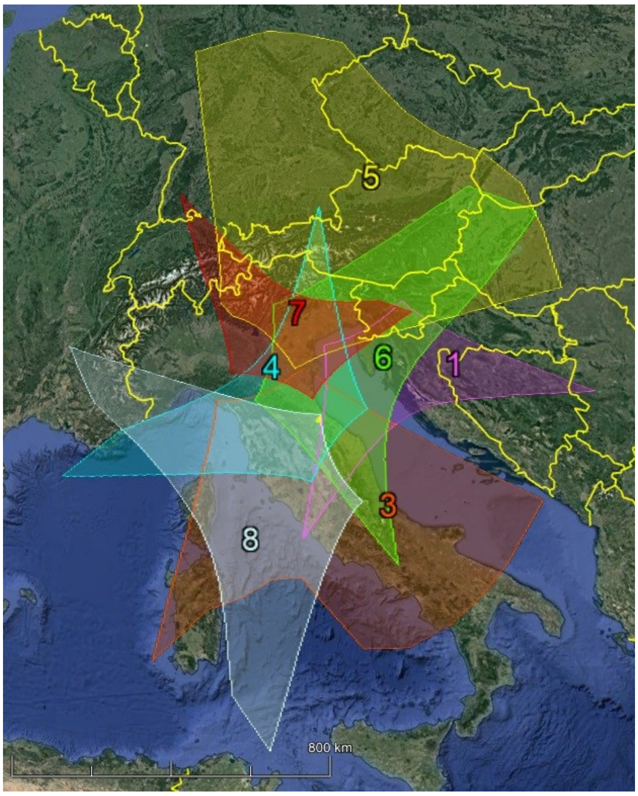

Figure 21 – GMN camera fields in 2023 intersected at 100 km elevation, for cameras active in Italy.

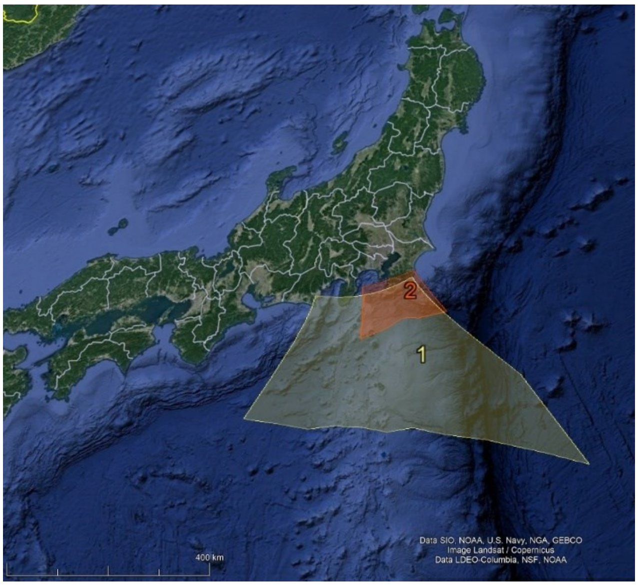

Figure 22 – GMN camera fields in 2023 intersected at 100 km elevation, for cameras active in Japan.

5.18 Korea (South)

A most impressive deployment of GMN cameras took place in 2022 in South Korea with a first few cameras obtaining orbits in September and as many as 47 GMN cameras installed in November and December 2022. The cameras were installed and pointed to obtain an optimal overlap resulting in 7711 orbits during the first year. In 2023 the number of cameras rapidly increased to 125 (!) collecting 34044 orbits. This fast deployment made the RMS network in South Korea a major contributor at a strategic geo location at the northern hemisphere for a 24 on 24-hour monitoring of meteor activity.

The dense coverage of overlapping camera fields in 2023 can be compared to the situation end of 2022 in *Figure 23*. If any RMS cameras get installed in South-Western Japan, these would generate many paired meteors with the Korean cameras.

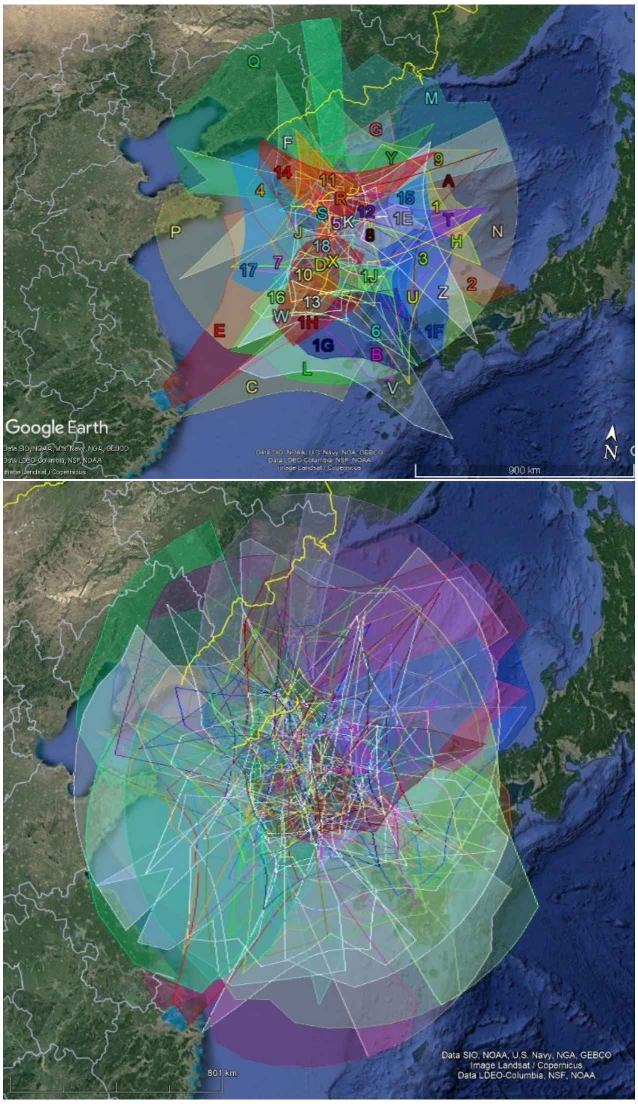

Figure 23 – GMN camera fields in 2022 (top) and in 2023 (bottom) intersected at 100 km elevation, for cameras active in South Korea.

5.19 Luxembourg

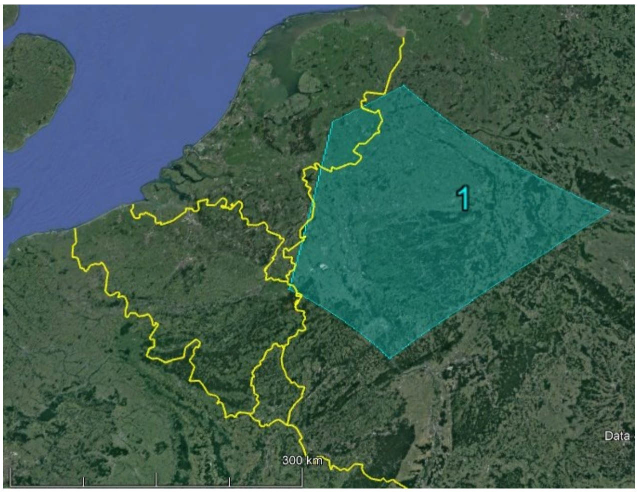

Figure 24 – GMN camera field in 2023 intersected at 100 km elevation, for cameras active in Luxembourg.

In October 2022 a first GMN camera got installed in Luxembourg contributing to 622 orbits combining with Belgian, Dutch, French, German and even Czech GMN cameras (*Figure 24*). In 2023 this camera had 2018 paired meteors with orbits. This camera covers a strategic volume of atmosphere for Belgian, Dutch, French and German cameras and cannot be missed.

5.20 Mexico

An impressive deployment of GMN cameras took place in Mexico in 2022. The first few installed cameras obtained the first orbits in February 2022 and soon 12 cameras got installed with a good overlap. A total of 1769 meteor orbits could be collected in 2022. The number of cameras increased to 15 in 2023 with 2953 orbits as result. The efforts in Mexico are crucial in getting coverage for both the northern and especially the southern hemisphere at these longitudes (*Figure 25*).

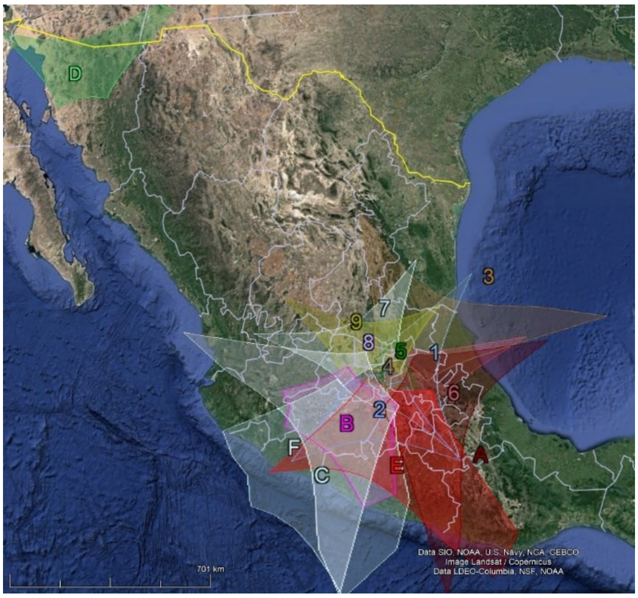

Figure 25 – GMN camera fields in 2023 intersected at 100 km elevation, for cameras active in Mexico.

5.21 Malaysia

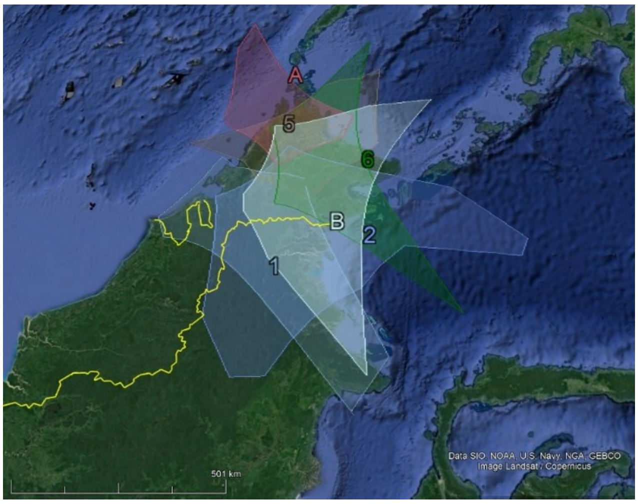

Figure 26 – GMN camera fields in 2023 intersected at 100 km elevation, for cameras active in Malaysia.

A first GMN camera had been installed in Malaysia in 2021 waiting for coverage from cameras installed at a suitable distance to get good triangulations. Some extra cameras got installed in 2022 and in June 2022 the first orbits were obtained. In total 50 orbits were obtained in 2022 with three cameras. In 2023 a ten-fold of orbits, 551, were collected with five cameras (*Figure 26*). Further extensions of the Malaysian network are very welcome.

5.22 Netherlands

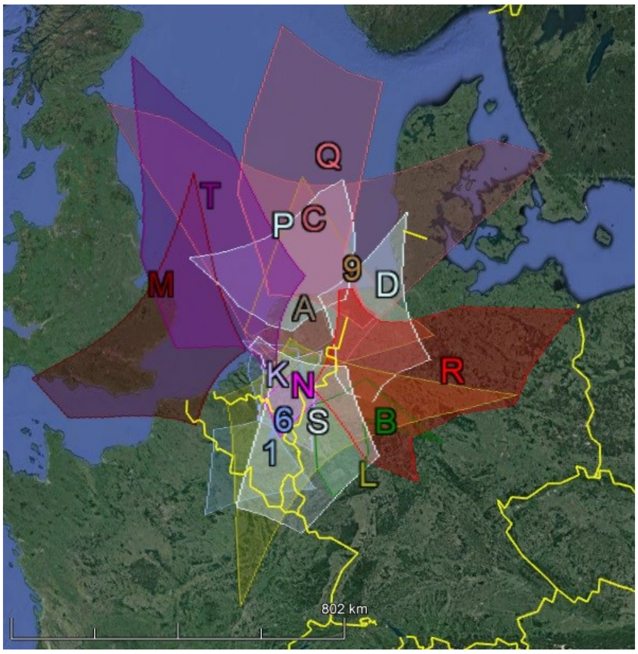

Figure 27 – GMN camera fields in 2023 intersected at 100 km elevation, for cameras active in the Netherlands.

The Netherlands started collecting orbits within GMN in August 2019 and had 278 orbits in its first year. The number of GMN cameras increased to 11 in 2020 with 4337 orbits as a result. The number of cameras remained unchanged in 2021 but the better overlap from neighboring countries resulted in 7605 orbits. Some cameras dropped off in 2022 and few new got installed, resulting in 9139 orbits with 13 cameras. In 2023, 14 Dutch RMS cameras had 9421 orbits (*Figure 27*). Dutch cameras get mainly multi-station coverage from cameras in Belgium, Germany, the UK and Denmark.

5.23 New Zealand

The first two GMN cameras were installed in July 2021 in New Zealand and 1146 orbits were obtained that year. From March 2022 more cameras were installed month by month with an impressive deployment of strategically placed well pointed cameras covering the huge surface of the country. With 28 active cameras at the end of 2022, 6280 orbits were recorded. The New Zealand GMN network, known as Fireballs Aotearoa, was further expanded in 2023 and with a total of 111 cameras 47436 orbits were obtained, making New Zealand one of the most important providers of orbit data for the Southern Hemisphere. The density of the camera coverage can be seen in *Figure 29* and compared to the situation one year earlier. Another 20 or so cameras are in states of install. The network has focused on having all the cameras hosted by members of the public, schools and observatories, and is now linked with the Royal Astronomical Society of New Zealand. Most of the country is now covered at 25 km elevation – assuming the weather is conducive! The monthly captures are now in the 1000s of

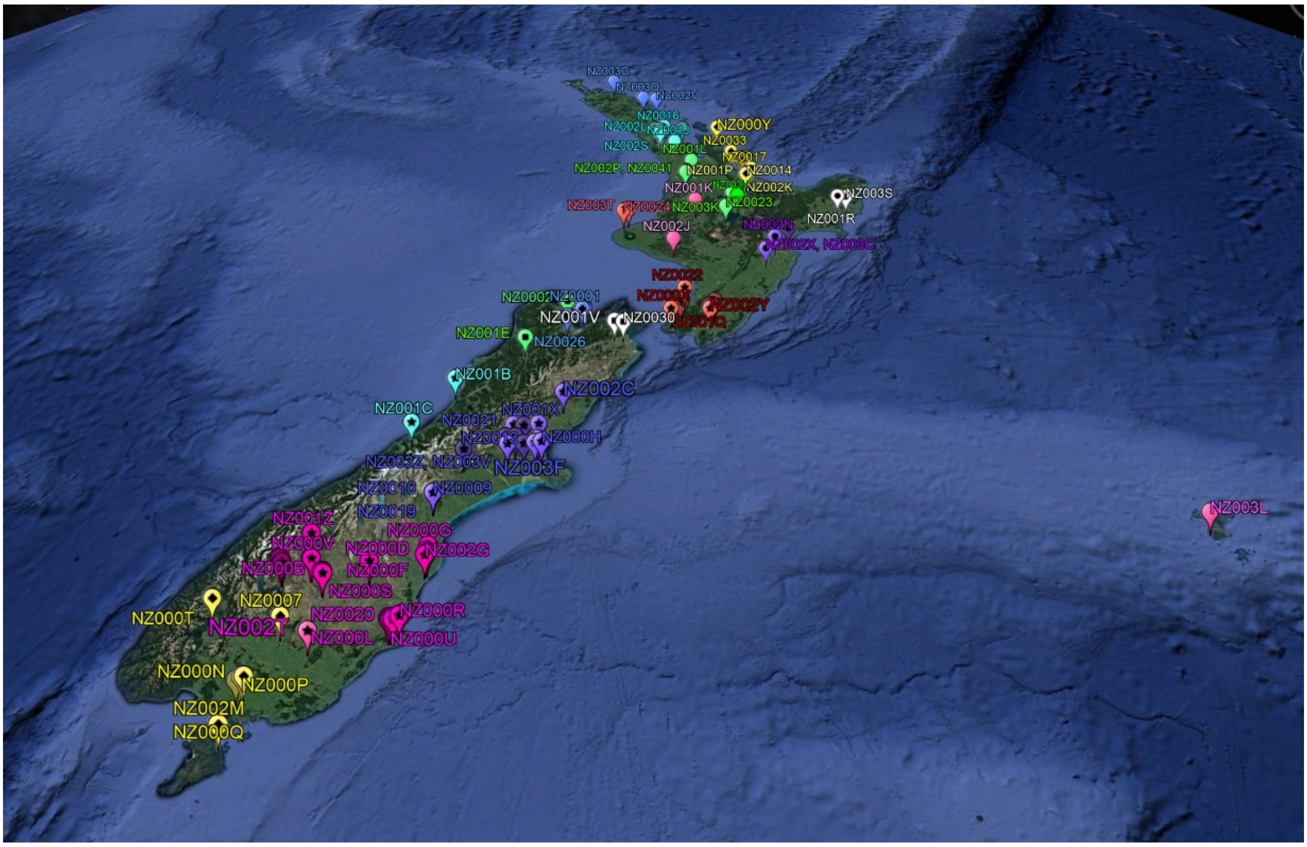

Figure 28 – GMN camera positions in New-Zealand, situation as end of 2023.

meteors, with more than 6300 in Jan 2024 whereas only 100–200 per month were detected 1.5 years ago. The network also contributed to optical identification of the Lamda Sculptorids, which is a meteor shower associated with Comet 46P/Wirtanen (Roggemans et al., 2024). There have been a number of impressive asteroidal and cometary fireballs detected and trajectories determined from the camera data, but we await the discovery of any meteorites.

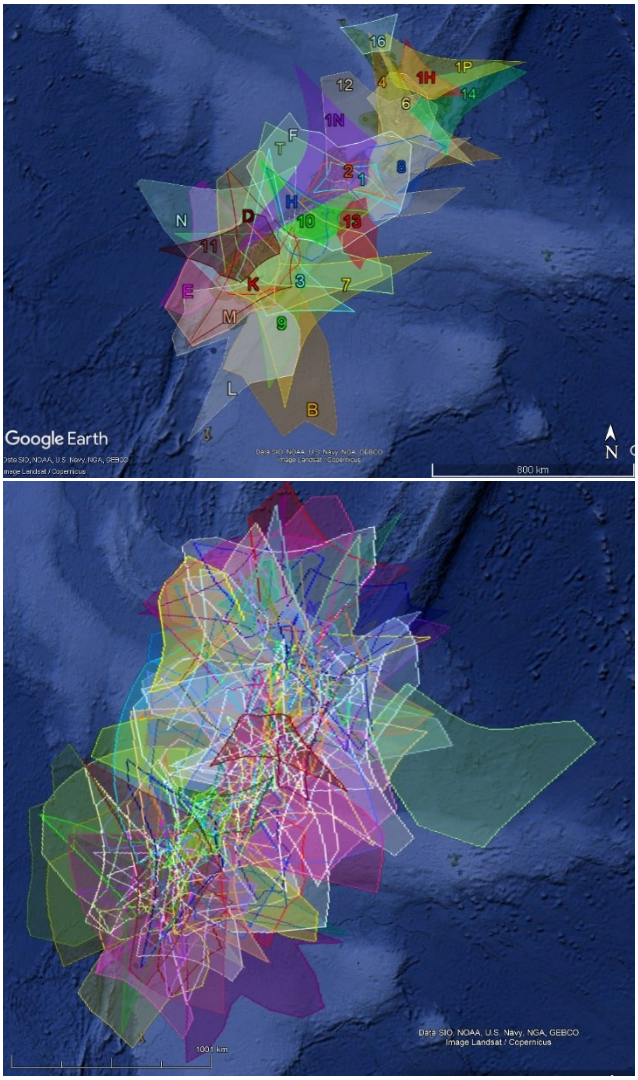

Figure 29 – GMN camera fields in 2022 (top) and in 2023 (bottom) intersected at 100 km elevation, for cameras active in New Zealand.

5.24 Poland

The first GMN camera got installed in September 2020 and remained long the only Polish GMN camera. In March 2022 two extra Polish GMN cameras got their first orbits. The cameras didn't function all the time but the number of orbits obtained increased from 67 in 2021 to 398 in 2022. The number of cameras remained unchanged in 2023 and collected 456 orbits (*Figure 30*). Polish GMN cameras get mainly paired meteors with cameras in stalled in Czechia.

5.25 Portugal

A first GMN camera got its first orbits in September 2022 in Portugal. A vast coverage from GMN cameras in Spain guarantees many paired meteors (*Figure 31*). In 2022, 398 orbits were recorded, in 2023 the total increased to 3322 orbits. Any extra cameras installed in the western part of the Iberian Peninsula would significantly improve the multi-station coverage.

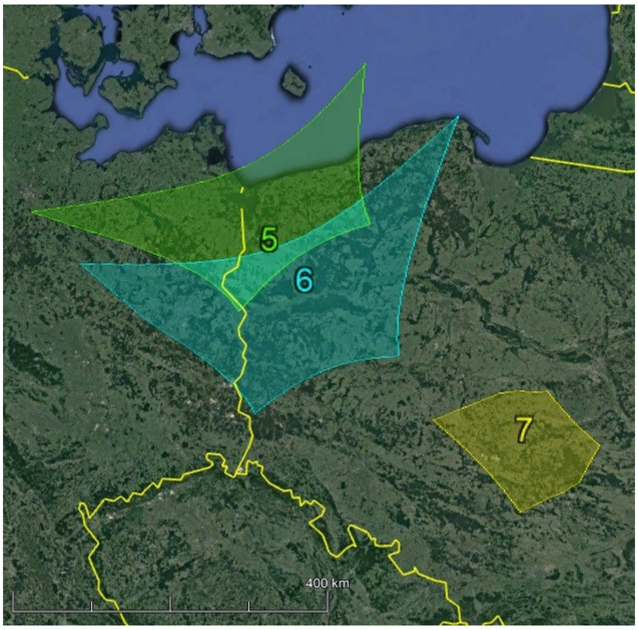

Figure 30 – GMN camera fields in 2023 intersected at 100 km elevation, for cameras active in Poland.

Figure 31 – GMN camera field in 2023 intersected at 100 km elevation, for cameras active in Portugal.

5.26 Romania

Romania was the only new country to install its first three RMS cameras in 2023 (*Figure 32*). Operational since October 2023 and despite unfavorable weather, 417 orbits were collected. These cameras had many paired meteors with Bulgarian, Croatian, Czech and Hungarian cameras. More cameras are planned for installation in 2024.

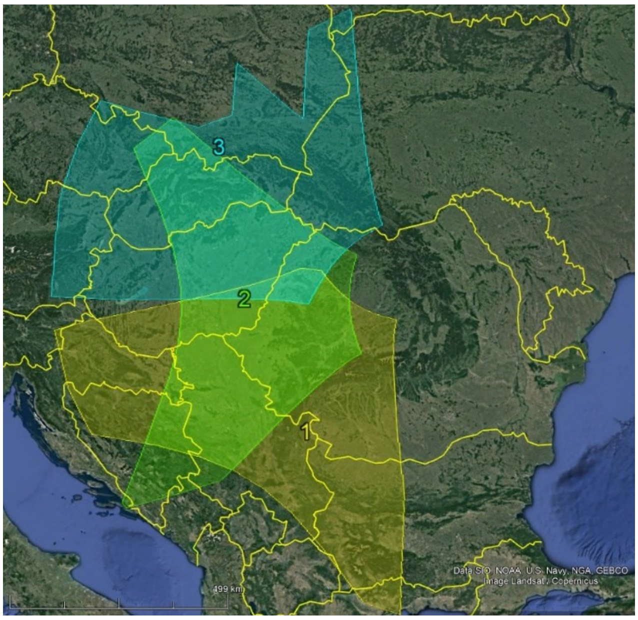

Figure 32 – GMN camera field in 2023 intersected at 100 km elevation, for cameras active in Romania.

5.27 Russia

The first two GMN cameras in Russia had orbits in July 2019. The first year had already 5715 orbits with 10 cameras. In 2020 the number of cameras increased to 21, good for as many as 13438 orbits. The number of RMS cameras having paired meteors remained stable at 21, but the number of orbits decreased to 6208 in 2021. Problems with the maintenance of some meteor stations reduced the number of paired observations. In 2022, 19 cameras in Russia had 5437 orbits. The number of Russian GMN cameras decreased further to 15 in 2023 and the number of paired meteors dropped to 1992. In total 12 of the formerly active cameras stopped contributing data. Some single RMS devices (*Figure 33*) got installed elsewhere in Russia, waiting for coverage from other RMS cameras at a suitable distance. Some cameras in the far east of Russia stopped uploading data.

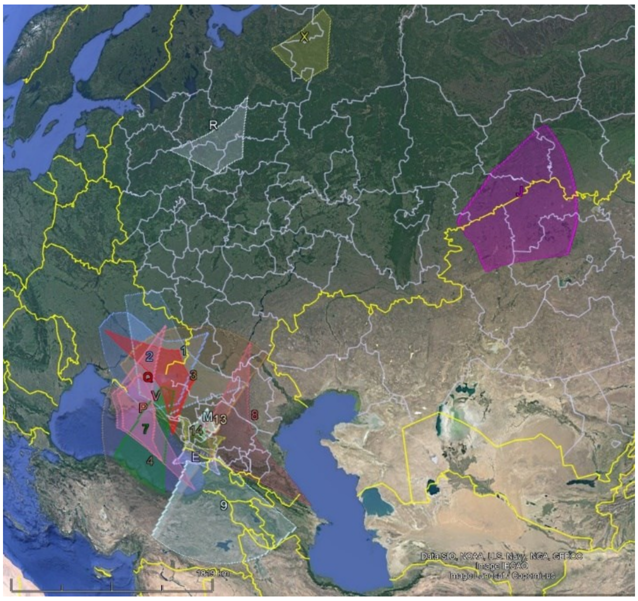

Figure 33 – GMN camera fields in 2023 intersected at 100 km elevation, for cameras active in Russia (West).

5.28 Singapore

A first camera got installed in 2022 and is waiting for multi-station partners, no orbits could be obtained yet in 2023 (*Figure 34*).

Figure 34 – GMN camera fields in 2023 intersected at 100 km elevation, for cameras active in Singapore.

5.29 Slovakia

Slovakia got its first camera in November 2021 with 37 paired meteors. In 2022, three GMN cameras got operational good for 2026 orbits. The number of cameras increased to four in 2023 and 5535 paired meteors with orbits were recorded by Slovakian cameras (*Figure 35*). Since the end of 2022, the Czech and Slovak GMN camera operators are grouped in the CSMON (Czech & Slovak Meteor Observation Network), which helps the new and current meteor enthusiasts to get on board.

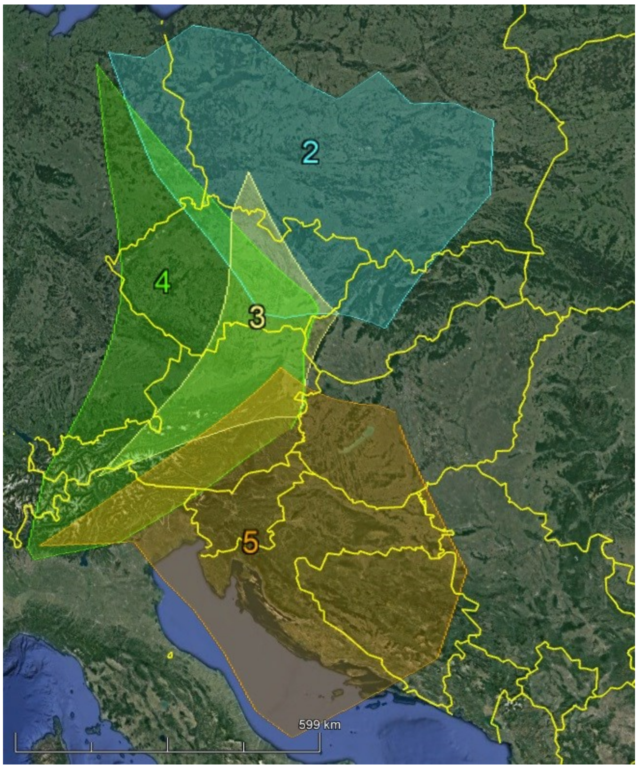

Figure 35 – GMN camera fields in 2023 intersected at 100 km elevation, for cameras active in Slovakia.

5.30 Slovenia

Slovenia got its first RMS contributing in August 2019 and a second RMS in August 2021. The coverage by cameras in neighboring Croatia resulted in 2753 orbits in 2019, 3999 in 2020 and 6001 in 2021. The two Slovenian cameras contributed to 5887 orbits in 2022. In 2023, four extra cameras were installed and 6789 orbits were collected (*Figure 36*).

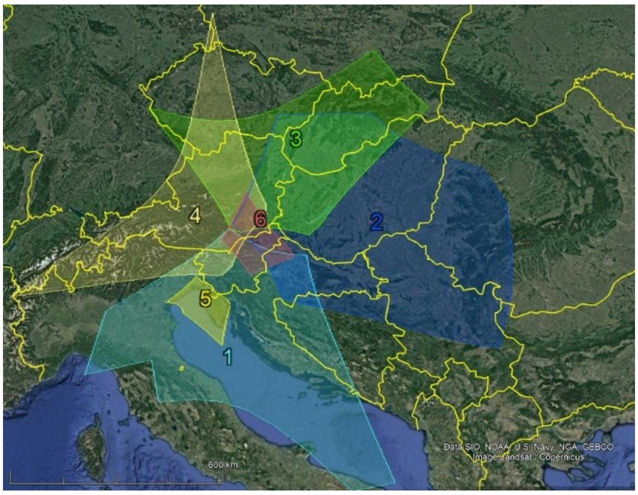

Figure 36 – GMN camera fields in 2023 intersected at 100 km elevation, for cameras active in Slovenia.

5.30 Spain

The GMN had its first orbits collected in Spain in April 2020. End of 2020, eight GMN cameras had collected 1207 orbits. A lot of progress was made in Spain in 2021 when the number of cameras increased from eight to 23. The 23 Spanish cameras were involved in 15113 multi-station events in 2021. The number of GMN cameras increased further to 30 in 2022 and resulted in 19301 orbits. In 2023, 22610 orbits were obtained with 35 cameras (*Figure 38*). Three cameras are installed at the Canary Islands (*Figure 37*).

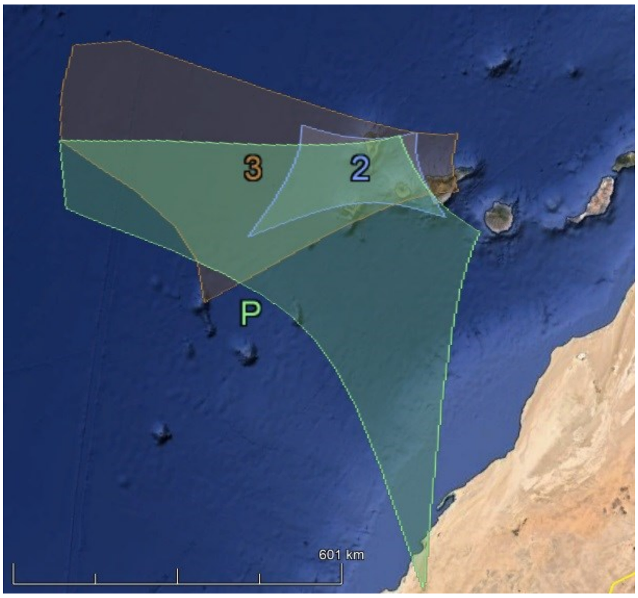

Figure 37 – GMN camera fields in 2023 intersected at 100 km elevation, for cameras active at the Canary Islands (Spain).

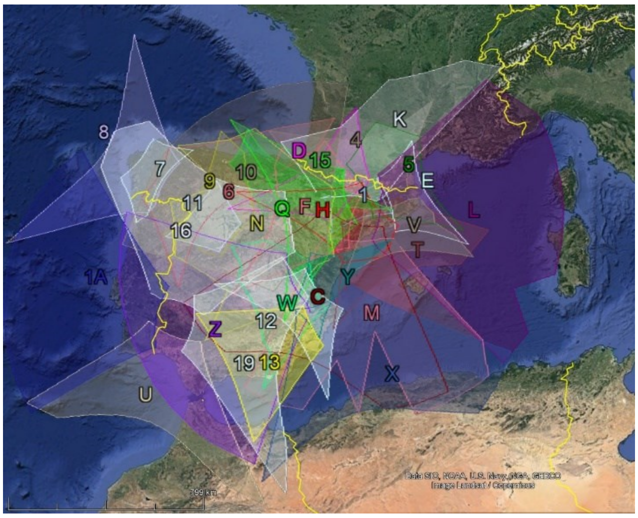

Figure 38 – GMN camera fields in 2023 intersected at 100 km elevation, for cameras active in Spain.

5.31 Switzerland

The first orbits were obtained in August 2021 but it took until May 2022 before extra cameras got installed and more orbits recorded. With five operational cameras 3439 orbits were obtained. The central location of Switzerland is ideal to obtain multi-station events with GMN cameras in the neighboring countries. The number of cameras remained unchanged in 2023 and the number of paired meteors increased to 4352 (*Figure 39*).

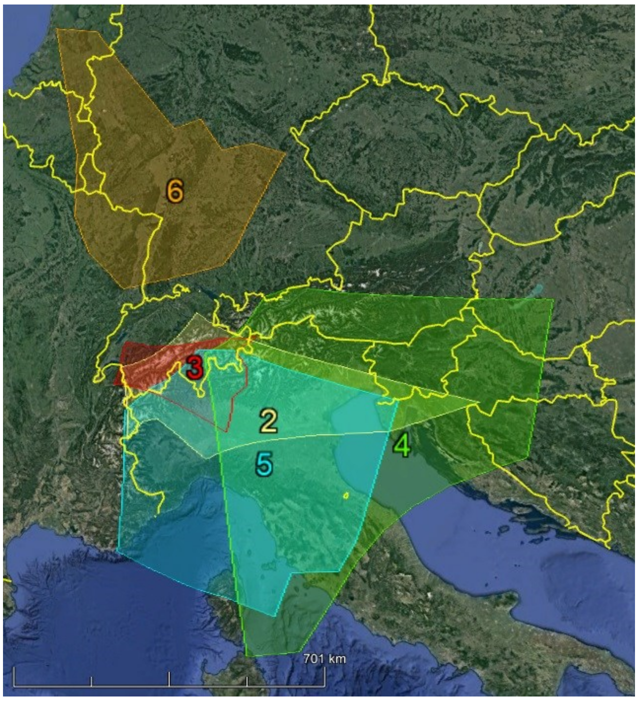

Figure 39 – GMN camera fields in 2023 intersected at 100 km elevation, for cameras active in Switzerland.

5.32 Ukraine

A first RMS camera contributes meteor data to Global Meteor Network in Ukraine, but so far, no paired meteors were recorded (*Figure 40*).

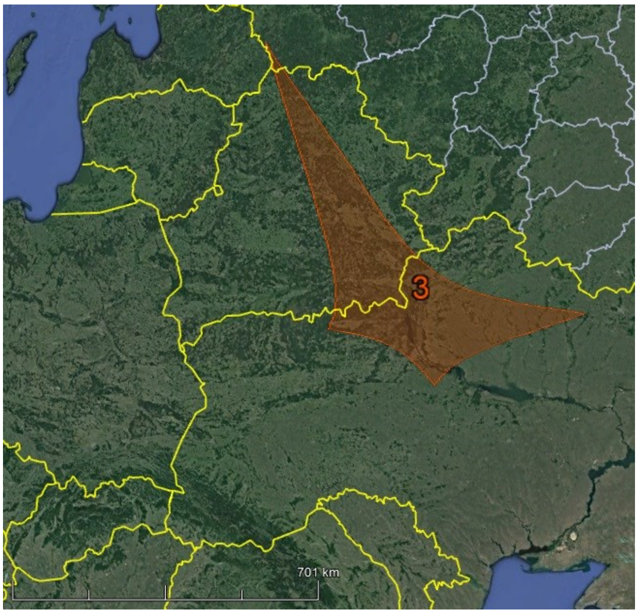

Figure 40 – GMN camera fields in 2023 intersected at 100 km elevation, for cameras active in Ukraine.

5.32 United Kingdom

The GMN got started with 13 cameras in 2020 in the UK and this number rapidly grew to 97 in 2021. The largest expansion came in 2022 when 169 cameras were contributing paired meteors. The network continued to grow throughout 2023 when 261 cameras contributed data (*Figure 41*). The number of orbits increased from 78652 in 2022 to 84688 orbits in 2023. The vast majority of these cameras are part of the UK Meteor Network which now provides complete coverage of the UK and Eire.

Cameras

Camera growth was similar to in 2023, rising from around 170 in January to 261 by year end. 224 of these are contributing to the UK Meteor Network and fourteen cameras dropped offline permanently during the year, typically due to changes in the owner's interests or relocations, though sadly in one case, due to the death of the operator.

In terms of coverage, the UK is now extremely densely covered, with many locations visible to as many as 40 cameras and at 70km altitude the entire of the UK and Eire is covered by at least two cameras, with coverage at 100km extending as far as Norway, Central France and Southern Germany. There is considerable overlap with the BeNeLux network, and potential for overlap with cameras across Europe.

Detections and matches

GMN records that UK cameras made around a million single-station detections. This is less than in 2022 however the reduction reflects improvements in RMS's ability to reject non-meteoric events and is a positive step.

These data contributed to 84688 orbit solutions in the GMN database (the UK Meteor Network, using the same solver but slightly different criteria, recorded 99600 orbits).

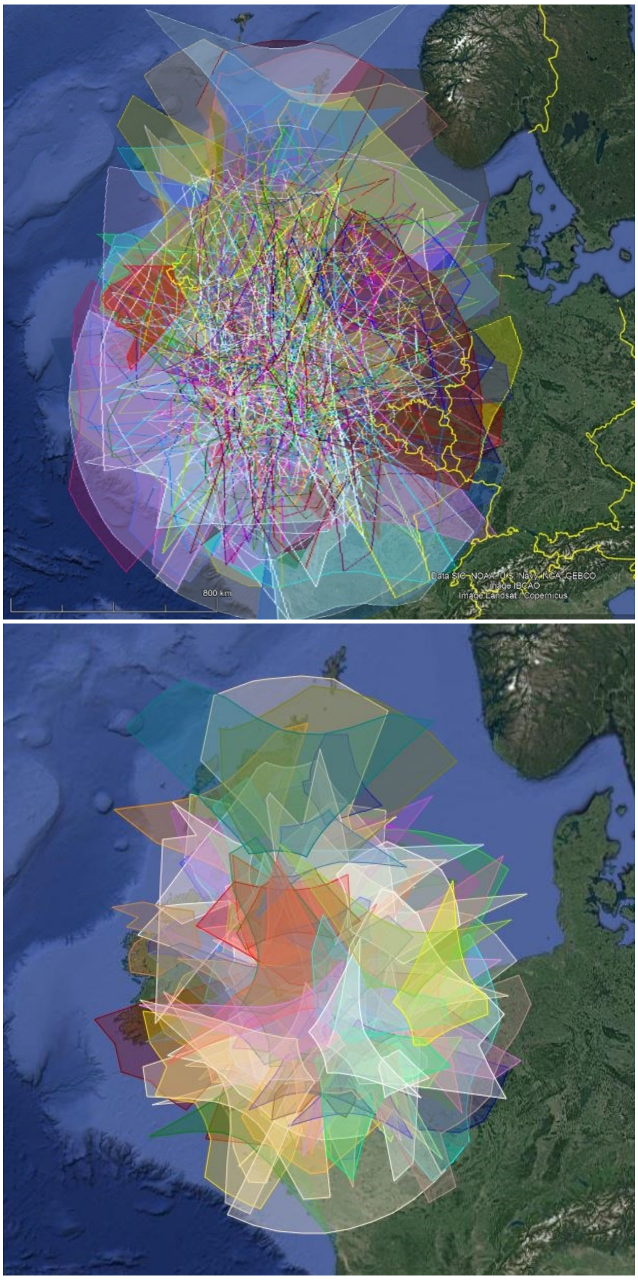

Figure 41 – GMN camera fields in 2023 intersected at 100 km elevation (top), and at 70 km elevation (bottom) for cameras active in the United Kingdom.

Matches were made as far afield as Norway, Germany and France, and on average, each detection involved five cameras, although some detections involved thirty or more cameras and one detection was picked up by 39 cameras.

On the other hand, RMS does occasionally miss earth-grazing and fireball meteors. This highlights the importance of engaging with the camera operators to encourage manual review of their data, whether via the GMN weblog or the UK Meteor Network's live-stream. Several fireballs were spotted by team members or even members of the public who were reviewing these sources and notified us of interesting events. The introduction of the GMN EventViewer tool has proved invaluable in this respect, allowing us to collect data on several fireballs that might otherwise have been missed.

The most interesting event of the year was the detection of 2023CX1, an asteroid that was detected by telescopic observers shortly before entering the atmosphere, and went on to deposit meteorites in Northern France. Several UK cameras detected this bolide, although it was so bright that some cameras were washed out and only three could be used in a solution.

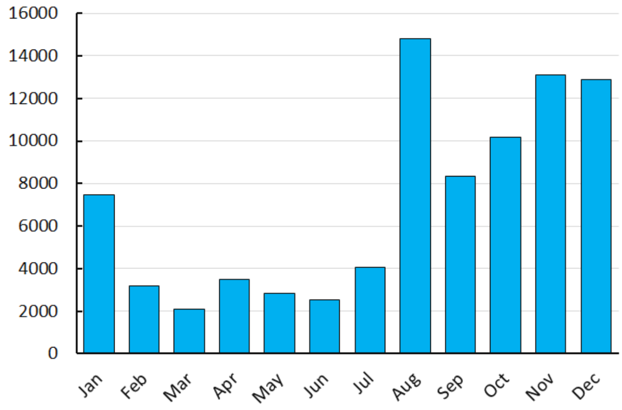

Figure 42 – UK matches in 2023 per month.

Showers

26466 shower meteors were measured in 2023. As in previous years the Perseid and Geminid showers dominate though the other autumn showers are well represented too. The top ten showers are shown in the table below.

Table 2 – Number of meteor shower matches in the UK.

Shower	UK Matches
PER	5393
GEM	4563
ORI	2033
STA	636
LEO	600
NTA	524
HYD	480
COM	359
QUA	298
LYR	206

Fireballs

UK cameras were involved in detection of 43 fireball meteors, the brightest of which was measured at magnitude –11 and occurred on the 30th of December, in addition to asteroid 2023CX1 which was recorded at magnitude –9. Five or six other fireballs may have dropped meteorites however most of these were over water or terrain that was too difficult to search, such as Dartmoor.

Looking Forward

Growth has slowed considerably, although several new cameras have been commissioned in the first three weeks of January 2024, and nearly 10,000 matched events have been recorded.

5.33 United States

The American New Mexico Meteor Array was the pioneering network of the GMN as it started to harvest meteors in December 2018 with six cameras, producing the first 497 orbits for GMN. It remained the only data provider for GMN until May 2019 when the first 3 Croatian cameras started to deliver orbits. At the end of 2019, the number of US cameras had increased to 20 when the network collected 27643 orbits that year. In 2020, the 33 operational cameras in the US collected as many as 50607 orbits. With 72 RMS cameras registering paired meteors in the US, a total of 91901 orbits were obtained in 2021.

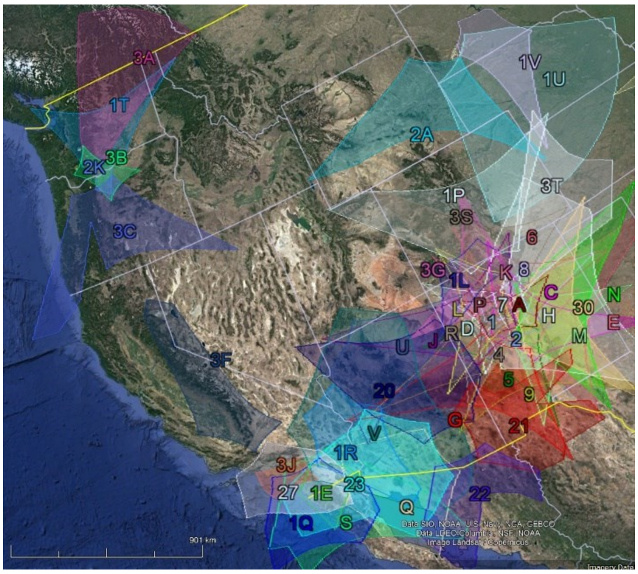

Figure 43 – GMN camera fields in 2023 intersected at 100 km elevation, for cameras in the western part of the USA.

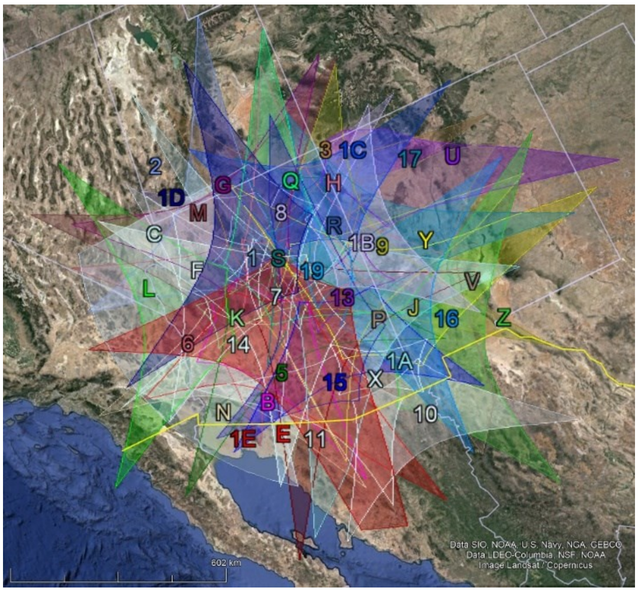

Figure 44 – GMN camera fields in 2023 intersected at 100 km elevation, for cameras of the Lowell Observatory in Arizona.

The number of GMN cameras involved in orbit determinations had increased to 100 in 2022, good for 114054 orbits. 2023 saw a further increase in cameras resulting in 120162 orbits.

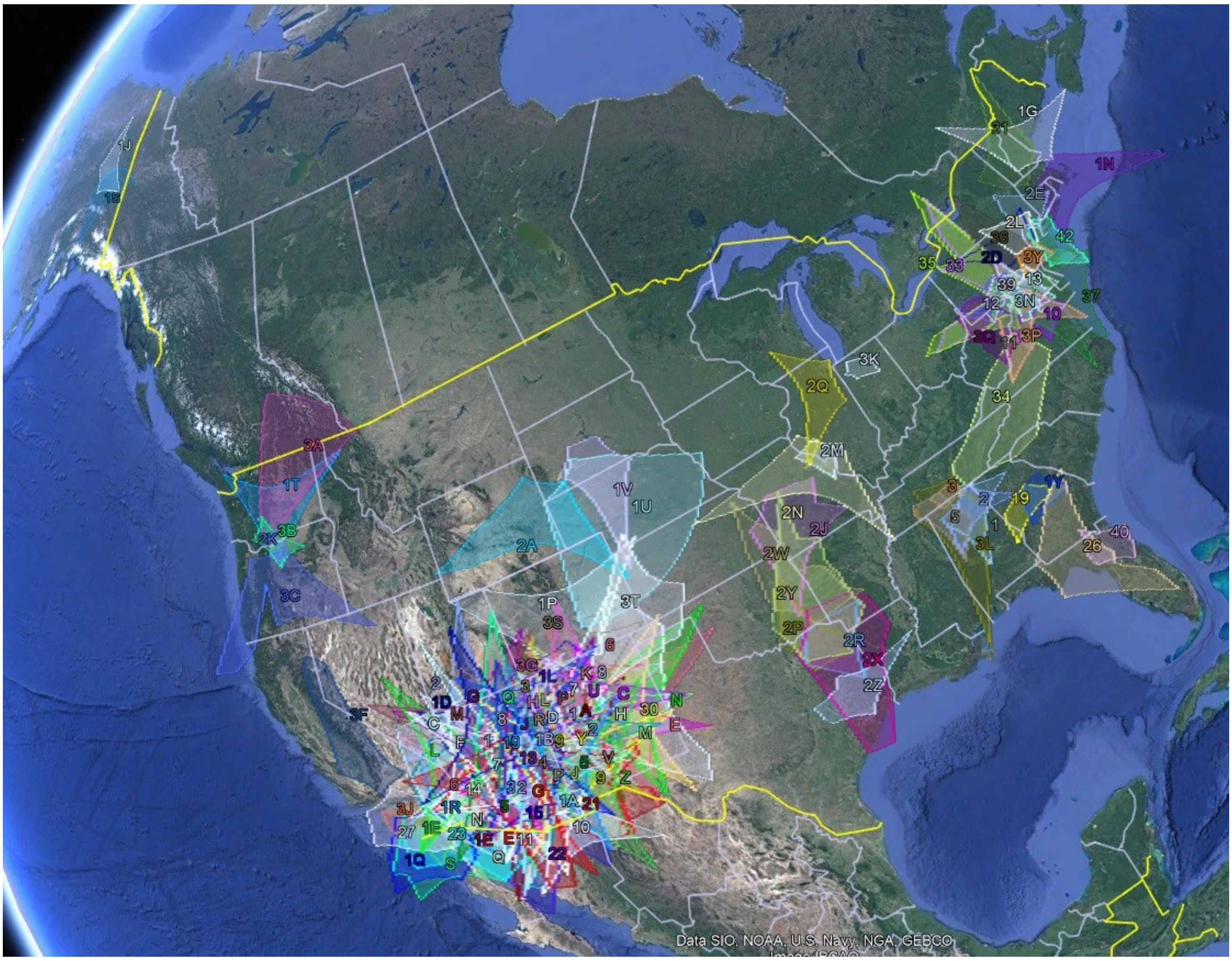

Figure 45 – GMN camera fields intersected at 100 km elevation, global view for cameras installed in the USA, status 2023.

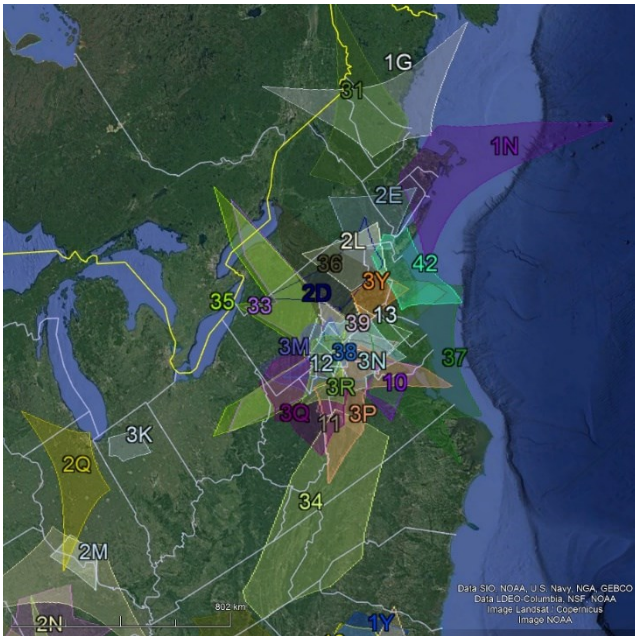

Figure 46 – GMN camera fields in 2023 intersected at 100 km elevation, for cameras in the north-eastern part of the USA.

Figure 45 shows the GMN status like it was at the end of 2023 with 128 GMN cameras in the US, most of which belong to the New Mexico Camera Array and the Lowell Observatory in Arizona. Both networks are independent in neighboring states but have a large overlap. *Figure 44* shows the situation for the Lowell network in Arizona. The Lowell Observatory cameras also benefit coverage from other GMN cameras in the state as well as in California (*Figure 43*).

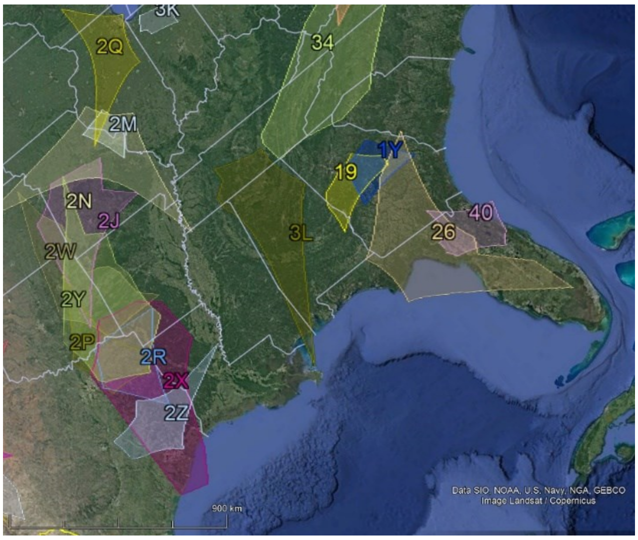

Figure 47 – GMN camera fields in 2023 intersected at 100 km elevation, for cameras in the south-eastern and central parts of the USA.

GMN camera networks are emerging at several other sites in the US (*Figure 45*). The network reaches till Alaska at 65° northern latitude. Several cameras installed near the East Coast, south of the Canadian border connect to the existing GMN network in Canada (*Figure 46*). The maps show where cameras in the US still wait for multi-station partners to set up cameras (*Figure 47*). Details are given in *Tables 5 and 6* for the Lowell network (USL), NASA network (USN) and USV network.

5.34 South Africa

The first two GMN cameras got installed end of 2022 but no paired meteors were obtained then. In 2023 the number of cameras increased to four and the first 200 orbits were obtained in South Africa (*Figure 48*).

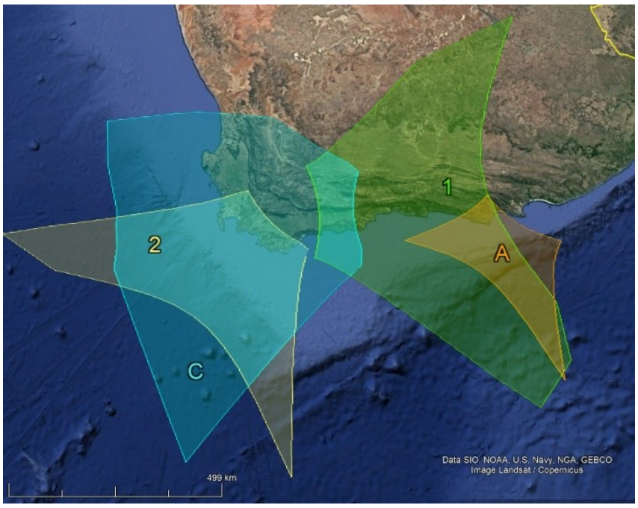

Figure 48 – GMN camera fields in 2023 intersected at 100 km elevation, for cameras active in South Africa.

6 GMN statistics 2023

When a first GMN status report got published, including all data until end October 2020, 140 operational cameras were involved and 144950 orbits had been collected (Roggemans, 2021). Meanwhile, we can compare five years of GMN work. *Figure 49* shows the accumulated number of orbits obtained and the number of contributing cameras during each calendar month. The rapid growth of the Global Meteor Network is obvious. The number of cameras involved in collecting orbits for GMN increased from 390 in 2021 to 700 in 2022 and 1066 at the end of 2023.

Table 3 shows that less than 30% of all orbits are collected during the first six months of each year, while more than 70% is obtained in the period July to December. The fast expansion of the Global Meteor Network also means that more cameras were available towards the end of each year than at the beginning of each year, what also influenced the number of orbits obtained. The most important cause for the difference in number of orbits between the first and last six months is the meteor activity itself. Apart from the most active major meteor showers like the Perseids, Taurids, Orionids, Leonids and Geminids, the overall meteor activity is much higher during the second half of the year. This can be seen very well in *Figure 49* where the blue curve has a much steeper increase each second half of the year.

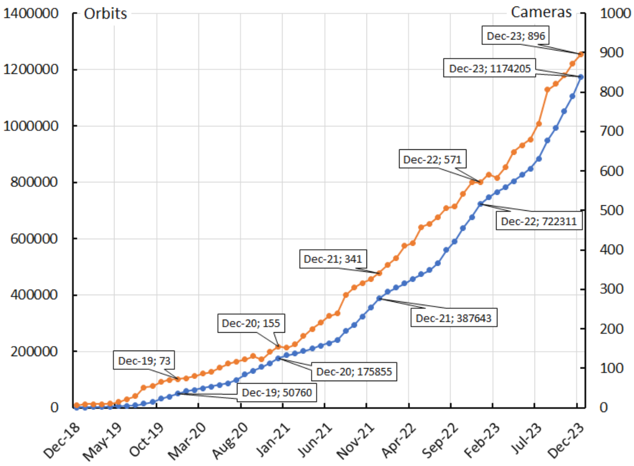

Figure 49 – The accumulated number of orbits (blue) and the actual number of operational cameras involved in triangulations (orange). The numbers at the end of each year are indicated.

Although 1066 different cameras contributed paired meteors during 2023, only 896 or 84% were successfully contributing during December. The explanation is that this report is based on the camera IDs which occur in the orbit dataset and thus successfully recorded paired meteors. Apart from the 896 successful cameras in December there were also a number of cameras functioning without having any paired meteors and thus not listed in the orbit dataset. Persistent unfavorable weather conditions sometimes prevent some cameras from getting paired meteors. A number of cameras struggled with technical issues. For instance, if a camera somehow is moved and has no calibration, no trajectories can be calculated.

Occasionally some hardware or network problem occur, if the connection with the camera board gets lost, the system may ping its camera unsuccessfully until the camera owner fixes the problem. Another hardware problem that is reported now and then is when the sd card crashes and needs replacement.

To prevent loss of valuable observing data, it is strongly recommended to look regularly at the camera status page[24] to check if all cameras report correctly to GMN.

In 2023, 430 new camera IDs contributed paired meteors to GMN, in total 1155 different camera IDs are listed in the orbit dataset, 89 of these camera IDs did not contribute to orbits in 2023, 25 of which didn't appear in the 2022 orbit data. *Table 6* lists the number of cameras active per country for each year since 2018. The number of camera IDs that contributed no camera data in 2023 has been also listed per country. In some cases, old devices were replaced by new, in other cases the camera owner somehow was unable to solve technical issues, had lack of time or lost interest. We know of at least two participants who have died.

[24] https://globalmeteornetwork.org/weblog/

Table 3 – Total number of orbits obtained by the Global Meteor Network cameras per calendar month for each year.

	2018	2019	2020	2021	2022	2023	Tot
January	–	564	7539	9919	23727	23972	65721
February	–	1284	5330	6529	14910	18602	46655
March	–	537	5101	8767	15409	16310	46124
April	–	876	7213	9655	15658	22713	56115
May	–	1242	5654	10217	16951	22050	56114
June	–	1523	5700	7954	13463	23125	51765
July	–	1961	10973	11325	25226	35109	84594
August	–	5387	19422	31292	47300	65155	168556
September	–	6058	14012	21189	29984	44174	115417
October	–	11978	13097	31501	48360	59134	164070
November	–	7710	13228	30381	37895	54030	143244
December	497	11143	17826	33059	45785	67520	175830
Totals	497	50263	125095	211788	334668	451894	1174205

Table 4 – Total number of operational cameras within the Global Meteor Network per calendar month.

	2018	2019	2020	2021	2022	2023	Tot
January	–	9	75	152	363	591	670
February	–	9	80	161	380	583	680
March	–	9	86	182	410	609	719
April	–	10	91	200	418	648	766
May	–	15	101	216	458	665	807
June	–	22	112	232	466	680	834
July	–	29	117	239	483	720	874
August	–	52	122	285	507	806	941
September	–	55	131	304	510	821	980
October	–	65	122	316	542	842	1004
November	–	71	142	326	571	873	1032
December	6	73	155	341	571	896	1067
Totals	6	76	173	390	700	1066	1155

One whose camera continued transmitting data until vegetation obstructed the camera field of view and the family switched off the system.

7 Meteor showers covered by GMN

Using the Working List of Meteor Showers[25] (Jenniskens et al., 2020; Jopek and Kaňuchová, 2017; Jopek and Jenniskens, 2011; Neslušan et al., 2020) as a reference, 425 of the showers listed could be associated with orbits collected by the Global Meteor Network. The number of orbits recorded for each of these showers is listed in *Table 7* for each year since 2018.

The GMN meteor shower association has been based on the table of Sun-centered ecliptic shower radiant positions given in Jenniskens et al. (2018). Many entrees of the Working List of Meteor Showers have no matching orbits in the GMN database yet. Some of the showers are periodic and display only some activity once every few years, some showers have been detected only by radar in a fainter range of magnitudes than what GMN cameras cover and others are known as daylight meteor showers. While GMN is getting better coverage at the southern hemisphere, more of the low declination meteor showers will get covered. For a number of listed meteoroid streams their absence in the GMN orbit database may be explained because the evidence for the existence of the shower could be missing. One of the goals of the GMN project is to help to identify ghost meteor showers that should be removed from the Working List.

[25] https://www.ta3.sk/IAUC22DB/MDC2022/Roje/roje_lista.php?corobic_roje=0&sort_roje=0

Table 5 – Total number of multi-station events contributing to an orbit result, recorded in each country for each year. The list is sorted on the country ID used in the camera ID. Subnetworks for some countries are counted in the grand total for the country.

	2018	2019	2020	2021	2022	2023	Total
Australia (AU)	0	0	0	1871	12460	41887	56218
Belgium (BE)	0	921	5500	8582	23174	25720	63897
Bulgaria (BG)	0	0	0	419	3877	3530	7826
Brazil (BR)	0	0	40	1645	2760	2331	6776
Canada (CA)	0	3599	10815	8809	16232	15023	54478
Canada (CAWE)	0	0	0	0	459	425	884
Canada (CAWT)	0	0	0	0	0	193	193
Switzerland (CH)	0	0	0	3	3439	4352	7794
Czech Republic (CZ)	0	0	163	464	2490	11269	14386
Germany (DE)	0	200	3963	7009	9128	12194	32494
Denmark (DK)	0	0	0	0	55	1386	1441
Spain (ES)	0	0	1207	15113	19301	22610	58231
Finland (FI)	0	0	0	0	41	90	131
France (FR)	0	0	3176	5601	11990	16682	37449
Greece (GR)	0	0	0	0	977	3375	4352
Croatia (HR)	0	12221	35099	38370	31329	27721	144740
Hungary (HU)	0	0	0	0	2114	7872	9986
Ireland (IE)	0	0	120	424	3490	1954	5988
Israel (IL)	0	0	553	2009	975	1096	4633
Italy (IT)	0	862	5384	5447	4943	5064	21700
Japan (JP)	0	0	0	0	0	629	629
South Korea (KR)	0	0	0	0	7711	34044	41755
Luxembourg (LU)	0	0	0	0	622	2018	2640
Mexico (MX)	0	0	0	0	1769	2953	4722
Malasia (MY)	0	0	0	0	50	501	551
Netherlands (NL)	0	278	4337	7605	9139	9421	30780
New Zealand (NZ)	0	0	0	1146	6280	47436	54862
Poland (PL)	0	0	35	67	398	456	956
Portugal (PT)	0	0	0	0	327	3322	3649
Romania (RO)	0	0	0	0	0	417	417
Russia (RU)	0	5715	13438	6208	5437	1992	32790
Slovenia (SI)	0	2753	3999	6001	5887	6789	25429
Slovakia (SK)	0	0	0	37	2026	5535	7598
United Kingdom (UK)	0	0	1889	27430	78652	84688	192659
USA (US)	497	27643	50607	91901	114054	120162	404864
USA (USL)	0	0	2149	51425	79647	64903	198124
USA (USN)	0	0	0	0	0	640	640
USA (USV)	0	0	0	0	3431	2099	5530
Erroneous entry (XX)	0	0	0	8	28	0	36
South Africa (ZA)	0	0	0	0	0	200	200

Table 6 – Total number of operational cameras in each country for each year. Inactive devices and cameras without orbits are not counted. The list is sorted on the country ID used in the camera ID. Subnetworks for some countries are counted in the grand total for the country. The column 2023 (0) lists the number of cameras which had paired meteors before 2023 but did not appear in the 2023 data.

	2018	2019	2020	2021	2022	2023	2023 (0)	Total
Australia (AU)	0	0	0	12	29	67	3	70
Belgium (BE)	0	4	4	10	20	24	1	25
Bulgaria (BG)	0	0	0	2	6	7	2	9
Brazil (BR)	0	0	2	13	20	34	1	35
Canada (CA)	0	11	18	29	58	67	16	83
Canada (CAWE)	0	0	0	0	7	8	0	8
Canada (CAWT)	0	0	0	0	0	8	0	8
Switzerland (CH)	0	0	0	1	5	5	0	5
Czech Republic (CZ)	0	0	3	4	6	20	0	20
Germany (DE)	0	4	10	12	18	19	3	22
Denmark (DK)	0	0	0	0	1	4	0	4
Spain (ES)	0	0	8	23	30	35	1	36
Finland (FI)	0	0	0	0	4	5	0	5
France (FR)	0	0	10	14	16	18	7	25
Greece (GR)	0	0	0	0	1	4	0	4
Croatia (HR)	0	23	32	48	45	41	14	55
Hungary (HU)	0	0	0	0	2	3	0	3
Ireland (IE)	0	0	2	3	5	5	1	6
Israel (IL)	0	0	3	6	5	6	2	8
Italy (IT)	0	1	1	5	5	7	0	7
Japan (JP)	0	0	0	0	0	2	0	2
South Korea (KR)	0	0	0	0	47	125	0	125
Luxembourg (LU)	0	0	0	0	1	1	0	1
Mexico (MX)	0	0	0	0	12	15	0	15
Malasia (MY)	0	0	0	0	3	5	1	6
Netherlands (NL)	0	2	11	11	13	14	5	19
New Zealand (NZ)	0	0	0	2	28	111	1	112
Poland (PL)	0	0	1	1	3	2	1	3
Portugal (PT)	0	0	0	0	1	1	0	1
Romania (RO)	0	0	0	0	0	3	0	3
Russia (RU)	0	10	21	21	19	15	12	27
Slovenia (SI)	0	1	1	2	2	6	0	6
Slovakia (SK)	0	0	0	1	3	4	0	4
United Kingdom (UK)	0	0	13	97	191	261	14	275
USA (US)	6	20	33	72	100	128	3	131
USA (USL)	0	0	9	36	47	45	2	47
USA (USN)	0	0	0	0	0	3	0	3
USA (USV)	0	0	0	0	2	2	0	2
Erroneous entry (XX)	0	0	0	1	1	0	1	1
South Africa (ZA)	0	0	0	0	0	4	0	4

Table 7 – Total number of orbits according to the meteor shower association (IAU number + code) for each year.

IAU	Meteor Shower	2018	2019	2020	2021	2022	2023	Total
Spor	Sporadics	188	27834	71186	115900	188413	318794	722315
CAP#1	alpha-Capricornids	0	139	793	641	1563	1840	4976
STA#2	SouthernTaurids	0	1388	1645	3417	5171	3575	15196
SIA#3	Southern iota-Aquariids	0	25	53	61	91	116	346
GEM#4	Geminids	200	2664	7309	12163	17950	19655	59941
SDA#5	Southern delta-Aquariids	0	350	1560	1570	4099	4138	11717
LYR#6	April Lyrids	0	46	733	1044	1431	1451	4705
PER#7	Perseids	0	1809	8615	14711	20480	22003	67618
ORI#8	Orionids	0	2771	3423	6900	12690	10417	36201
DRA#9	October Draconids	0	4	3	10	10	6	33
QUA#10	Quadrantids	3	139	919	1710	2172	1017	5960
EVI#11	eta-Virginids	0	5	102	424	408	82	1021
KCG#12	kappa-Cygnids	0	51	237	2554	305	107	3254
LEO#13	Leonids	0	426	912	1598	2247	2362	7545
URS#15	Ursids	5	134	336	259	560	402	1696
HYD#16	sigma-Hydrids	7	557	778	2116	1994	2737	8189
NTA#17	Northern Taurids	1	963	1332	2476	2803	2397	9972
AND#18	Andromedids	0	61	126	1034	316	216	1753
MON#19	December Monocerotids	12	184	330	791	727	1291	3335
COM#20	Comae Berenicids	17	367	762	925	2183	1686	5940
AVB#21	alpha-Virginids	0	15	155	194	226	368	958
LMI#22	Leonis Minorids	0	109	134	269	451	436	1399
EGE#23	Epsilon Geminids	0	168	198	597	825	624	2412
NOA#25	Northern October delta-Arietids	0	145	170	234	330	437	1316
NDA#26	Northern delta-Aquariids	0	203	687	894	1390	1265	4439
KSE#27	kappa-Serpentids	0	3	17	45	46	54	165
SOA#28	Southern October delta-Arietids	0	180	324	663	354	576	2097
ETA#31	eta-Aquariids	0	218	647	1607	2961	2575	8008
NIA#33	Northern iota-Aquariids	0	108	187	292	351	382	1320
ZCY#40	zeta-Cygnids	0	32	362	607	829	347	2177
DLI#47	mu-Virginids	0	7	99	73	203	205	587
TAH#61	tau-Herculids	0	0	0	1	1241	1	1243
GDE#65	gamma-Delphinids	0	1	5	22	27	36	91
SSG#69	Southern mu-Sagittariids	0	31	87	113	161	354	746
SLY#81	September Lyncids	0	15	98	149	101	197	560
ODR#88	omicron-Draconids	0	4	20	21	53	31	129
PVI#89	January pi-Virginids	0	1	41	114	189	105	450
NCC#96	Northern delta-Cancrids	1	45	153	197	451	204	1051
SCC#97	Southern delta-Cancrids	1	81	223	227	584	272	1388
PIH#101	pi-Hydrids	0	152	272	533	919	649	2525
ACE#102	alpha-Centaurids	0	0	0	0	39	40	79
BTU#108	beta-Tucanids	0	0	0	0	0	28	28
AAN#110	alpha-Antliids	0	3	26	19	94	48	190
DME#130	delta-Mensids	0	0	0	0	3	57	60
ELY#145	eta-Lyrids	0	10	63	202	265	181	721
NOP#149	Northern May Ophiuchids	0	7	25	23	24	61	140
SOP#150	Southern May Ophiuchids	0	3	22	44	21	70	160

IAU	Meteor Shower	2018	2019	2020	2021	2022	2023	Total
EAU#151	epsilon-Aquilids	0	15	71	74	123	303	586
NOC#152	Northern Daytime omega-Cetids	0	2	4	7	9	12	34
SSC#161	Southern omega-Scorpiids	0	9	5	27	16	50	107
NZC#164	Northern June Aquilids	0	143	602	617	1321	1005	3688
SZC#165	Southern June Aquilids	0	32	108	131	324	408	1003
JBO#170	June Bootids	0	0	5	3	36	5	49
ARI#171	Daytime Arietids	0	6	19	34	40	46	145
JPE#175	July Pegasids	0	43	254	351	690	669	2007
PHE#176	July Phoenicids	0	2	1	24	109	221	357
OCY#182	omicron-Cygnids	0	1	19	19	36	34	109
PAU#183	Piscis Austrinids	0	9	55	73	89	104	330
GDR#184	July gamma-Draconids	0	10	140	84	214	127	575
EUM#186	epsilon-Ursae Majorids	0	1	12	5	21	22	61
PCA#187	psi-Cassiopeiids	0	11	45	63	127	80	326
XRI#188	Daytime xi-Orionids	0	0	1	0	0	0	1
BPE#190	beta-Perseids	0	11	52	60	174	75	372
ERI#191	eta-Eridanids	0	88	232	321	596	642	1879
UCE#194	upsilon-Cetids	0	51	108	168	320	272	919
BIN#195	beta-Indids	0	0	1	6	5	0	12
AUD#197	August Draconids	0	176	464	582	806	714	2742
AUR#206	Aurigids	0	58	152	259	336	157	962
SPE#208	September epsilon-Perseids	0	196	422	813	854	833	3118
BAU#210	beta-Aurigids	0	84	267	304	512	340	1507
KLE#212	Daytime kappa-Leonids	0	2	4	10	8	24	48
NPI#215	Northern delta-Piscids	0	71	120	138	254	237	820
SPI#216	Southern delta-Piscids	0	20	47	38	79	175	359
NDR#220	nu-Draconids	0	39	123	125	157	169	613
DSX#221	Daytime Sextantids	0	7	4	27	46	34	118
SOR#225	sigma-Orionids	0	71	114	228	364	310	1087
XDR#242	xi-Draconids	0	33	60	165	158	136	552
ZCN#243	zeta-Cancrids	0	2	2	13	10	26	53
NHD#245	November Hydrids	0	13	39	127	101	131	411
AMO#246	alpha-Monocerotids	0	25	30	41	81	80	257
NOO#250	November Orionids	1	396	489	1340	1590	953	4769
ALY#252	alpha-Lyncids	0	2	5	9	15	8	39
CMI#253	December Canis Minorids	1	65	96	166	320	189	837
ORN#256	Northern chi-Orionids	8	172	185	380	560	423	1728
ORS#257	Southern chi-Orionids	3	279	385	759	1066	971	3463
OCT#281	October Camelopardalids	0	27	11	57	159	55	309
FTA#286	omega-Taurids	0	51	39	89	295	206	680
DSA#288	Southern December delta-Arietids	3	46	69	74	228	259	679
DNA#289	Northern December delta-Arietids	0	20	23	144	113	96	396
TPU#307	tau-Puppids	0	1	0	6	12	31	50
PIP#308	January pi-Puppids	1	28	32	62	119	108	350
MVE#318	mu-Velids	0	15	27	52	96	107	297
JLE#319	January Leonids	0	0	9	7	25	13	54
OSE#320	omega-Serpentids	0	1	1	2	1	0	5
LBO#322	lambda-Bootids	0	0	6	16	40	56	118

IAU	Meteor Shower	2018	2019	2020	2021	2022	2023	Total
XCB#323	xi-Coronae Borealids	0	0	26	48	69	65	208
EPR#324	epsilon-Perseids	0	1	13	3	13	17	47
EPG#326	epsilon-Pegasids	0	12	63	94	127	59	355
SSE#330	sigma-Serpentids	0	2	3	0	8	4	17
AHY#331	alpha-Hydrids	1	30	100	130	367	62	690
OCU#333	October Ursae Majorids	0	51	72	182	194	295	794
DAD#334	December alpha-Draconids	5	271	419	1068	1139	606	3508
XVI#335	December chi-Virginids	1	68	95	145	207	289	805
DKD#336	December kappa-Draconids	1	129	54	385	182	423	1174
NUE#337	nu-Eridanids	0	403	786	1543	2290	1849	6871
OER#338	omicron-Eridanids	0	243	272	612	779	718	2624
PSU#339	psi-Ursae Majorids	0	45	37	178	105	150	515
TPY#340	theta-Pyxidids	2	41	74	114	256	194	681
XUM#341	January xi-Ursae Majorids	0	0	28	40	66	133	267
HVI#343	h-Virginids	0	18	189	28	29	7	271
FHE#345	f-Herculids	0	2	31	69	134	49	285
XHE#346	x-Herculids	0	6	50	100	152	84	392
BPG#347	beta-Pegasids	0	0	1	8	5	5	19
ARC#348	April rho-Cygnids	0	12	92	112	262	205	683
LLY#349	lambda-Lyrids	0	0	3	7	8	6	24
JMC#362	June mu-Cassiopeiids	0	9	37	92	111	44	293
PPS#372	phi-Piscids	0	111	572	662	1601	952	3898
ALN#376	August Lyncids	0	4	11	22	34	45	116
OLP#384	October Leporids	0	24	21	64	72	74	255
OBC#386	October beta-Camelopardalids	0	37	49	93	196	115	490
CTA#388	chi-Taurids	0	145	141	439	481	288	1494
THA#390	November theta-Aurigids	3	50	107	193	254	693	1300
NDD#391	November delta-Draconids	0	2	2	13	6	0	23
NID#392	November i-Draconids	0	37	76	167	138	126	544
ACA#394	alpha-Canis Majorids	1	35	26	75	124	107	368
GCM#395	gamma-Canis Majorids	2	34	65	61	157	132	451
GUM#404	gamma-Ursae Minorids	0	0	35	29	84	162	310
DPI#410	delta-Piscids	0	3	12	17	59	98	189
CAN#411	c-Andromedids	0	31	222	317	632	439	1641
SIC#416	September iota-Cassiopeiids	0	5	46	76	54	82	263
SOL#424	September-October Lyncids	0	29	99	127	297	178	730
FED#427	February eta-Draconids	0	1	7	5	31	11	55
DSV#428	December sigma-Virginids	5	87	194	337	602	395	1620
ACB#429	alpha-Coronae Borealids	0	6	28	21	132	115	302
JIP#431	June iota-Pegasids	0	3	17	10	67	106	203
ZCS#444	zeta-Cassiopeiids	0	34	193	330	531	624	1712
KUM#445	kappa-Ursae Majorids	0	30	81	192	153	154	610
DPC#446	December phi-Cassiopeiids	0	24	17	102	86	40	269
AAL#448	April alpha-Librids	0	2	11	14	30	52	109
AED#450	April epsilon-Delphinids	0	3	26	42	60	49	180
CAM#451	Camelopardalids	0	4	1	2	6	6	19
MPS#456	May psi-Scorpiids	0	57	159	259	351	390	1216
JEC#458	June epsilon-Cygnids	0	5	44	74	48	128	299

IAU	Meteor Shower	2018	2019	2020	2021	2022	2023	Total
JEO#459	June epsilon-Ophiuchids	0	41	16	3	43	110	213
LOP#460	lambda-Ophiuchids	0	0	0	3	0	0	3
AXC#465	August xi-Cassiopeiids	0	7	31	74	116	96	324
AOC#466	August omicron-Cetids	0	0	15	30	34	52	131
LAQ#473	lambda-Aquariids	0	16	34	36	58	104	248
ICE#476	iota-Cetids	0	9	38	27	34	60	168
TCA#480	tau-Cancrids	0	131	149	395	634	439	1748
NZP#486	November zeta-Perseids	0	11	30	26	76	43	186
NSU#488	November sigma-Ursae Majorids	0	13	21	25	59	45	163
DEL#494	December Lyncids	0	39	59	207	170	169	644
DAB#497	December alpha-Bootids	0	4	15	23	51	52	145
FPL#501	February pi-Leonids	0	1	31	51	43	52	178
DRV#502	December rho-Virginids	2	58	81	186	235	173	735
AIC#505	August iota-Cetids	0	69	186	262	439	439	1395
FEV#506	February epsilon-Virginids	0	14	127	196	478	360	1175
UAN#507	upsilon-Andromedids	0	25	121	170	434	211	961
JRC#510	June rho-Cygnids	0	1	19	54	64	98	236
RPU#512	rho-Puppids	0	17	53	71	96	185	422
OMC#514	omega-Capricornids	0	0	18	24	48	120	210
OLE#515	omicron-Leonids	0	31	73	138	278	189	709
FMV#516	February mu-Virginids	0	6	81	90	208	116	501
ALO#517	April lambda-Ophiuchids	0	1	5	29	52	30	117
AHE#518	April 102-Herculids	0	1	13	4	20	27	65
BAQ#519	beta-Aquariids	0	8	12	41	79	31	171
MBC#520	May beta-Capricornids	0	5	23	44	41	90	203
AGC#523	August gamma-Cepheids	0	31	94	133	270	103	631
LUM#524	lambda-Ursae Majorids	0	19	14	91	135	35	294
SLD#526	Southern lambda-Draconids	0	18	26	104	93	92	333
EHY#529	eta-Hydrids	4	88	144	315	390	473	1414
ECV#530	eta-Corvids	0	6	45	83	206	211	551
GAQ#531	gamma-Aquilids	0	11	43	107	120	94	375
JXA#533	July xi-Arietids	0	15	61	90	191	212	569
THC#535	theta-Cetids	0	0	4	9	18	29	60
FSO#536	47-Ophiuchids	0	1	1	2	5	0	9
TTB#543	22-Bootids	0	4	7	7	19	16	53
JNH#544	January nu-Hydrids	0	3	25	17	81	20	146
XCA#545	xi-Cassiopeiids	0	2	6	9	36	13	66
FTC#546	43-Cassiopeiids	0	17	86	95	115	149	462
KAP#547	kappa-Perseids	0	92	368	564	1083	689	2796
FAN#549	49-Andromedids	0	5	75	79	152	156	467
PSO#552	pi6-Orionids	0	61	183	388	471	361	1464
OCP#555	October gamma-Camelopardalids	0	23	32	83	148	85	371
PTA#556	phi-Taurids	0	16	13	65	110	81	285
SFD#557	64-Draconids	0	100	125	309	344	191	1069
MCB#559	beta-Canis Majorids	0	10	18	28	56	42	154
SSX#561	6-Sextantids	1	10	33	40	94	64	242
DOU#563	December omega-Ursae Majorids	3	38	59	46	171	88	405
SUM#564	61-Ursae Majorids	0	14	23	17	53	23	130

IAU	Meteor Shower	2018	2019	2020	2021	2022	2023	Total
OHY#569	omicron-Hydrids	0	16	48	65	225	225	579
FBH#570	February beta-Herculids	0	6	19	16	81	48	170
TSB#571	26-Bootids	0	1	11	14	31	28	85
SAU#575	63-Aurigids	0	7	19	23	40	60	149
CHA#580	chi-Andromedids	0	16	53	37	120	67	293
NHE#581	90-Herculids	0	11	103	166	235	190	705
JBC#582	January beta-Craterids	0	3	23	49	108	80	263
GCE#584	Cepheids-Cassiopeiids	0	22	56	86	153	102	419
THY#585	33-Hydrids	1	9	24	38	78	73	223
FNC#587	59-Cygnids	0	6	18	33	60	25	142
FCA#589	50-Cancrids	0	13	38	66	115	62	294
VCT#590	10-CanumVenaticids	0	1	5	2	9	5	22
ZBO#591	zeta-Bootids	0	3	30	40	69	49	191
PON#592	91-Piscids	0	3	9	16	24	39	91
TOL#593	28-Lyncids	0	17	26	80	96	126	345
RSE#594	Serpentids-Coronae Borealids	0	0	3	2	3	27	35
POS#599	72-Ophiuchids	0	8	96	190	351	173	818
ICT#601	iota-Craterids	1	4	5	7	17	28	62
KCR#602	kappa-Craterids	0	0	5	27	51	37	120
FAR#608	14-Aurigids	0	4	14	35	39	64	156
TLY#613	31-Lyncids	0	5	19	90	61	104	279
THD#618	12-Hydrids	0	1	5	7	26	12	51
XCS#623	xi2-Capricornids	0	33	123	134	309	814	1413
XAR#624	xi-Arietids	0	214	330	288	676	523	2031
LTA#625	lambda-Taurids	0	43	123	98	298	492	1054
LCT#626	lambda-Cetids	0	171	53	340	563	42	1169
NPS#627	nu-Piscids	0	79	37	239	293	122	770
STS#628	s-Taurids	0	175	134	415	3472	258	4454
ATS#629	A2-Taurids	0	126	170	220	464	706	1686
TAR#630	tau-Arietids	0	183	164	611	521	537	2016
DAT#631	delta-Arietids	0	192	63	449	656	227	1587
NET#632	November eta-Taurids	0	54	138	344	141	774	1451
PTS#633	p-Taurids	2	75	52	172	172	401	874
TAT#634	tau-Taurids	0	150	256	267	682	606	1961
ATU#635	A1-Taurids	0	67	388	665	337	1090	2547
MTA#636	m-Taurids	0	59	25	177	112	182	555
FTR#637	f-Taurids	0	69	95	236	515	663	1578
DZT#638	December zeta-Taurids	2	10	11	37	40	97	197
AOA#640	August omicron-Aquariids	0	123	413	479	768	1117	2900
DRG#641	December rho-Geminids	0	1	10	4	5	0	20
JLL#644	January lambda-Leonids	1	39	60	83	147	231	561
BCO#647	beta-Comae Berenicids	0	10	61	114	137	82	404
TAL#648	22-Aquilids	0	18	188	265	478	317	1266
OAV#651	68-Virginids	0	27	65	144	237	385	858
OSP#652	omicron-Serpentids	0	4	18	35	48	36	141
RLY#653	R-Lyrids	0	6	63	67	155	71	362
APC#655	April phi-Capricornids	0	1	2	3	6	29	41
GSG#657	gamma-Sagittariids	0	1	6	16	13	27	63

IAU	Meteor Shower	2018	2019	2020	2021	2022	2023	Total
EDR#658	epsilon-Draconids	0	2	27	35	54	19	137
EPS#660	epsilon-Scorpiids	0	3	21	50	36	61	171
OTH#661	110-Herculids	0	1	17	35	49	25	127
MXA#664	May xi-Aurigids	0	0	0	1	1	0	2
MUC#665	May upsilon-Cygnids	0	3	30	42	55	64	194
JMP#668	June mu-Pegasids	0	2	20	22	41	52	137
MCY#671	mu-Cygnids	0	0	5	11	22	9	47
HNJ#672	June 9-Herculids	0	2	5	22	11	0	40
FCL#677	43-Camelopardalids	0	0	0	5	4	0	9
MUA#679	mu-Aquariids	0	10	19	41	53	56	179
JEA#680	June epsilon-Arietids	0	7	10	13	24	22	76
OAQ#681	omicron-Aquariids	0	4	19	21	28	48	120
JTS#683	June theta-Serpentids	0	0	8	6	4	20	38
JPS#685	June beta-Pegasids	0	3	11	5	38	37	94
JRD#686	June rho-Draconids	0	1	3	8	20	26	58
KDP#687	kappa-Delphinids	0	1	7	4	5	8	25
TAC#689	tau-Capricornids	0	17	64	46	151	160	438
ZCE#691	zeta-Cetids	0	1	2	20	42	15	80
EQA#692	epsilon-Aquariids	0	32	165	331	518	159	1205
ANP#693	August nu-Perseids	0	23	55	93	200	147	518
OMG#694	omicron-Geminids	0	59	130	219	317	217	942
APA#695	August psi-Aurigids	0	9	13	12	36	34	104
OAU#696	omicron-Aurigids	0	8	30	41	73	79	231
AET#698	August eta-Taurids	0	4	40	47	84	81	256
BCE#701	beta-Cepheids	0	2	10	8	23	37	80
ASP#702	August 78-Pegasids	0	1	9	7	13	13	43
OAN#704	omicron-Andromedids	0	53	191	281	408	197	1130
ZPI#706	zeta-Piscids	0	28	59	110	162	174	533
BPX#707	beta-Pyxidids	0	0	1	3	16	15	35
RLM#708	R-Leonis Minorids	0	0	2	18	32	46	98
FDC#712	February delta-Cygnids	0	3	16	14	28	21	82
CCR#713	chi-Cancrids	0	2	12	10	17	25	66
RPI#714	rho-Piscids	0	56	120	167	318	181	842
ACL#715	alpha-Camelopardalids	0	145	363	641	945	557	2651
OCH#716	October chi-Andromedids	0	43	56	145	213	109	566
NGB#720	November gamma-Bootids	0	8	3	19	21	16	67
DAS#721	December alpha-Sextantids	0	12	10	42	25	23	112
FLE#722	15-Leonids	0	16	16	73	49	45	199
LAP#724	lambda-Piscids	0	0	0	0	1	0	1
DEG#726	December epsilon-Geminids	3	15	35	6	81	76	216
ISR#727	iota-Serpentids	1	4	6	1	19	6	37
PGE#728	phi-Geminids	0	8	8	5	35	26	82
DCO#729	delta-Corvids	0	2	10	3	17	13	45
ATV#730	April theta-Virginids	0	1	11	3	7	7	29
FGV#732	February gamma-Virginids	0	4	17	24	43	41	129
MOC#734	March omicron-Cygnids	0	1	14	15	18	11	59
XIP#736	xi-Perseids	0	2	6	14	33	27	82
FNP#737	59-Perseids	0	2	7	11	30	4	54

IAU	Meteor Shower	2018	2019	2020	2021	2022	2023	Total
RER#738	rho-Eridanids	0	1	11	28	46	78	164
LAR#739	lambda-Arietids	0	3	12	31	61	36	143
OSD#745	October 6-Draconids	0	22	41	81	128	83	355
EVE#746	e-Velids	0	19	24	202	373	942	1560
JKL#747	January kappa-Leonids	0	13	44	87	192	52	388
JTL#748	January theta-Leonids	0	6	32	44	176	92	350
NMV#749	North. March gamma-Virginids	0	13	84	113	193	0	403
SMV#750	South. March gamma-Virginids	0	20	122	178	358	229	907
KCE#751	kappa-Cepheids	0	38	83	91	150	87	449
AAC#752	April alpha-Capricornids	0	0	0	0	2	0	2
MID#755	May iota-Draconids	0	0	5	8	19	6	38
CCY#757	chi-Cygnids	0	19	508	48	56	47	678
VOL#758	Volantids	0	0	0	2	0	0	2
ZPH#768	zeta-Phoenicids	0	0	0	0	11	0	11
SCO#771	sigma-Columbids	0	1	0	4	8	27	40
ILU#783	iota-Lupids	0	0	1	0	3	0	4
KVE#784	kappa-Velids	0	0	5	43	155	99	302
TCD#785	theta-Carinids	0	0	0	10	53	75	138
SXP#786	6-Puppids	0	2	4	1	15	10	32
MBE#792	March beta-Equuleids	0	0	0	2	3	6	11
KCA#793	kappa-Cancrids	0	0	8	6	28	14	56
SED#796	September epsilon-Draconids	0	19	9	62	97	34	221
EGR#797	epsilon-Gruids	0	0	0	4	17	0	21
ADS#802	June Aquariids	0	2	14	15	29	46	106
LSA#803	lambda-Sagittariids	0	5	11	43	68	69	196
FLO#807	February Leonids	0	11	100	130	176	126	543
XCD#810	October Cetids	0	29	16	57	116	62	280
NAA#812	November alpha-Aurigids	0	6	19	22	36	64	147
CVD#814	January Canum Venaticids	0	1	11	9	55	48	124
UMS#815	August Ursae Majorids	0	1	10	9	20	16	56
CVT#816	February Canum Venaticids	0	2	15	19	34	23	93
OAG#818	October Aurigids	0	9	11	13	24	30	87
NUT#822	nu-Taurids	0	0	4	9	19	52	84
FCE#823	56-Cetids	0	14	33	39	82	85	253
DEX#824	December Sextantids	0	2	16	12	34	45	109
XIE#825	xi-Eridanids	0	10	11	22	19	69	131
ILI#826	iota1-Librids	0	9	52	60	134	126	381
NPE#827	nu-Pegasids	0	1	17	25	42	52	137
TPG#828	31-Pegasids	0	0	1	1	3	0	5
JSP#829	July 77-Pegasids	0	6	19	28	43	113	209
SCY#830	63-Cygnids	0	3	40	24	69	46	182
GPG#831	gamma-Pegasids	0	4	9	21	33	44	111
LEP#832	Leporids	0	4	5	9	29	27	74
KOR#833	kappa-Orionids	0	10	8	20	37	34	109
ACU#834	April theta-Centaurids	0	1	1	6	5	9	22
JDP#835	June delta-Pavonids	0	0	0	1	0	0	1
ABH#836	April beta-Herculids	0	0	2	7	18	22	49
CAE#837	Caelids	0	2	0	2	20	30	54

IAU	Meteor Shower	2018	2019	2020	2021	2022	2023	Total
ODS#838	October delta-Sextantids	0	2	0	5	2	0	9
PSR#839	phi-Serpentids	0	1	9	19	21	29	79
TER#840	Tau4-Eridanids	0	0	4	9	3	17	33
DHE#841	delta-Herculids	0	1	7	26	58	25	117
CRN#842	A-Carinids	0	0	0	6	27	0	33
DMD#843	December mu-Draconids	1	9	9	9	21	13	62
DTP#844	December theta-Pyxidids	0	17	8	60	42	61	188
OEV#845	October eta-Virginids	0	0	1	1	0	0	2
TSC#846	tau-Sculptorids	0	0	0	0	2	0	2
BEL#847	beta-Leonids	0	4	1	15	12	12	44
OPE#848	omicron-Perseids	0	2	5	4	11	8	30
SZE#849	September zeta-Eridanids	0	1	15	19	23	48	106
MBA#850	May beta-Aquariids	0	0	2	8	7	0	17
BEC#851	beta-Carinids	0	0	0	0	1	0	1
AST#852	alpha-Sculptorids	0	0	0	0	5	0	5
ZPA#853	zeta-Pavonids	0	0	0	0	3	0	3
PCY#854	psi-Cygnids	0	3	28	49	98	69	247
ATD#855	August tau-Draconids	0	0	3	11	9	18	41
EMO#856	epsilon-Monocerotids	0	6	12	14	29	17	78
EVO#857	eta-Volantids	0	0	0	0	1	0	1
FPB#858	February phi-Bootids	0	8	34	36	163	81	322
MTB#859	March12-Bootids	0	2	8	22	49	21	102
PAN#860	psi-Andromedids	0	0	4	14	32	22	72
JXS#861	June xi1-Sagittariids	0	3	7	3	7	33	53
SSR#862	16-Scorpiids	0	1	12	28	62	48	151
TLR#863	12-Lacertids	0	0	5	12	13	26	56
JSG#864	June 66-Pegasids	0	0	1	9	9	20	39
JES#865	June epsilon-Serpentids	0	4	5	6	16	25	56
ECB#866	epsilon-Coronae Borealids	0	2	7	12	12	6	39
FPE#867	52-Pegasids	0	3	8	3	38	17	69
PSQ#868	psi3-Aquariids	0	1	4	2	8	23	38
UCA#869	upsilon1-Cassiopeiids	0	0	16	8	28	29	81
JPG#870	July eta-Pegasids	0	0	12	9	13	10	44
DCD#871	delta-Cepheids	0	0	6	5	11	11	33
ETR#872	epsilon-Triangulids	0	1	10	15	29	39	94
OMI#873	omicron-Cetids	0	3	7	12	18	21	61
PXS#874	September xi-Perseids	0	8	36	38	60	113	255
TEI#875	tau9-Eridanids	0	12	11	25	40	24	112
ROR#876	rho-Orionids	0	9	11	15	35	43	113
OHD#877	omega-Hydrids	0	6	9	26	29	41	111
OEA#878	October epsilon-Aurigids	0	3	4	4	8	23	42
ATI#879	alpha-Taurids	0	6	8	26	39	58	137
YDR#880	Y-Draconids	0	16	22	45	74	50	207
TLE#881	theta-Leonids	0	3	1	15	17	9	45
PLE#882	phi-Leonids	0	3	8	9	14	20	54
NMD#883	November mu-Draconids	0	1	6	3	0	0	10
NBP#884	November beta-Pyxidids	0	0	3	2	17	29	51
DEV#885	December epsilon-Virginids	0	4	12	8	20	16	60

IAU	Meteor Shower	2018	2019	2020	2021	2022	2023	Total
ACV#886	alpha-Corvids	2	2	7	18	63	24	116
DZB#887	December zeta-Bootids	0	7	12	10	23	13	65
SCV#888	6-Corvids	0	0	2	7	8	21	38
YOP#889	Y-Ophiuchids	0	0	1	2	8	6	17
ESU#890	eta-Scutids	0	1	3	5	8	10	27
FSL#891	February sigma-Leonids	0	6	30	29	90	44	199
MCN#892	March Centaurids	0	0	0	3	9	5	17
EOP#893	eta-Ophiuchids	0	0	21	37	59	71	188
JMD#894	June mu-Draconids	0	3	18	25	21	0	67
OAB#895	October alpha-Comae Berenicids	0	0	0	1	3	0	4
OTA#896	130-Taurids	0	8	20	12	48	61	149
OUR#897	October alpha-UrsaeMinorids	0	9	2	22	27	10	70
SGP#898	September gamma-Piscids	0	5	12	24	10	30	81
EMC#899	epsilon-Microscopiids	0	1	0	5	20	29	55
BBO#900	beta-Bootids	0	2	28	61	173	44	308
TLC#901	34-Lyncids	0	1	5	5	15	21	47
DCT#902	delta-Cetids	0	11	18	30	48	86	193
OAT#903	October alpha-Triangulids	0	8	13	9	25	35	90
OCO#904	omicron-Columbids	0	2	4	13	6	50	75
MXD#905	March xi-Draconids	0	0	4	8	6	11	29
ETD#906	eta-Draconids	0	4	26	22	59	27	138
MCE#907	mu-Cepheids	0	0	8	19	27	17	71
SEC#909	September epsilon-Columbids	0	0	1	6	6	0	13
BTC#910	beta2-Cygnids	0	3	30	24	63	26	146
TVU#911	21-Vulpeculids	0	3	18	39	75	49	184
BCY#912	beta-Cygnids	0	0	30	58	77	46	211
FVI#913	41-Virginids	0	0	0	0	1	0	1
AGE#914	alpha-Geminids	0	0	3	0	2	0	5
DNO#915	delta-Normids	0	0	0	2	2	41	45
ATH#916	April 21-Herculids	0	0	0	0	4	0	4
OVI#917	omicron-Virginids	0	1	1	2	1	0	5
TAG#918	theta-Aurigids	0	4	7	14	32	18	75
ICN#919	iota-Centaurids	0	0	1	1	3	17	22
XSC#920	xi-Scorpiids	0	5	10	28	47	53	143
JLC#921	July lambda-Capricornids	0	3	21	8	27	27	86
PPE#922	August phi-Pegasids	0	1	2	2	9	0	14
FBO#923	15-Bootids	0	0	1	1	5	0	7
SAN#924	62-Andromedids	0	1	3	21	5	26	56
EAN#925	eta-Andromedids	0	3	3	3	15	23	47
OMH#926	October mu-Hydrids	0	0	0	1	2	0	3
OCR#1033	omega-Carinids	0	0	0	0	0	6	6
ARD#1130	Arids	0	0	0	6	0	1	7
OZP#1131	October zeta-Perseids	0	0	0	14	8	0	22
	Totals	497	50263	125095	211788	334668	451894	1174205

Table 7 serves as an inventory of what the GMN orbit database has available until end 2023. Of course, the number of shower members detected depends on the criteria used to associate a meteor with a known meteor shower radiant. The GMN shower association criterion assumes that meteors within 1° in solar longitude, within 3° in radiant, and within 10% in geocentric velocity of a shower reference location are members of that shower. Further details about the shower association are explained in Moorhead et al. (2020). This is a rather strict criterion since meteor showers often have a larger dispersion in radiant position and velocity. Therefore, using the orbit similarity criteria (Drummond, 1981; Southworth and Hawkins, 1963; Jopek, 1993) will certainly detect more shower candidates but at the risk of including sporadic orbits that fulfil similarity criteria by pure chance.

In 2023 Global Meteor Network detected some new meteor showers and contributed data about poorly known new meteor showers. The growing coverage of GMN cameras in Australia and New Zealand confirmed the unusual activity of the omega-Carinids in 2023 (Šegon et al., 2023a). In January 2023 two new meteor shower were discovered, one in Draco (Šegon et al., 2023b) and one in Bootes (Šegon et al., 2023c). GMN also confirmed the enhanced activity of the February Hydrids (FHY#1032) in 2023 (Jenniskens, 2023a). In May 2023 a possible new meteor shower was discovered in Sagitta (Šegon et al., 2023d). In December 2023, GMN recorded the first meteors from comet 46P/Wirtanen, confirming the predictions of theoretical models (Roggemans et al., 2023b).

More information and detailed documentation about meteor showers can be found in the new reference work "Atlas of Earth's Meteor Showers" that appeared in October 2023 (Jenniskens, 2023b).

The main goal of the GMN, not to let any meteor shower activity pass unnoticed is being achieved. Whenever some unexpected meteor activity occurs, the Global Meteor Network has good chances to cover it.

Acknowledgment

This report is based on the data of the Global Meteor Network which is released under the CC BY 4.0 license[26]. We thank all the participants in the Global Meteor Network project for their contribution and perseverance, operators whose cameras provided the data used in this work and contributors who made important code contributions The Global Meteor Network results were obtained thanks to the efforts of the following volunteers (list cut-off date as it was at the end of 2023):

Adam Mullins, Aden Walker, Adrian Bigland, Adriana Roggemans, Alain Marin, Alaistar Brickhill, Alan Beech, Alan Maunder, Alan Pevec, Alan Pickwick, Alan Decamps, Alan Cowie, Alastair Emerson, Aled Powell, Alejandro Barriuso, Aleksandar Merlak, Alex Bell, Alex Haislip, Alex Hodge, Alex Jeffery, Alex Kichev, Alex McConahay, Alex Pratt, Alex Roig, Alex Aitov, Alexander Wiedekind-Klein, Alexandre Alves, Alfredo Dal' Ava Júnior, Alison Scott, Amy Barron, Anatoly Ijon, Andre Rousseau, Andre Bruton, Andrea Storani, Andrei Marukhno, Andres Fernandez, Andrew Campbell-Laing, Andrew Challis, Andrew Cooper, Andrew Fiamingo, Andrew Heath, Andrew Moyle, Andrew Washington, Andrew Fulher, Andrew Robertson, Andy Stott, Andy Sapir, Ange Fox, Angel Sierra, Angélica López Olmos, Anna Johnston, Ansgar Schmidt, Anthony Hopkinson, Anthony Pitt, Anthony Kesterton, Anton Macan, Anton Yanishevskiy, Antony Crowther, Anzhari Purnomo, Arie Blumenzweig, Arie Verveer, Arnaud Leroy, Attila Nemes, Barry Findley, Bart Dessoy, Bela Szomi Kralj, Bernard Côté, Bernard Hagen, Bev M. Ewen-Smith, Bill Cooke, Bill Wallace, Bill Witte, Bill Carr, Bill Thomas, Bob Evans, Bob Greschke, Bob Hufnagel, Bob Marshall, Bob Massey, Bob Zarnke, Bob Guzik, Brenda Goodwill, Brendan Cooney, Brendon Reid, Brian Chapman, Brian Murphy, Brian Rowe, Brian Hochgurtel, Wyatt Hochgurtel, Brian Mitchell, Bruno Bonicontro, Callum Potter, Carl Elkins, Carl Mustoe, Carl Panter, Charles Thody, Charlie McCormack, Chris Baddiley, Chris Blake, Chris Dakin, Chris George, Chris James, Chris Ramsay, Chris Reichelt, Chris Chad, Chris O'Neill, Chris White, Chris Jones, Chris Sale, Christian Wanlin, Christine Ord, Christof Zink, Christophe Demeautis, Christopher Coomber, Christopher Curtis, Christopher Tofts, Christopher Brooks, Chuck Goldsmith, Chuck Pullen, Ciaran Tangney, Claude Boivin, Claude Surprenant, Clive Sanders, Colin Graham, Colin Marshall, Colin Nichols, Con Stoitsis, Craig Young, Creina Beaman, Daknam Al-Ahmadi, Damien Lemay, Damien McNamara, Damir Matković, Damir Šegon, Damjan Nemarnik, Dan Klinglesmith, Dan Pye, Daniel Duarte, Daniel J. Grinkevich, Daniela Cardozo Mourão, Danijel Reponj, Danko Kočiš, Dario Zubović, Dave Jones, Dave Mowbray, Dave Newbury, Dave Smith, David Akerman, David Attreed, David Bailey, David Brash, David Castledine, David Hatton, David Leurquin, David Price, David Rankin, David Robinson, David Rollinson, David Strawford, David Taylor, David Rogers, David Banes, David Johnston, David Rees, David Cowan, David Greig, David Hickey, David Colthorpe, Dean Moore, Debbie Godsiff, Denis Bergeron, Denis St-Gelais, Dennis Behan, Derek Poulton, Didier Walliang, Dimitris Georgoulas, Dino Čaljkušić, Dmitrii Rychkov, Dominique Guiot, Don Anderson, Don Hladiuk, Dorian Božičević, Dougal Matthews, Douglas Sloane, Douglas Stone, Dustin Rego, Dylan O'Donnell, Ed Breuer, Ed Harman, Edd Stone, Edgar Mendes Merizio, Edison José Felipe Pérezgómez Álvarez, Edson Valencia Morales, Eduardo Fernandez Del Peloso, Edward Cooper, Ehud Behar, Eleanor Mayers, Emily Barraclough, Enrico Pettarin, Enrique Arce, Enrique Chávez Garcilazo, Eric Lopez, Eric Toops, Errol Balks, Erwin van Ballegoij, Erwin Harkink, Eugene Potapov, Ewan Richardson, Fabricio Borges, Fernando Dall'Igna, Fernando Jordan, Fernando Requena, Filip Matković, Filip Mezak, Filip Parag, Fiona Cole, Florent Benoit,

[26] https://creativecommons.org/licenses/by/4.0/

Francis Rowsell, François Simard, Frank Lyter, Frantisek Bilek, Gabor Sule, Gaétan Laflamme, Gareth Brown, Gareth Lloyd, Gareth Oakey, Garry Dymond, Gary Parker, Gary Eason, Gavin Martin, Gene Mroz, Geoff Scott, Georges Attard, Georgi Momchilov, Germano Soru, Gilton Cavallini, Gordon Hudson, Graeme Hanigan, Graeme McKay, Graham Stevens, Graham Winstanley, Graham Henstridge, Graham Atkinson, Graham Palmer, Greg Michael, Greg Parker, Gustav Frisholm, Gustavo Silveira B. Carvalho, Guy Létourneau, Guy Williamson, Guy Lesser, Hamish Barker, Hamish McKinnon, Haris Jeffrey, Harri Kiiskinen, Hartmut Leiting, Heather Petelo, Heriton Rocha, Hervé Lamy, Herve Roche, Holger Pedersen, Horst Meyerdierks, Howard Edin, Hugo González, Iain Drea, Ian Enting Graham, Ian Lauwerys, Ian Parker, Ian Pass, Ian A. Smith, Ian Williams, Ian Hepworth, Ian Collins, Igor Duchaj, Igor Henrique, Igor Macuka, Igor Pavletić, Ilya Jankowsky, Ioannis Kedros, Ivan Gašparić, Ivan Sardelić, Ivica Ćiković, Ivica Skokić, Ivo Dijan, Ivo Silvestri, Jack Barrett, Jacques Masson, Jacques Walliang, Jacqui Thompson, James Davenport, James Farrar, James Scott, James Stanley, James Dawson, Jamie Allen, Jamie Cooper, Jamie McCulloch, Jamie Olver, Jamie Shepherd, Jan Hykel, Jan Wisniewski, Janis Russell, Janusz Powazki, Jason Burns, Jason Charles, Jason Gill, Jason van Hattum, Jason Sanders, Javor Kac, Jay Shaffer, Jean Francois Larouche, Jean Vallieres, Jean Brunet, Jean-Baptiste Kikwaya, Jean-Fabien Barrois, Jean-Louis Naudin, Jean-Marie Jacquart, Jean-Paul Dumoulin, Jean-Philippe Barrilliot, Jeff Holmes, Jeff Huddle, Jeff Wood, Jeff Devries, Jeffrey Legg, Jeremy Taylor, Jesse Stayte, Jesse Lard, Jessica Richards, Jim Blackhurst, Jim Cheetham, Jim Critchley, Jim Fordice, Jim Gilbert, Jim Rowe, Jim Seargeant, Jochen Vollsted, Jocimar Justino, John W. Briggs, John Drummond, John Hale, John Kmetz, John Maclean, John Savage, John Thurmond, John Tuckett, John Waller, John Wildridge, John Bailey, Jon Bursey, Jonathan Alexis Valdez Aguilar, Jonathan Eames, Jonathan Mackey, Jonathan Whiting, Jonathan Wyatt, Jonathon Kambulow, Jorge Augusto Acosta Bermúdez, Jorge Oliveira, Jose Carballada, Jose Galindo Lopez, José María García, José-Luis Martín, Josip Belas, Josip Krpan, Jost Jahn, Juan Luis Muñoz, Jure Zakrajšek, Jürgen Dörr, Jürgen Ketterer, Justin Zani, Karen Smith, Karl Browne, Kath Johnston, Kees Habraken, Keith Maslin, Keith Biggin, Keith Christie, Ken Jamrogowicz, Ken Lawson, Ken Gledhill, Kevin Gibbs-Wragge, Kevin Morgan, Kevin Faure, Klaas Jobse, Korado Korlević, Kyle Francis, Lachlan Gilbert, Larry Groom, Laurent Brunetto, Laurie Stanton, Lawrence Saville, Lee Hill, Leith Robertson, Len North, Leslie Kaye, Lev Pustil'Nik, Lexie Wallace, Lisa Holstein, Llewellyn Cupido, Logan Carpenter, Lorna McCalman, Louw Ferreira, Lovro Pavletić, Lubomir Moravek, Luc Turbide, Lucia Dowling, Luciano Miguel Diniz, Ludger Börgerding, Luis Fabiano Fetter, Maciej Reszelsk, Magda Wisniewska, Manel Colldecarrera, Marc Corretgé Gilart, Marcel Berger, Marcelo Domingues, Marcelo Zurita, Marcio Malacarne, Marco Verstraaten, Margareta Gumilar, Marián Harnádek, Mariusz Adamczyk, Mark Fairfax, Mark Gatehouse, Mark Haworth, Mark McIntyre, Mark Phillips, Mark Robbins, Mark Spink, Mark Suhovecky, Mark Williams, Mark Ward, Marko Šegon, Marshall Palmer, Marthinus Roos, Martin Breukers, Martin Richmond-Hardy, Martin Robinson, Martin Walker, Martin Woodward, Martin Connors, Martyn Andrews, Mary Waddingham, Mary Hope, Mason McCormack, Mat Allan, Matej Mihelčić, Matt Cheselka, Matthew Howarth, Megan Gialluca, Mia Boothroyd, Michael Cook, Michael Mazur, Michael O'Connell, Michael Krocil, Michael Camilleri, Michael Kennedy, Michał Warchoł, Michel Saint-Laurent, Miguel Diaz Angel, Miguel Preciado, Mike Breimann, Mike Hutchings, Mike Read, Mike Shaw, Mike Ball, Milan Kalina, Minesh Patel, Miranda Clare, Mirjana Malarić, Muhammad Luqmanul Hakim Muharam, Murray Forbes, Murray Singleton, Murray Thompson, Myron Valenta, Nalayini Brito, Nawaz Mahomed, Ned Smith, Nedeljko Mandić, Neil Graham, Neil Papworth, Neil Waters, Neil Petersen, Nelson Moreira, Neville Vann, Nial Bruce, Nicholas Hill, Nicholas Ruffier, Nick Howarth, Nick James, Nick Moskovitz, Nick Norman, Nick Primavesi, Nick Quinn, Nick Russel, Nick Powell, Nick Wiffen, Nicola Masseroni, Nigel Bubb, Nigel Evans, Nigel Owen, Nigel Harris, Nikola Gotovac, Nikolay Gusev, Nikos Sioulas, Noah Simmonds, Norman Izsett, Ollie Eisman, Pablo Canedo, Paraksh Vankawala, Pat Devine, Patrick Franks, Patrick Poitevin, Patrick Geoffroy, Patrik Kukić, Paul Cox, Paul Dickinson, Paul Haworth, Paul Heelis, Paul Kavanagh, Paul Ludick, Paul Prouse, Paul Pugh, Paul Roche, Paul Roggemans, Paul Stewart, Paul Huges, Pedro Augusto Hay Day, Penko Yordanov, Pete Graham, Pete Lynch, Peter G. Brown, Peter Campbell-Burns, Peter Davis, Peter Eschman, Peter Gural, Peter Hallett, Peter Jaquiery, Peter Kent, Peter Lee, Peter McKellar, Peter Meadows, Peter Stewart, Peter Triffitt, Peter Leigh, Peter Felhofer, Pető Zsolt, Phil James, Philip Gladstone, Philip Norton, Philippe Schaak, Phillip Wilhelm Maximilian Grammerstorf, Pierre Gamache, Pierre de Ponthière, Pierre-Michael Micaletti, Pierre-Yves Pechart, Pieter Dijkema, Predrag Vukovic, Przemek Nagański, Radim Stano, Rajko Sušanj, Raju Aryal, Ralph Brady, Raoul van Eijndhoven, Raul Truta, Raul Elias-Drago, Reinhard Kühn, Remi Lacasse, Renato Cássio Poltronieri, René Tardif, Richard Abraham, Richard Bassom, Richard Croy, Richard Davis, Richard Fleet, Richard Hayler, Richard Johnston, Richard Kacerek, Richard Payne, Richard Stevenson, Richard Severn, Rick Fischer, Rick Hewett, Rick James, Ricky Bassom, Rob Agar, Rob de Corday Long, Rob Saunders, Rob Smeenk, Robert Longbottom, Robert McCoy, Robert Saint-Jean, Robert D. Steele, Robert Veronneau, Robert Peledie, Robin Boivin, Robin Earl, Robin Rowe, Roel Gloudemans, Roger Banks, Roger Morin, Roland Idaczyk, Rolf Carstens, Romulo Jose, Ron James Jr, Roslina Hussain, Ross Skilton, Ross Dickie, Ross Welch, Russell Jackson, Russell Brunton, Ryan Frazer, Ryan Harper, Salvador Aguirre, Sam Green, Sam Hemmelgarn, Sam Leaske, Sarah Tonorio, Scott Kaufmann, Sebastian Klier, Seppe Canonaco, Seraphin Feller, Serge Bergeron, Sergio Mazzi, Sevo Nikolov, Simon Cooke-Willis, Simon Holbeche, Simon Maidment, Simon McMillan, Simon Minnican, Simon Parsons, Simon Saunders, Simon Fidler, Simon Oosterman, Simon Peterson, Simon lewis, *Sofia Ulrich, Srivishal Sudharsan, Stacey Downton, Stan Nelson, Stanislav Korotkiy, Stanislav Tkachenko, Stef Vancampenhout, Stefan Frei, Stephane Zanoni, Stephen Grimes, Stephen Nattrass, Steve Berry, Steve Bosley, Steve Carter, Steve Dearden, Steve Homer, Steve Kaufman, Steve Lamb, Steve Rau, Steve Tonkin, Steve Trone, Steve Welch, Steve Wyn-Harris, Steven Shanks, Steven Tilley, Stewart Doyle, Stuart Brett, Stuart Land, Stuart McAndrew, Sue Baker Wilson, Sylvain Cadieux, Tammo Jan Dijkema, Terry Pundiak, Terry Richardson, Terry Simmich, Terry Young, Thiago Paes, Thomas Blog, Thomas Schmiereck, Thomas Stevenson, Tihomir Jakopčić, Tim Burgess, Tim Claydon, Tim Cooper, Tim Gloudemans, Tim Havens, Tim Polfliet, Tim Frye, Tioga Gulon, Tobias Westphal, Tom Warner, Tom Bell, Tommy McEwan, Tommy B. Nielsen, Torcuill Torrance, Tosh White, Tracey Snelus, Trevor Clifton, Ubiratan Borges, Urs Wirthmueller, Uwe Glässner, Vasilii Savtchenko, Ventsislav Bodakov, Victor Acciari, Viktor Toth, Vincent McDermott, Vladimir Jovanović, Waily Harim, Warley Souza, Washington Oliveira, Wenceslao Trujillo, William Perkin, William Schauff, William Stewart, William Harvey, William Hernandez, Wullie Mitchell, Yakov Tchenak, Yfore Scott, Yohsuke Akamatsu, Yong-Ik Byun, Yozhi Nasvadi, Yuri Stepanychev, Zach Steele, Zané Smit, Zbigniew Krzeminski, Željko Andreić, Zhuoyang Chen, Zoran Dragić, Zoran Knez, Zoran Novak, Asociación de Astronomía de Marina Alta, Costa Blanca Astronomical Society, Perth Observatory Volunteer Group, Royal Astronomical Society of Canada Calgary Centre.*

References

Dijkema T. J. (2022). “Visualizing meteor ground tracks on the meteor map”. *eMetN*, **7**, 73–75.

Drummond J. D. (1981). “A test of comet and meteor shower associations”. *Icarus*, **45**, 545–553.

Gural P. and Šegon D. (2009). “A new meteor detection processing approach for observations collected by the Croatian Meteor Network (CMN)”. *WGN, the Journal of the IMO*, **37**, 28–32.

Harman E., Eschman P., Massey B., and Olivera W. (2023). “Using GUI RMS on Linux to support multiple cameras”. *eMetN*, **8**, 185–196.

Jenniskens P., Baggaley J., Crumpton I., Aldous P., Pokorny P., Janches D., Gural P. S., Samuels D., Albers J., Howell A., Johannink C., Breukers M., Odeh M., Moskovitz N., Collison J., Ganju S. (2018). “A survey of southern hemisphere meteor showers”. *Planetary and Space Science*, **154**, 21–29.

Jenniskens P., Jopek T.J., Janches D., Hajduková M., Kokhirova G.I., Rudawska R. (2020). “On removing showers from the IAU Working List of Meteor Showers”. *Planetary and Space Science*, **182**, id. 104821.

Jenniskens P. (2023a). “February Hydrids (FHY#1032) in 2023”. *eMetN*, **8**, 181–182.

Jenniskens P. (2023b). Atlas of Earth’s Meteor Showers. Elsevier, USA, ISBN: 978-0-443-23577-1, 824 pages.

Jopek T. J. (1993). “Remarks on the meteor orbital similarity D-criterion”. *Icarus*, **106**, 603–607.

Jopek T. J. and Jenniskens P. M. (2011). “The Working Group on Meteor Showers Nomenclature: A History, Current Status and a Call for Contributions”. In Meteoroids: The Smallest Solar System Bodies, *Proceedings of the Meteoroids Conference* held in Breckenridge, Colorado, USA, May 24-28, 2010. Edited by W.J. Cooke, D.E. Moser, B.F. Hardin, and D. Janches, NASA/CP-2011-216469., 7–13.

Jopek T. J. and Kaňuchová Z. (2017). “IAU Meteor Data Center - the shower database: A status report”. *Planetary and Space Science*, **143**, 3–6.

Moorhead A. V., Clements T. D., Vida D. (2020). “Realistic gravitational focusing of meteoroid streams”. *Monthly Notices of the Royal Astronomical Society*, **494**, 2982–2994.

Mroz E. J. (2021). “Optimizing Camera Orientation for the New Mexico Meteor Array”. *eMetN*, **6**, 562–567.

Neslušan L., Poručan V., Svoreň J., Jakubík M. (2020). “On the new design othe IAU MDC portal”. *WGN, Journal of the International Meteor Organization*, **48**, 168–169.

Roggemans P., Cambell-Burns P., McIntyre M., Šegon D. and Vida D. (2023). “Global Meteor Network report 2022”. *eMetN*, **8**, 77–98.

Roggemans P., Vida D., Scott J.M., Jenniskens P., Šegon D., and Rollinson D. (2024). “First observed meteors from comet 46P/Wirtanen (lambda-Sculptorids, LSC)”. *eMetN*, **9**, 6–14.

Šegon D., Vida D., Roggemans P., Wood J., Boothroyd M., Fraser R., Hanigan G., Poulton D., Scott G., Scott J. and Zink C. (2023a). “2023 activity omega-Carinids (OCR#1033)”. *eMetN*, **8**, 74–76.

Šegon D., Vida D., Roggemans P. (2023b). “New meteor shower in Draco”. *eMetN*, **8**, 171–176.

Šegon D., Vida D., Roggemans P. (2023c). “New meteor shower in Bootes”. *eMetN*, **8**, 177–180.

Šegon D., Vida D., Roggemans P. (2023d). “A possibly new meteor shower in Sagitta”. *eMetN*, **8**, 246–251.

Southworth R. R. and Hawkins G. S. (1963). “Statistics of meteor streams”. *Smithson. Contrib. Astrophys.*, **7**, 261–286.

Vida D., Zubović D., Šegon D., Gural P. and Cupec R. (2016). “Open-source meteor detection software for low-cost single-board computers”. In: Roggemans A. and Roggemans P., editors, *Proceedings of the International Meteor Conference*, Egmond, the Netherlands, 2-5 June 2016. International Meteor Organization, pages 307–318.

Vida D., Gural P., Brown P., Campbell-Brown M., Wiegert P. (2020a). “Estimating trajectories of meteors: an observational Monte Carlo approach - I. Theory”. *Monthly Notices of the Royal Astronomical Society*, **491**, 2688–2705.

Vida D., Gural P., Brown P., Campbell-Brown M., Wiegert P. (2020b). “Estimating trajectories of meteors: an observational Monte Carlo approach - II. Results”. *Monthly Notices of the Royal Astronomical Society*, **491**, 3996–4011.

Vida D., Šegon D., Gural P. S., Brown P. G., McIntyre M. J. M., Dijkema T. J., Pavletić L., Kukić P., Mazur M. J., Eschman P., Roggemans P., Merlak A., Zubrović D. (2021). “The Global Meteor Network – Methodology and first results”. *Monthly Notices of the Royal Astronomical Society*, **506**, 5046–5074.

Vida D., Blaauw Erskine R. C., Brown P. G., Kambulow J., Campbell-Brown M., Mazur M. J. (2022). “Computing optical meteor flux using global meteor network data”. *Monthly Notices of the Royal Astronomical Society*, **515**, 2322–2339.

Zubović D., Vida D., Gural P. and Šegon D. (2015). “Advances in the development of a low-cost video meteor station”. In: Rault J.-L. and Roggemans P., editors, *Proceedings of the International Meteor Conference*, Mistelbach, Austria, 27-30 August 2015. International Meteor Organization, pages 94–97.

December 2023 report CAMS-BeNeLux

Carl Johannink

Am Ollenkamp 4, 48599 Gronau, Germany
c.johannink@t-online.de

A summary of the activity of the CAMS-BeNeLux network during the month of December 2023 is presented. This month we collected a total of 21696 meteors resulting in 2751 orbits.

1 Introduction

In December the Earth crosses dust of the Geminids, one of the highlights of meteor observing. Some nice minor streams are visible too. Combined with high sporadic activity this is a very attractive month for all meteor observers. After the bit disappointing month November, we hoped for better circumstances this month.

2 December 2023 statistics

December 2023 was again a somber month. Only a handful of complete clear nights occurred in large parts of the BeNeLux. And although the number of cameras and stations increased significantly compared to December months in the past, we have captured only 2751 orbits, resulting from 21696 captured meteors.

In 4 nights, we could capture no orbit at all, and there were only a small number of nights during which we could collect more than 100 orbits. So, a meager result this year. See *Figure 1*.

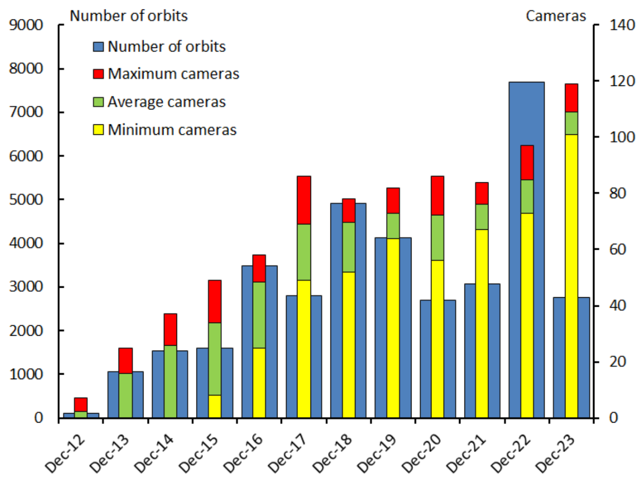

Figure 1 – Comparing December 2023 to previous months of December in the CAMS-BeNeLux history. The blue bars represent the number of orbits, the red bars the maximum number of cameras capturing in a single night, the green bars the average number of cameras capturing per night and the yellow bars the minimum number of cameras.

Table 1 – Number of orbits and active cameras in the BeNeLux during the month of December in the period 2012–2023.

Year	Nights	Orbits	Stations	Max. Cams	Min. Cams	Mean Cams
2012	12	117	6	7		2.4
2013	23	1053	10	25		15.7
2014	19	1540	14	37		25.8
2015	27	1589	15	49	8	33.8
2016	25	3492	21	58	25	48.3
2017	25	2804	22	86	49	68.9
2018	23	4908	21	78	52	69.8
2019	28	4124	21	82	64	72.8
2020	24	2693	24	86	56	72.4
2021	25	3072	25	84	67	76.0
2022	27	7680	31	97	73	84.8
2023	27	2751	41	119	101	109.0
Total	285	35823				

The highest number of orbits in one night was recorded in the nights of December 11–12 and December 17–18, approximately 300 orbits each night. As said earlier, compared with December 2022, the number of stations, and consequently the number of active cameras, has increased significantly (see *Table 1*).

Rob Smeenk added 4 more RMS cameras (3192–3195) at Kalenberg, the Netherlands.

This month, only 42.6% of all simultaneous meteors were captured by more than two stations. This confirms the bad weather this month. This number is even a bit lower than in November 2023.

On average, nearly 109 cameras at 41 stations were active during this month. Every night, at least 101 cameras captured meteors. The highest number of active cameras was 119 for a single night. These numbers are significantly higher than last year (*Figure 1*). Unfortunately, the number of orbits was hampered by bad weather.

3 Conclusion

Results for December 2023 are, when compared to other years, only modest, although the number of cameras increased significantly.

Acknowledgement

Many thanks to all participants in the CAMS-BeNeLux network for their dedicated efforts. The CAMS-BeNeLux team was operated by the following volunteers during the month of December 2023:

Stéphane Barré (Colombey-Les-Belles, France, RMS 3907), *Hans Betlem* (Woold, Netherlands, Watec 3071, 3072, 3073, 3074, 3075, 3076, 3077 and 3078), *Jean-Marie Biets* (Wilderen, Belgium, Watec 3180, 3181, 3182 and 3183), *Ludger Boergerding* (Holdorf, Germany, RMS 3801), *Günther Boerjan* (Assenede, Belgium, RMS 3823), *Martin Breukers* (Hengelo, Netherlands, Watec 320, 321, 322, 323, 324, 325, 326 and 327, RMS 319, 328 and 329), *Jean Brunet* (Fontenay le Marmion, France, RMS 3911), *Seppe Canonaco* (Genk, RMS 3818 and 3819), *Pierre de Ponthiere* (Lesve, Belgium, RMS 3816 and 3826), *Bart Dessoy* (Zoersel, Belgium, Watec 804, 805, 806), *Tammo Jan Dijkema* (Dwingeloo, Netherlands, RMS 3199), *Isabelle Ansseau, Jean-Paul Dumoulin, Dominique Guiot* and *Christian Wanlin* (Grapfontaine, Belgium, Watec 814, 815, RMS 3817, 3843, 3844 and 3845), *Uwe Glässner* (Langenfeld, Germany, RMS 3800), *Roel Gloudemans* (Alphen aan de Rijn, Netherlands, RMS 3197), *Luc Gobin* (Mechelen, Belgium, Watec 3890, 3891, 3892 and 3893), *Tioga Gulon* (Nancy, France, Watec 3900 and 3901), *Tioga Gulon* (Chassignolles, France, RMS 3910), *Robert Haas* (Alphen aan de Rijn, Netherlands, Watec 3160, 3161, 3162, 3163, 3164, 3165, 3166 and 3167), *Robert Haas* (Texel, Netherlands, Watec 811 and 812), *Kees Habraken* (Kattendijke, Netherlands, RMS 3780, 3781, 3782 and 3783), *Klaas Jobse* (Oostkapelle, Netherlands, Watec 3030, 3031, 3032, 3033, 3034, 3035, 3036 and 3037), *Carl Johannink* (Gronau, Germany, Watec 3100, 3101, 3102), *Reinhard Kühn* (Flatzby, Germany, RMS 3802), *Hervé Lamy* (Dourbes, Belgium, Watec 394 and 395, RMS 3825 and 3841), *Hervé Lamy* (Humain, Belgium, RMS 3821 and 3828), *Hervé Lamy* (Ukkel, Belgium, Watec 393 and 817), *Hartmut Leiting* (Solingen, Germany, RMS 3806), *Arnoud Leroy* (Gretz-Armainvielliers, France, RMS3909), *Horst Meyerdierks* (Osterholz-Scharmbeck, Germany, RMS 3807), *Koen Miskotte* (Ermelo, Netherlands, Watec 3051, 3052, 3053 and 3054), *Pierre-Yves Péchart* (Hagnicourt, France, RMS 3902, 3903, 3904, 3905, 3906 and 3908), *Eduardo Fernandez del Peloso* (Ludwigshafen, Germany, RMS 3805), *Tim Polfliet* (Gent, Belgium, Watec 396, RMS 3820 and 3840), *Steve Rau* (Oostende, Belgium, RMS 3822), *Steve Rau* (Zillebeke, Belgium, Watec 3850 and 3852, RMS 3851 and 3853), *Paul and Adriana Roggemans* (Mechelen, Belgium, RMS 3830 and 3831, Watec 3832, 3833, 3834, 3835, 3836 and 3837), *Jim Rowe* (Eastbourne, England, RMS 3703), *Philippe Schaack* (Roodt-sur-Syre, Luxemburg, RMS 3952), *Hans Schremmer* (Niederkruechten, Germany, Watec 803), *Rob Smeenk* (Assen, Netherlands, RMS 3196), *Rob Smeenk* (Kalenberg, Netherlands, RMS 3192, 3193, 3194 and 3195), *Erwin van Ballegoij* (Heesh, Netherlands Watec 3148 and 3149), *Stef Vancampenhout* (Vorselaar, Belgium, RMS 3842), *Andy Washington* (Clapton, England, RMS 3702).

Annual report 2023 CAMS-BeNeLux

Carl Johannink

Am Ollenkamp 4, 48599 Gronau, Germany

c.johannink@t-online.de

A summary of the activity of the CAMS-BeNeLux network during the year 2023 is presented. The year 2023 brought a mix of good and bad conditions for astronomical observations. The best months were especially the months June and September. In November and December on the other hand, many cloudy nights culminated in only modest results, despite the larger number of cameras involved in our network. 57190 orbits could be collected during 331 different nights which corresponds to 90,7% of all 365 nights in 2023. The months January, June, and September had the best scores ever for these months since the start of the network in 2012.

1 Introduction

In 2023, the network continued to grow steadily with new stations, especially in France and Germany. In the Netherlands three new stations, all equipped with RMS cameras, participated. *Rob Smeenk* added one camera at Assen and four cameras in Kalenberg. *Roel Gloudemans* added his camera in Alphen aan de Rijn to the network. In Germany cameras in Ludwigshafen (*Eduardo Fernandez del Peloso*), Solingen (*Hartmut Leiting*) and Osterholz-Scharmbeck, near Bremen (*Horst Meyerdierks*), were added. In France, *Pierre-Yves Péchart* in Hagnicourt, added four additional cameras to the CAMS network. Further on *Stéphane Barré* (Colombey-Les_Belles), *Arnoud Leroy* (Gretz-Armainvilliers), *Jean Brunet* (Fontenay le Marmion) and *Tioga Gulon* (Chassignolles) participated each with one RMS-camera.

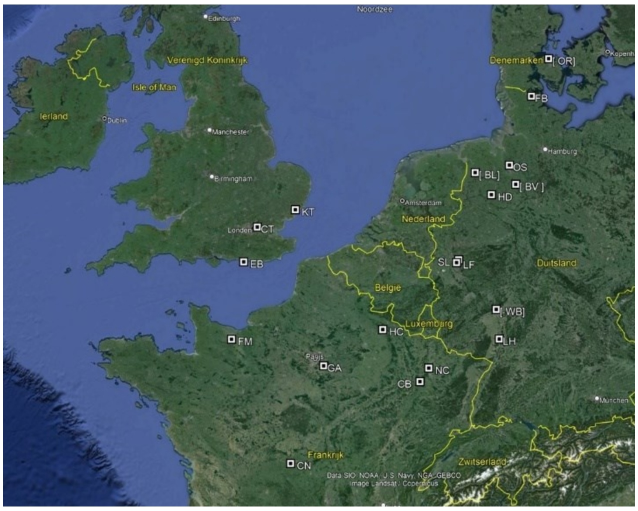

Figure 1 – Sites beyond the BeNeLux countries which are participating in CAMS-BeNeLux. Future expansions between brackets.

Expansions took place mainly on the southern and eastern flanks of our network. But also, two cameras in England were added to our network, one located in Clapton, and operated by *Andy Washington*, and one located in Kirton and operated by *Martin Richmond-Hardy*. Unfortunately, Martin passed away soon after he started providing data to CAMS.

In the course of 2024, a number of sites in Germany, and also one in Denmark, have been added. *Figure 1* shows all active locations outside the BeNeLux, with the locations that will participate in 2024 indicated between brackets.

2 CAMS-BeNeLux 2023 statistics

The year 2023 started with a very good result for the month of January. This was followed by four months that showed more or less an average to above-average picture.

June was a real outlier with a record harvest of orbits. No wonder: in this month we got sunshine for an average of more than 10 hours a day! July and August were very changeable, but thanks to clear nights at the right moments, they still produced great scores. After a top production in September, slowly but surely results started to decline in October. The precipitation amounts rose to record amounts, so the number of recorded meteors remained quite modest.

Table 1 presents an overview of the results during each month and the annual total.

Table 1 – Results for each month in 2023 (data CAMS-BeNeLux).

Month	Orbits	Ranking
January 2023	2291	1st
February 2023	3543	2nd
March 2023	1328	4th
April 2023	2888	3rd
May 2023	2734	2nd
June 2023	2889	1st
July 2023	3966	4th
August 2023	12074	2nd
September 2023	11331	1st
October 2023	7404	4th
November 2023	3991	6th
December 2023	2751	7th
2023 (year)	57190	2nd

The months of November and December were quite gloomy, mainly for that reason this year's total score lagged somewhat behind on 2022. Thanks to the excellent months of January, June and September, the annual total was still good for the second highest annual score with 57190 orbits, see also *Table 2*.

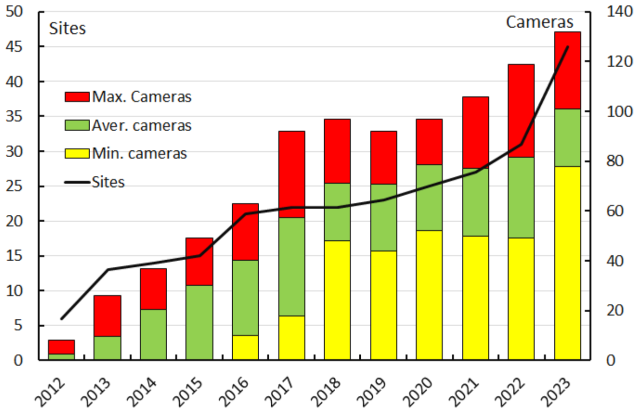

Figure 2 – The evolution of the number of cameras and camera sites, active during each year.

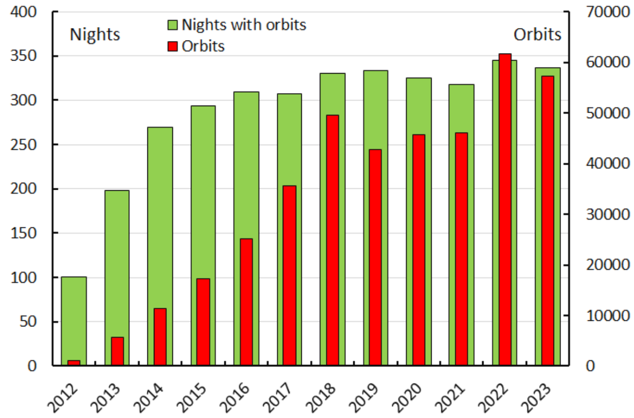

Figure 3 – The number of nights per year during which at least one orbit was obtained and the total number of orbits collected during each year.

Table 2 – Number of orbits collected since 2012 (data CAMS-BeNeLux).

Year	Orbits
2012	1079
2013	5684
2014	11288
2015	17259
2016	25187
2017	35591
2018	49627
2019	42746
2020	45743
2021	45985
2022	61619
2023	57190
Total	398998

The number of participating cameras increased by 25 during the year, but some cameras active in 2022 in the Netherlands were no longer operated. As mentioned earlier, the expansion is nearly completely due to new cameras in France and Germany. *Figure 2* shows how the maximum number of different cameras that contributed orbits increased year after year. Having many cameras is good to have, but for the coverage of a camera network it is important to have as many as possible of these capturing all nights, 7 on 7. Unfortunately, due to technical and personal problems of camera operators a number of cameras is not always available. *Figure 2* shows that during 2023 the average and minimum number of cameras increased thanks to the deployment of reliable fully automated systems.

Despite the rather unfavorable climate for astronomy in the BeNeLux more than 300 out of 365 nights allowed to obtain orbits since 2016 (*Figure 3*). The number of clear nights combined with the number of available cameras determines the chances to obtain orbits. With 345 nights with orbits 2022 was the best year ever with 2023 doing a bit less good with 337 nights. Also 2018 and 2019 were exceptional good years.

3 CAMS worldwide

CAMS is a global project in which different networks around the world participate all using the same software. Results for all networks are given in *Table 3*. CAMS-BeNeLux contributed to more than 11% of the total score for 2023. It remains amazing that with the well-known temperate climatic conditions we can still achieve this result in our regions.

Table 3 – Worldwide results of all CAMS networks in 2023.

CAMS network	2023	2022	2021
LOCAMS (Arizona, USA)	107857	106596	76232
Namibia	73960	81197	99659
BeNeLux	56741	61619	47023
California (USA)	40118	52130	39683
Chile	37606	49051	51350
Australia	59948	38114	54893
UAE	33585	32597	16294
Florida (USA)	25255	26454	24554
New Zealand	23426	16856	21661
Arkansas (USA)	12713	18972	15868
Texas (USA)	11709	19063	17449
South Afrika	7422	7867	8726
Maryland (USA)	0	2384	5140
Turkey	758	1605	1323
Brazil	29	105	144
India	0	0	0
Total	491127	514610	479999

When CAMS-BeNeLux started, the aim was to collect at least 100 orbits for every night of the year. Over the past 12 years, we have more than achieved this goal. *Table 4* shows an overview of the number of orbits that have been collected on each calendar night of the year up to and including 31 December 2023.

Table 4 – Cumulated daily tally with the total number of orbits obtained by CAMS-BeNeLux for each calendar date, period 2012–2023.

TOTAL	01-02	02-03	03-04	04-05	05-06	06-07	07-08	08-09	09-10	10-11	11-12	12-13	13-14	14-15	15-16	16-17	17-18	18-19	19-20	20-21	21-22	22-23	23-24	24-25	25-26	26-27	27-28	28-29	29-30	30-31	31-01	
January	137	807	1385	545	572	320	648	633	576	302	144	381	393	273	509	515	966	780	921	1244	653	178	28	162	242	244	239	402	413	533	229	15374
February	117	251	469	437	524	845	506	516	257	434	648	1258	1304	843	1121	418	625	469	275	681	687	700	908	1161	1008	1131	1277	634	169			19673
March	574	653	428	457	509	524	573	442	395	518	422	435	359	328	335	330	494	648	572	371	587	639	632	738	577	637	739	379	618	479	455	15847
April	466	451	627	555	481	362	345	588	504	666	644	547	751	617	673	699	977	857	1444	1349	1474	1716	863	385	684	780	490	283	434	365		21077
May	515	679	477	665	795	559	548	813	297	420	478	609	721	741	536	420	572	438	520	562	428	173	530	568	553	460	545	718	478	680	799	17297
June	610	419	335	319	382	484	309	446	584	468	523	580	709	543	604	581	379	511	251	619	580	615	522	659	662	420	536	641	689	383		15363
July	695	856	810	397	968	789	742	873	530	933	690	782	557	973	707	851	1614	1242	990	1098	1097	1199	976	912	890	576	792	954	2111	1492	1357	29453
August	1707	1809	1894	1674	2843	3353	2767	2411	3250	4444	3876	9055	7806	2367	2739	1287	1551	2089	1380	1871	1704	2400	2049	2309	1595	1648	1780	1685	1272	1366	1566	79547
September	1948	1869	1564	1795	2211	1856	2099	1914	2238	1692	1434	1094	2251	2130	1749	1551	1753	1894	1688	2240	2333	1696	1772	2152	1347	1825	1436	1692	2012	1144		54379
October	1163	1353	1123	1820	1776	1408	1653	3018	2137	2297	1534	1340	1814	1924	2262	1105	1707	1604	1405	1631	2243	2669	2156	1916	1117	1535	2915	1531	1884	1827	1745	55612
November	1648	1548	1776	1657	1494	1910	2194	1119	1530	1186	1419	1428	1909	1018	1020	1453	1718	1025	1271	786	1622	1563	919	1371	1101	412	715	1219	1000	522		39553
December	567	1055	1045	1451	730	819	942	1257	1477	1403	1993	4320	2765	2768	1346	918	1370	837	803	1185	655	205	226	489	554	939	830	683	1427	409	355	35823
																																398998

less than 100 orbits

100 orbits or more, but less than 500 orbits

500 orbits or more, but less than 1000 orbits

1000 orbits or more

In the meantime, we already have more than 1000 orbits available in more than 41% of the number of nights. The night 23–24 January remains 'the outlier' in this overview. The large harvest of orbits that we achieved in February is remarkable, despite the low meteor activity in this month. The explanation for this is that after 2014 the number of hours of sunshine in February in our regions was almost always well above normal.

Only in 2017 and 2020 did the number of hours of sunshine remain below the typical average for February. The long nights under clear sky conditions then provide such remarkable results.

Acknowledgments

Many thanks to all operators in the CAMS-BeNeLux network for their work and quick delivery of data. The CAMS-BeNeLux network was operated by the following volunteers in 2023:

Stéphane Barré (Colombey-Les-Belles, France, RMS 3907), *Hans Betlem* (Woold, Netherlands, Watec 3071, 3072, 3073, 3074, 3075, 3076, 3077 and 3078), *Felix Bettonvil* (Utrecht, Netherlands, Watec 376), *Jean-Marie Biets* (Wilderen, Belgium, Watec 3180, 3181, 3182 and 3183), *Ludger Boergerding* (Holdorf, Germany, RMS 3801), *Günther Boerjan* (Assenede, Belgium, RMS 3823), *Martin Breukers* (Hengelo, Netherlands, Watec 320, 321, 322, 323, 324, 325, 326 and 327, RMS 319, 328 and 329), *Jean Brunet* (Fontenay le Marmion, France, RMS 3911), *Seppe Canonaco* (Genk, RMS 3818 and 3819), *Pierre de Ponthiere* (Lesve, Belgium, RMS 3816 and 3826), *Bart Dessoy* (Zoersel, Belgium, Watec 397, 398, 804, 805, 806, 888 and RMS 3827), *Tammo Jan Dijkema* (Dwingeloo, Netherlands, RMS 3199), *Isabelle Ansseau, Jean-Paul Dumoulin, Dominique Guiot and Christian Wanlin* (Grapfontaine, Belgium, Watec 814, 815, RMS 3814, 3817, 3843, 3844 and 3845), *Uwe Glässner* (Langenfeld, Germany, RMS 3800), *Roel Gloudemans* (Alphen aan de Rijn, Netherlands, RMS 3197), *Luc Gobin* (Mechelen, Belgium, Watec 3890, 3891, 3892 and 3893), *Tioga Gulon* (Nancy, France, Watec 3900 and 3901), *Tioga Gulon* (Chassignolles, France, RMS 3910), *Robert Haas* (Alphen aan de Rijn, Netherlands, Watec 3160, 3161, 3162, 3163, 3164, 3165, 3166 and 3167), *Robert Haas* (Texel, Netherlands, Watec 811, 812 and 813), *Kees Habraken* (Kattendijke, Netherlands, RMS 3780, 3781, 3782 and 3783), *Klaas Jobse* (Oostkapelle, Netherlands, Watec 3030, 3031, 3032, 3033, 3034, 3035, 3036 and 3037), *Carl Johannink* (Gronau, Germany, Watec 3100, 3101, 3102), *Reinhard Kühn* (Flatzby, Germany, RMS 3802), *Hervé Lamy* (Dourbes, Belgium, Watec 394 and 395, RMS 3825 and 3841), *Hervé Lamy* (Humain, Belgium, RMS 3821 and 3828), *Hervé Lamy* (Ukkel, Belgium, Watec 393 and 817), *Hartmut Leiting* (Solingen, Germany, RMS 3806), *Arnoud Leroy* (Gretz-Armainvielliers, France, RMS3909), *Horst Meyerdierks* (Osterholz-Scharmbeck, Germany, RMS 3807), *Koen Miskotte* (Ermelo, Netherlands, Watec 3051, 3052, 3053 and 3054), *Pierre-Yves Péchart* (Hagnicourt, France, RMS 3902, 3903, 3904, 3905, 3906 and 3908), *Eduardo Fernandez del Peloso* (Ludwigshafen, Germany, RMS 3805), *Tim Polfliet* (Gent, Belgium, Watec 396, RMS 3820 and 3840), *Steve Rau* (Oostende, Belgium, RMS 3822), *Steve Rau* (Zillebeke, Belgium, Watec 3850 and 3852, RMS 3851 and 3853), *Martin Richmond-Hardy* (Kirton, England, RMS 3701), *Paul and Adriana Roggemans* (Mechelen, Belgium, RMS 3830 and 3831, Watec 3832, 3833, 3834, 3835, 3836 and 3837), *Jim Rowe* (Eastbourne, England, RMS 3703), *Philippe Schaack* (Roodt-sur-Syre, Luxemburg, RMS 3952), *Hans Schremmer* (Niederkruechten, Germany, Watec 803), *Rob Smeenk* (Assen, Netherlands, RMS 3196), *Rob Smeenk* (Kalenberg, Netherlands, RMS 3192, 3193, 3194 and 3195), *Jan Thoemel* (Luxembourg, Watec 3950), *Erwin van Ballegoij* (Heesh, Netherlands Watec 3148 and 3149), *Stef Vancampenhout* (Vorselaar, Belgium, RMS 3842), *Andy Washington* (Clapton, England, RMS 3702).

January 2024 report CAMS-BeNeLux

Carl Johannink

Am Ollenkamp 4, 48599 Gronau, Germany
c.johannink@t-online.de

A summary of the activity of the CAMS-BeNeLux network during the month of January 2024 is presented. This month gave an above average number of hours of sunshine. As a result, a new record number of orbits could be collected: 4966 orbits derived from a total of 16838 meteors.

1 Introduction

From visual observations in the past, it is known that in the course of the month of January, sporadic activity begins to decrease. The Quadrantids at the start of January mark also the end of the series of major streams that produce displays since the month of July. Results for January strongly depend on the weather.

2 January 2024 statistics

January was also on the mild side in 2024 with an average temperature of 4 degrees. Often this means cloudy and gloomy conditions at night, but this year there were two short periods of clear weather. As a result, January 2024 was a bit sunnier than the climatological average. Something we had only seen in the CAMS years so far in 2017. Most hours of sunshine occurred during January 8–10 and January 26–27. And although meteor activity is decreasing then, we could collect a record number of orbits for this month during these three nights starting on January 8th. So far, the record number of orbits was 660 during the Quadrantid maximum in 2020. Starting with January 8–9 we collect 711, 673 and 742 orbits per night, actually, completely without any major shower activity.

The main reason for these high numbers of orbits is the growth of the number of cameras in our network, especially in 2023. Only three nights remained without any orbit at all (January 12–13, 13–14 and 25–26). Together with the year 2022 this is a record low number. In all other years there were at least six nights without any orbit. Unfortunately, the weather was bad around the Quadrantids maximum. On January 4–5 we collected 142 orbits, but in the previous nights, the number of orbits was limited to a few dozen. A total of 16838 meteors were captured by all 45 active stations, resulting in 4966 orbits. Nearly 55% of these simultaneous meteors were captured by more than two stations. This percentage is a bit lower than what we had in 2023. At least 96 of all 126 cameras at 44 stations were active each night, 126 cameras at the most, see *Table 1*. This month we could welcome two new stations. *Jürgen Dörr* in Wiesbaden (Germany) delivers now data obtained by his RMS-camera. *Holger Pedersen* in Otterup (Denmark) joined our network too. These cameras are both pointed in western direction. They give a better coverage for the areas just south of Belgium and the north of Germany and the Netherlands.

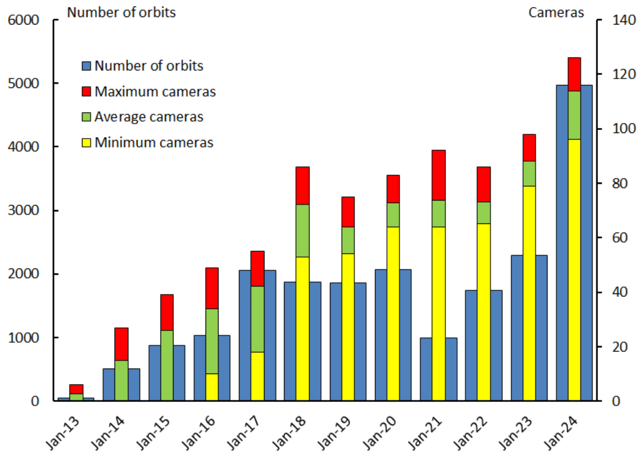

Figure 1 – Comparing January 2024 to previous months of January in the CAMS-BeNeLux history. The blue bars represent the number of orbits, the red bars the maximum number of cameras capturing in a single night, the green bars the average number of cameras capturing per night and the yellow bars the minimum number of cameras.

Table 1 – Number of orbits and active cameras in CAMS-BeNeLux during the month of January in the period 2013–2024.

Year	Nights	Orbits	Stations	Max. Cams	Min. Cams	Mean Cams
2013	7	49	6	6	–	2.6
2014	21	514	11	27	–	14.8
2015	22	880	14	39	–	26.1
2016	25	1037	15	49	10	34.0
2017	23	2058	18	55	18	42.3
2018	25	1878	22	86	53	72.1
2019	22	1857	20	75	54	64
2020	23	2075	21	83	64	72.9
2021	22	991	26	92	64	73.7
2022	28	1744	25	86	65	73.2
2023	25	2291	32	98	79	88.1
2024	28	4966	44	126	96	113.7
Total	271	20340				

3 Conclusion

Results for January 2024 are the best in the history of CAMS-BeNeLux, mainly thanks to the increase in the number of stations and the number of cameras.

Acknowledgement

Many thanks to all participants in the CAMS-BeNeLux network for their dedicated efforts. The CAMS-BeNeLux team was operated by the following volunteers during the month of January 2024:

Stéphane Barré (Colombey-Les-Belles, France, RMS 3907), *Hans Betlem* (Woold, Netherlands, Watec 3071, 3072, 3073, 3074, 3075, 3076, 3077 and 3078), *Felix Bettonvil* (Utrecht, Netherlands, Watec 376), *Jean-Marie Biets* (Wilderen, Belgium, Watec 3180, 3181, 3182 and 3183), *Ludger Boergerding* (Holdorf, Germany, RMS 3801), *Günther Boerjan* (Assenede, Belgium, RMS 3823), *Martin Breukers* (Hengelo, Netherlands, Watec 320, 321, 322, 323, 324, 325, 326 and 327, RMS 319, 328 and 329), *Jean Brunet* (Fontenay le Marmion, France, RMS 3911), *Seppe Canonaco* (Genk, RMS 3818 and 3819), *Pierre de Ponthiere* (Lesve, Belgium, RMS 3816 and 3826), *Bart Dessoy* (Zoersel, Belgium, Watec 804, 805, 806), *Tammo Jan Dijkema* (Dwingeloo, Netherlands, RMS 3199), *Jürgen Dörr* (Wiesbaden, Germany, RMS 3810), *Isabelle Ansseau, Jean-Paul Dumoulin, Dominique Guiot* and *Christian Wanlin* (Grapfontaine, Belgium, Watec 814, 815, RMS 3817, 3843, 3844 and 3845), *Uwe Glässner* (Langenfeld, Germany, RMS 3800), *Roel Gloudemans* (Alphen aan de Rijn, Netherlands, RMS 3197), *Luc Gobin* (Mechelen, Belgium, Watec 3890, 3891, 3892 and 3893), *Tioga Gulon* (Nancy, France, Watec 3900 and 3901), *Tioga Gulon* (Chassignolles, France, RMS 3910), *Robert Haas* (Alphen aan de Rijn, Netherlands, Watec 3160, 3161, 3162, 3163, 3164, 3165, 3166 and 3167), *Robert Haas* (Texel, Netherlands, Watec 811 and 812), *Kees Habraken* (Kattendijke, Netherlands, RMS 3780, 3781, 3782 and 3783), *Klaas Jobse* (Oostkapelle, Netherlands, Watec 3030, 3031, 3032, 3033, 3034, 3035, 3036 and 3037), *Carl Johannink* (Gronau, Germany, Watec 3100, 3101, 3102), *Reinhard Kühn* (Flatzby, Germany, RMS 3802), *Hervé Lamy* (Dourbes, Belgium, Watec 394 and 395, RMS 3825 and 3841), *Hervé Lamy* (Humain, Belgium, RMS 3821 and 3828), *Hervé Lamy* (Ukkel, Belgium, Watec 393 and 817), *Hartmut Leiting* (Solingen, Germany, RMS 3806), *Arnoud Leroy* (Gretz-Armainvielliers, France, RMS3909), *Horst Meyerdierks* (Osterholz-Scharmbeck, Germany, RMS 3807), *Koen Miskotte* (Ermelo, Netherlands, Watec 3051, 3052, 3053 and 3054), *Pierre-Yves Péchart* (Hagnicourt, France, RMS 3902, 3903, 3904, 3905, 3906 and 3908), *Holger Pedersen* (Otterup, Denmark, RMS 3501), *Eduardo Fernandez del Peloso* (Ludwigshafen, Germany, RMS 3805), *Tim Polfliet* (Gent, Belgium, Watec 396, RMS 3820 and 3840), *Steve Rau* (Oostende, Belgium, RMS 3822), *Steve Rau* (Zillebeke, Belgium, Watec 3850 and 3852, RMS 3851 and 3853), *Paul and Adriana Roggemans* (Mechelen, Belgium, RMS 3830 and 3831, Watec 3832, 3833, 3834, 3835, 3836 and 3837), *Jim Rowe* (Eastbourne, England, RMS 3703), *Philippe Schaack* (Roodt-sur-Syre, Luxemburg, RMS 3952), *Hans Schremmer* (Niederkruechten, Germany, Watec 803), *Rob Smeenk* (Assen, Netherlands, RMS 3196), *Rob Smeenk* (Kalenberg, Netherlands, RMS 3192, 3193, 3194 and 3195), *Erwin van Ballegoij* (Heesh, Netherlands Watec 3148 and 3149), *Andy Washington* (Clapton, England, RMS 3702).

A successful Geminid campaign from Portugal

Jaap van 't Leven and Koen Miskotte

Dutch Meteor Society
k.miskotte@upcmail.nl

An overview is presented of visual meteor observations during the Geminids 2023.

1 Introduction

The Geminids are one of the most beautiful meteor showers to observe. But also, a difficult one: the chance of a clear sky in December in the Netherlands is less than 10%. But the southern locations in Europe are certainly also no guarantee for success either. For Koen, it also became apparent in September (due to suddenly imposed holidays by the company where he works), that he had no more days off. So, in September Koen had already resigned himself to the fact that it would be a Dutch campaign with a small chance of success.

In October Jaap booked a house near Monchique in the Algarve. More precisely, near the very small village of Umbria. The goal was to be in the region where the occultation of the star Betelgeuse by asteroid 319 Leona on December 12, 2023 at 1^h12^m UT would occur. This asteroid would cover the red star for a maximum of 11 seconds. According to predictions, Betelgeuse would disappear completely for a brief time, other sources spoke of a decrease in brightness of up to 3 magnitudes. In addition, Jaap planned to observe the Geminids as well, which would have their maximum on the night of December 14–15.

At the end of November, it turned out that Koen had worked so many hours extra that he could take a whole week off. And luckily the boss agreed. The weather predictions have been looked at a bit, but at the end of November they were still not sure: it could still go either way. This had to do with the position of a high-pressure area located off the Portuguese coast, or a little further away in the west or just above the Iberian Peninsula. On Tuesday, December 5, Koen booked the same flight as Jaap’s, to and from Faro. Outbound flight December 9, return flight December 16, good for a week of counting Geminids if the weather permits!

2 Equipment

To cover the Betelgeuse occultation, Jaap brought a Watec 902H2 video camera with a 12mm Pentax lens. Combined with a GPS and a so-called time inserter, each individual video frame is given a text with accurate location and time data. This video image is then saved on a laptop. By combining observations with similar equipment, all kinds of information can be gathered, the shape and size of the asteroid, the shape and size of Betelgeuse and its

Figure 1 – Our rented house as seen from the garden.

Table 1 – Overview of the visual observations.

Date 12/2023	Period UT Start	End	$T_{eff.}$	Lm	GEM	MON	HYD	ANT	DLM	COM	URS	SPO	Total
10–11	22^h40^m	05^h08^m	6.00	6.60	73	9	8	5	~	3	~	47	145
13–14	20^h37^m	05^h45^m	8.50	6.60->6.70	620	18	10	9	~	7	3	99	766
14–15	18^h40^m	05^h30^m	8.85	6.50->6.70	519	12	10	11	2	7	1	70	632
15–16	23^h17^m	03^h17^m	4.00	6.60	29	1	4	7	3	3	2	44	93
4 nights			27.35		1241	40	32	32	5	20	6	260	1636

atmosphere, etc. For the overview, a Canon EOS R6ii camera with a 50mm lens would also be running in movie mode. For the Geminids, we relied on Canon EOS R and R6ii cameras with Sigma 14 and 24mm lenses.

3 Our observations

On Saturday afternoon we left from Schiphol Airport after a half hour delay. The take-off seemed to proceed normally until after half an hour we clearly noticed that the plane was turning. At the same time, the captain of the flight reports that damage occurred to one of the cockpit windows during take-off and that, just to be on the safe side, they are flying back to see if they can continue flying to Faro. After returning to Schiphol Airport, it turned out that it was not possible to continue flying, but fortunately a new Transavia plane was ready. We arrived in Faro at 21^h UT after a bumpy flight and a very hard landing. We got our luggage quickly and the rental car arrived quickly. It was 0^h00^m UT when we arrive at the rented house.

There were clear skies but there was also some fog. Yet we saw that the starry sky looked great. The weather predictions indicated that we would probably miss the Betelgeuse occultation, but there was hope for the Geminids.

During the day of December 10, we looked for a suitable place for the visual observations and the cameras. Since there were no other observers in Southern Portugal there will be no simultaneous photographic sessions. So, it was all about the beautiful pictures. A bit of a problem were the numerous cork oaks around the house. But this also gave nice opportunities. In front of our house, which was located on a slope facing north, there was a dead cork oak without leaves. It really contrasted beautifully with the starry sky! This could well become the most photographed tree in Portugal!

During the day, an extremely bright security lamp that illuminated the entire garden was rendered “harmless” with some tape and plastic around the sensor. Other outdoor lighting could be turned off with a switch inside. Due to the large number of cork oaks, it was not possible to look at the starry sky undisturbed from the garden. The view south and east was also largely blocked by the hill and trees. After some searching in the area, it was decided to observe on the street. It was a dead-end asphalt road situated underneath our house with one more house at the end. So, no traffic was expected, with the exception of the residents of that other house. The view there was perfect towards the north. But there was also a lighting problem here. There was a rechargeable (solar) streetlight mounted on the tree. On a cloudy day it usually turned off after two hours, but on a sunny day it usually took three or four hours. The solution to this was an observation location next to the house. But there was more obstruction in Koen’s FOV for about 10%. So as soon as the streetlight shut down, Koen moved to the street.

December 10–11, 2023

This night would be clear. Koen first wents to sleep for a few hours, Jaap got to work with a Watec 902H2 Ultimate with a 12 mm lens to test some things for the Betelgeuse occultation. Koen was aiming for a four-hour visual session, but this went so well without any fatigue that it ended up being six hours. The observations started at 22^h40^m UT. After one minute the first +3 Geminid was already seen. And while recording, meteor number 2 also appeared! While flaring, a beautiful –6 Monocerotid (22^h42^m UT) moved down to the northwestern horizon! The Canon Ra with the 14 mm captured this fireball nicely. This was a great start to this campaign! The Geminids were also alive, loud and clear, the hourly counts were between 10 and 15. Smaller meteor showers such as the Coma Berenicids, Monocerotids, and sigma Hydrids were also clearly active. In total, Koen counted 145 meteors during effectively 6 hours. See also *Table 1*.

Figure 2 – The spectacular Monocerotid of December 12, 2023, 22^h42^m UT. When zoomed in, many small flares are visible. Camera: Canon EOS Ra with a Sigma Art 14 mm at F 2.0, ISO 3200 and 6 seconds exposure time. © Jaap van ‘t Leven.

December 11–12, 2023

During the day of December 11th, it turned out that observing the Betelgeuse occultation from the south-west of Portugal would be difficult. A lot of clouds and fog were forecasted with only a small chance of clear spells. Satellite images were continuously consulted during the evening and night, but the clouds and fog were very persistent. At one point the fog was so thick that it seemed to be raining. After the dense fog dissolved a bit, stars occasionally appeared in small clear parts of the sky, so we set up the equipment anyway. However, around the time of the occultation, no star was visible and so we packed up the equipment again. Fortunately, positive messages came from the east of Spain; there, many observers were able to observe the occultation under good conditions. From a first quick analysis, the predicted central line of the occultation appeared to have been slightly further north than calculated.

Figure 3 – Find the cameras. Four of Jaap's cameras ready for action!

December 12–13, 2023

During the day, Jaap was busy positioning his cameras. Because of the many trees it took a bit of planning. Ultimately, one of his cameras ended up on a large pergola via a clamp with a ball head. And this camera would also produce the most beautiful photos. As predicted, December 12–13 was also cloudy. We used this night to catch up on some sleep so that we could go into the two marathon nights as fit as possible. We looked outside a few times, but it was always completely cloudy.

Figure 4 – The beautiful, improvised setup of a Canon R6ii and the Sigma ART 14 mm lens on a sturdy pergola. This setup produced the most beautiful pictures.

December 13–14, 2023

After a gray start, blue patches of sky soon became visible that day: the first clear spells arrived. However, it took until sunset before it became completely clear. During the day we did some shopping and went out for some dinner. That saved time, because, the days were also short here and the nights were very long in December. At dusk Jaap set up his cameras and as soon as it got dark, they were all open. The cameras all worked on batteries that needed to be changed every 2 to 3 hours. Because the maximum was not expected until the evening of December 14, Koen decided to sleep for another 2 hours after dinner. Wake up at 20^h UT, have a coffee and then go outside! Expectations were not too high in terms of numbers and thinking of 2015 with Carl Johannink and Sietse Dijkstra in the Black Forest (southern Germany) when especially the first hours showed rather low activity. It was 20^{h}37^m UT when Koen signed in. The sky was perfectly clear (limiting magnitude 6.6), comparable to the first night of this observation campaign. During the night the sky would further improve, and the limiting magnitude increased to 6.7.

The Geminid activity? That really was not disappointing. With hourly counts ranging from 40 to well into the 90s, that was not bad at all. Minute counts of 4 or 5 were sometimes followed by a minute-long period with no Geminids. Regularly two appeared at the same time, but there were also times with several in just a few seconds. As expected, few bright Geminids, especially the first few hours when only a few Geminids of 0 and –1 were seen. Koen was occasionally accompanied by Jaap when he had no camera duties. To continue the long observational session, Koen decided to take two longer breaks, every three hours (between 23^{h}38^m and 00^{h}00^m UT and between 03^{h}00^m and 03^{h}15^m UT). The impression is that the activity is less than December 13–14, 2007, but equal or slightly higher than 2015. Anyway, calculations will really provide a definitive answer.

A first Geminid fireball was seen at 00^{h}40^m UT, in the corner of the eye and right between two treetops and straight through Leo's sickle. About magnitude –4 or –5. It would turn out to be the only one this night, but from that moment on brighter Geminids such as a few of –3 appeared. Koen's three magnitude distributions that night also show a steadily decreasing of the average brightness. When the radiant culminated, between 80 and 90 Geminids could be seen per hour. It was 05^{h}45^m UT when we decided to stop, with in mind the next buzzy night. Koen actually counted 766 meteors in 8.50 hours. Photographically, 63 meteors were captured in 9 hours by Jaap with the 14mm, compared to 47 meteors in 10 hours with the 24mm. We were very satisfied, the first night was in the bag!

Figure 5 – Beautiful image of a bright –5 Geminid on December 15, 2023, at 03^{h}00^m UT with the dead cork oak in the foreground. A second faint Geminid is visible below the fireball. Camera: Canon R6ii, Sigma ART 14mm F 2.2, ISO 6400, 6 seconds exposure.

Figure 6 – This is how we like it. Bright blue skies on December 14!

December 14–15, 2023

With a maximum predicted by IMO on December 14, 19^h UT, it was ideal to observe earth grazers. However, caution was required, because if the maximum felt a few hours later (which often happens when a double maximum occurs), we would be in a dip and things could easily be disappointing. The Geminid radiant appeared just after 18^h30^m UT above the horizon. Everything was ready and the cameras started making pictures around that time. This night Koen used his Sony Alpha AIIs camera with a Sigma ART 20 mm F 1.4 lens. He started his visual observations because of the early time next to the house (because of the streetlight on the tree), which was at 18^h40^m UT. There was still a little bit of twilight, but the limiting magnitude was already around 6.5. The transparency/contrast of the starry sky was excellent. It took five minutes before the first earth grazer, a +1 Geminid, appeared, low in a north-northeast direction, disappearing as seen from our vantage point behind a tree. Yes, there they were again! And so more appeared. Koen observed for 80 minutes and counted 24 Geminids: sometimes several in a few minutes, sometimes nothing was to be seen for 5 or 6 minutes. The brightest earth grazers were the most beautiful: you could see them slowing down, fall apart or just dissolve, a very beautiful view to see! The cameras also captured a number of earth grazers.

Koen took a break between 20^h10^m and 20^h57^m UT and some coffee and fruit were consumed. Unfortunately, the streetlight still appeared to be on after this, so he continued observing from the spot next to the house. The Geminids activity had increased, obviously due to the climbing radiant. But not many bright Geminids were seen. Just before 22^h00^m UT the streetlight appeared to be off and Koen quickly moved to the street. At 22^h15^m UT restart with an unobstructed view and a limiting magnitude well above 6.6. After 1 minute, Koen saw the most beautiful Geminid of this campaign, a –3 Geminid moved low above the eastern horizon, and it had a wake (tail) that moved like a flame in a strong wind. Exceptionally that this was seen so beautiful. Shortly afterwards a –2 Geminid: ah, would we now get the nice bright stuff? Well, no, but more –1 and –2 Geminids appeared. But actually, it was never convincing in terms of numbers of bright Geminids. The number of Geminids per hour were good with maximum hourly counts near 100 around radiant culmination (~02^h45^m UT). However, after 3^h30^m UT there was a rapid decline in numbers, which halved in a short while. Fortunately, the number of bright Geminids increased somewhat, so at

Figure 7 – Two Geminid Earth grazers in one 6 second shot! December 14, 2023, 20^h49^m UT. Canon R6ii, Sigma Art 14mm F 2.0 (ISO 6400, 6 seconds).

Figure 8 – Another nice catch from the camera on the pergola. A –3 Geminid on December 14, 22^h17^m UT. Camera: Canon R6ii, Sigma ART 14mm F 2.2, ISO 6400 and 6 seconds exposure time.

02^{h}45^m UT a –4 Geminid, 02^{h}47^m UT a –3, –1 and +1 Geminid were simultaneously seen and at 03^{h}00^m UT a –5 Geminid (see *Figure 5*). At 05^{h}25^m UT: another –5 Geminid, this one diving "into" the tree to the east and emerging again underneath! Some short flashes of light were visible from behind the tree. All in all, we got the impression that the decreasing mean brightness of the Geminids was not as convincing as for example in 2007 (also from Portugal). Anyway, final calculations together with data from other visual observers should provide more details about this. And of course, we did not really know what had appeared behind the trees and mountain. Koen observed this night between 18^{h}40^m and 05^{h}30^m UT, which is almost 11 hours, but due to some longer breaks, the net observing time was 8.85 hours, this night yielded 632 meteors.

Jaap let his cameras run until dusk and then went to bed. In 11 hours, 220 meteors were photographed with the 14mm. The 24mm captured 105 meteors in 9 hours.

December 15–16, 2023

The last night in Umbria would also be a clear one. Due to the two long previous nights, the start was now later again. Jaap only used a Canon R6ii with the 14 mm. Koen did one single visual session between 23^{h}17^m and 03^{h}17^m UT. Wow! What a peace at the firmament: The Geminids only showed up sporadically with a maximum hourly count of 9. In the last hour, this value halved again. Koen counted a total of 96 meteors in 4.00 hours. Jaap's 14mm was no longer as busy as the night before; 34 meteors in 10.5 hours.

In the evening of December 16th, we flew back to Schiphol. We look back on a highly successful campaign. It was just a pity that we didn't see the Betelgeuse cover.

About spectrograms of meteor echoes at different stages of the radiant position – an AI/ML-investigation

Wilhelm Sicking

Augustin-Wibbelt-Straße 13, 48712 Gescher, Germany
wil.sicking@gmail.com

Spectrograms of meteor echoes at different stages of the radiant position of the Quadrantid 2024 shower were examined. The analysis of the January 4th data shows a very surprising result: Spectrograms of meteor echoes close in time to the notch differ significantly from spectrograms of ordinary meteor echoes. They are rather small, have a jagged surface and are similar to the spectrograms of satellites, which have a comb-like structure due to their metal surface. The reason for this could be that, for geometric reasons, only the hot plasma head with similar reflection properties to metal reflects the radar waves. When the meteor trail reflects the waves, the usual soft spectrograms are created.

The effect was discovered because the ML-software mistook meteor echoes for satellite echoes due to their similarity. The second part of this article presents a new neural network with a new class that can recognize these echoes. Data from the Perseids were analyzed with the new model. As with the 2024 Quadrantids, different echoes can be observed in the different phases of the shower. The histogram of the jagged echoes shows, for example, when the radiant of the shower has passed the 0° azimuth mark.

1 Introduction

I was able to record the Quadrantid 2024 echoes on January 4th without interference, allowing a new study of the notch. Notches in meteor histograms are known from the literature. According to Felix Verbelen (Verbelen, 2019) and personal communication with him, there are notches in all major streams. He found that the number of underdense reflections will drastically decrease when the elevation of the meteor radiant becomes high (say above some 60 degrees above the local horizon). At the same time, the number of overdense (and thus long duration reflections) will increase. Wolfgang Kaufmann (Kaufmann, 2020) postulated that due to the Doppler shift, the meteor echo can lie outside the normal receiver bandwidths and is therefore not registered. In my meteor work (Sicking, 2022a) I proposed a mechanism according to which the notch is created by the geometric relationships between transmitter, receiver and radiant. An extensive work by Mike German (German, 2023) precisely explains the geometric relationships in meteor observation.

According to my own work, there are pronounced notches in the Arietids (Sicking, 2022a), in the Geminids (Sicking, 2024) *Figure 11*, and in the Quadrantids, this work. The Perseids show at most a faint notch (Sicking, 2022b) and this work. The new Quadrantid 2024 data should now provide further interesting insights into the notch.

2 Setup

A right hand circularly polarized 4-element Cross-Yagi antenna is used to receive the meteor echoes. The elevation is approximately 30° and it faces south towards Dijon in France. My antennas are mounted in the attic so the configuration can be easily changed. A low-noise preamplifier with a frequency range of 140–150 MHz and a noise figure of 0.25 dB is connected directly to the antenna. The receiver is an Icom IC-R8600. Spectrum-Lab (SL) from Wolfgang Buescher (DL4YHF) is used as recording software. SL generates plots at 20 second intervals with corresponding date and time in the file name, which are later analyzed using machine learning-based software developed by me (Sicking, 2024). The three-class model mask_rcnn_model.061-0.417564.h5 was used for detection.

The ML-software not only counts the echoes, but also determines their size. The neural network was trained with 3D-spectrograms. If an echo is detected, a box is drawn in debug mode and labelled with the score. The program places a polygon over the detected echo that is filled with a transparent color. The area of this polygon (not the box) is logged as the size of the meteor. The plots generated in debug mode and the original Spectrum-Lab plots were then processed into the figures.

3 Results and discussion

3.1 About the Quadrantids

The first two images, *Figures 1 and 2*, document the respective day and provide a first impression. The satellite echoes, the interference and the noise floor are also documented. *Figure 1* shows the raw data from January 4th 2024. The green dots represent the meteor echoes. The sizes of the echoes are plotted logarithmically. A dip around 8h AM, the notch, is clearly visible. *Figure 2* is an hourly histogram. The yellow histogram shows the rate and the red histogram shows the rate weighted by the sizes of the meteors. The size of the meteors is taken from the spectrograms, see Setup section. The blue histogram usually shows satellite echoes. Near the notch, the number of echoes detected as satellites by the ML-software

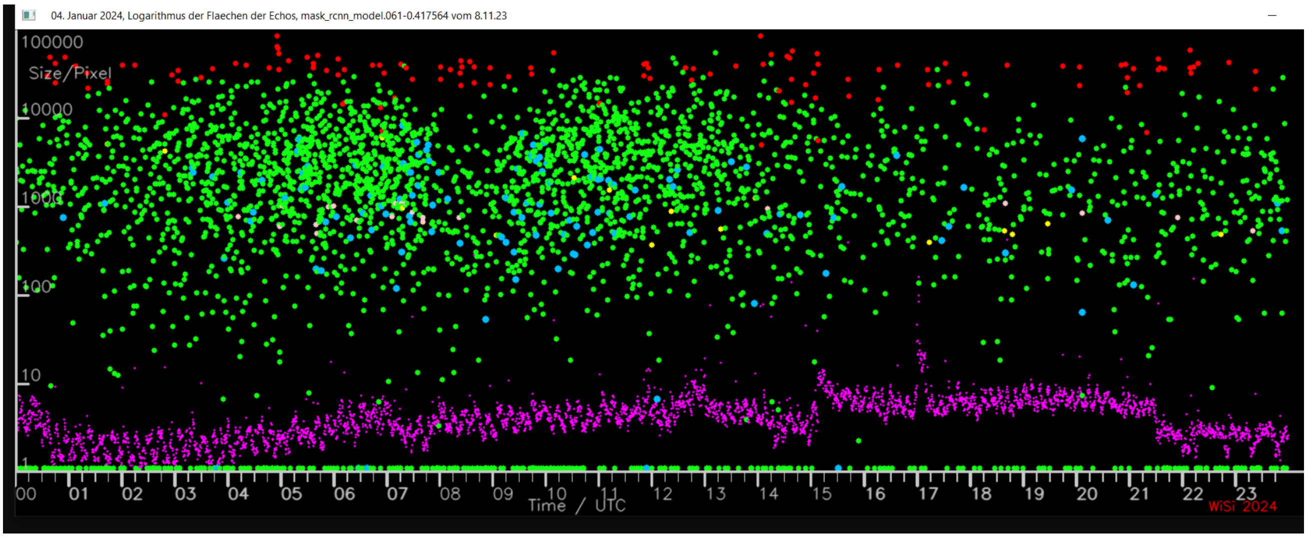

Figure 1 – Measured meteor sizes as a function of time, recorded on January 4th 2024. Each green dot represents an echo. 2962 echoes were recorded. A drastic decrease in the rate can be seen at 8h AM. The blue dots represent satellite echoes. For clarity they were plotted slightly larger than the green meteor echoes. An unusually large number of satellite echoes are registered near the notch. An explanation of this is given in the text. The purple curve shows the background noise. The red and pink dots show detected interference. There were no significant disturbances that could have distorted the result.

increases and decreases with the rise and fall of positively detected meteors. This is obviously an artefact. The following analysis shows that these are also meteor echoes, but due to their unusual surface structure they were mistaken for satellite echoes by the ML-software.

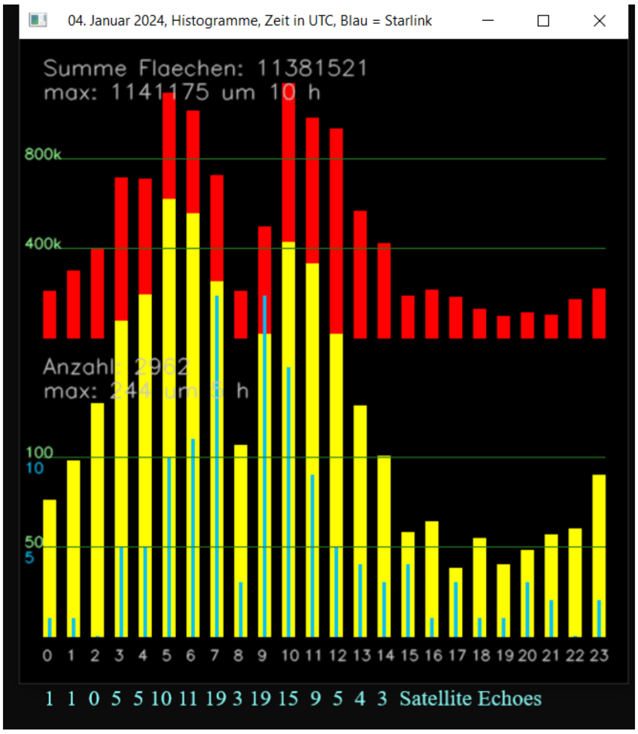

Figure 2 – The yellow histogram shows the rate and the red histogram shows the rate weighted by the sizes of the meteors. The notch at 8h AM is clearly pronounced. The number of echoes detected as satellites by the ML-software (blue) increases and decreases with the rise and fall of positively detected meteors at the notch. This is an artefact of the ML-software, see text.

About the observation of Quadrantid meteors with the GRAVES radar

First, I examined the azimuth of the radiant of the Quadrantids using Stellarium–Web. The star 44 Boötis was chosen as the radiant because, according to the CMOR radar, it occupied approximately the position of the radiant of the Quadrantids. At 7h51m AM the azimuth Dijon / 44 Boötis is 0° and the elevation of the star is 89°. At this time the radiant is in front of or over the GRAVES radar, so that the meteor tracks run towards the transmitter. Meteor tracks and radar waves then meet (more or less) head-on in a line.

Although GRAVES and my cross–Yagi are directional antennas that look south with a certain opening angle, meteor echoes can be received from all directions because of the back- and side lobes, see e.g. Mike German (German, 2023) and posts in the Astronomy forum[27,28]. There are examples where echoes were received at the GRAVES and BRAMS frequencies at the same time. In my work (Sicking, 2022b) it was shown that an omnidirectional antenna, a vertically polarized Discone, detects significantly more Perseid echoes than the directional antenna. That shows that echoes can also be detected overhead and north of GRAVES. The radiant does not have to be in the main lobes of the antennas. Of course, the observer receives the strongest echoes from the south often with the typical GRAVES glitches. Also because of the high power of the GRAVES radar, meteor detection works in all directions.

The high elevation angle of the radiant is not the reason for the notch. Lower elevation angles also create notches. For example, the elevation of the Arietids at the notch is 66° (Sicking, 2022a). The heights around the notch in the case of the Quadrantids 2024, viewed from Dijon, are:

---

27 https://forum.astronomie.de/threads/meteorecho-mit-graves-und-brams-gleichzeitig-erwischt.316517/

28 https://forum.astronomie.de/threads/parallel-aufzeichnung-von-brams-meteor-echos-und-graves-meteor-echos.308016/

- $6^h = 71°$ sin(71) = 0.946
- $7^h = 81°$ sin(81) = 0.987
- $8^h = 88°$ sin(88) = 0.999
- $9^h = 78°$ sin(78) = 0.978
- $10^h = 68°$ sin(68) = 0.927

In contrast, the increase and decrease in the "visibility" of the meteor follows the sine around 0°. At an azimuth of 0°, the trail is not illuminated by the radar waves because it is hidden by the head. But at 20°, for example, 34% (sin(20) = 0.342) is "visible". For this reason, the notch has a slim shape. For elevation, 20° only means a change in the second decimal place, see above.

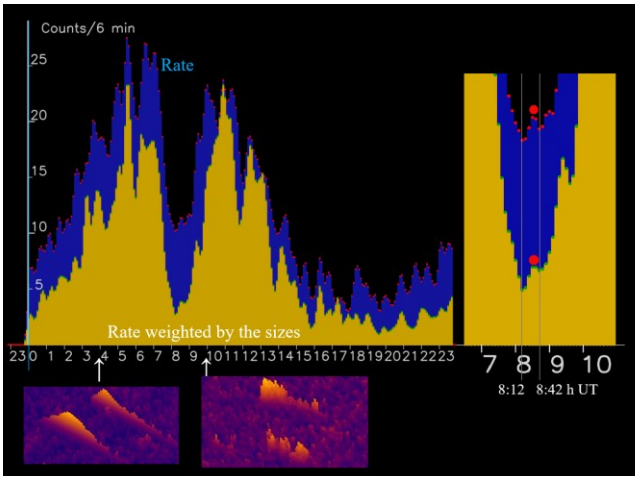

Figure 3 – The figure shows two histograms with a time resolution of 6 minutes. This allows details such as the In-Line-Peak to be displayed. One spectrogram from 3^h54^m AM from before the notch (smooth) and one spectrogram from near the notch (jagged) from 9^h58^m AM have been included, see also the Figures below. The inset on the right shows enlarged the In-Line-Peak, see the red dots. The histograms are smoothed with a fixed Gaussian like filter with the coefficients 0.31, 0.74, 1.0, 0.74 and 0.31.

Examination of the notch

The notch of the high-resolution histogram in *Figure 3* shows two minima and the In-Line-Peak (Sicking, 2022a), see the red dots. The first minimum appears at 8^h12^m AM, the second minimum at 8^h42^m AM. The cause of the time difference between the 0° azimuth of 44 Boötis (7^h51^m AM) and the first minimum of the notch (8^h12^m AM) is still unclear. From my understanding the times should be identical. Of course, the In-Line-Peak is weak, so the peak and minima could simply be noise like the other peaks. However, I observed the In-Line-Peak in the Arietids (Sicking, 2022a), see for example *Figure 8* in the article and also in the Geminids (Sicking, 2024) see *Figure 11* in the article, so perhaps they are real signals after all. Further investigations will follow.

Examination of the echoes at the notch

Spectrograms from four times before and one after the notch are shown in *Figures 4 to 8*. The aim is to examine the change in meteor echoes and the increase in satellite echoes towards the notch. I chose the plots so that as many echoes as possible are combined in one image in order to keep the number of images as low as possible. Because of the importance of the statement, there were five figures.

Figure 4 from 3^h54^m AM shows meteor echoes commonly seen. They have the typical curved, often Gaussian shape and a smooth surface. There are of course other forms of echoes, but they don't play a role here.

The notch occurs because the echoes become smaller and at some point, are no longer perceptible. This will be examined in more detail in the next section. However, the shape of the echoes also changes drastically towards the notch: They have a jagged surface, see *Figures 5, 6, 7 and*

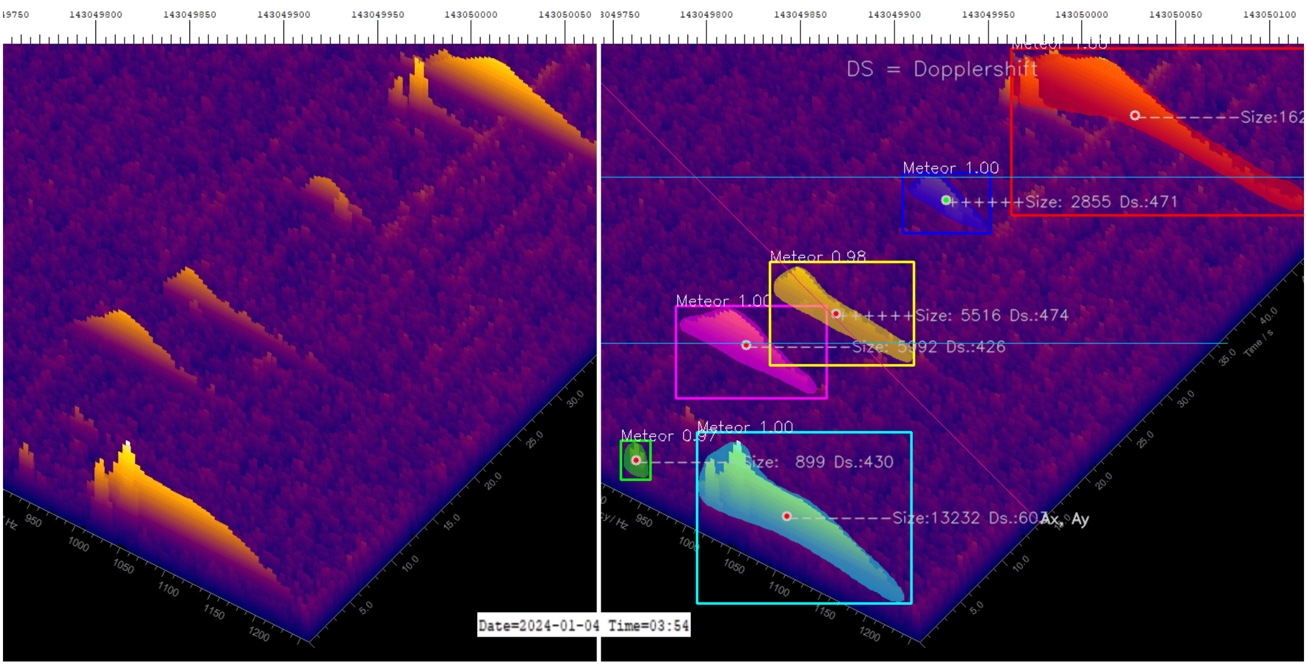

Figure 4 – At 3^h54^m AM, examples of "normal" echoes. The original Spectrum-Lab Echoes are shown in the left half of the picture. The echoes examined with the AI software are shown on the right. The colorful polygons represent the sizes of the echoes. For details see my AI work (Sicking, 2024).

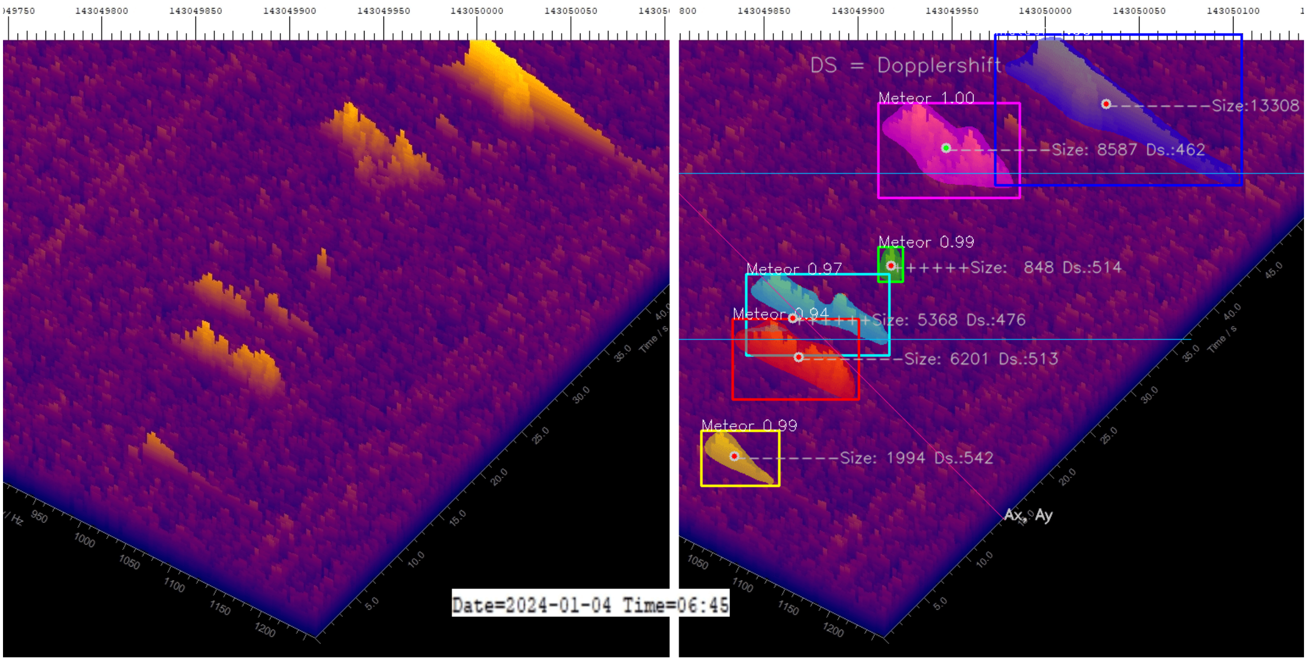

Figure 5 – At 6^{h}45^{m} AM, the echoes show clearly a jagged surface, but are still correctly recognized by the ML-software.

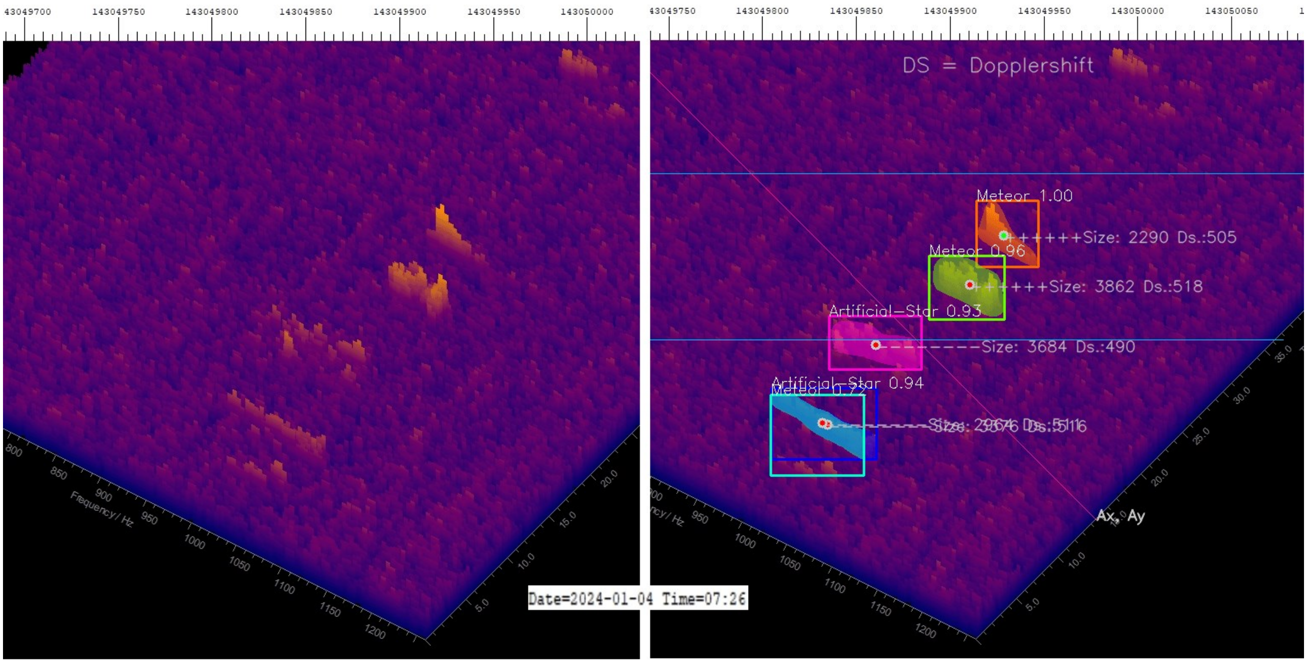

Figure 6 – At 7^{h}26^{m} AM, the echoes are very small and are almost no longer observable. Two faint echoes are recognized as satellites.

8. It is now clear why the number of satellite echoes increases near the notch: Some echoes are more similar to satellite echoes, than they look like normal meteor echoes used in training the ML-model.

From this it can be concluded that *Figures 5 to 8* show spectrograms of meteor echoes in which essentially only the head was exposed to the radar waves. The hot plasma head apparently has similar reflection properties to the surface of the satellites, which produce echoes with a comb-like structure due to their metal surface (Sicking, 2024). If the trace also reflects, a softer echo is created, according to my hypothesis.

With previous meteoroid streams I already noticed that echoes near the notch are jagged. The increase in satellite echoes near the notch occurred for the first time in the 2024 Quadrantids.

Finally, the fact that near the notch the number of echoes detected as satellites by the ML-software increases and decreases with the rise and fall of positively detected meteors shows that there is a systematic relationship.

Such spectrograms are not contained in the training data of the ML-model used, or are only contained sporadically. However, the reason for the notch is not the wrongly

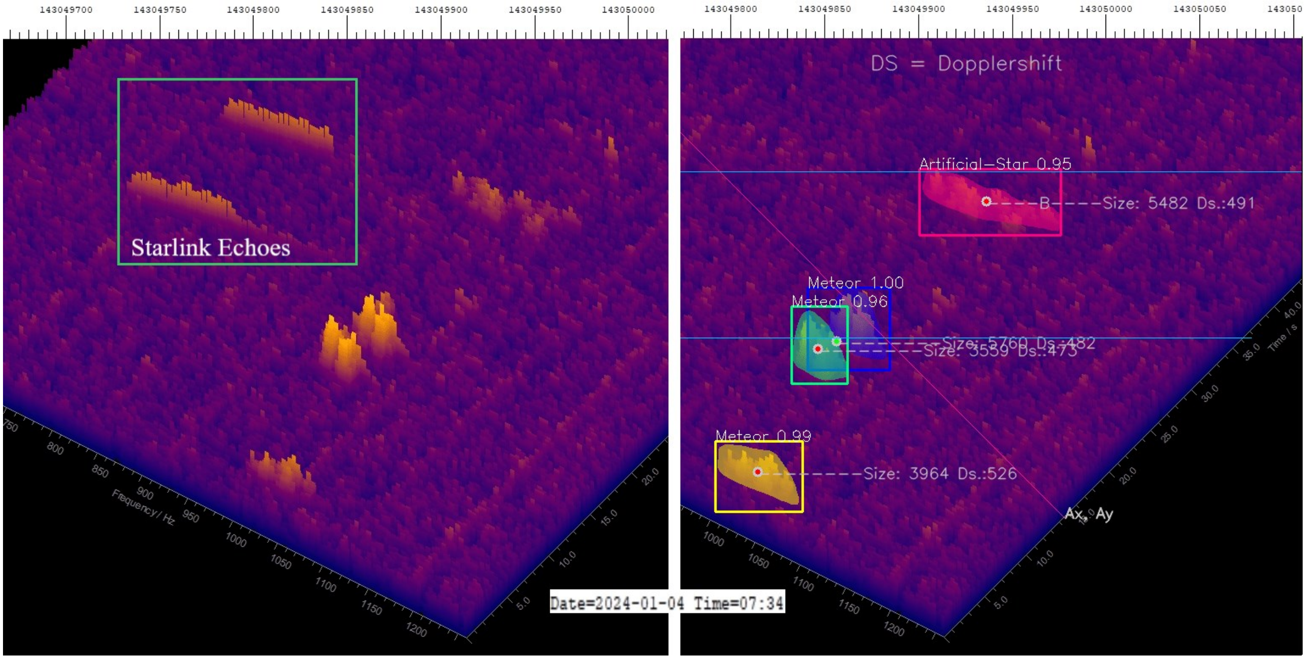

Figure 7 – At 7ʰ34ᵐ AM. An echo (magenta) is incorrectly recognized as a satellite. The inset at the top left shows real Starlink echoes for comparison.

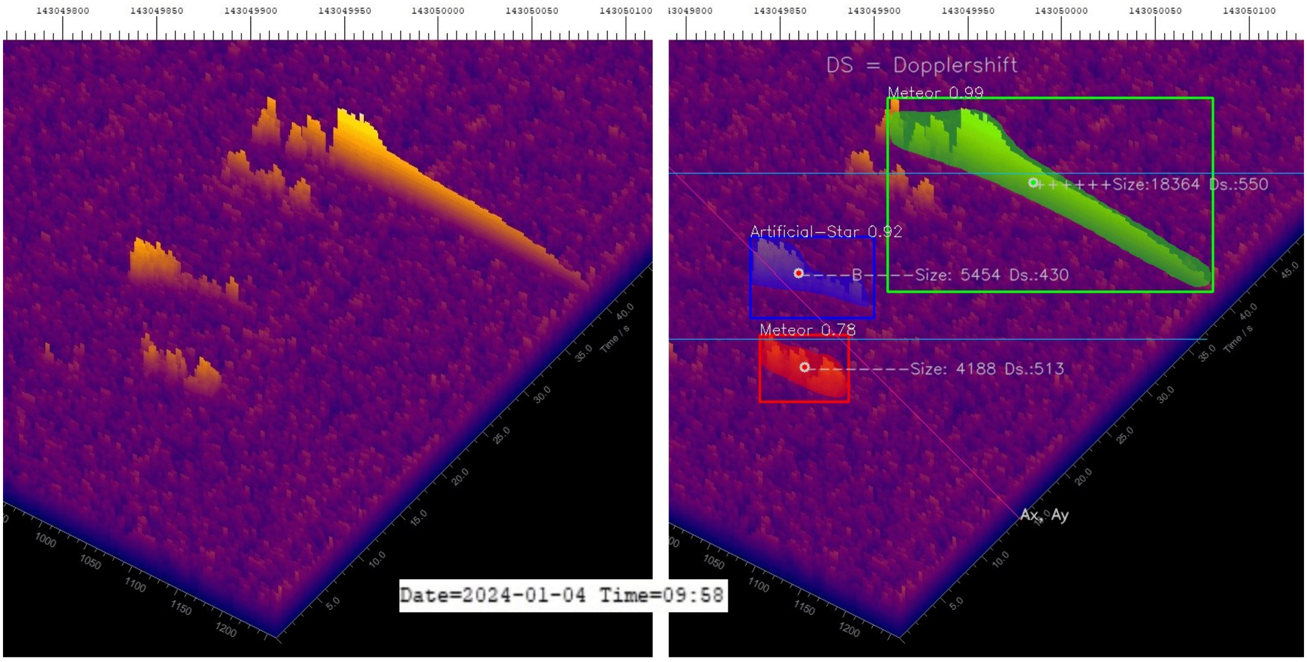

Figure 8 – At 9ʰ58ᵐ AM. Of the four echoes, only two are recognized as meteors. The red echo also has a bad score of 0.78, the blue echo is recognized as a satellite and an echo is not recognized at all.

detected or undetected echoes. At 7ʰ AM 198 meteor echoes were recorded. Another 19 echoes were mistaken for satellites, representing an error of about 10%. The notch is also recorded by other observers.

Examination of the rates and the rates weighted by the sizes of the echoes

Figure 9 shows the echoes divided into four classes of sizes. The most important result is shown by the yellow trace, which represents the small echoes: The small echoes have a (secondary) maximum at the minimum of the notch, see the yellow dot. The amount of the larger meteors is decreasing. This does not mean that the number of small echoes has increased, but it means that large echoes now appear smaller due to perspective and appear in the class of small echoes. The maximum of the yellow trace in the minimum of the notch is therefore a confirmation of the theory that geometric conditions as described above cause the notch.

3.2 An extension of the neural network from three to four classes

The Quadrantids 2024 of January 4ᵗʰ contain many spectrograms of meteors with a jagged structure, as shown above. A lot of these echoes were incorrectly detected as satellites. I therefore trained a new neural network with the data from this day.

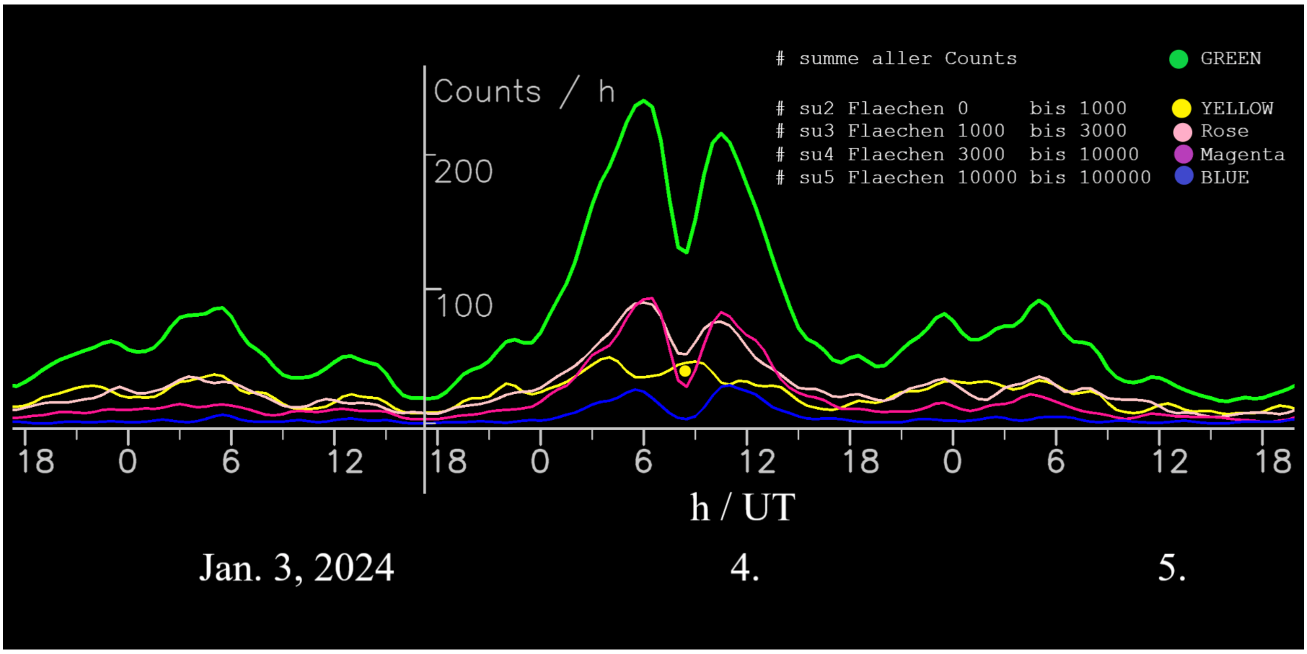

Figure 9 – Meteor rates for different echo sizes of the 2024 Quadrantids over three days. The blue line represents the rate of large echoes (10000 to 100000 pixels), the purple/magenta line shows the medium sized echoes (3000 to 10000 pixels), the pink line shows the echoes (1000 to 3000 pixels) and the yellow line shows the small echoes (below 1000 pixels). Finally, the green curve shows the rate of all echoes summed up. The yellow trace (echoes under 1000 pixels) shows a maximum (see yellow dot) where the notch and all other meteor sizes have a minimum. The histograms are smoothed with a fixed Gaussian like filter with the coefficients 0.25, 0.71, 1.0, 0.71 and 0.25.

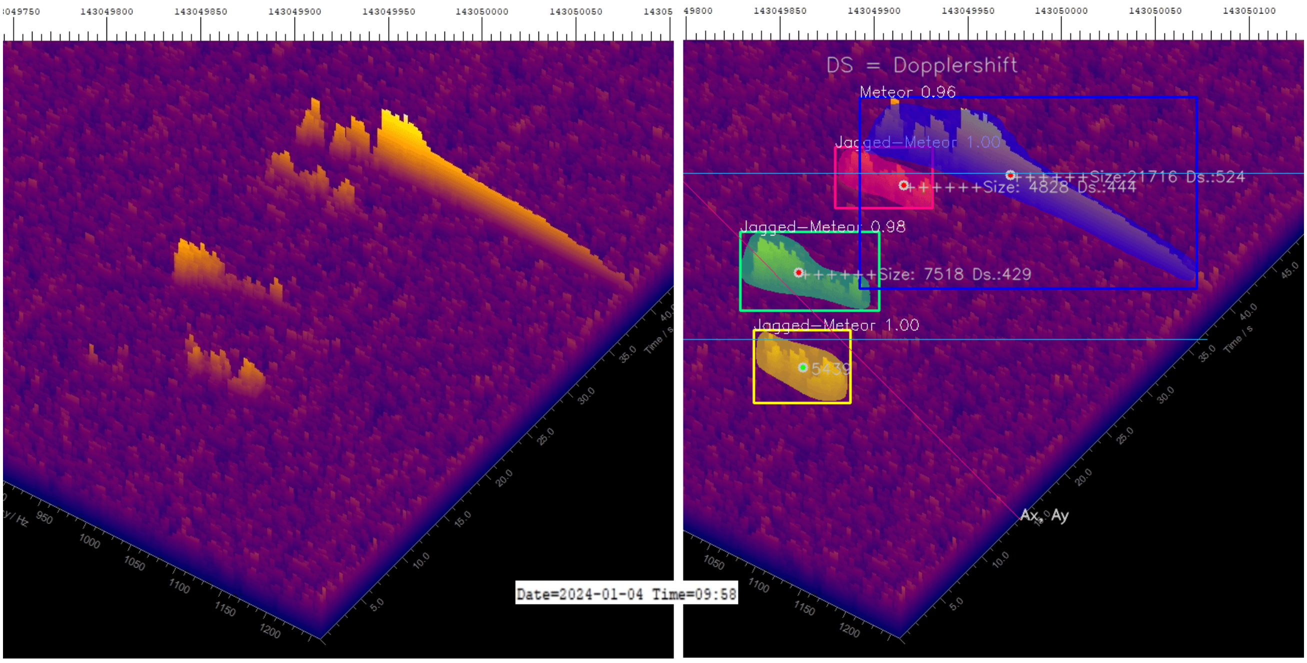

Figure 10 – At 9^h58^m AM. *Figure 10* is based on the same Spectrum-Lab diagram as *Figure 8*. With the new 4-class model, all meteor echoes are correctly detected: three as jagged echoes, one as normal echo. In *Figure 8*, only two echoes were correctly detected. This plot is not included in the training data. It was saved for testing and demonstration purposes.

The model used so far with the three classes “Artificial Star”, “Background” and “Meteor” is based on 506 Spectrum-Lab plots, which contain multiples of signals. Now I have labelled a new class with 93 plots and almost 200 echoes of jagged spectrograms. The echoes are from near the Quadrantid notch from 6^h AM to 9^h59^m AM on January 4th 2024. The old model still contained around 20 jagged echoes. This explains that they were partially recognized. These have been transferred to the new so called Jagged-Meteor class. The new 4-class model now also recognizes the jagged spectrograms, see *Figure 10*. The same Spectrum-Lab plot as in *Figure 8* was used. With the new 4-class model, all meteor echoes are correctly recognized: three as jagged echoes, one as a normal echo. Of course, the plot is not included in the training data set.

I wasn’t actually supposed to study the January 4th Quadrantids with the new model because the echoes were used in training. Nevertheless, I would like to show the

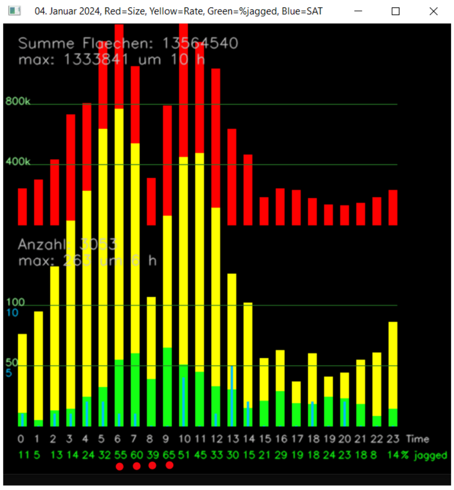

Time	0	1	2	3	4	5	6	7	8	9	10	11	12	13	14	15	16	17	18	19	20	21	22	23
Rate	76	95	132	170	195	246	263	234	107	174	223	226	181	126	102	56	63	37	60	41	44	55	61	86
Jagged	8	5	17	24	46	78	145	141	42	113	113	101	59	38	15	12	18	7	11	10	10	10	5	12
Jagged %	11	5	13	14	24	32	55	60	39	65	51	45	33	30	15	21	29	19	18	24	23	18	8	14

Figure 11 – The figure shows the analysis of the data from January 4th 2024 with the new model. The yellow and red histograms show the rates and the size-weighted rate of the meteors as in *Figure 2*. The rate, i.e. the yellow histogram, is listed again with numbers in the second line. The values contain all positively detected meteors and jagged meteors. Line three shows the number of jagged echoes it contains. The fourth line is the percentage of jagged echoes, i.e. the number of jagged echoes/total number × 100%. These values are plotted in the green histogram. It must be remembered that data from 6h–9h AM (see the red dots) were used in training. The old model counted 2962 meteor echoes and 127 satellite echoes. That's a total of 3089 echoes. The new model counts 3053 meteor echoes and 25 satellite echoes. That's a total of 3078 echoes.

evaluation to demonstrate the new model, see *Figure 11*. It shows a similar output to *Figure 2*. The yellow and red histograms show the rate and the size-weighted rate of the echoes. The jagged echoes are included in these values. The green histogram is new. It shows the percentage of jagged echoes.

The satellite echoes no longer correlate with the meteor echoes. The proportion of jagged echoes provides interesting insights. For example, 65% of jagged echoes are present at 9h AM. This is a significant difference from midnight. However, it must be remembered that data from 6h–9h AM (see the red dots) were used in training. In the next chapter, I used this method to examine data that were not used in training.

First results achieved with the new neural network

The following analysis of the Perseids 2022 shows the possibilities of the method very clearly. The model is not yet perfect and still needs to be fed with additional label data. Occasionally, double detection of normal and jagged echoes occurs. However, I have checked all analyses using a high score method: Only echoes with a probability greater than or equal to 98% were analyzed. This does not change the statement. One example is shown below.

I selected the data from August 10th to 14th 2022 because no data from these days were used for training and there was relatively little interference.

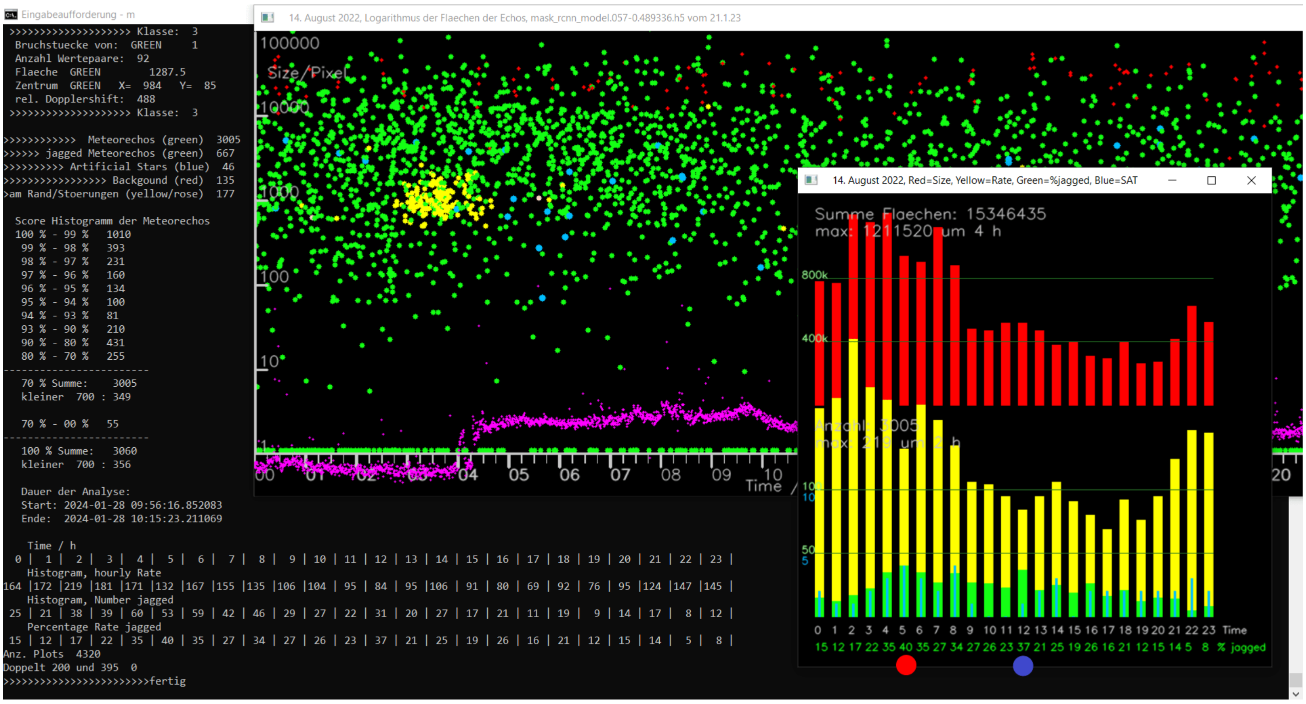

Figure 12 – This shows an example of the output of my ML-software from August 14, 2022. The data from the inset on the right are included in *Figure 14* . From 3h AM, many moon echoes were received, see the accumulation of yellow dots. The percentage of the jagged echoes has a maximum at 5h AM, indicating, that the radiant has crossed the 0° mark, see the red dot. However, there is a second maximum at 12h PM, see the blue dot. In combination with the small notch, one can conclude that there was a second radiant, see text.

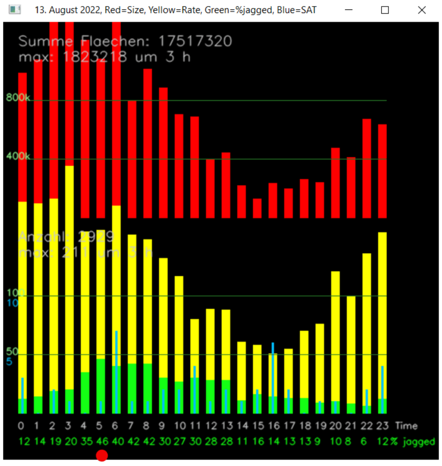

Time	0	1	2	3	4	5	6	7	8	9	10	11	12	13	14	15	16	17	18	19	20	21	22	23	h / UT
Rate	180	179	183	211	155	156	177	152	148	132	117	80	89	88	61	58	51	55	70	76	121	100	136	154	Aug.13
Jagg	21	25	34	42	54	71	71	64	62	40	32	24	25	25	7	9	7	7	9	7	12	8	8	18	Aug.13
Jagg%	12	14	19	20	35	46	40	42	42	30	27	30	28	28	11	16	14	13	13	9	10	8	6	12	Aug.13
Score >= 0.7 3005 Echoes																									
Jagg%	15	12	17	22	35	40	35	27	34	27	26	23	37	21	25	19	26	16	21	12	15	14	5	8	Aug.14
Jagg%	12	14	19	20	35	46	40	42	42	30	27	30	28	28	11	16	14	13	13	9	10	8	6	12	Aug.13
Jagg%	8	12	8	10	25	35	31	34	26	22	18	31	22	18	32	7	13	27	22	17	11	17	15	10	Aug.12
Jagg%	8	4	5	11	18	40	32	31	19	22	21	23	34	18	20	10	20	16	25	15	15	22	9	18	Aug.11
Jagg%	8	5	8	11	25	32	29	20	29	21	33	17	17	22	19	12	15	17	14	17	19	17	13	14	Aug.10
Score >= 0.98 1403 Echoes																									
Jagg%	6	6	6	14	24	35	25	10	21	12	14	15	34	3	9	12	5	12	3	3	6	3	4	2	Aug.14
Score >= 0.99 1010 Echoes																									
Jagg%	5	7	3	13	26	48	21	10	29	15	17	19	45	0	6	12	4	14	4	3	9	3	3	1	Aug.14

Figure 13 – The histogram shows the analysis of the data from August 13th 2022 with the new model. The yellow and red histograms show the rate and the size-weighted rate of the meteors as in *Figure 2*. The rate, i.e. the yellow histogram, is listed again with numbers in the second row. The values contain all positively detected meteors and jagged meteors. Row three shows the number of jagged echoes it contains. The fourth line is the percentage of jagged echoes, i.e. the number of jagged echoes/total number × 100%. These values are plotted in the green histogram. The remaining rows show the percentage of jagged echoes from August 10th to 14th. With the exception of 10th August the percentage of jagged echoes has a maximum at 5h AM, see the values marked in red. The last two rows show an evaluation from August 14th, in which the score was set to 0.98 and 0.99. The blue dots indicate a local maximum on the same day.

Figure 12 shows an example of the output of my ML–software from August 14th, 2022. The data from the inset are included in the table in *Figure 13*. Similar plots were evaluated from August 10th to 14th and summarized in the table.

From 3h AM, many moon echoes were received, see the accumulation of yellow dots. This shows how powerful the GRAVES radar is.

The table in *Figure 13* shows that on almost all days the percentage rate of jagged echoes has a maximum around 5h. In order to compare this time with the azimuth of the Perseids, I determined the 0° azimuth of the radiant using Stellarium–Web.

The star HD15449 was chosen as the position of the Perseid radiant. It has an azimuth of 0° and an elevation of 79° at 5h43m AM on August 14th.

However also eta Persei (6h02m AM, 0° Az., 81° El.) and gamma Persei (6h17m AM, 0° Az., 83° El.) may be good candidates.

These times fit with the maximum of percentage of jagged echoes at 5h AM. Also, a small notch can be seen in the histograms from August 13th and 14th 2022 at this time.

However, upon closer inspection, there are two maxima in the green histogram in *Figure 13* that are similar to those of the Quadrantids (*Figure 11*), only significantly weaker. Such notches are actually faintly visible in the table. The numerical values on August 13th are 5h = 46%, 6h = 40%

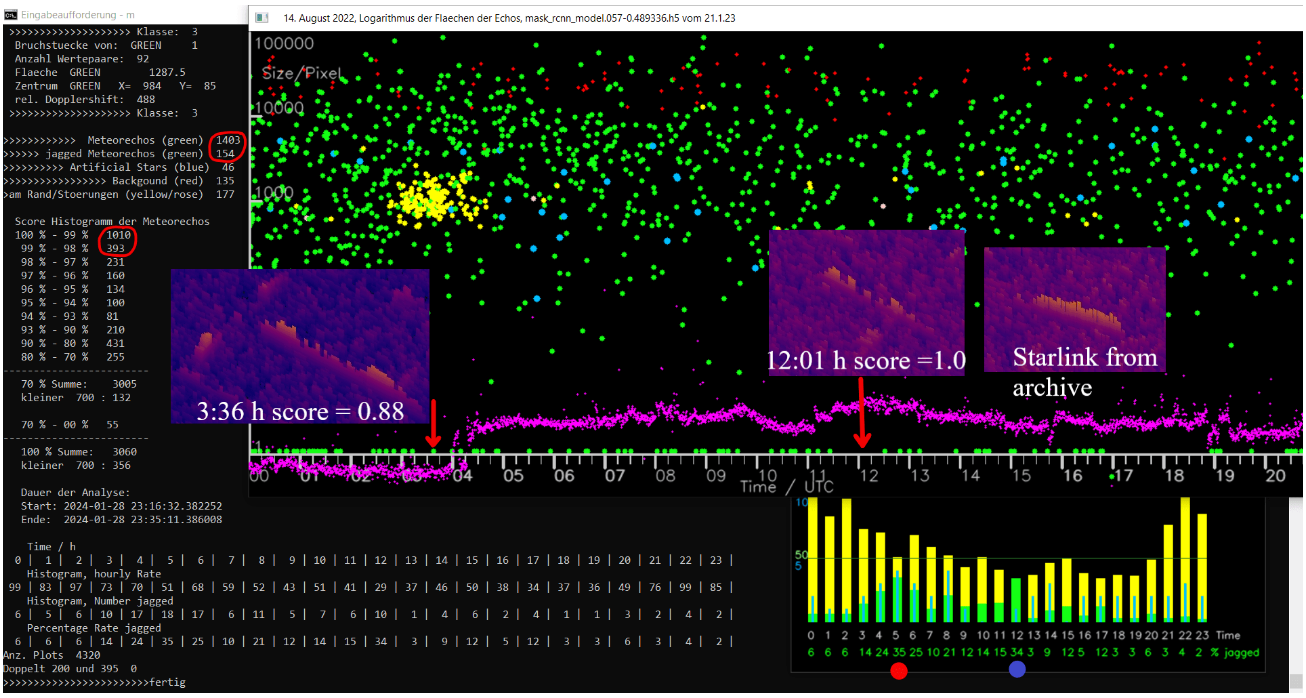

Figure 14 – The same day as *Figure 12*, August 14th. However, only values that have a probability of better than or equal to 98% were included in the analysis. The values are included in the table in *Figure 13*. The insets show examples of the background. The comparison shows that the noise in the plot is shown greatly enlarged and the level should have no influence. The inset on the left side shows two moon echoes and a jagged meteor with a score of 0.88, see also the graphical abstract. The middle inset shows a jagged meteor with a score of 1.0 from 12h AM. It belongs to the postulated burst. The echo in the inset on the right is a starlink echo from archive for comparison, see text.

and 7^h = 42%. On August 12th the corresponding values are 5^h = 35%, 6^h = 31%, 7^h = 34%. The radiant passage at 0° was therefore closer to 6^h AM, which corresponds well with the times of the three stars.

A burst and the high score test

At 12^h PM on August 14th, the percentage of jagged spectrograms is quite high at 37%, see the blue dots in *Figures 12, 13 and 14*. According to my work (Sicking, 2022b), there was a small outburst at this time.

In order to prevent errors, e.g. due to double detection or false detection, I also carried out all evaluations with a high score. Only values whose probability is greater than or equal to 98% were included in the evaluation. *Figure 14* shows an evaluation using this method from August 14th. Of the 3005 echoes in *Figure 12*, only 1403 echoes meet the criterion. Although there are fewer but better points in the evaluation, the test confirms the result of *Figure 12*: The two maximums at 5^h AM and 12^h PM remain. A final test with a score of 0.99 confirms the result and increases the two maxima even further, see the last entry in the table in *Figure 13*.

Figure 14 also shows three insets. This is intended to show that the noise floor has no influence on the quality of the echoes. A comparison with a Starlink satellite is also shown. One difference between the satellite echo and the meteor echo is the angle created by the different Doppler shift. The jagged echo from 12^h PM has a score of 1.0. The satellite has a score of 0.98, in its class of course.

To the errors

In *Figures 12 and 14* it appears that the green histogram correlates with the satellites up to 7^h AM. This is not a systematic error. On other days, the distribution of satellite echoes is random, see e.g. *Figure 13*. The satellite scale is also stretched by a factor of 10 compared to the scale for the rate. There are only four satellite echoes at 5^h AM. Two of them are unrecognized meteors. Of course, the software does not work without errors. There are double and false recognitions. I therefore repeated the evaluations using the high score method. Only echoes with a probability greater than or equal to 98% were evaluated. That's about half, see *Figure 13*. This should reveal an error in the system. However, the high score method confirmed the result of the overall analysis, see *Figure 14* and the table in *Figure 13*, last two rows.

Finally, I only examined one stream over several days and not several streams with perhaps only one day. This makes it easier to identify errors and outliers.

What do I want to do with it?

So far, my approach has been to detect weak showers observing the notch, because a notch is easier to detect than a broad maximum. This is also used, for example, for the minimum bearing. Radio-amateurs use the procedure in the so-called "Foxhunting". According to this work, the azimuth passage can be extracted directly from the shape of the spectrograms, as the echoes are "smooth" far from the 0° / 180° azimuth passage and "jagged" near and at the passage. The method also appears to be sensitive: A (secondary) maximum at 5^h AM can already be seen on August 10th and a second maximum at 12^h PM on August 14th probably indicates a second radiant.

Further investigations will follow. For further measurements I will test another location in the near future, see (Sicking, 2024) *Figure 12*. This is a location without interference, at least when there is no contest operation.

4 Conclusion

Inspired by an obvious artefact, I examined spectrograms at different stages of the radiant position of the Quadrantid 2024 shower. The work shows that spectrograms taken near the notch are different from spectrograms taken at other times. It is concluded that spectrograms could be used to identify meteors where the radar waves hit the meteor head-on and illuminate only the plasma head.

In addition, the theory that geometric conditions cause the notch has been experimentally proven.

In the second part of the article, a new neural network was presented. The new model appears to be well suited to studying meteor spectrograms at different stages of the shower. The percentage of jagged spectrograms provides interesting insights into the showers and will be used to study future showers and sporadic meteors. This is going to be exciting.

Acknowledgment

Many thanks to *Mike German*, *Stefanie Lück*, *Kerstin Sicking*, *Ulrich Sperberg* and *Felix Verbelen* for proofreading and for the many comments. My special thanks go to *Mike German*, who made many detailed comments and suggestions for improvement. This greatly enhanced this article.

References

German M. T. (2023). "Utilizing Video Meteor Trails to Understand Radio Meteor Detection". *WGN, Journal of the IMO*, **51**, 72–92.

Kaufmann W. (2020). "Limitations of the observability of radio meteor head echoes in a forward scatter setup". *WGN, Journal of the International Meteor Organization*, **48**, 12–16.

Sicking W. (2022a). "A Notch in the Arietids Radio Data and a new so called In-Line-Effect". *eMetN*, **7**, 331–335.

Sicking W. (2022b). "Radio observations on the Perseids and some other showers in August and September 2022". *eMetN*, **7**, 407–410.

Sicking W. (2024). "Meteor detection using Artificial Intelligence and Machine Learning". *eMetN*, **9**, 29–36.

Verbelen F. (2019). “Meteor velocity derived from head echoes obtained by a single observer using forward scatter from a low powered beacon”. *WGN, Journal of the International Meteor Organization*, **47**, 49–54.

Quadrantids 2024 by radio meteor observations

Hirofumi Sugimoto[1] **and Hiroshi Ogawa**[2]

[1] **The Nippon Meteor Society**
hiro-sugimoto@kbf.biglobe.ne.jp

[2] **The International Project for Radio Meteor Observations**
h-ogawa@amro-net.jp

The Quadrantids 2024 showed a much higher activity than on average during past years. The peak was recorded with *AL* = 8.3 ± 1.3 and a ZHR_r = 226 ± 5 at $\lambda_\odot$ = 283.04°– 283.17° (2024 January 4, 6^h30^m – 9^h30^m UT). Also, a sub-peak has been observed after the main peak which reached *AL* = 7.4 ± 1.1 and a ZHR_r = 135 ± 14 at $\lambda_\odot$ = 283.43°– 283.55° (2024 January 4, 15^h30^m – 18^h30^m UT). As a result, this activity has been observed separately as two components, one was the regular activity which had *AL* = 8.5 at $\lambda_\odot$ = 283.13° and the other was a sub-peak with *AL* = 6.5 at $\lambda_\odot$ = 283.47°. The enhanced regular activity such as in 2024 has been also observed in the past. On the other hand, however, a strong sub-peak after the main peak has never been observed in past.

1 Introduction

The Quadrantids are one of most famous annual meteor showers. The regular peak reaches Zenithal Hourly Rate (ZHR) = 80 at $\lambda_\odot$ = 283.15° (Rendtel, 2023). For 2024, the regular peak was predicted at $\lambda_\odot$ = 283.15° (January 4, 9^h00^m UT).

Radio meteor observing allows to obtain a complete activity profile even with bad weather and during daytime. Besides, the International Project for Radio Meteor Observations (IPRMO) has been organized to analyze the entire meteor shower activity without any radiant problems in 2001 (Ogawa et al., 2001). During past research, the activity profiles were derived from worldwide radio data from the Radio Meteor Observation Bulletin (RMOB).

The Quadrantid activity has also been analyzed by IPRMO. The average value for the period of the past 10 years has an Activity Level Index (*AL*) = 4.5 at $\lambda_\odot$ = 283.15° (Ogawa, 2022). Besides, Ogawa and Steyaert (2017) described that the maximum was sometimes observed with a higher activity than during most annual returns.

This paper reports the result obtained for the Quadrantids 2024 using worldwide radio meteor observations.

2 Method

To analyze the worldwide radio meteor observation data, the meteor activity is calculated by the "Activity Level Index: *AL*(t)" (Ogawa et al., 2001) and the estimated Zenithal Hourly Rate: ZHR_r(t) (Sugimoto, 2017). A lot of meteor showers have already been analyzed by this method.

3 Results

3.1 Activity Level Index

Figure 1 shows the result for the Activity Level Index. A gray line means an average for the period of past 10 years by IPRMO. A main peak was detected with *AL* = 8.3 ± 1.3 at $\lambda_\odot$ = 283.04° (January 4, 6^h30^m). The maximum peak was one and a half times stronger in activity. Although the peak time was earlier than for the past average, it seems that this was caused by a few reports. A second peak was observed at $\lambda_\odot$ = 283.43° (January 4, 15^h30^m). The *AL* reached 7.4 ± 1.1, the second peak was weaker than the main peak.

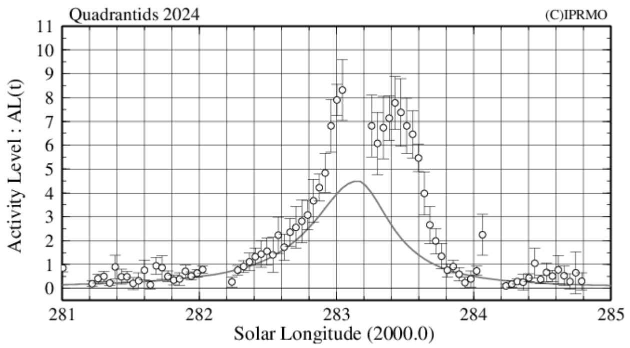

Figure 1 – The activity Level Index for the Quadrantids 2024 using 39 datasets from 10 countries (gray line: average for the period of the past 10 years).

Figure 2 shows an estimated activity profile using a Lorentz profile. A first peak had *AL* = 8.5 at $\lambda_\odot$ = 283.13° (January 4, 8^h30^m) with *FWHM* = –0.25°/+0.15° and a second peak had *AL* = 6.5 at $\lambda_\odot$ = 283.47° (January 4, 16^h30^m) with *FHWM* = –0.15°/+0.15°. The first peak was at the same time as the regular maximum ($\lambda_\odot$ = 283.15°).

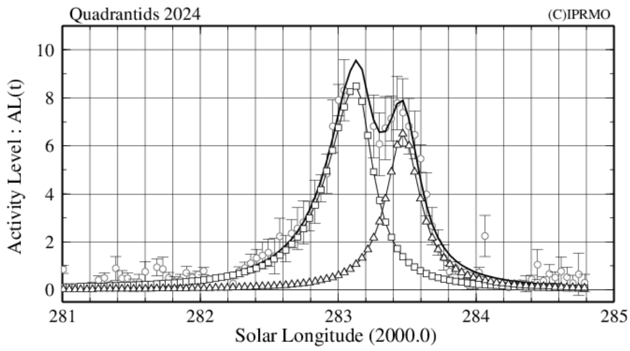

Figure 2 – The components of the Activity Level Index for the Quadrantids 2024 (squares: component of the first peak, triangles: second peak, solid line: first and second peak).

3.2 Estimated ZHR_r

Since the Activity Level Index is difficult to compare to visual observations, an estimated ZHR_r was calculated in *Figure 3*. The first peak reached $ZHR_r = 226 \pm 5$ at $\lambda_\odot = 283.17°$ (January 4, 9^h30^m). Although this is later than in *Figure 1*, it is difficult to conclude when exactly a first peak occurred because there was not enough data available. A second peak has been recorded with $ZHR_r = 135 \pm 14$ at $\lambda_\odot = 283.55°$ (January 4, 18^h30^m). This peak occurred later and weaker than in *Figure 1*, both figures have large error margins around the time of the second peak. Therefore, it is difficult to conclude when a second peak occurred.

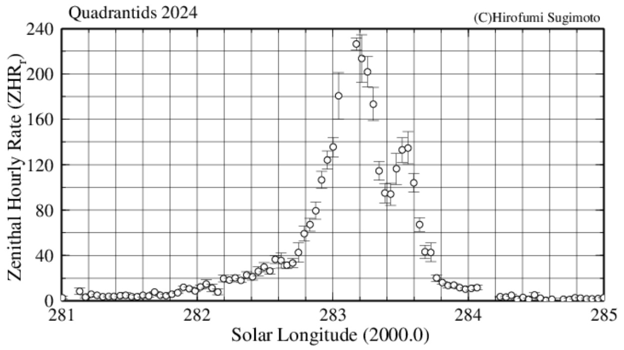

Figure 3 – The ZHR_r-distribution for the Quadrantids 2024 using 41 datasets.

4 Discussion

4.1 Influence of the zenithal effect

Section 3 described that the Quadrantids 2024 had two peaks. When a radiant of a meteor shower which has an average geocentric velocity is located near the zenith, the number of meteor echoes decrease temporary. This is called the "zenithal effect". The radiant of the Quadrantids comes near the zenith for most observing stations in the Northern hemisphere. Therefore, it is necessary to consider which data to use.

This study has already taken into account this effect and data from locations with the radiant located near the zenith as well as with the radiant at too low elevation had been removed. Therefore, it can be concluded that the double peak was not caused by the zenithal effect.

4.2 Past records

The Quadrantids sometimes show a strong activity. A recent result with $AL = 7.8 \pm 1.1$ has been recorded at $\lambda_\odot = 283.11°$ in 2021. A value of $AL = 7.5$ had been estimated for the main component (Ogawa and Sugimoto 2021). Moreover, other surprisingly rich activities have been observed in 2021, 2019, 2016, 2014, 2004 and 2002 since this project started in 2001 (*Table 1*).

A double peak has also been detected in the past. *Figure 4* and *Table 2* show a similar case in 2024. Although a sub peak after the main peak has been detected, it has never reached an activity as strong as in 2024. The activity level in 2024 was two or three times higher than in past years.

On the other hand, a sub-peak did not only occur after the main peak but also before the main peak such as in 2021 and in 2019.

Table 1 – Strong main activity peaks recorded during past years (average for the period of 2002–2023).

Year	Peak $\lambda_\odot$	Activity Level
2004	283.31°	9.0
2014	283.11°	8.0
2016	283.14°	8.0
2019	283.17°	8.5
2021	283.11°	7.5
2024	283.13°	8.5
average	283.15°	4.5

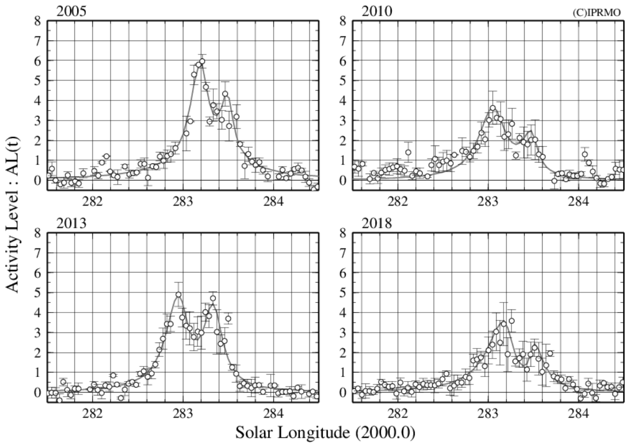

Figure 4 – Similar results from past years comparable to the 2024 Quadrantids. (solid line: estimated activity profile (main + sub-peak component).

Table 2 – Sub-peaks that occurred after the main peak in past years.

Year	Peak $\lambda_\odot$	Activity Level	ZHR_r
2005	283.51°	3.0	85 ($\lambda_\odot = 283.51°$)
2010	283.48°	2.0	45 ($\lambda_\odot = 283.52°$)
2013	238.33°	4.0	65 ($\lambda_\odot = 283.50°$)
2018	238.51°	2.0	45 ($\lambda_\odot = 283.56°$)
2024	283.47°	6.5	110 ($\lambda_\odot = 283.55°$)

5 Conclusion

Radio meteor observations in the world detected a double peak in 2024. The main peak (at $\lambda_\odot = 283.13°$) produced higher activity than the long-term average. A high activity such as in 2024 has also been observed during several years in the past.

A sub-peak after the main peak has also been observed in the past. But the activity level in 2024 was much higher than during past Quadrantid displays.

Acknowledgment

The worldwide radio data were provided by the Radio Meteor Observation Bulletin (RMOB). We wish to thank *Pierre Terrier* for developing and hosting rmob.org.

References

Ogawa H., Toyomasu S., Ohnishi K., and Maegawa K. (2001). "The Global Monitor of Meteor Streams by Radio Meteor Observation all over the world". In, Warmbein Barbara, editor, Proceeding of the Meteoroids 2001 Conference, 6-10 August 2001, Swedish Institute of Space Physics, Kiruna, Sweden. ESA Publications Division, European Space Agency, Noordwijk, The Netherlands, pages 189–191.

Ogawa H. and Steyaert C. (2017). "Major and daytime meteor showers using global radio meteor observations covering the period of 2001-2016". *WGN, Journal of the IMO*, **45**, 98–106.

Ogawa H. and Sugimoto H. (2021). "Quadrantids 2021 with Worldwide Radio Meteor Observations". *eMetN*, **6**, 271–273.

Ogawa H. (2022). "Long-Term Studies of Major and Daytime Meteor Showers using Worldwide Radio Meteor Observations". *WGN, Journal of the IMO*, **50**, 148–157.

Rendtel J. (2023). "2024 Meteor Shower Calendar". International Meteor Organization.

Sugimoto H. (2017). "The new method of estimating ZHR using Radio Meteor Observations". *eMetN*, **2**, 109–110.

Radio observations of meteors in January–December 2023

Ivan Sergei

Mira Str.40-2, 222307, Molodechno, Belarus
astroseriv@yandex.by

This article presents a summary report of the radio observations made in the period January to December 2023.

1 Introduction

The observations were carried out at a private astronomical observatory near the town of Molodechno (Belarus) at the place of Polyani. A 5 element-antenna directed to the west was used, a car FM-receiver was connected to a laptop with as processor an Intel Atom CPU N2600 (1.6 GHz). The software to detect signals is Metan (author – Carol from Poland). Observations are made on the operating frequency 88.6 MHz (the FM radio station near Paris broadcasts on this frequency). The "France Culture" radio broadcast transmitter (100 kW) which I use is at about 1550 km from my observatory which has been renewed in 1997. The method of listening at a radiophone is more "sensitive" in terms of detecting meteor signals compared to the method of automatic detection, so it is more interesting. Regular (daily) observations 3–5 times a day are of scientific value, because they have uniformity, as performed on the same equipment.

2 Listening for radio echoes on 88.6 MHz

In order to save observation time and to increase the efficiency of listening for the radio meteor echoes in order to obtain a more complete observation series, I made a modification to the method with the introduction of a definition of "synthetic" hourly rate numbers (*Figures 1–12*).

Listening to the radio signals for 10 minutes with extrapolation of the data to 1 hour was done about 3 to 5 times a day. At the times of the maxima of the main meteoroid streams, the counting of meteor echoes was performed on average every 2–3 hours in order to get a better coverage of the observational series. This was done in order to control the level of the hourly rates as well as to distinguish between periods of tropospheric passage and other natural radio interference.

The maximum Quadrantid (#0010) activity was recorded at 11^h50^m UT 04 January 2023 ($\lambda_\odot = 283.50°$), while the traditional estimated moment of maximum should have occurred around 03^h UT 04 January 2023 ($\lambda_\odot = 283.155°$). Most likely the peak of the shower was short-lived and I missed it.

February is a quiet month - the activity of hourly radio signals monotonically decreased from an average of 40 at the beginning of the month to an average of 20.

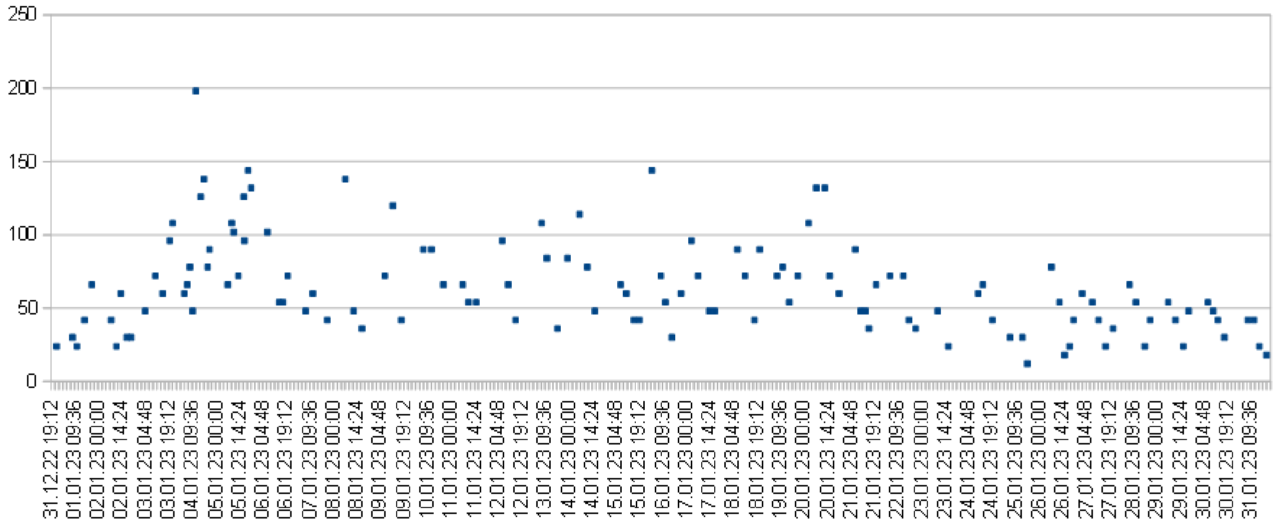

Figure 1 – The result with the calculated hourly numbers of meteor echoes by listening to the radio signals during January 2023.

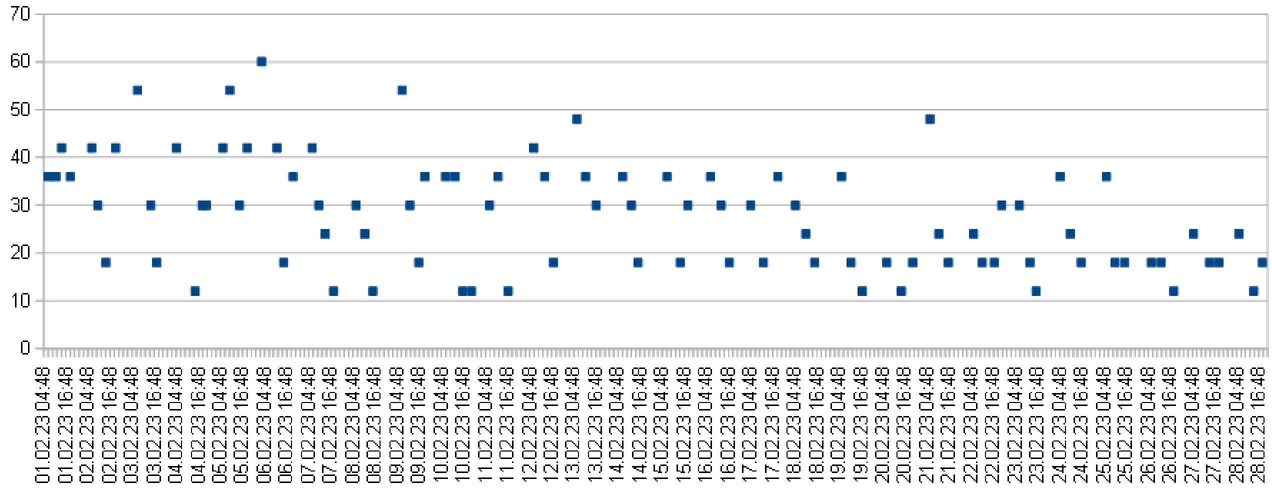

Figure 2 – The result with the calculated hourly numbers of meteor echoes by listening to the radio signals during February 2023.

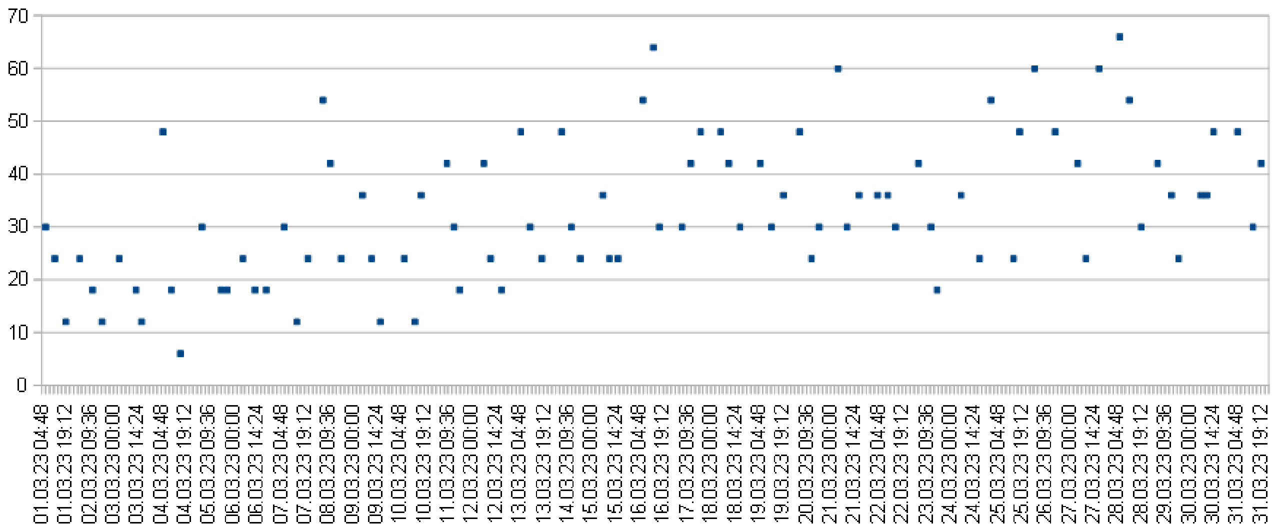

Figure 3 – The result with the calculated hourly numbers of meteor echoes by listening to the radio signals during March 2023.

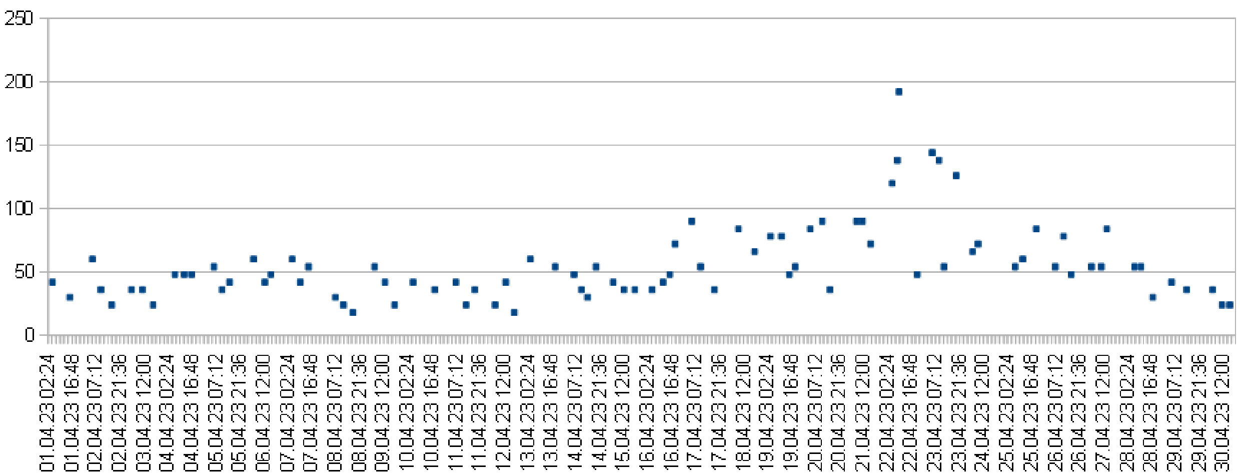

Figure 4 – The result with the calculated hourly numbers of meteor echoes by listening to the radio signals during April 2023.

March is also a quiet month, with the activity graph “opposite” to that for February. The average hourly activity of signals grows from 20 to 40 signals per hour.

The Lyrid (LYR, #0006) maximum was recorded on April 22–23 at 150 signals per hour.

The broad maximum of the eta Aquariids (ETA, #0031) was recorded from May 5 to 8 with radio meteor activity at 250 per hour. On May 7, there is one observation with an activity of 400 signals per hour, which was not confirmed by subsequent observations.

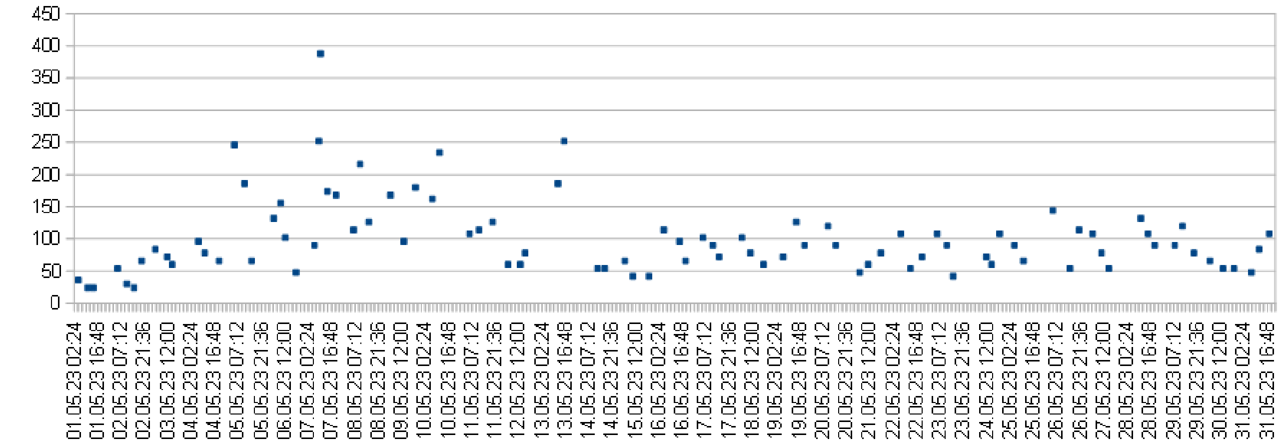

Figure 5 – The result with the calculated hourly numbers of meteor echoes by listening to the radio signals during May 2023.

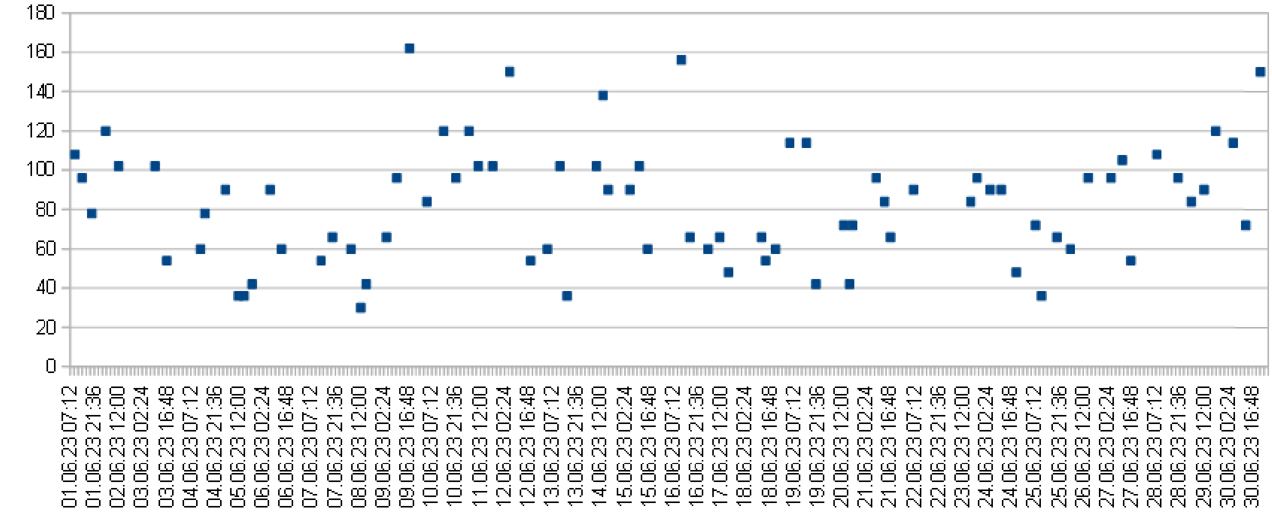

Figure 6 – The result with the calculated hourly numbers of meteor echoes by listening to the radio signals during June 2023.

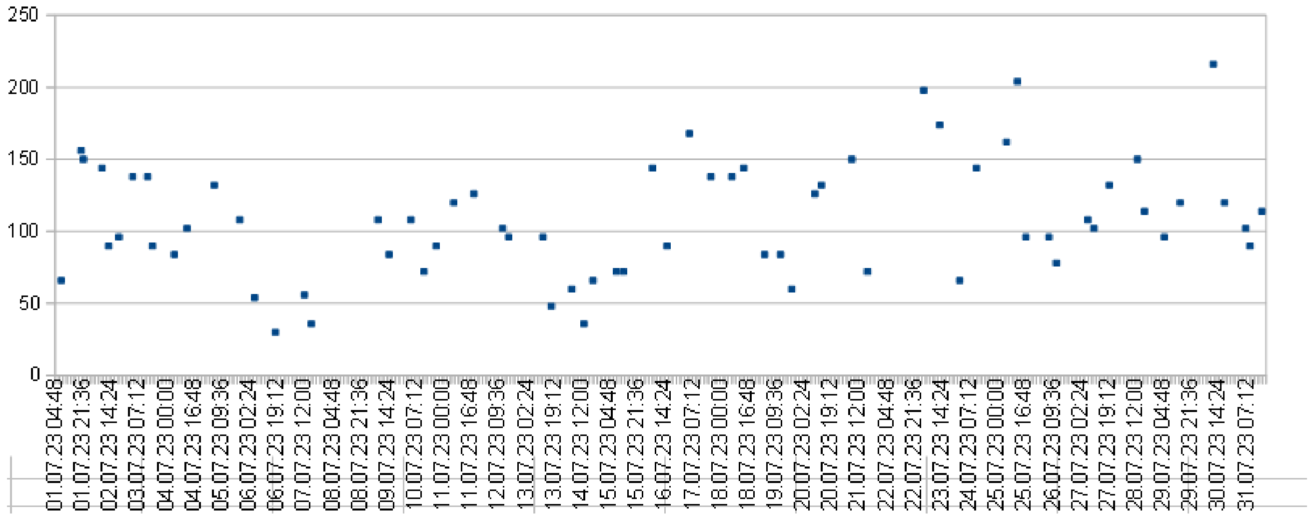

Figure 7 – The result with the calculated hourly numbers of meteor echoes by listening to the radio signals during July 2023.

In June, the activity trend resembles sinusoidal oscillations with several maxima of different intensity. The first broad maxima with a peak near June 12 may belong to the Daytime Arietids (ARI, #00171) and zeta-Perseids (ZPE, #0172). According to IMO, the peak of the daily ZPE (#0172) is around June 10, which coincides well with my radio observations.

The maximum of the Perseid (#0007) activity was recorded in the interval August 12–14 with a level of 600 signals per hour. The peaks on October 8 and October 22 likely belong to the Draconids (DRA, #0009) and Orionids (ORI, #0008), respectively.

The blurry faint peak around Nov. 10–11 may belong to the Northern Taurids (NTA, #0017). The more pronounced peaks on November 17–18 and November 22–23 can belong to the Leonids (LEO, #0013) and December Monocerotids (MON, #0019), respectively.

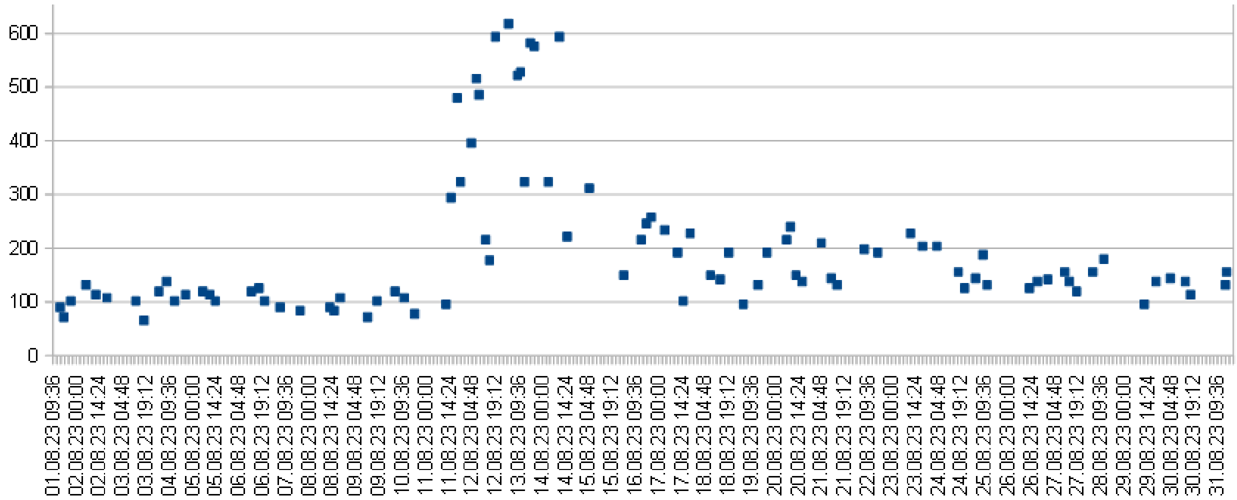

Figure 8 – The result with the calculated hourly numbers of meteor echoes by listening to the radio signals during August 2023.

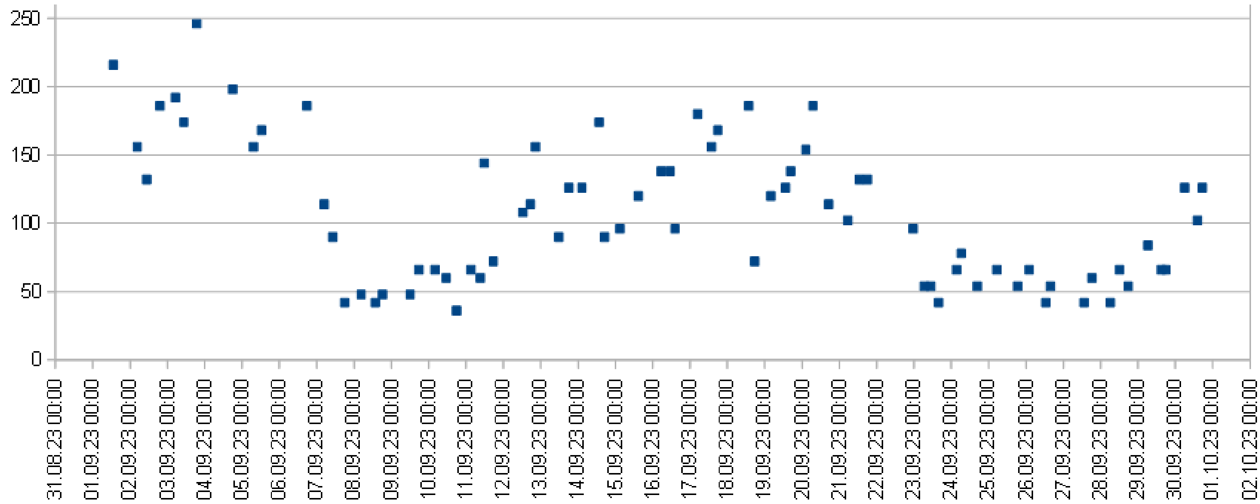

Figure 9 – The result with the calculated hourly numbers of meteor echoes by listening to the radio signals during September 2023.

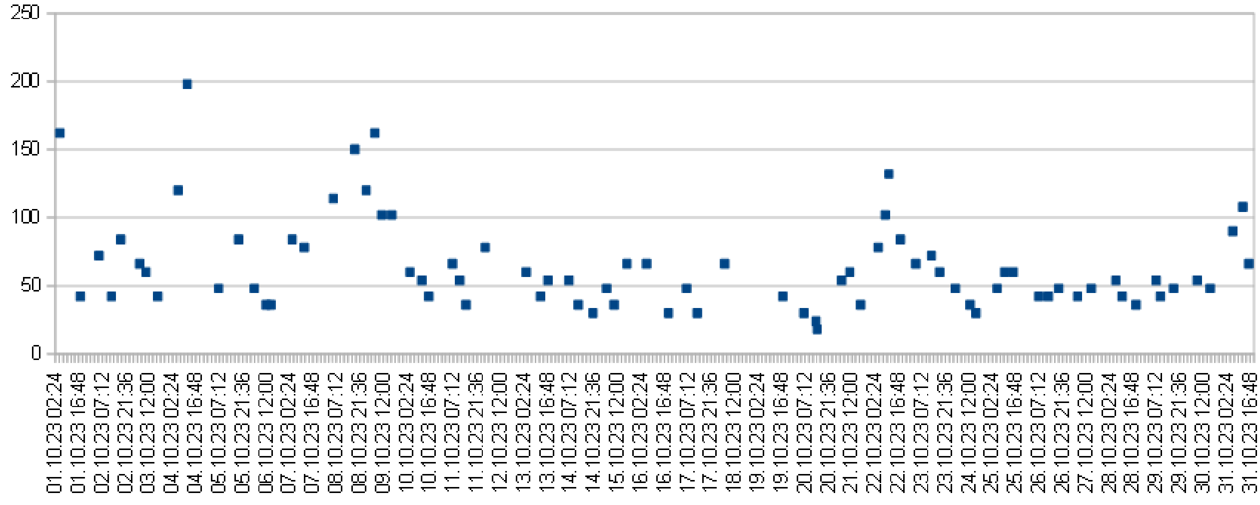

Figure 10 – The result with the calculated hourly numbers of meteor echoes by listening to the radio signals during October 2023.

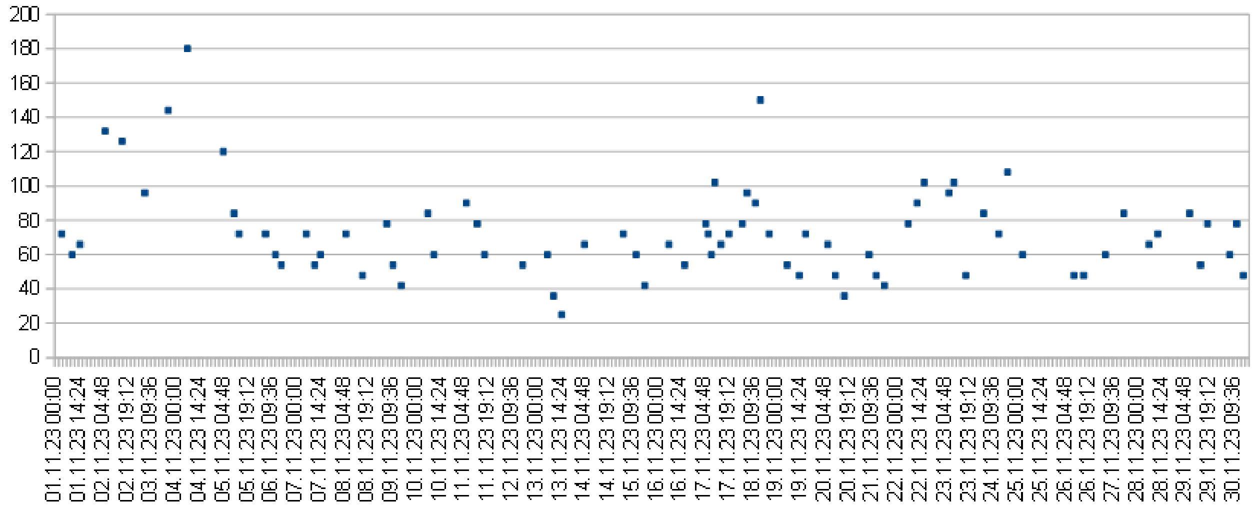

Figure 11 – The result with the calculated hourly numbers of meteor echoes by listening to the radio signals during November 2023.

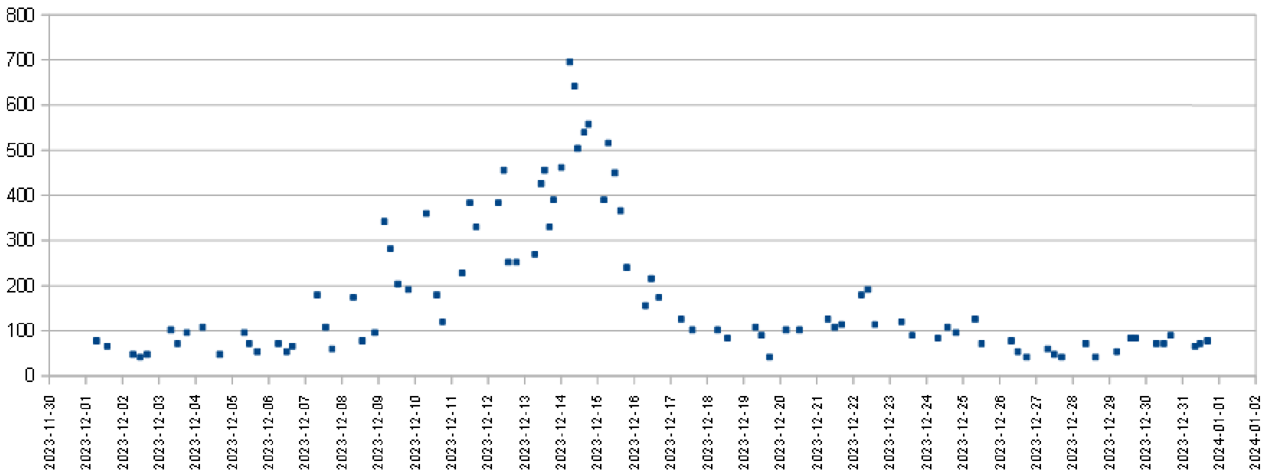

Figure 12 – The result with the calculated hourly numbers of meteor echoes by listening to the radio signals during December 2023.

The primary peak of the Geminids (GEM, #0004) at the level of 650–700 signals occurred during the interval 05^h40^m–08^h40^m UT on 14 December 2023. Within this interval the antenna "looks" in the radiant area (western direction). The second peak was registered with activity at an average of about 550 signals per hour during the interval 15^h10^m–17^h55^m UT on December 14, which almost coincides with the traditional maximum at 19^h16^m UT on 14 December 2023 ($\lambda_{\odot} = 262.2°$). The peak on December 22 probably belongs to the Ursids (URS, #0015).

3 Automatic detection of meteor signals on 88.6 MHz

Figures 13–15 show the results of automatic observations for January, August, and December 2023. During the year, experiments were underway to increase the sensitivity of the `Methane` program in terms of meteor signal detection. From December 5 to 24, a more sensitive program threshold for meteor events had been set.

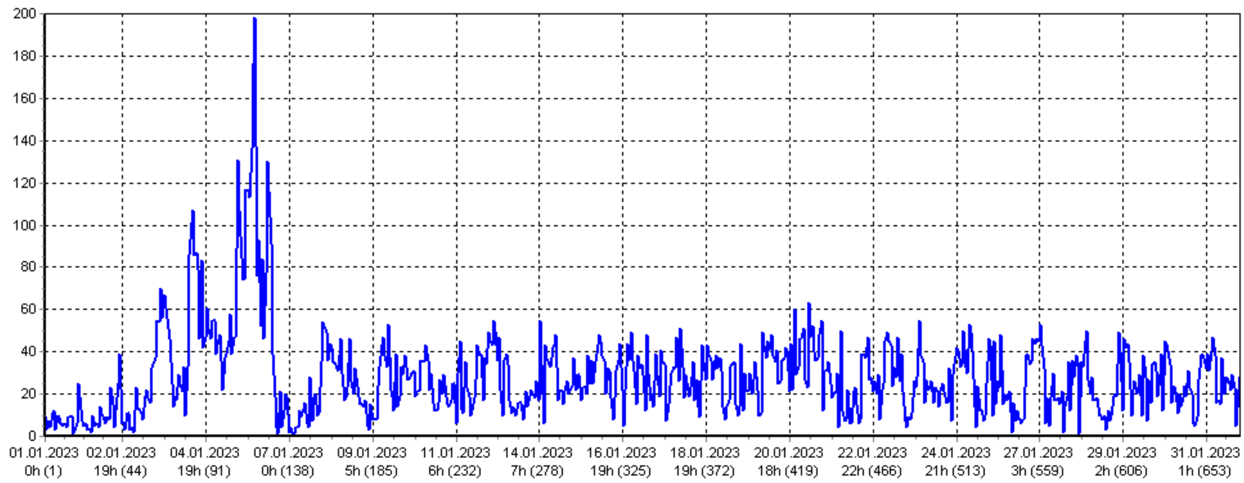

Figure 13 – The result of automatic detection of meteor signals for January 2023 using the `Methane` program.

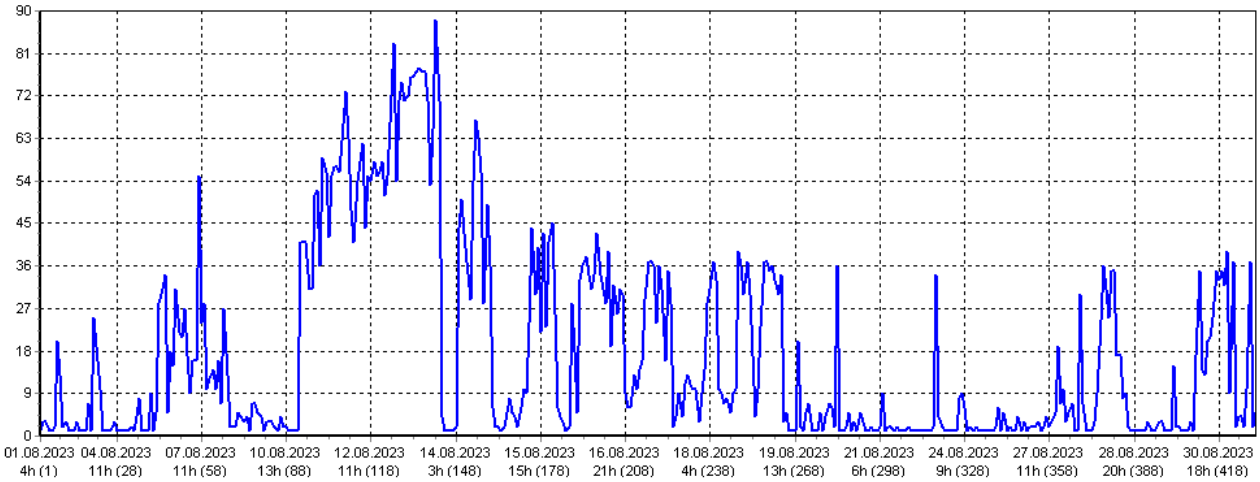

Figure 14 – The result of automatic detection of meteor signals for August 2023 using the `Methane` program.

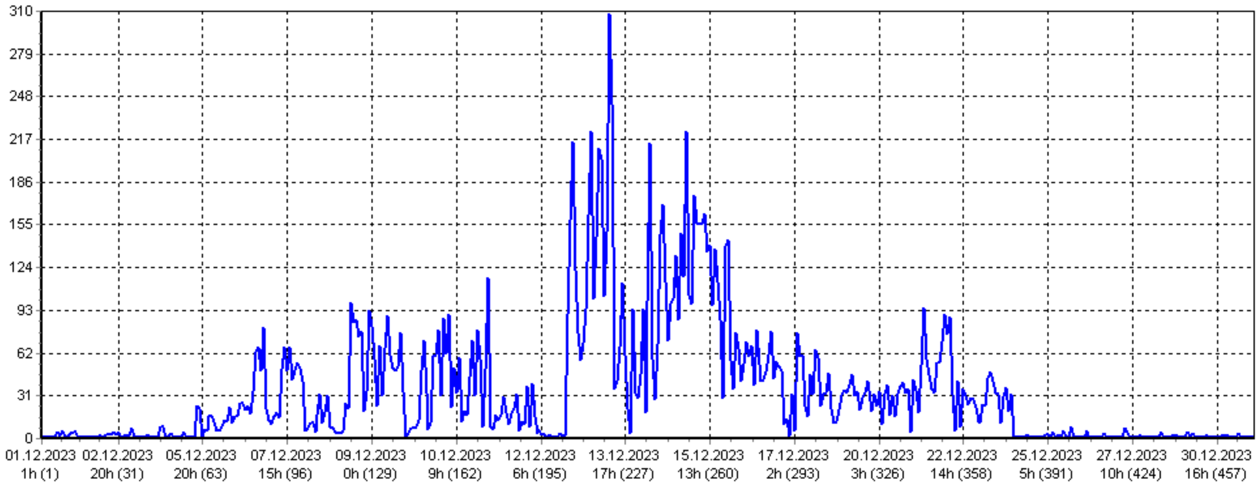

Figure 15 – The result of automatic detection of meteor signals for December 2023 using the Methane program.

4 Conclusion

The method of counting the radio meteor echoes by listening is about 3 times more sensitive than the method using automatic detection of meteor echo signals with music or speech. Experiments are underway to increase the sensitivity of the `Metan` software for automatic detection of meteor signals. The method of listening to the radio echoes is very interesting, because it allows you to "scan" the dynamics of the total meteor background over a long time, to identify periods of low activity, periods of high activity, as well as outbursts and the peak activity of the most prominent meteoroid streams. Not all maxima in the meteor shower plots could be classified with known meteor streams from the IMO meteor shower working list data (meteor calendar). Probably some unidentified maxima are the result of some enhanced activity of one or a superposition of several minor meteor showers, which are detected by video networks.

Acknowledgment

I would like to thank *Sergey Dubrovsky* for the software he developed for data analysis and processing of radio observations (software Rameda). I thank *Carol* from Poland for the `Metan` software. Thanks to *Paul Roggemans* for his help in the lay-out and the correction of this article.

References

Rendtel J. (2023). "Meteor Shower Calendar". IMO.

Radio meteors December 2023

Felix Verbelen

Vereniging voor Sterrenkunde & Volkssterrenwacht MIRA, Grimbergen, Belgium
felix.verbelen@gmail.com

An overview of the radio observations during December 2023 is given.

1 Introduction

The graphs show both the daily totals (*Figure 1 and 2*) and the hourly numbers (*Figure 3 and 4*) of "all" reflections counted automatically, and of manually counted "overdense" reflections, overdense reflections longer than 10 seconds and longer than 1 minute, as observed here at Kampenhout (BE) on the frequency of our VVS-beacon (49.99 MHz) during the month of December 2023.

The hourly numbers, for echoes shorter than 1 minute, are weighted averages derived from:

$$N(h) = \frac{n(h-1)}{4} + \frac{n(h)}{2} + \frac{n(h+1)}{4}$$

No lightning activity was observed and local interference remained quite low during this month.

The eye-catchers were of course the Geminids, which reached their peak in the period December 13–15, with the long-lasting overdenses clearly peaking later than the underdense.

The Ursids showed a maximum on December 22 as expected. This is best seen in the daily graphs.

Other interesting showers were active, especially during the first week of the month.

Over the entire month, 13 reflections longer than 1 minute were observed here. Attached please find a selection of these and of other interesting reflections (*Figures 5 to 16*). Many more of these are available on request.

In addition to the usual graphs, you will also find the raw counts in cvs-format[29] from which the graphs are derived. The table contains the following columns: day of the month, hour of the day, day + decimals, solar longitude (epoch J2000), counts of "all" reflections, overdense reflections, reflections longer than 10 seconds and reflections longer than 1 minute, the numbers being the observed reflections of the past hour.

[29] https://www.emeteornews.net/wp-content/uploads/2024/01/202312_49990_FV_rawcounts.csv

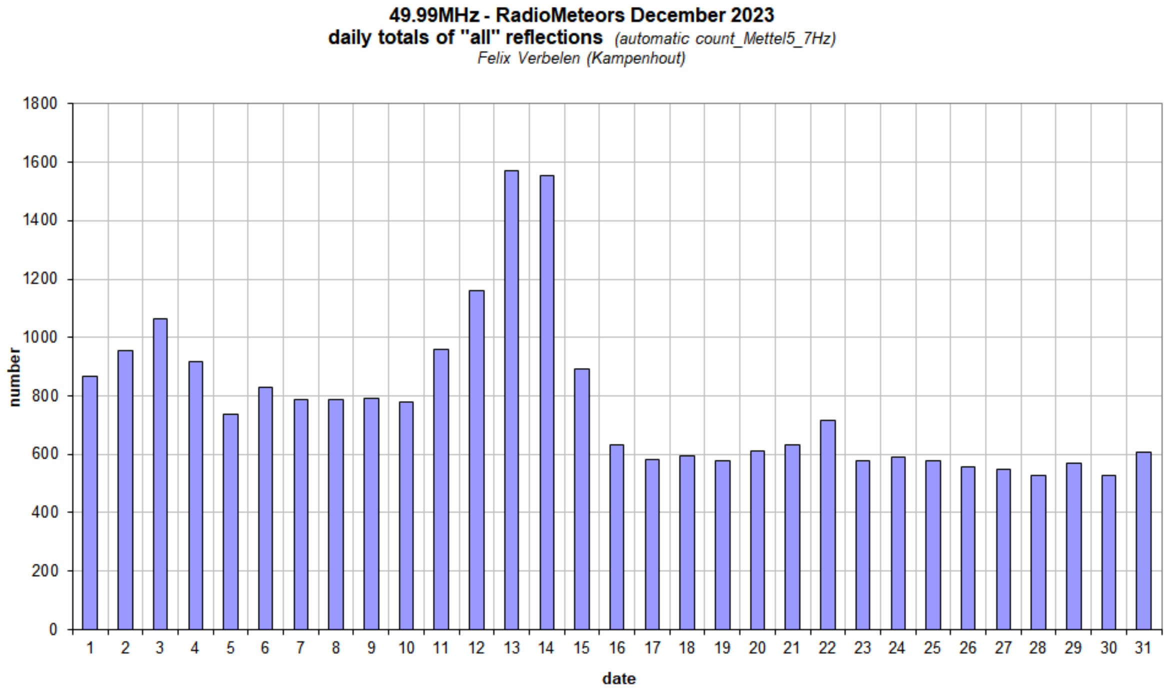

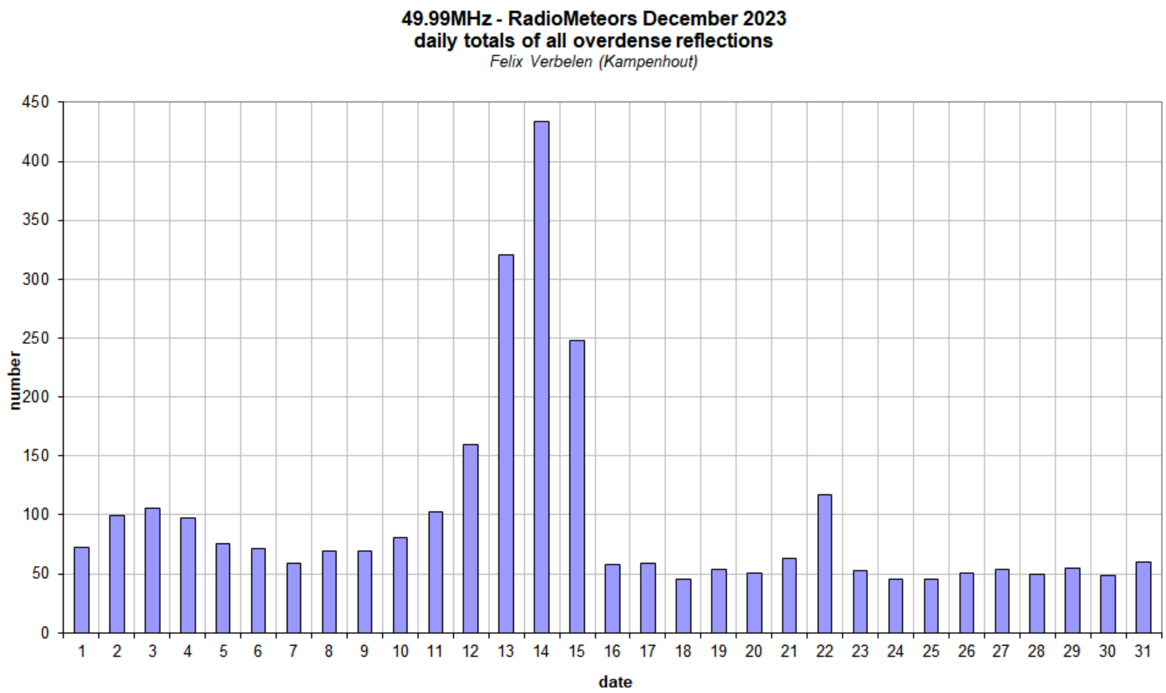

Figure 1 – The daily totals of "all" reflections counted automatically, and of manually counted "overdense" reflections, as observed here at Kampenhout (BE) on the frequency of our VVS-beacon (49.99 MHz) during December 2023.

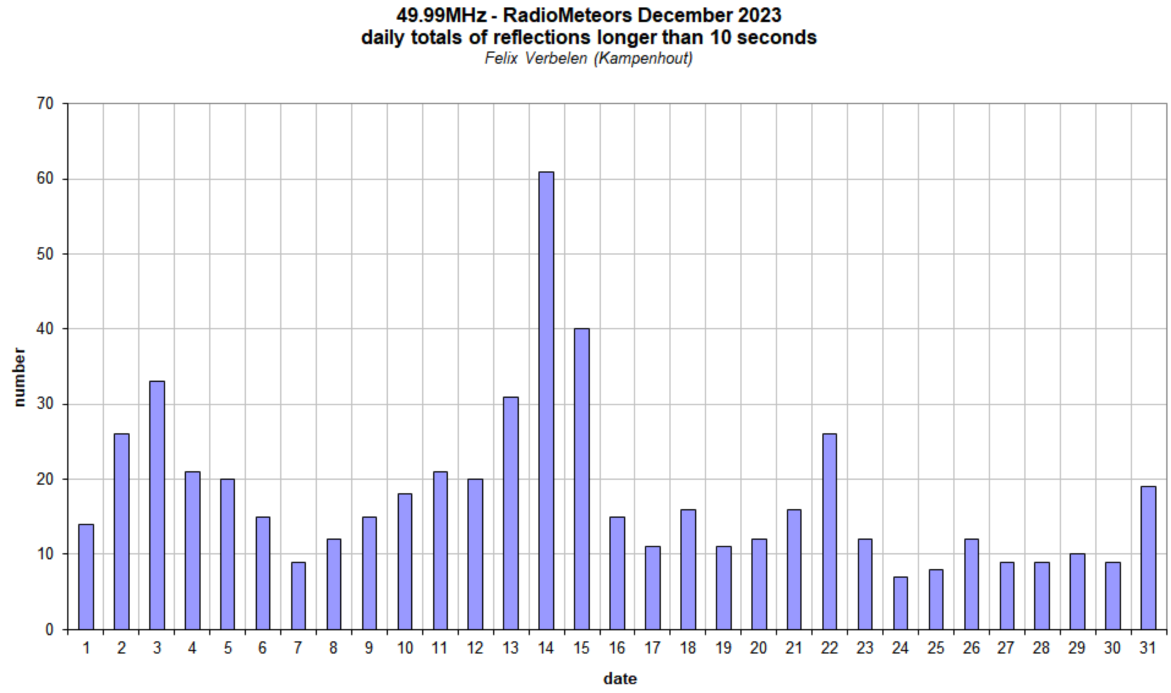

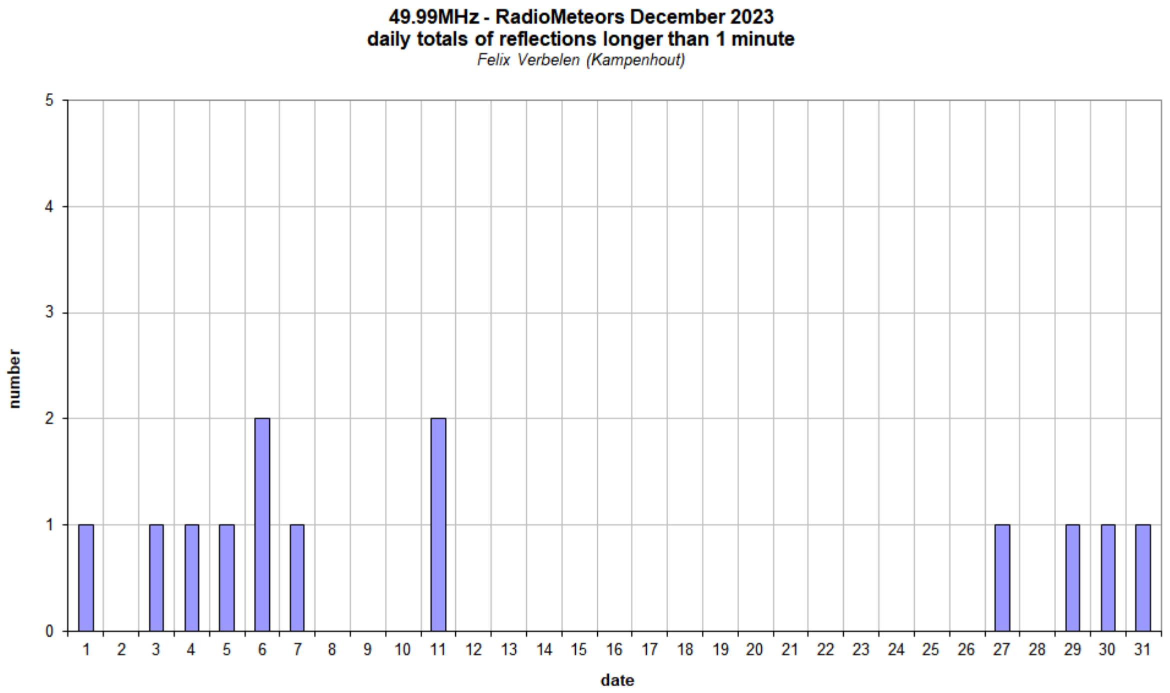

Figure 2 – The daily totals of overdense reflections longer than 10 seconds and longer than 1 minute, as observed here at Kampenhout (BE) on the frequency of our VVS-beacon (49.99 MHz) during December 2023.

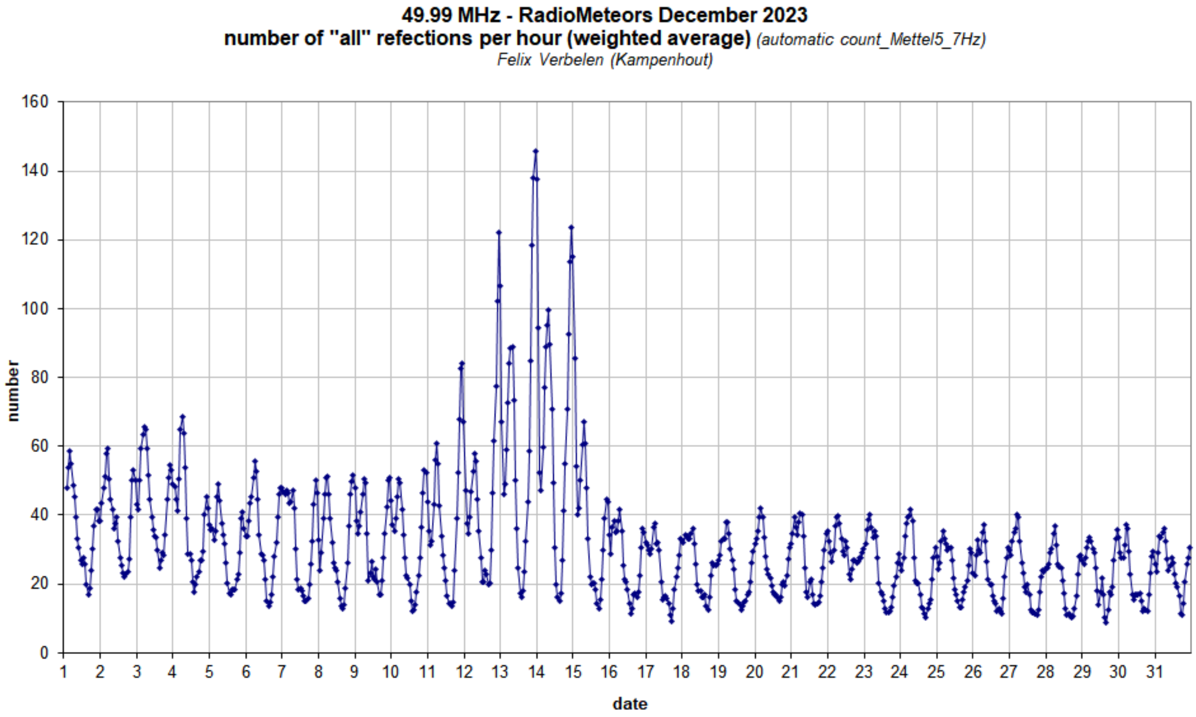

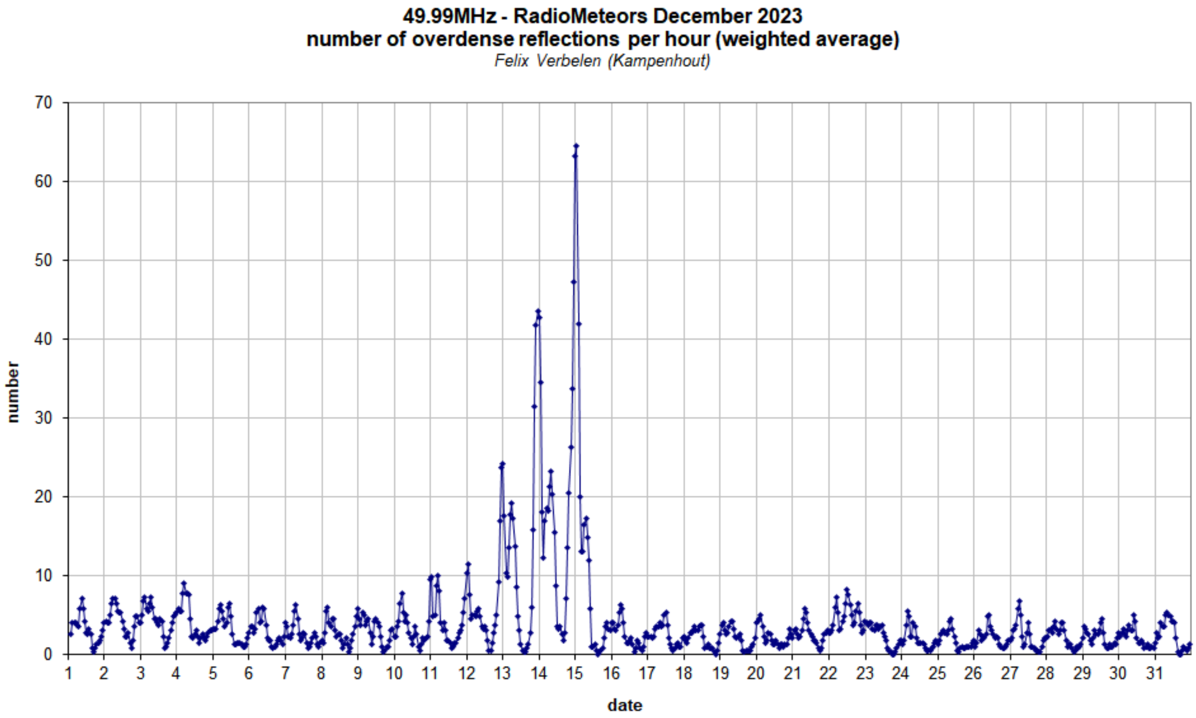

Figure 3 – The hourly numbers of "all" reflections counted automatically, and of manually counted "overdense" reflections, as observed here at Kampenhout (BE) on the frequency of our VVS-beacon (49.99 MHz) during December 2023.

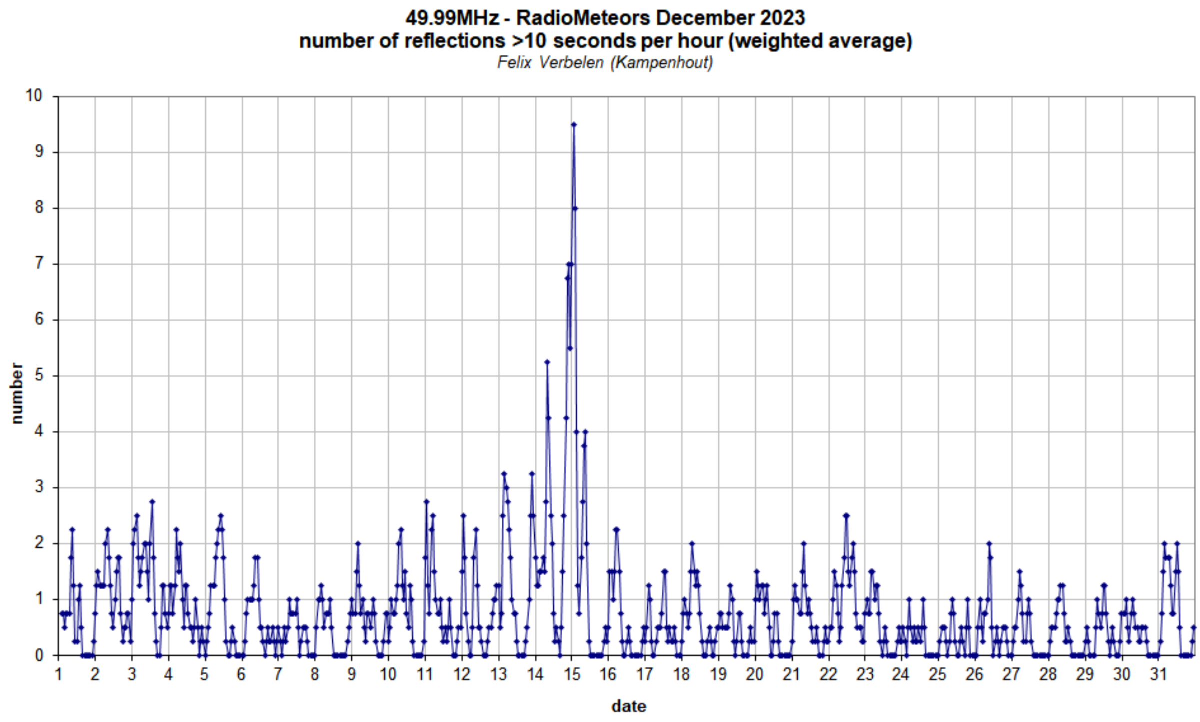

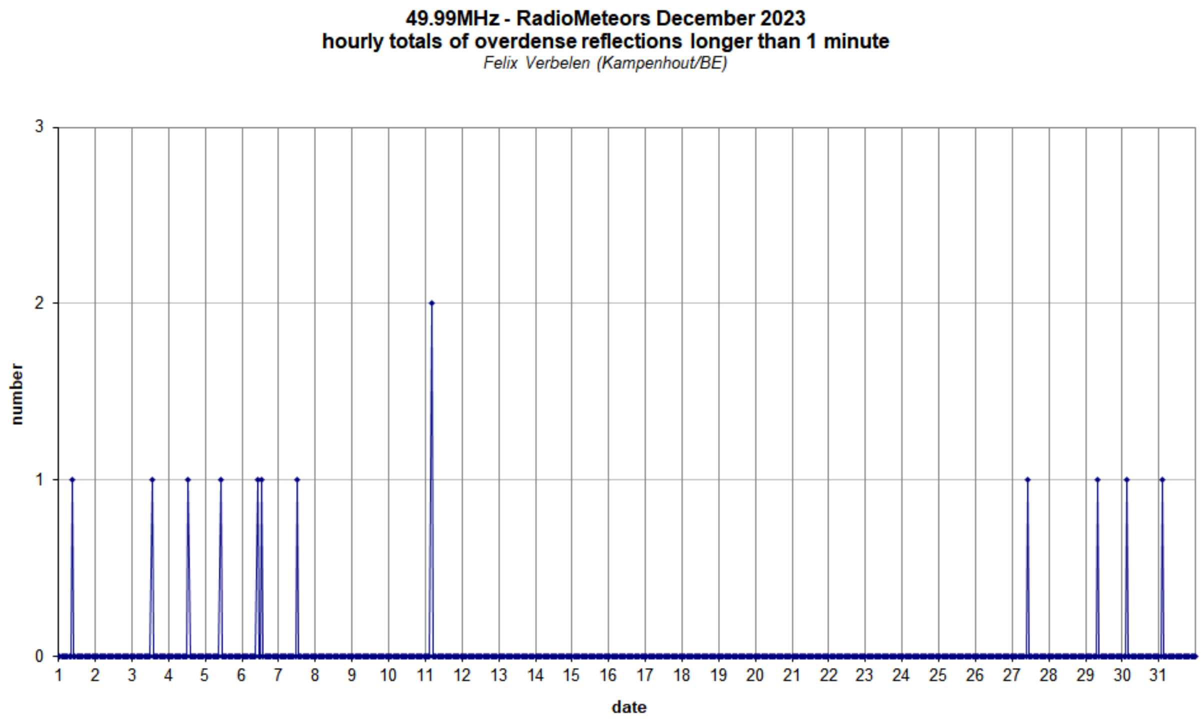

Figure 4 – The hourly numbers of overdense reflections longer than 10 seconds and longer than 1 minute, as observed here at Kampenhout (BE) on the frequency of our VVS-beacon (49.99 MHz) during December 2023.

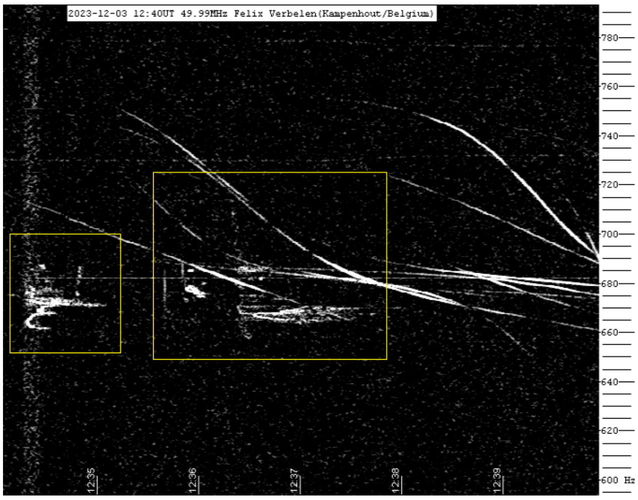

Figure 5 – Meteor echo 3 December 2023, 12^{h}40^{m} UT.

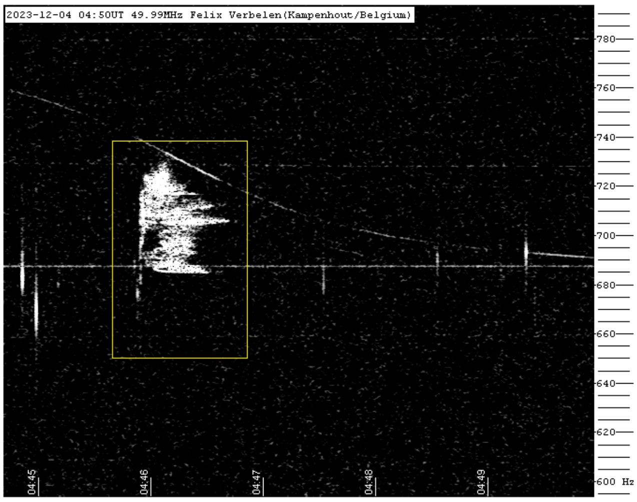

Figure 6 – Meteor echo 4 December 2023, 04^{h}50^{m} UT.

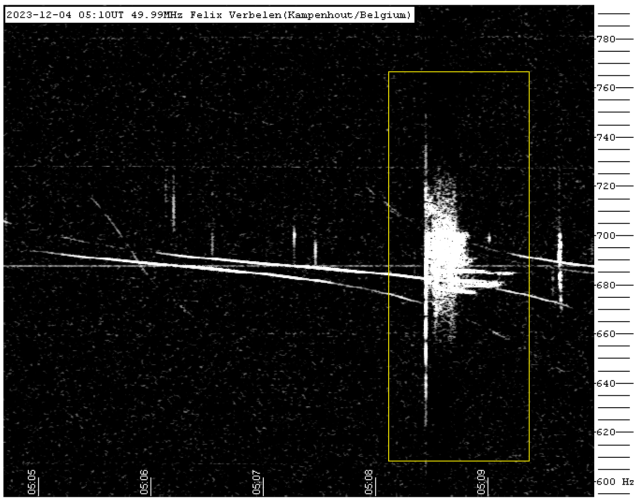

Figure 7 – Meteor echo 4 December 2023, 05^{h}10^{m} UT.

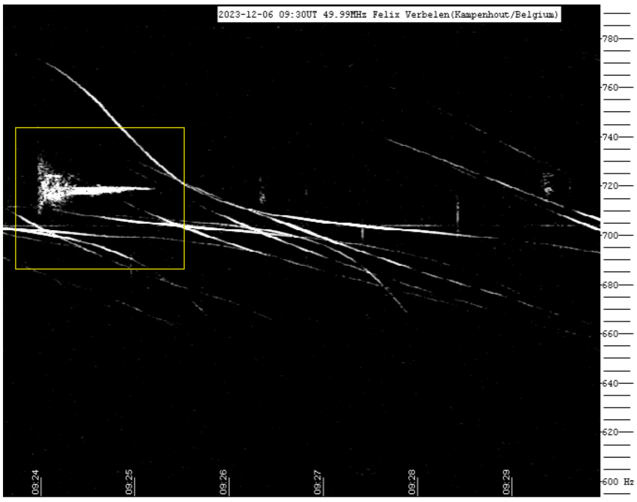

Figure 8 – Meteor echo 6 December 2023, 09^{h}30^{m} UT.

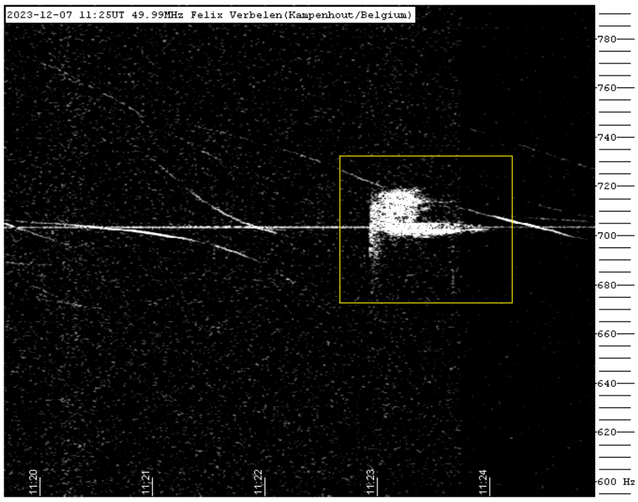

Figure 9 – Meteor echo 7 December 2023, 11^{h}25^{m} UT.

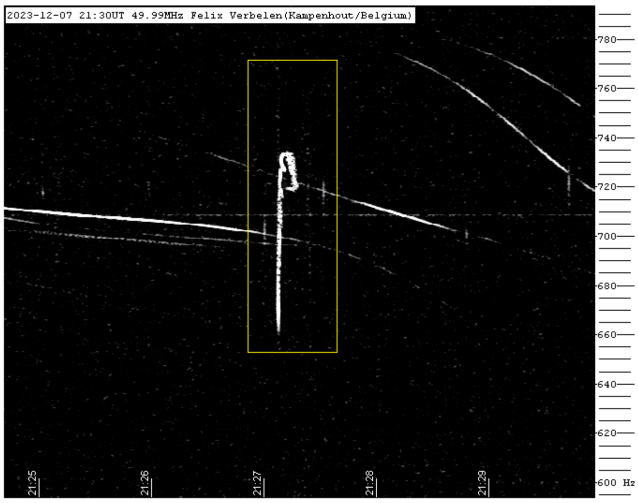

Figure 10 – Meteor echo 7 December 2023, 21^{h}30^{m} UT.

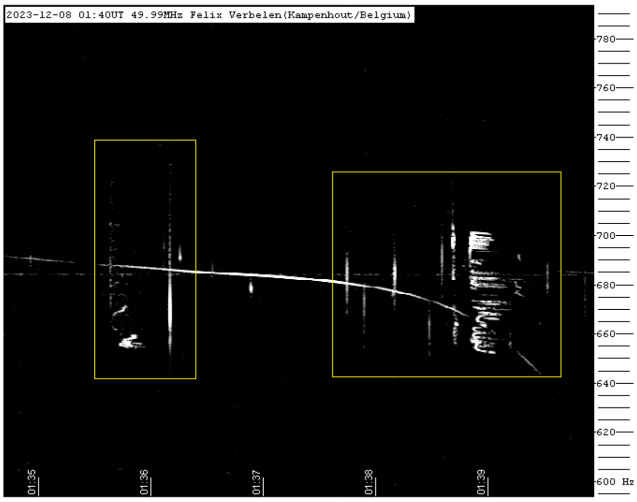

Figure 11 – Meteor echo 8 December 2023, 01^{h}40^{m} UT.

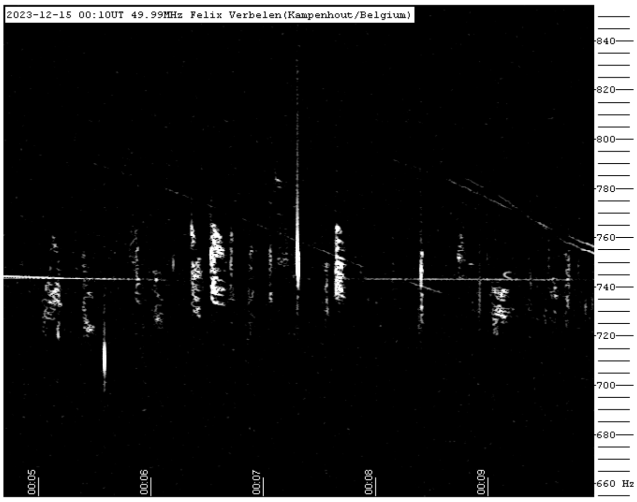

Figure 14 – Meteor echo 15 December 2023, 00^{h}10^{m} UT.

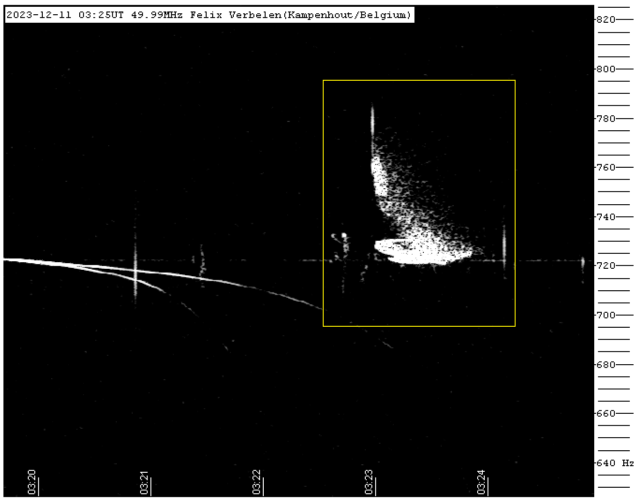

Figure 12 – Meteor echo 11 December 2023, 03^{h}25^{m} UT.

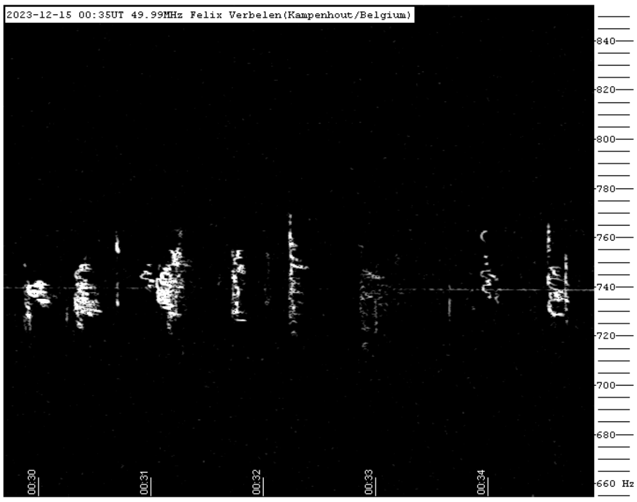

Figure 15 – Meteor echo 15 December 2023, 00^{h}35^{m} UT.

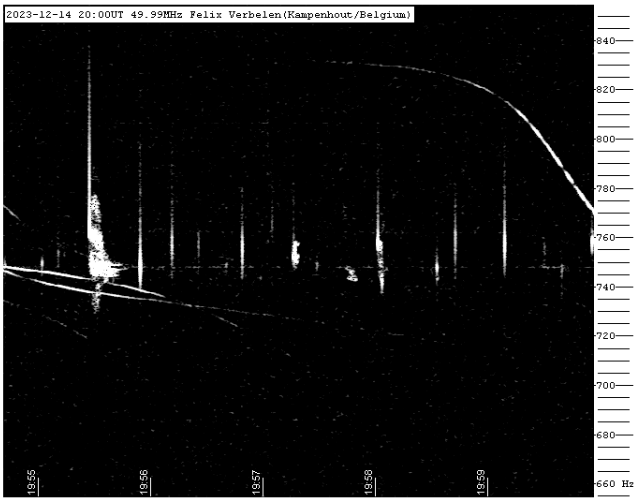

Figure 13 – Meteor echo 14 December 2023, 20^{h}00^{m} UT.

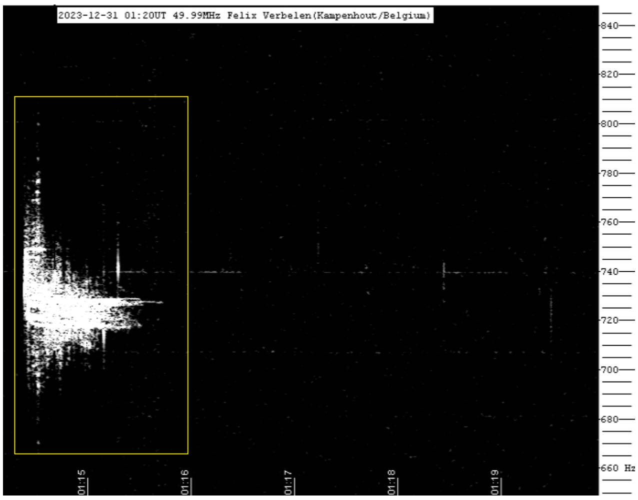

Figure 16 – Meteor echo 31 December 2023, 01^{h}20^{m} UT.

Radio meteors January 2024

Felix Verbelen

Vereniging voor Sterrenkunde & Volkssterrenwacht MIRA, Grimbergen, Belgium
felix.verbelen@gmail.com

An overview of the radio observations during January 2024 is given.

1 Introduction

The graphs show both the daily totals (*Figure 1 and 2*) and the hourly numbers (*Figure 3 and 4*) of "all" reflections counted automatically, and of manually counted "overdense" reflections, overdense reflections longer than 10 seconds and longer than 1 minute, as observed here at Kampenhout (BE) on the frequency of our VVS-beacon (49.99 MHz) during the month of January 2024.

The hourly numbers, for echoes shorter than 1 minute, are weighted averages derived from:

$$N(h) = \frac{n(h-1)}{4} + \frac{n(h)}{2} + \frac{n(h+1)}{4}$$

Local interference and unidentified noise remained moderate to low during this month and weak lightning activity was observed only on January 3rd. Also, the solar activity remained relatively moderated during this month, with nevertheless some nice type III eruptions as shown for example in *Figures 5 and 6*.

The eye-catchers were of course the Quadrantids/Boötids, peaking on January 4th. Attached are some pictures of their activity (*Figures 7 to 12*).

Although the general activity was, as expected, quite low during the remainder of the month, several minor showers and brief outbursts were observed.

Over the entire month 5 reflections longer than 1 minute were observed. A selection of these, together with a number some other interesting reflections are included (Figures 13 to 18). Many more are available on request.

In addition to the usual graphs, you will also find the raw counts in cvs-format[30] from which the graphs are derived. The table contains the following columns: day of the month, hour of the day, day + decimals, solar longitude (epoch J2000), counts of "all" reflections, overdense reflections, reflections longer than 10 seconds and reflections longer than 1 minute, the numbers being the observed reflections of the past hour.

[30] https://www.emeteornews.net/wp-content/uploads/2024/02/202401_49990_FV_rawcounts.csv

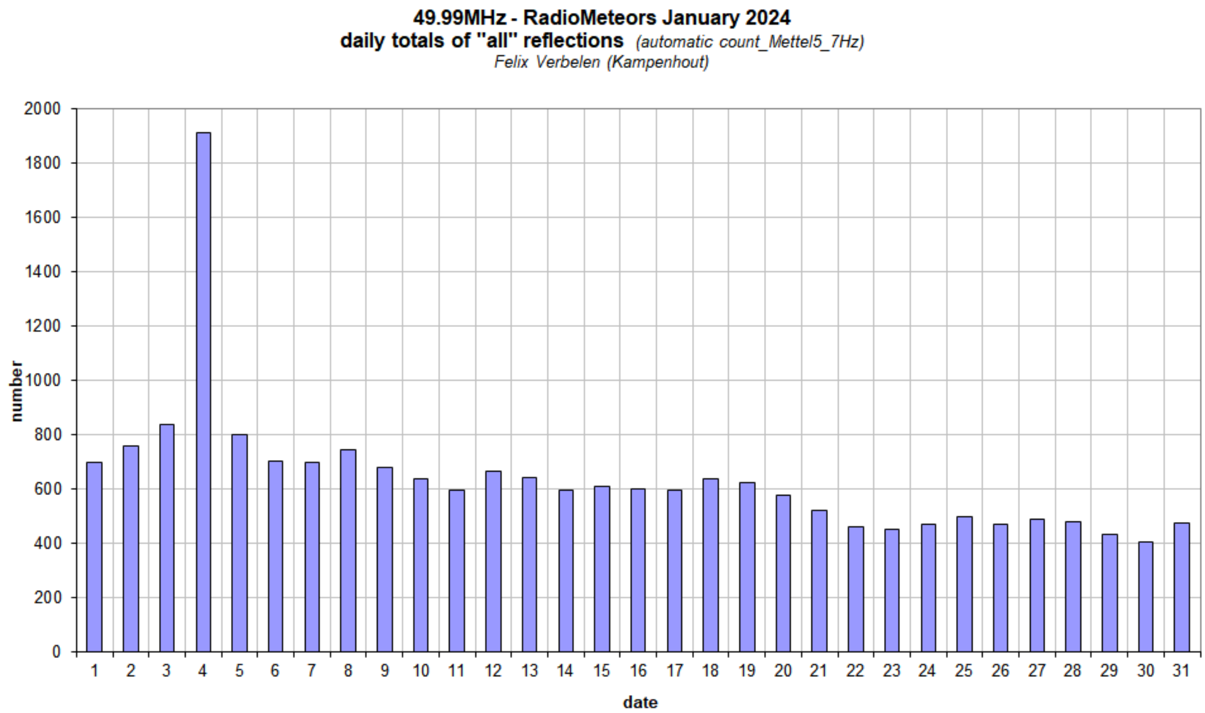

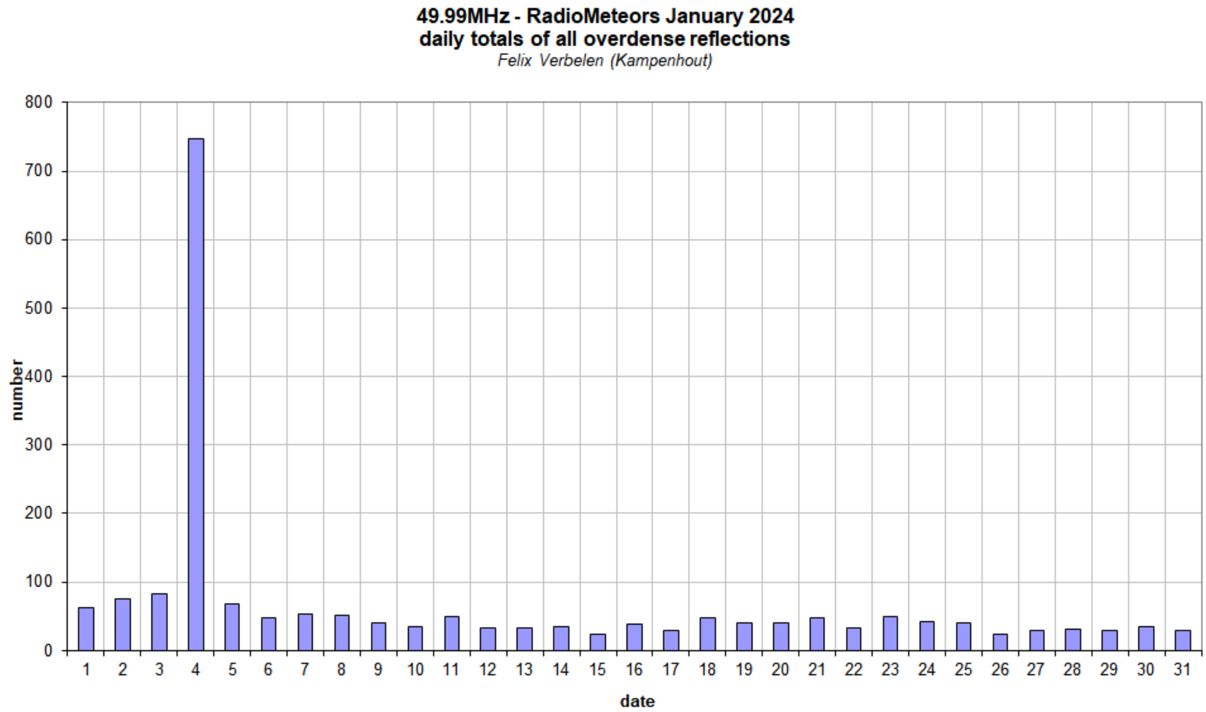

Figure 1 – The daily totals of "all" reflections counted automatically, and of manually counted "overdense" reflections, as observed here at Kampenhout (BE) on the frequency of our VVS-beacon (49.99 MHz) during January 2024.

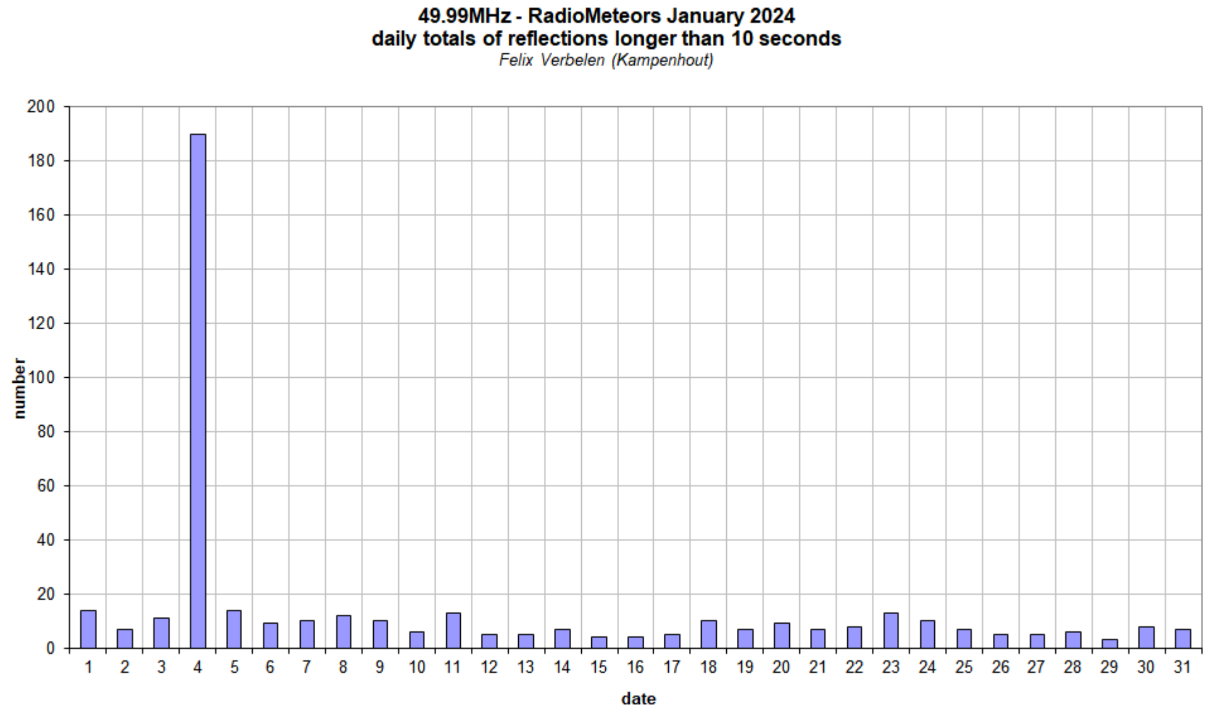

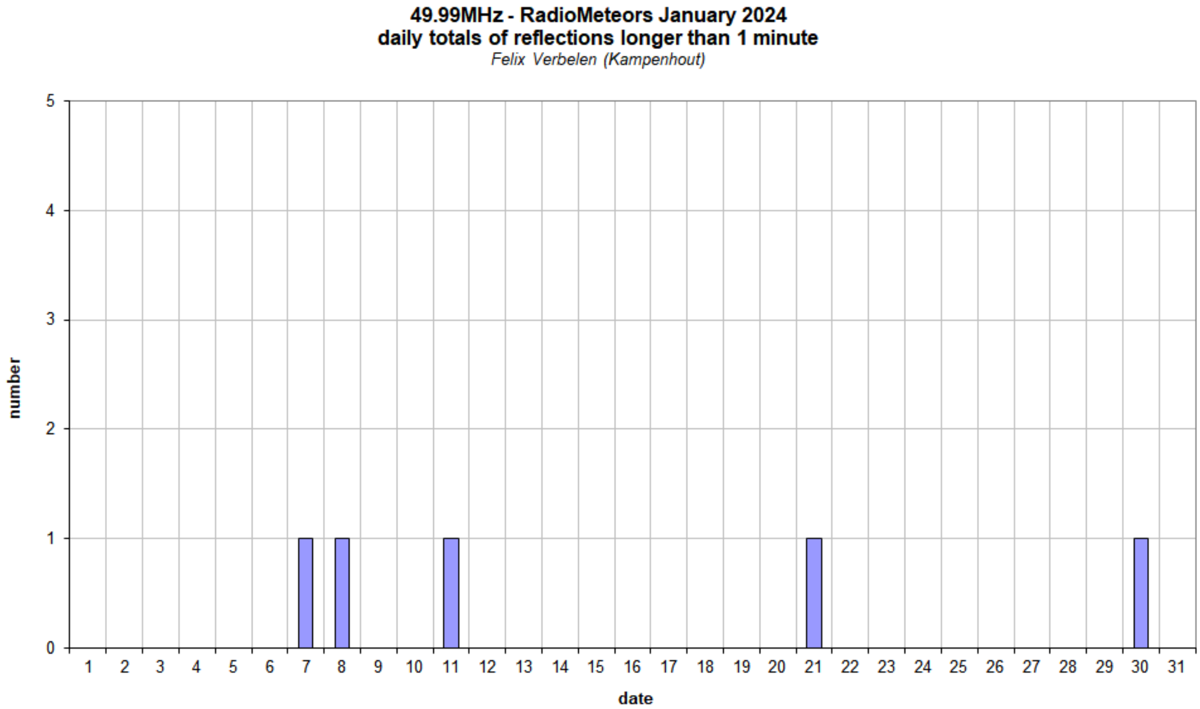

Figure 2 – The daily totals of overdense reflections longer than 10 seconds and longer than 1 minute, as observed here at Kampenhout (BE) on the frequency of our VVS-beacon (49.99 MHz) during January 2024.

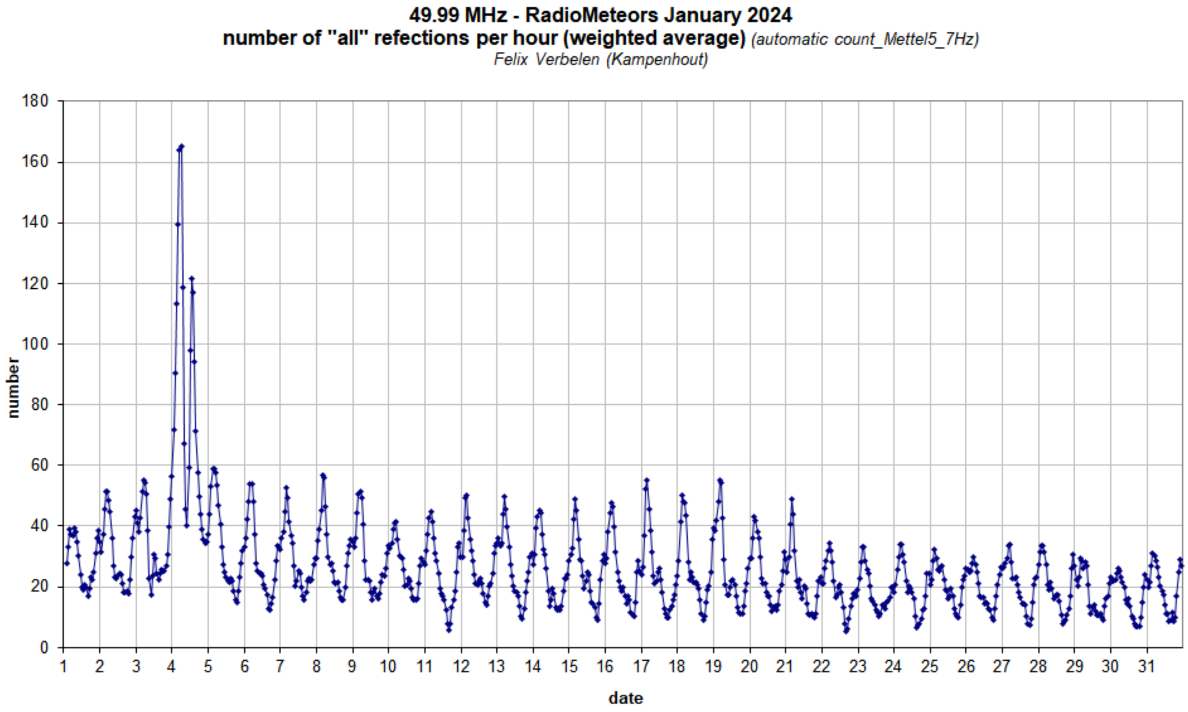

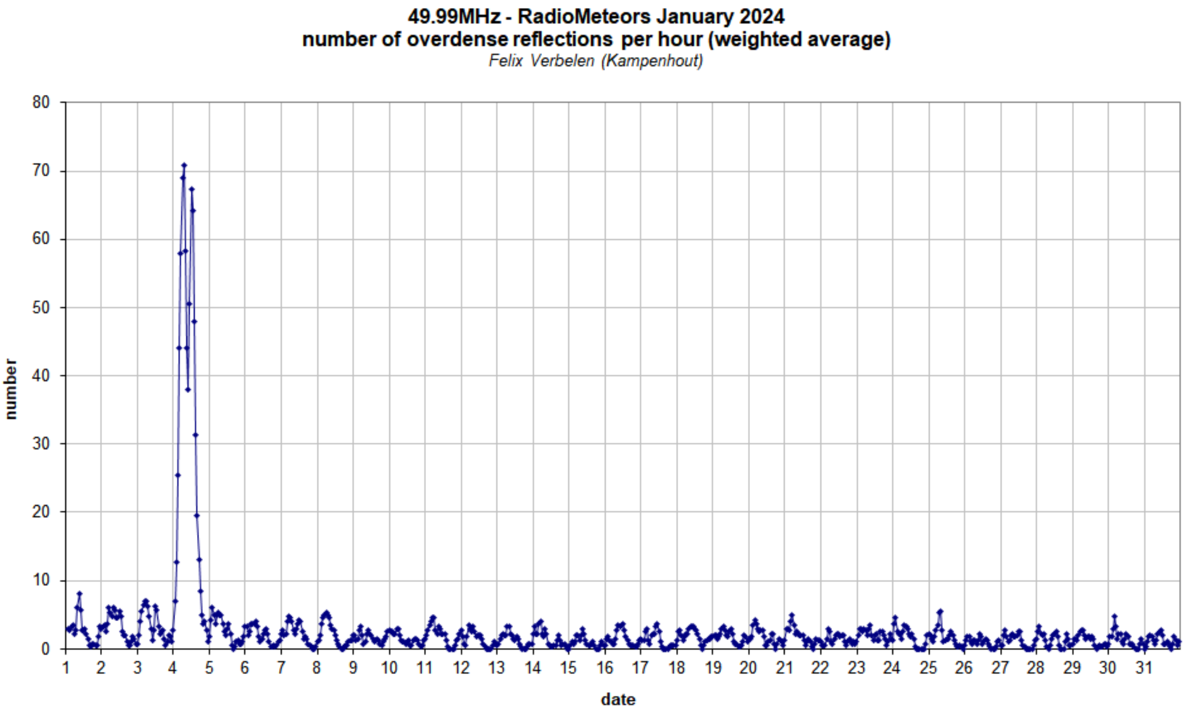

Figure 3 – The hourly numbers of "all" reflections counted automatically, and of manually counted "overdense" reflections, as observed here at Kampenhout (BE) on the frequency of our VVS-beacon (49.99 MHz) during January 2024.

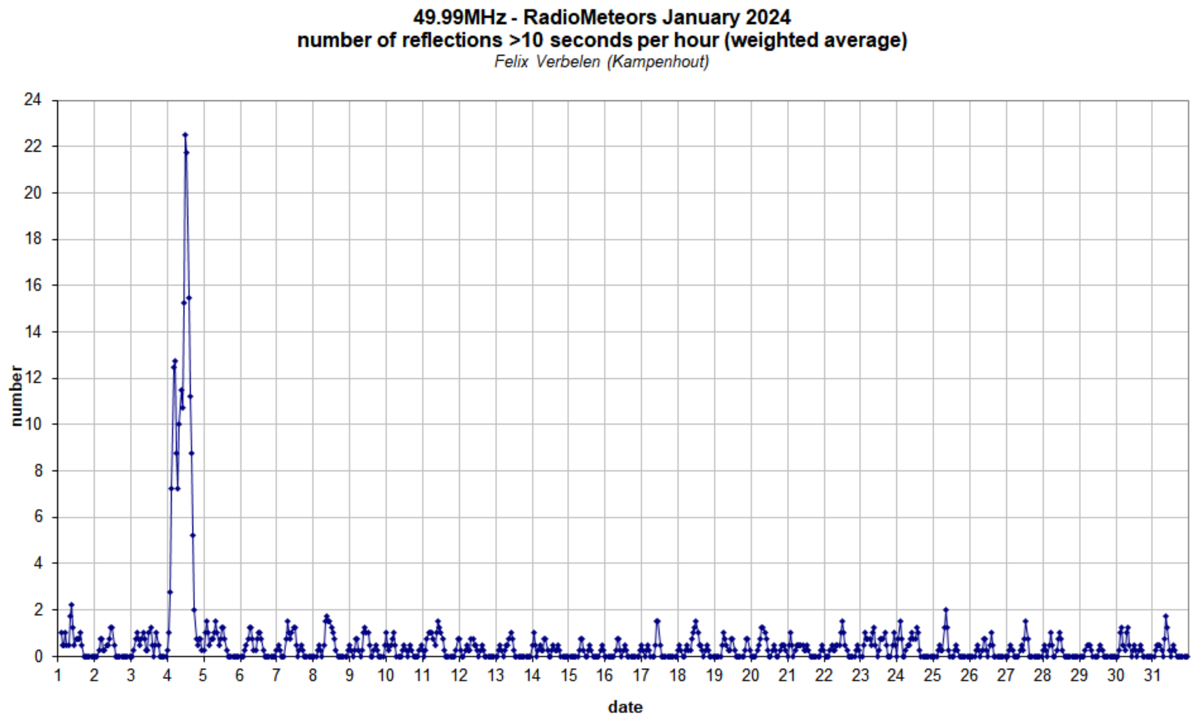

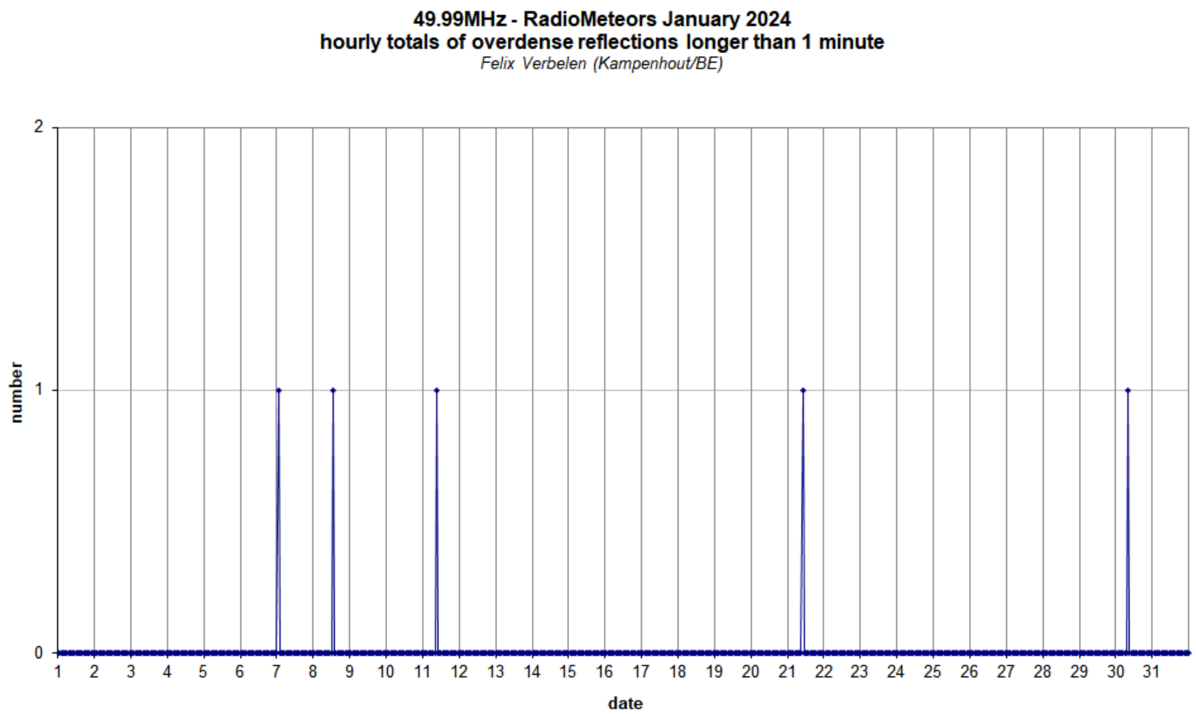

Figure 4 – The hourly numbers of overdense reflections longer than 10 seconds and longer than 1 minute, as observed here at Kampenhout (BE) on the frequency of our VVS-beacon (49.99 MHz) during January 2024.

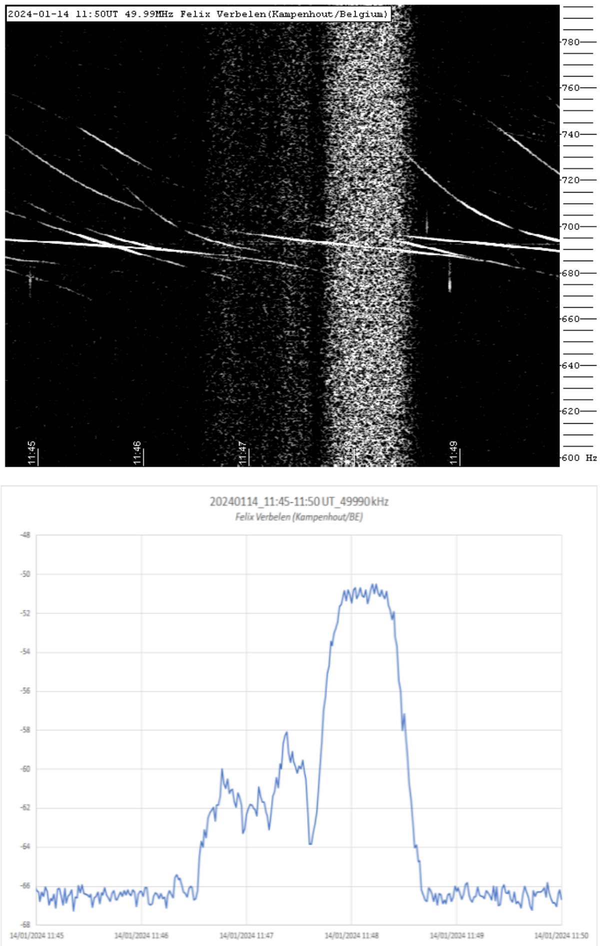

Figure 5 – solar activity with some nice type III eruptions.

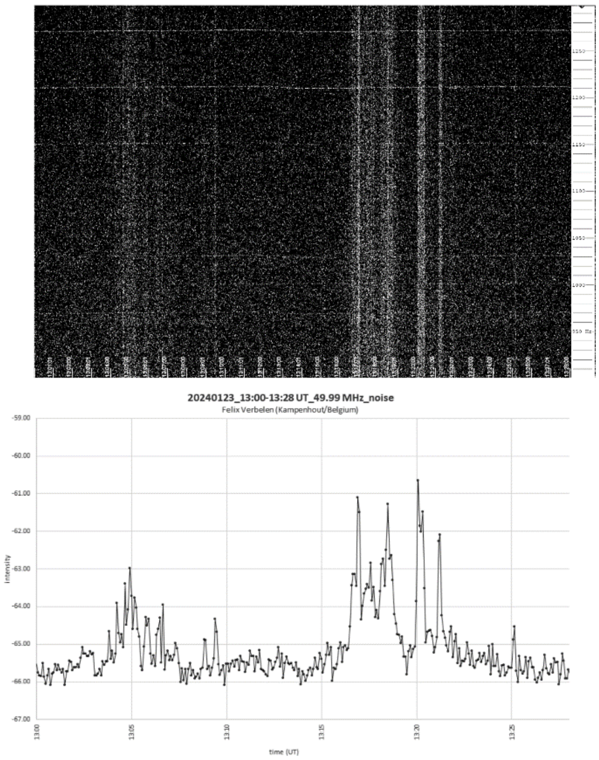

Figure 6 – solar activity with some nice type III eruptions.

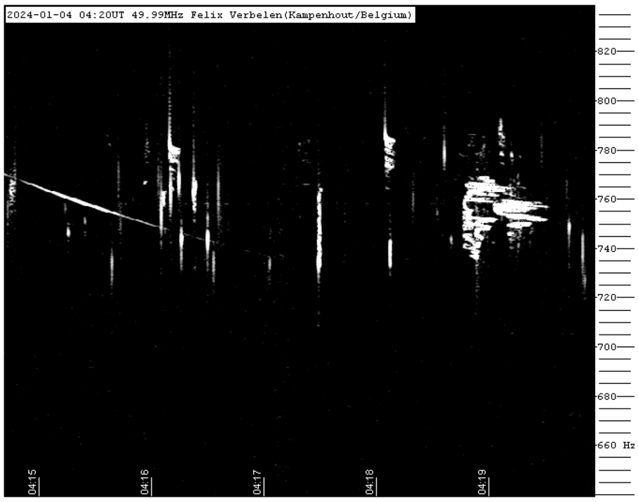

Figure 7 – Meteor echo 4 January 2024, 04^h20^m UT.

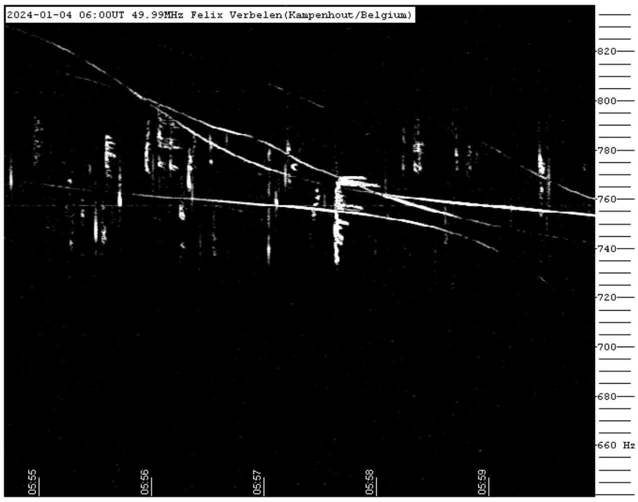

Figure 8 – Meteor echo 4 January 2024, 06^h00^m UT.

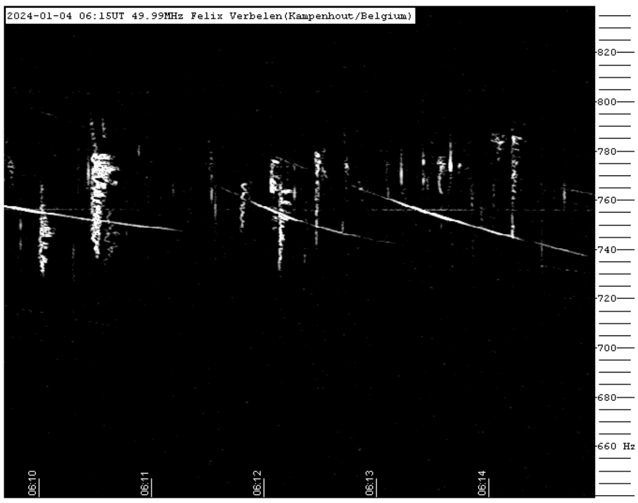

Figure 9 – Meteor echo 4 January 2024, 06^h15^m UT.

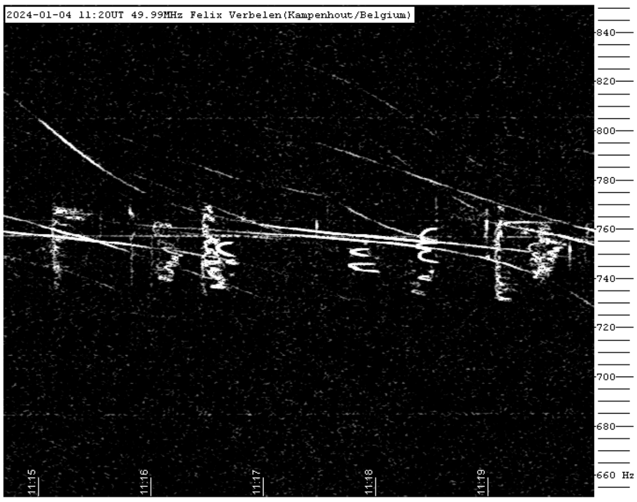

Figure 10 – Meteor echo 4 January 2024, 11^h20^m UT.

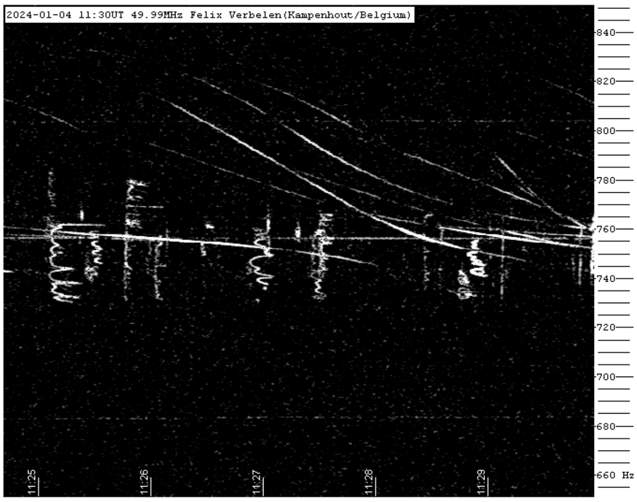

Figure 11 – Meteor echo 4 January 2024, 11^h30^m UT.

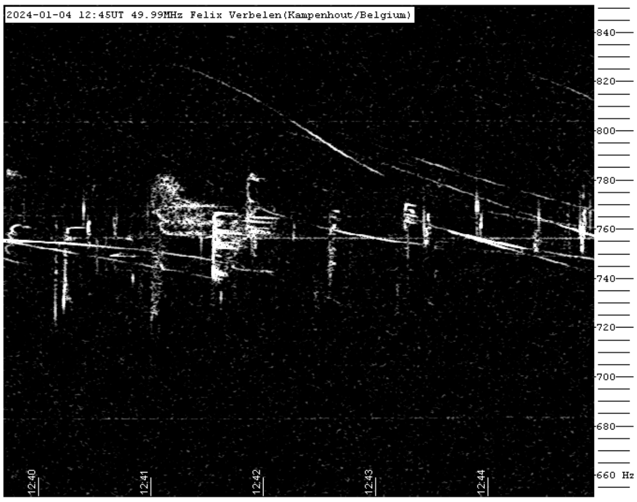

Figure 12 – Meteor echo 4 January 2024, 12^h45^m UT.

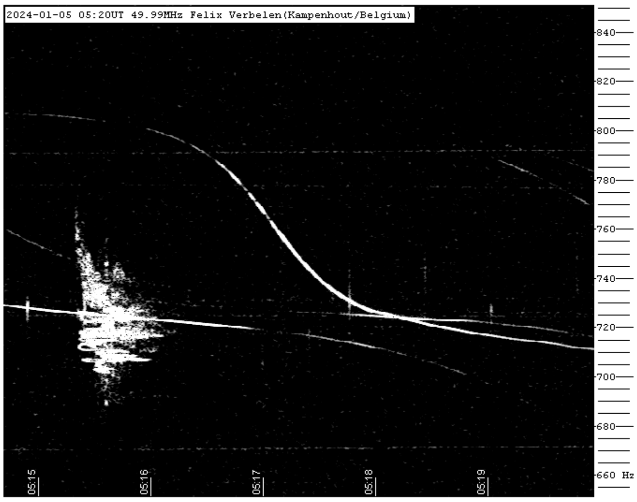

Figure 13 – Meteor echo 5 January 2024, 05^h20^m UT.

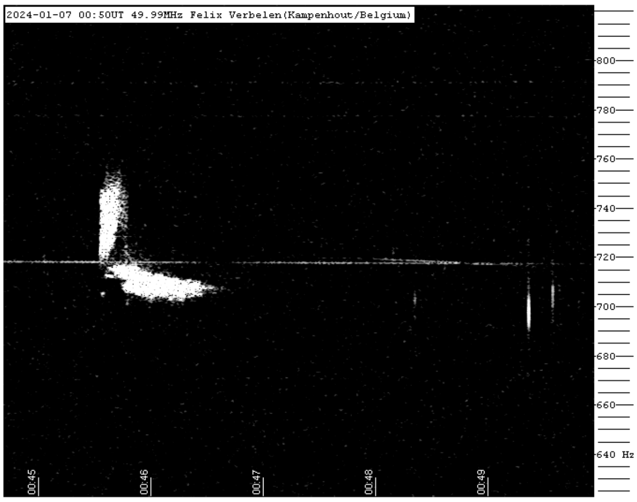

Figure 14 – Meteor echo 7 January 2024, 00^h50^m UT.

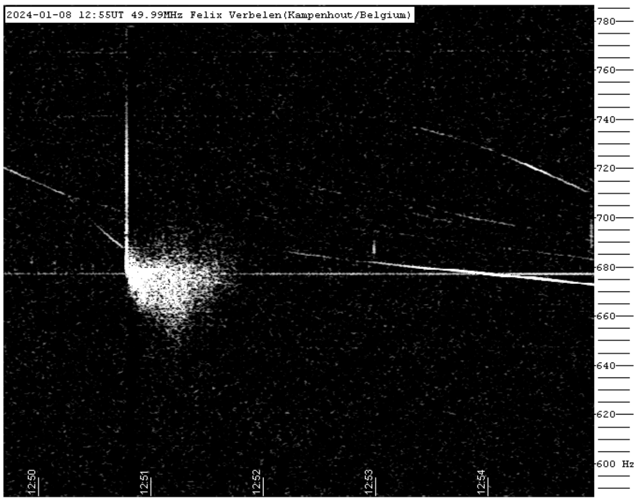

Figure 15 – Meteor echo 8 January 2024, 12^h55^m UT.

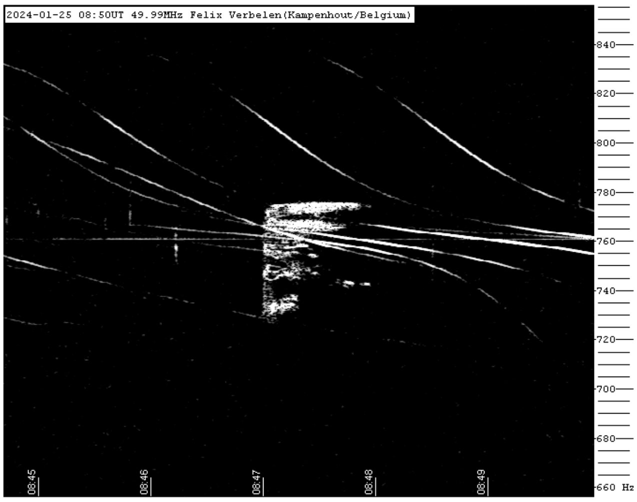

Figure 16 – Meteor echo 25 January 2024, 08^h50^m UT.

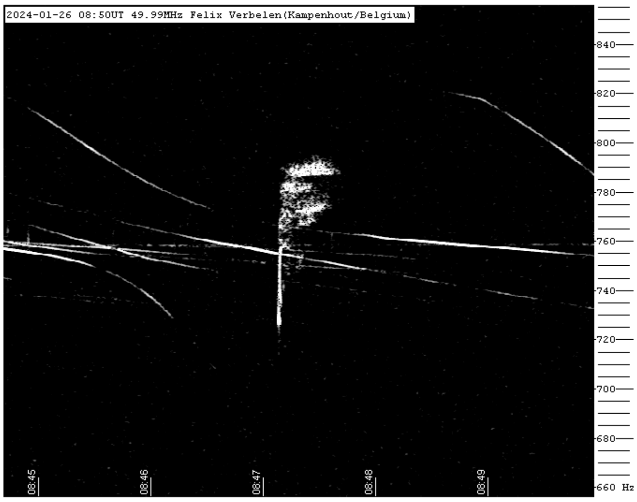

Figure 17 – Meteor echo 26 January 2024, 08^h50^m UT.

Figure 18 – Meteor echo 30 January 2024, 07^h15^m UT.

Radio observations in January 2024

Ivan Sergei

Mira Str.40-2, 222307, Molodechno, Belarus
astroseriv@yandex.by

This article presents the results of radio observations made in January 2024.

1 Introduction

The observations were carried out at a private astronomical observatory near the town of Molodechno (Belarus) at the place of Polyani. A 5 element-antenna directed to the west was used, a car FM-receiver was connected to a laptop with as processor an Intel Atom CPU N2600 (1.6 GHz). The software to detect signals is MetAN (author – Carol from Poland). Observations are made on the operating frequency 88.6 MHz (the FM radio station near Paris broadcasts on this frequency). The "France Culture" radio broadcast transmitter (100 kW) I use is at about 1550 km from my observatory which has been renewed in 1997.

Figure 1 – New TECSUN PL-310ET meteor radio receiver.

On January 12 afternoon the new radio receiver TECSUN PL-310 ET (*Figure 1*) was put into operation, providing a more accurate search for the operating frequency around 88.6 MHz. The new operating frequency 88.58 MHz was selected. The peculiarity of this receiver is its good noise immunity, sensitivity and selectivity. The range covered by the SpectrumLab program is very good, which allows a visual search for bolide radio signals.

2 Automatic observations

The maximum hourly count of QUA meteor numbers (#0010), occurred at 04^h–06^h UT on January 04, 2024, which agrees well with the IMO meteor calendar data at 03^h40^m UT on January 4 ($\lambda_\odot = 283.15°$).

3 Listening to radio echoes on 88.6 MHz

In order to save observation time and to increase the efficiency of listening for the radio meteor echoes in order to obtain a more complete observation series, I made a modification to the method with the introduction of a definition of "synthetic" hourly rate numbers (*Figure 4*).

Listening for the radio signals during 10 minutes with extrapolation of the data to 1 hour was done about 3 to 5 times a day. At the times of the maxima of the main meteoroid streams, the counting of meteor echoes was performed on average every 2–3 hours in order to get a better coverage of the observational series. This was done in order to control the level of the hourly rates as well as to distinguish between periods of tropospheric passage, E-layer activity and other natural radio interferences. The total effective observing time was 138 synthetic hours. The calculated hourly rate data are given in order to compare with the hourly activity rate values obtained by the method of automatic hourly signal detection.

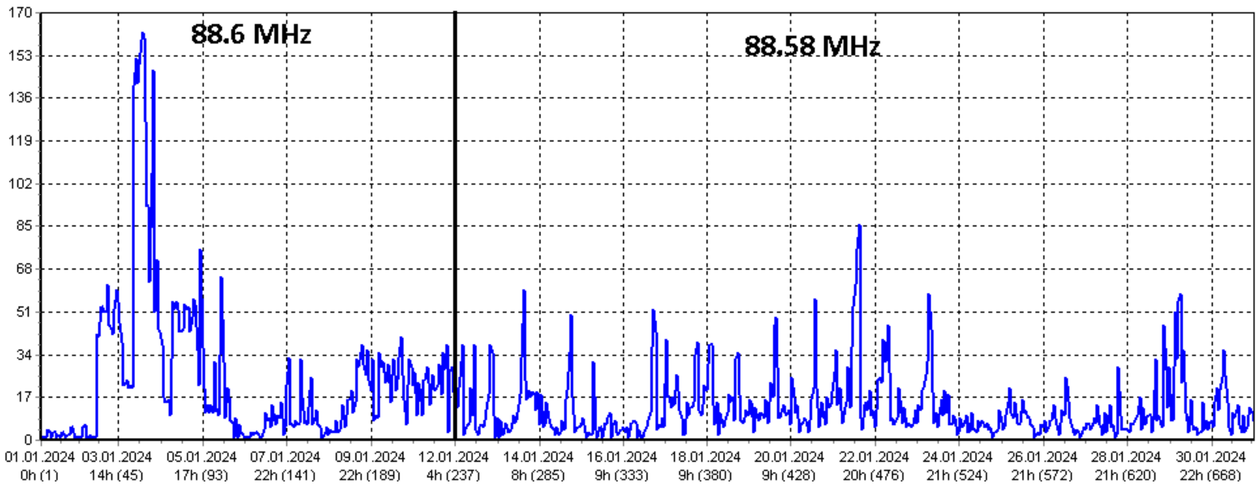

Figure 2 – Radio meteor echo counts at 88.6 MHz for January 2024.

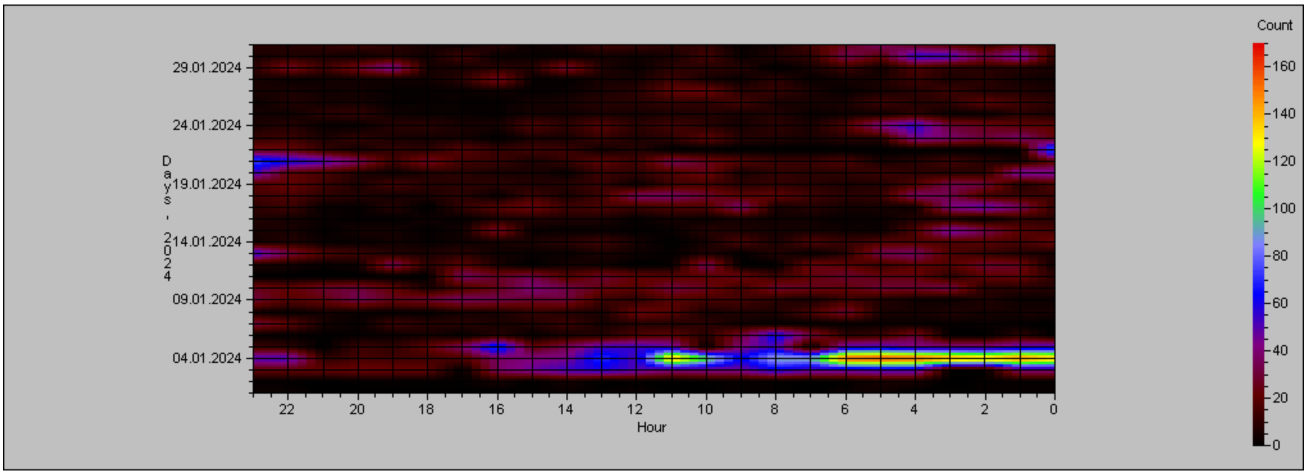

Figure 3 – Heatmap for radio meteor echo counts at 88.6 MHz for January 2024.

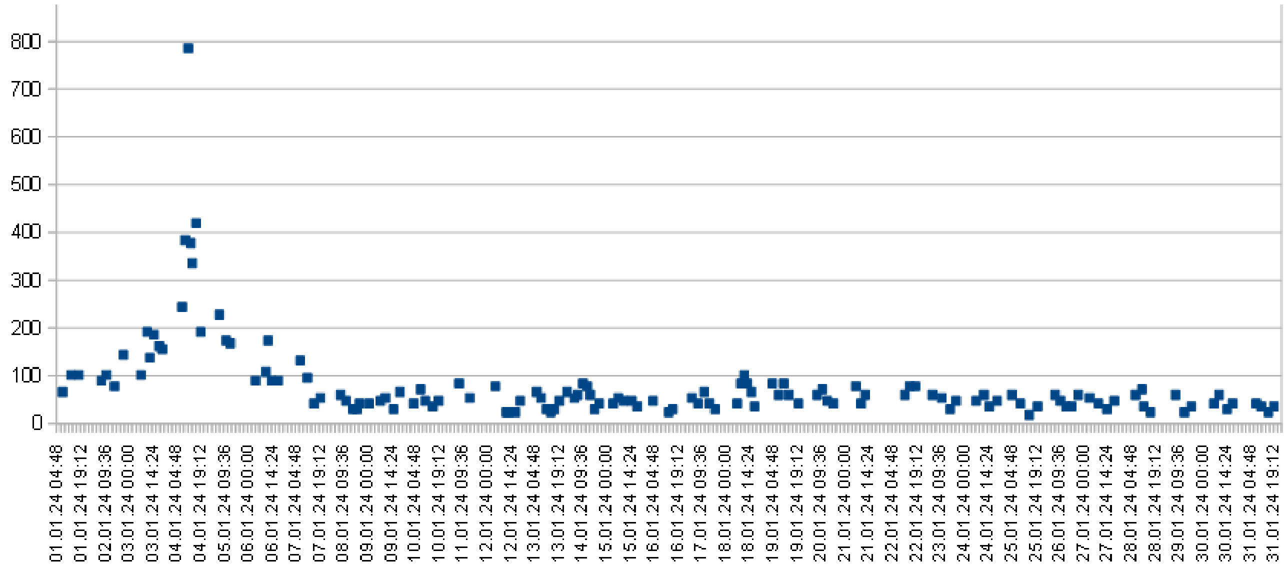

Figure 4 – The result with the calculated hourly numbers of meteor echoes by listening to the radio signals during January 2024.

There is no confirmation for the peak activity of the Quadrantid meteor shower (QUA#0010) recorded at almost 800 signals per hour, most likely a statistical random fluctuation from the overall trend. The shower activity at 400 signals per hour can be considered as real.

The method of listening by ear is not suitable to detect the time of maximum activity, but it is suitable for determining the approximate level of maximum activity, because very weak signals are detected when listening by ear, which cannot be detected by automatic methods in the FM-band.

4 Method of visual counting of meteor signals in SpectrumLab

Given the very good resolution range of the SpectrumLab program with the new radio receiver, it is very easy to count meteors visually. For the selection of signals in the frequency range 300–1500 Hz I used as criterion a signal length of 5 Hz and a level greater than ~ –48 dB (with an average noise level of about –55 dB). Screenshots in $\lambda_{\odot}$ were saved every 10 minutes. The time resolution is sufficient to detect signals with a duration from 0.5 sec. *Figure 5* shows the daily activity of meteor signals after January 12.

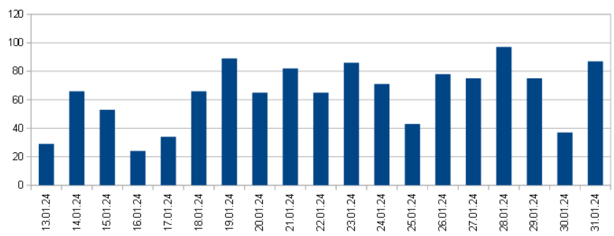

Figure 5 – Daily activity of meteor signals by counting the exhoes visually in SpectrumLab.

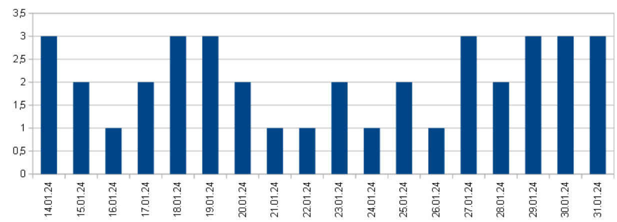

Figure 6 – Daily activity of meteor signals by counting the meteor echoes in SpectrumLab with a duration of the signals from 10 to 60 sec.

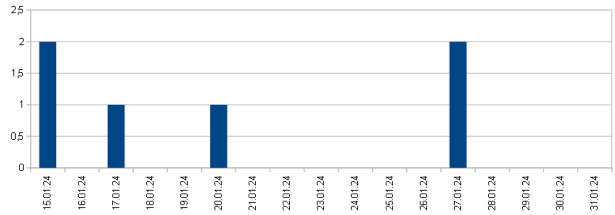

Figure 7 – Daily activity of meteor signals by counting the meteor echoes in SpectrumLab with a duration of signals from 60 seconds and longer.

5 Fireballs in the radio band

Phenomena (*Figure 10–12*) with wide trails and smaller amplitude can occur at long distances, also the signal arrives outside the antenna pattern (e.g., from an easterly direction).

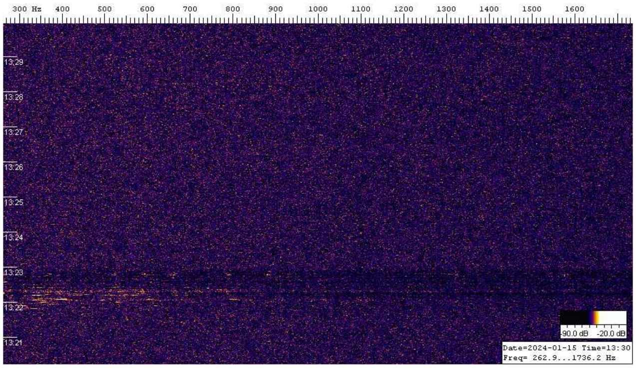

Figure 8 – Fireball 15 January 2024 at 10^h22^m UT.

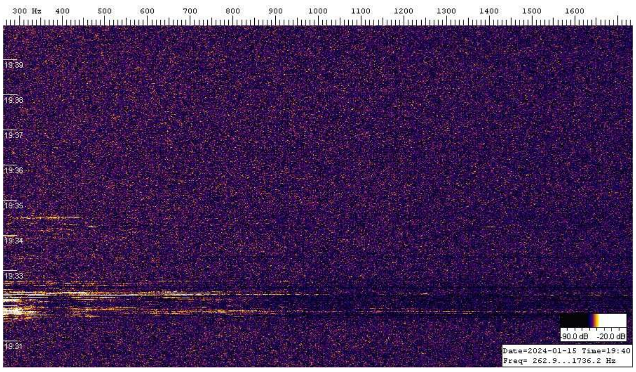

Figure 9 – Fireball 15 January 2024 at 16^h31^m UT.

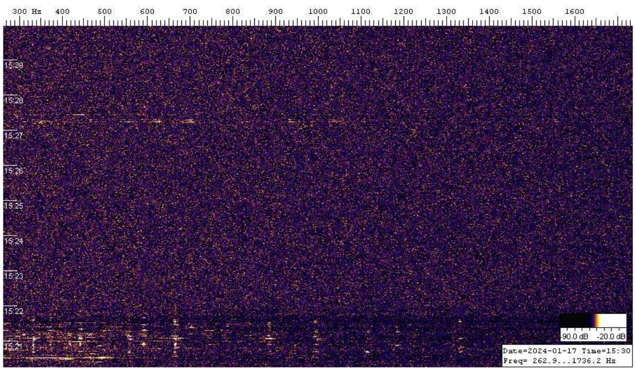

Figure 10 – Firebal 17 January 2024 at 12^h21^m UT.

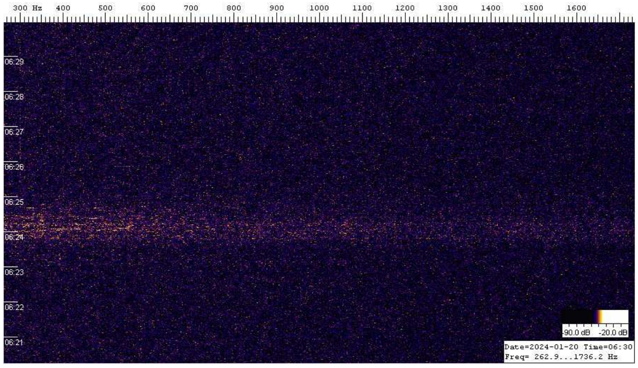

Figure 11 – Firebal 20 January 2024 at 03^h24^m UT.

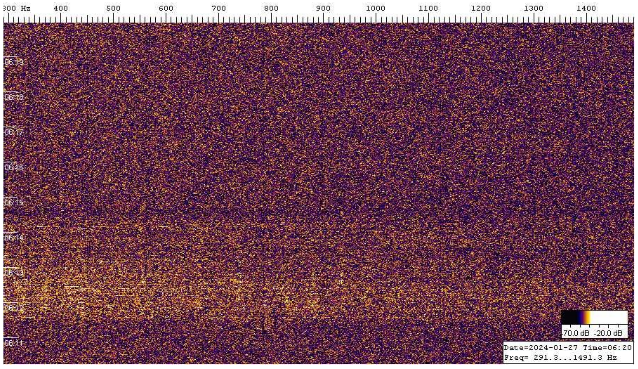

Figure 12 – Firebal 27 January 2024 at 03^h14^m UT.

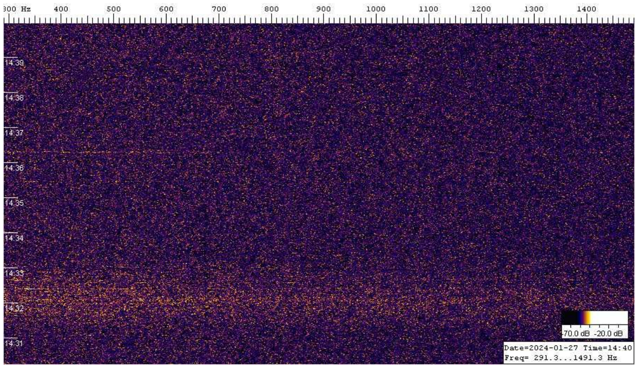

Figure 13 – Fireball 27 January 2024 at 11^h32^m UT.

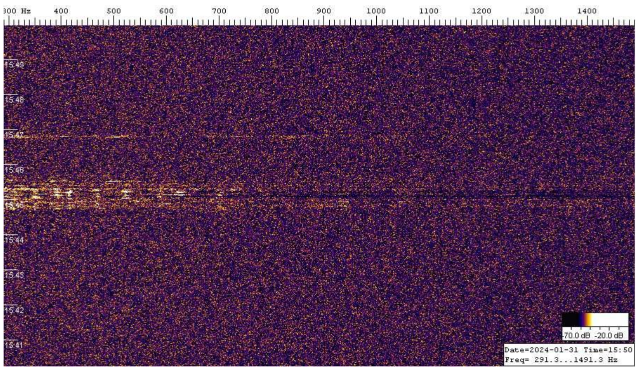

Figure 14 – Fireball 31 January 2024 at 12^h45^m UT.

6 Conclusion

The method of counting radio meteor echoes by listening is about 3 times more sensitive than the method using automatic detection of meteor echo signals. The method of listening to the radio echoes is very interesting, because it allows you to “scan” the dynamics of the total meteor background over a long time, to identify periods of low activity, periods of high activity, as well as outbursts and the peak activity of the most prominent meteoroid streams. Not all maxima in the meteor shower plots could be classified with known meteor showers from the IMO meteor shower working list data (meteor calendar). Probably some unidentified maxima are the result of some enhanced activity of one shower or a superposition of several minor meteor showers, which are detected by video networks.

Acknowledgment

I would like to thank *Sergey Dubrovsky* for the software he developed for data analysis and processing of radio observations (software Rameda). I thank Carol from Poland for the Metan software. Thanks to *Paul Roggemans* for his help in the lay-out and the correction of this article.

References

Rendtel J. (2024). "Meteor Shower Calendar". IMO.

A fireball over NW Bulgaria, December 9th 2023

Ventsislav Bodakov

Stellar Society, Sofia, Bulgaria
venzibo@gmail.com

A fireball appeared on 2023 December 9 at 20^h52^m UT and was recorded by two Bulgarian Global Meteor Network cameras. The trajectory and the orbit of the fireball could be computed.

1 Introduction

Saturday evening on December 9th, 2023 a few members of our astronomical association "Stellar Society" were doing tests at our recently automated remote observatory at Rozhen astronomical site, Bulgaria. We have two RMS cameras installed there and in addition to their primary purpose we are using their "live view" (live_maxpixel_enable) to monitor the sky conditions at least in a part of the sky. The live maxpixel JPEG is fetched from the stations at regular intervals and presented at a simple but useful web page. This is where I noticed the fireball at 20^h52^m UTC, it lit the entire frame of the two cameras, overexposing the area around it (*Figure 1*). I was sure that something must have exploded there.

Figure 1 – The fireball as recorded from the BG000B FF file.

Both stations at Rozhen have captured the fireball, as their FoV slightly overlaps. BG000B got the fireball until it went down exploding behind trees, and BG0003 had it only partially as it moved out of the frame even earlier.

The sky was generally clear at that moment, there was some haze though, which can be seen in the FF files. This haze together with the brightness of the fireball and the explosion itself saturated the camera sensor preventing the meteor detector algorithm to detect this event as a regular meteor. The algorithm seeks the frames for a well-defined "centroid" of a meteor, which is hard or impossible to be determined in case of an overexposed, exploding fireball with haze in the sky. Consequently, there was no detection entry in the file *radiants.txt, no presence in the detected stack and no FF file in Archive directory. However, the brightness of the event triggered the fireball detector and it created an uncompressed "region-of-interest" video as FR file in the Archive directory.

The fact that this fireball was not detected as a regular meteor, which will also not appear on the Meteor map[31], could be a reminder that it is always good to check the captured stack and captured thumbs in the archive as otherwise such fireballs might be missed.

The RMS camera network in Bulgaria is in development since March 2021 and the coverage is not yet the best. This fireball was also seen from one other camera (BG0004, 80km away), while other cameras were hampered by clouds. However, the explosion was so intense that all cameras irrespective of their pointing direction recorded an increase in sky brightness at the time of the fireball.

2 Fireball analysis

For this situation where the meteor detector missed a bright fireball, I was advised in Global Meteor Network forum[32] to perform an "Advanced Multi-station meteor analysis". For this task I used Mark McIntyre's guide "Advanced Meteor Analysis[33]" and the thorough video guide[34] by Denis Vida. The software of RMS and the trajectory solver WMPL (WesternMeteorPyLib) were installed on an Ubuntu 20.04.6 LTS virtual machine.

For the fireball manual reduction in SkyFit2 I used the FR files for both stations, along with their respective platepar, config and CALSTARS files. The uncompressed FR files can be better compared to the compressed FF when performing a manual data reduction. Once this process is done for each camera, SkyFit2 generates a respective ECSV file as a result. This file contains data about the meteor position as coordinates in time. As a second step in multi-station analysis these ECSV files were analyzed and solved by WMPL with the additional option of 20 runs of the Monte Carlo method for a possible optimization of the error margins (Vida et al., 2020a; 2020b; 2021).

The report generated by WMPL showed that the stations had a very good agreement on the trajectory. The spatial

[31] https://tammojan.github.io/meteormap/
[32] https://globalmeteornetwork.groups.io/g/main
[33] https://markmcintyreastro.co.uk/advanced-meteor-analysis/
[34] https://www.youtube.com/watch?v=ao3J9Jf0iLQ

residuals were grouped within 60 meters root-mean-square deviation of the solution for BG000B (*Figure 2*) and 25 for BG0004 (*Figure 3*).

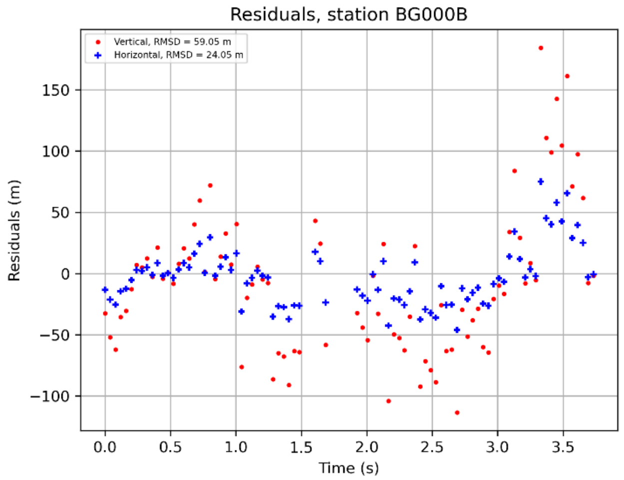

Figure 2 – BG000B residuals.

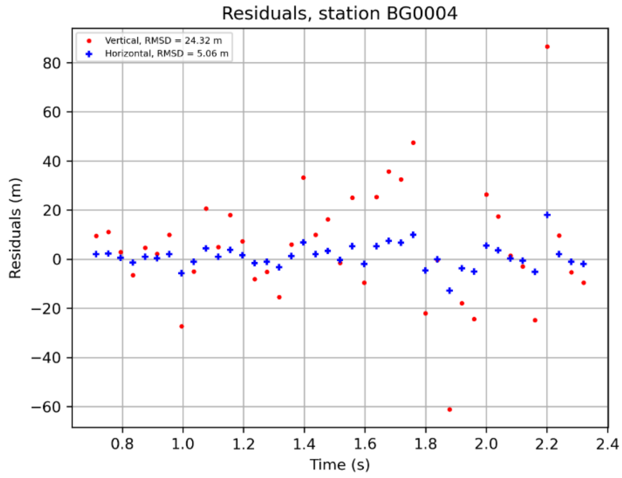

Figure 3 – BG0004 residuals.

The cameras and the fireball have a convergence angle of 26.72°, well above the minimum of 3° for a successful trajectory estimation.

A Google Earth 3D visualization was generated with WMPL's Utils.TrajectoryKML tool (*Figure 4*) and can be viewed as a YouTube video[35].

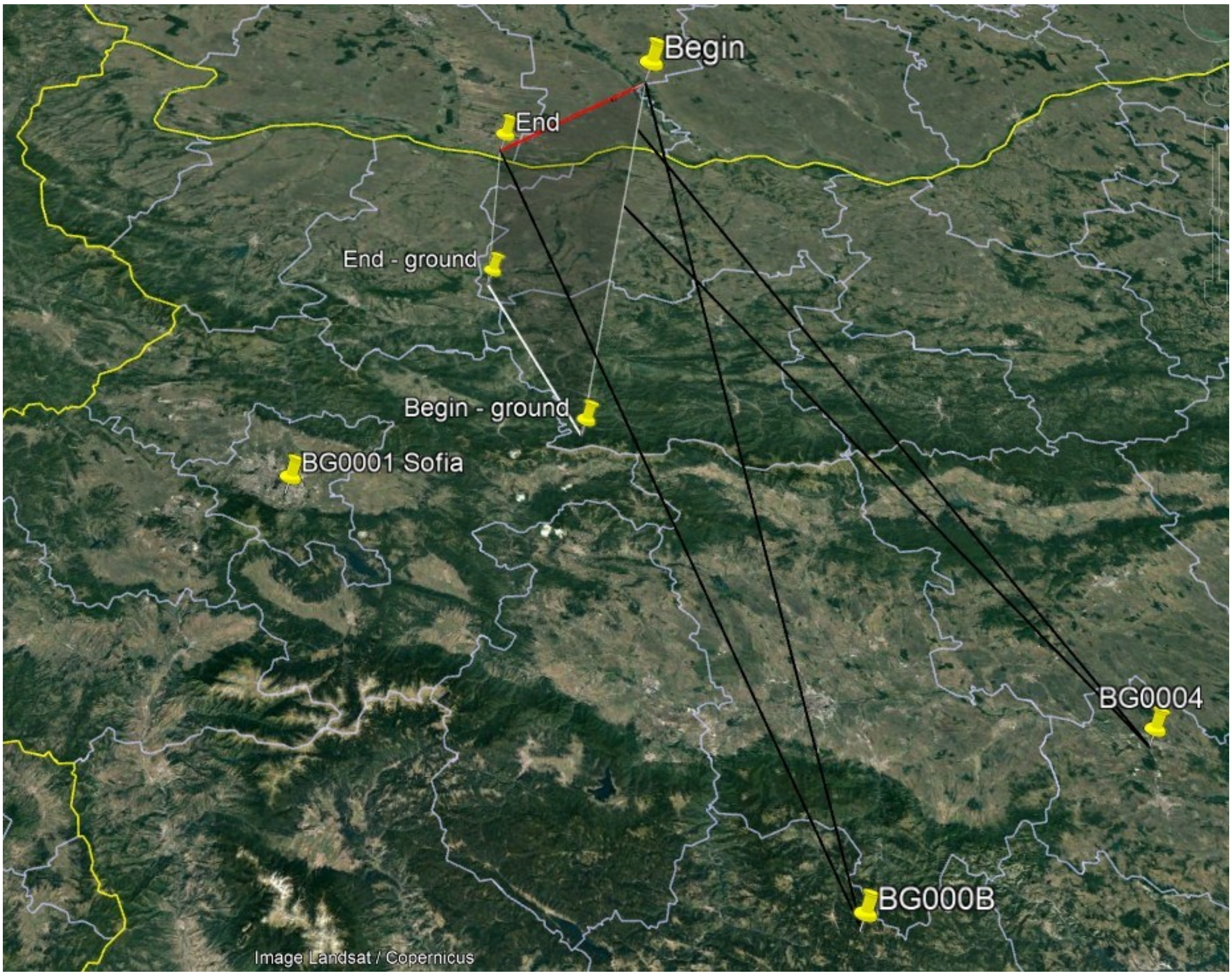

Figure 5 – Google Earth 3D visualization of the fireball trajectory.

[35] https://youtu.be/SguTmh_UdZM

3 The results

The meteor had an entry velocity of 21.9 km/s and an average velocity of 21.62 km/s, which indicates a slow meteor. All the relevant data radiant and orbit data has been listed *Table 1*. The Tisserand's parameter with respect to Jupiter as perturbing body, indicates an asteroidal origin with T_j = 4.0. No meteor shower could be associated so that this fireball has been classified as a sporadic.

Table 1 – The orbital elements for the fireball observed on 2023, December 9, at. 20^{h}52^m UT above N.W. Bulgaria.

Epoch	JD: 2460288.369
$\lambda_{\odot}$ (°)	257.18
α_g (°)	69.37 ± 0.02
δ_g (°)	–1.1 ± 0.04
v_g (km/s)	18.79 ± 0.003
$\lambda - \lambda_{\odot}$ (°)	170.33 ± 0.02
β (°)	–22.95 ± 0.04
H_b (km)	104.57 ± 0.02
H_e (km)	44.82 ± 0.01
a (AU)	2.532 ± 0.003
q (AU)	0.737903 ± 0.0001
e	0.708637 ± 0.0003
ω (°)	66.71 ± 0.03
Ω (°)	77.19
i (°)	12.46 ± 0.02
Π (°)	143.91 ± 0.03
T_j	4.03 ± 0.01

Figure 5 shows the ground track, the black cross marks the lowest height at which the fireball was captured. As mentioned above the meteor went out of the FoV in BG0004 and behind trees in BG000B. The estimated begin point of the trajectory is at 104.6 km and the end point at 44.8 km. The special residuals in height are shown in *Figure 6*.

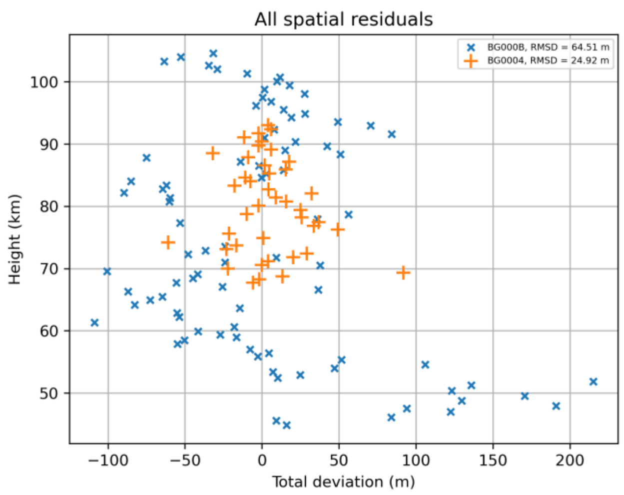

Figure 6 – Spatial residuals in height.

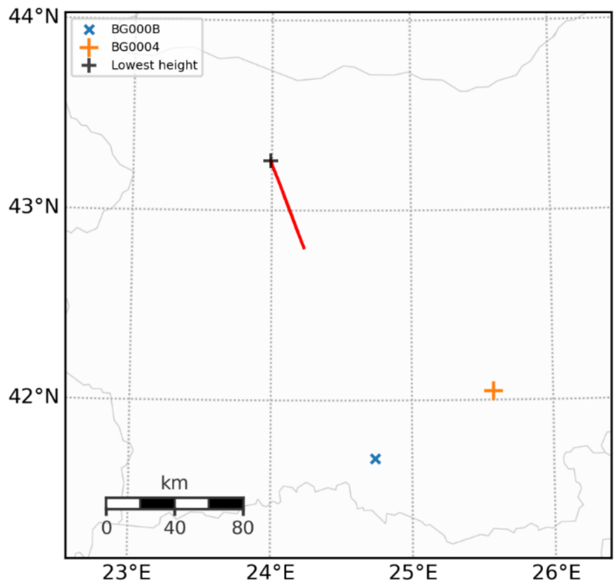

Figure 5 – Ground track of the fireball.

The orbit estimation shows that the fireball came from the asteroid belt with an inclination of 12.4° (*Figures 7 and 8*).

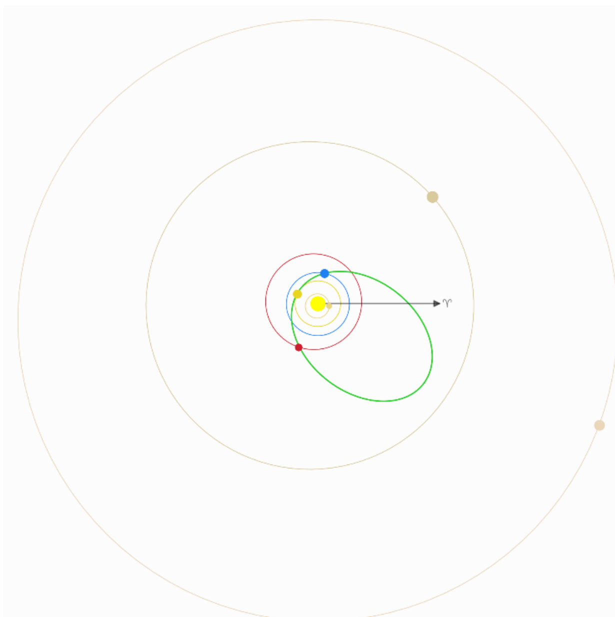

Figure 7 – The fireball orbit, top view.

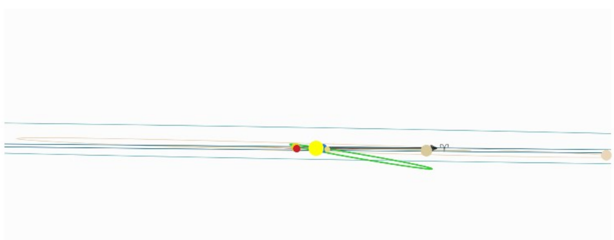

Figure 8 – The fireball orbit, side view.

Acknowledgment

I thank Penko Yordanov for providing BG0004 data.

References

Vida D., Gural P., Brown P., Campbell-Brown M., Wiegert P. (2020a). “Estimating trajectories of meteors: an observational Monte Carlo approach - I. Theory”. *Monthly Notices of the Royal Astronomical Society*, **491**, 2688–2705.

Vida D., Gural P., Brown P., Campbell-Brown M., Wiegert P. (2020b). “Estimating trajectories of meteors: an observational Monte Carlo approach - II. Results”. *Monthly Notices of the Royal Astronomical Society*, **491**, 3996–4011.

Vida D., Šegon D., Gural P. S., Brown P. G., McIntyre M. J. M., Dijkema T. J., Pavletić L., Kukić P., Mazur M. J., Eschman P., Roggemans P., Merlak A., Zubrović D. (2021). “The Global Meteor Network – Methodology and first results”. *Monthly Notices of the Royal Astronomical Society*, **506**, 5046–5074.

Fireball over North East of France, January 9, 2024

Tioga Gulon

6, rue Rodin, F-54710 Fléville-devant-Nancy, France
france.allsky.camera@gmail.com

On January 9, 2024, at $21^h55^m45.0^s$ UTC, an object entered almost perpendicularly into the atmosphere and produced a fireball over the North East of France.

1 Introduction

On the night of Tuesday January 9, at about 22^h55^m CEST, a fireball has been observed from a vast region including the BeNeLux (*Figure 1*). On the IMO website, 81 people[36], mainly from Belgium, the Netherlands and Germany, reported to having seen a meteor for a few seconds with a brightness equivalent to the Full Moon.

Five All-sky cameras from the Fripon network recorded the event and their calculations motivated their team to spend a day searching for a meteorite. Cameras from the Global Meteor Network and the CAMS network, with smaller fields of view, also recorded the fireball.

Figure 1 – Map of 81 eyewitnesses of the event 2024/198 on the IMO page.

2 Observations

Figure 2 – The fireball as recorded on BE000P (courtesy: Paul Roggemans).

The sky was cloudy over the north-eastern quarter of France, preventing French cameras to record the fireball (*Figure 3*).

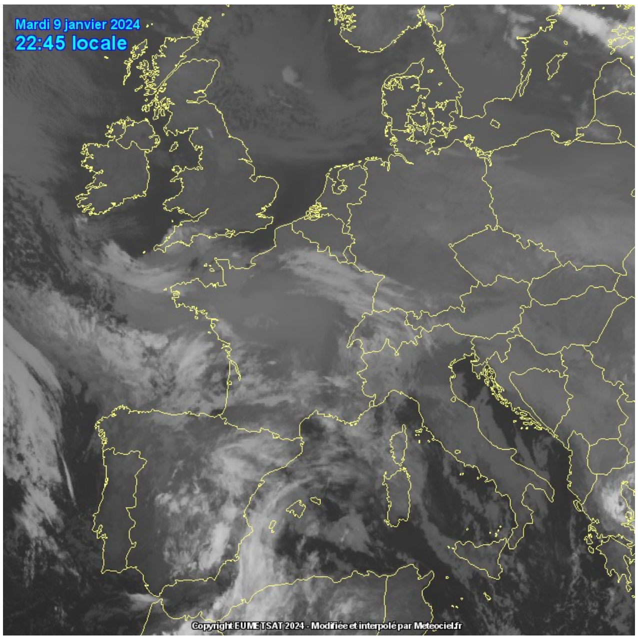

Figure 3 – Infrared satellite weather image 2024 January 09, 21^h45^m UTC (courtesy : EUMETSAT/meteociel.fr).

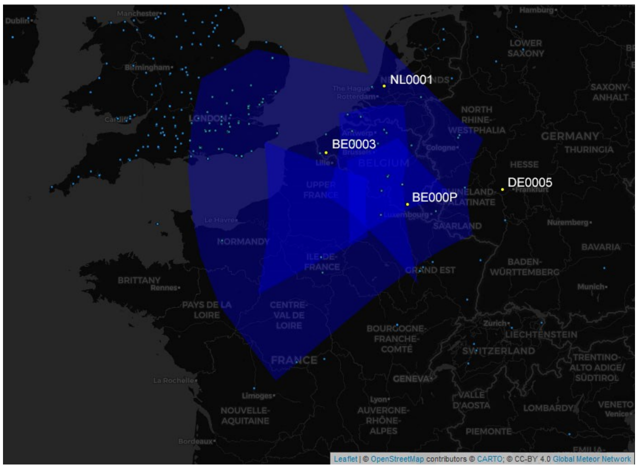

Figure 4 – Cameras field of view at 100 km of height (courtesy : GMN/ tammojan[37]).

Four stations of the Global Meteor Network (*Figure 4*) and CAMS-BeNeLux have captured the event: BE000P

[36] https://fireball.imo.net/members/imo_view/event/2024/198

[37] https://tammojan.github.io/meteormap/

(*Figure 2*) and BE0003 in Belgium, DE0005 in Germany and NL0001 in the Netherlands.

Figure 5 – The fireball as recorded from BE0003 (courtesy : Steve Rau).

Figure 6 – The fireball as recorded from DE0005 (courtesy : Jurgen Dörr).

Figure 7 – The fireball as recorded from NL0001 (courtesy : Kees Habraken).

3 Fireball analysis

All these cameras work with an RPi Meteor Station. The night's video files are stored in a "Captured" folder as compressed images FF*.fits in 10-second image sequences. Then they are analyzed, at the end of the night, the astrometry is carried out, and the meteor captures are duplicated in an "Archived" folder. In the case of a bright event, the program stores a raw image sequence of the object in the "Captured" folder as FR*.bin file.

As explained in the video guide[38] by Denis Vida and Mark McIntyre's guide[39] "Advanced Meteor Analysis", I analyzed each four captures by a manual reduction with the software SkyFit2 and after a multi-station triangulation analysis, the trajectory was derived using the WMPL (WesternMeteorPyLib) trajectory solver.

I used the uncompressed FR*.bin video files, which are better suited for manual reduction, for the first part of the trajectory on BE000P, for the capture on BE0003 and for the second part on DE0005. Compressed FF*.fits video files were used for the second part of the trajectory on BE000P (called BE000P_2) and for the low-light fireball video capture on NL0001.

WMPL solved the trajectory with an option of 20 good simulations. The spatial residuals better than 200 meters and a smooth curve of the state vector show a good correlation between the different sets of reduced data.

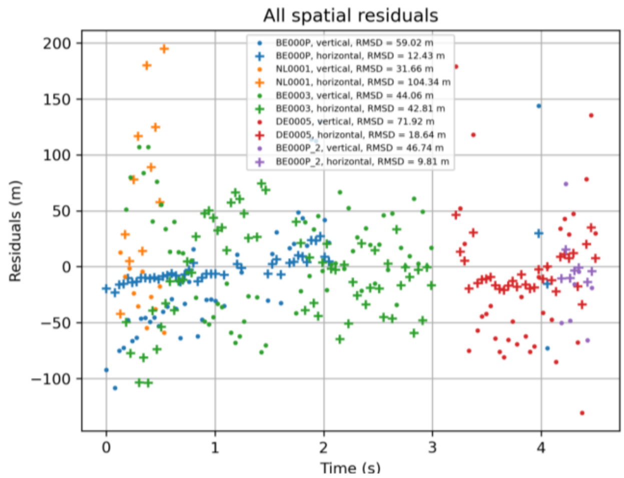

Figure 8 – Horizontal and vertical spatial residuals for all captures in function of time.

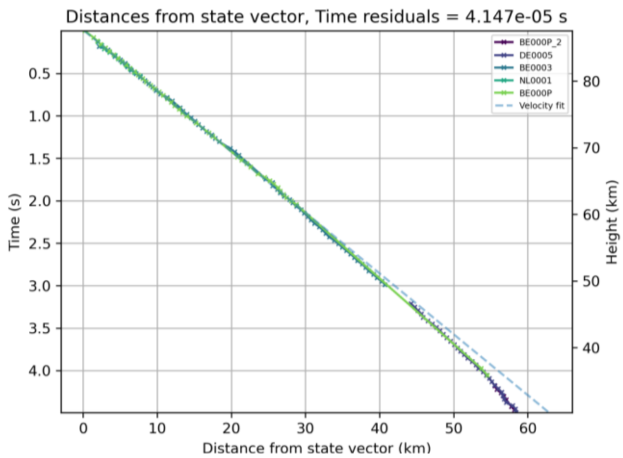

Figure 9 – Distances from the state vector.

4 Trajectory result

At 21^h^45^m^55^s^ UTC, on January 9th, 2024, the object penetrated into the atmosphere with an almost vertical trajectory, an entrance angle of 81° and a low velocity of 14 km/s. The luminous path started at an elevation of about 87 km and ended at 30 km, with a total duration of 4.5 seconds. The trajectory parameters indicate good chances for the survival of the object through the atmosphere and a short strewn field if any meteorites got dropped.

[38] https://youtu.be/ao3J9Jf0iLQ?t=4809

[39] https://markmcintyreastro.co.uk/advanced-meteor-analysis/

Figure 10 – 3D view of the trajectory.

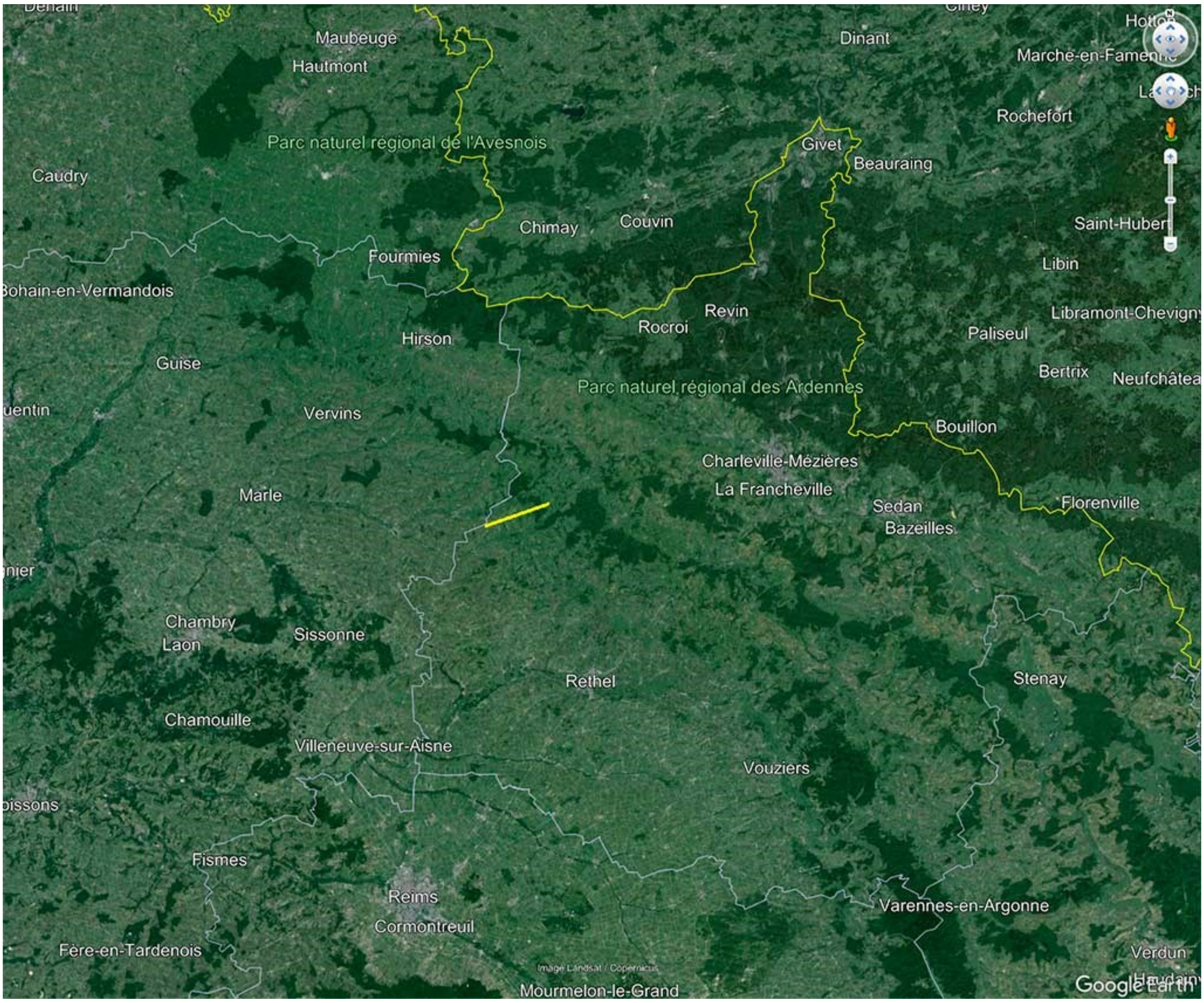

Figure 11 – Ground path of the trajectory on Google Earth map.

Unfortunately, the manual reduction could not give a good indication of the magnitude of the fireball and therefore it's difficult to estimate the size of the object.

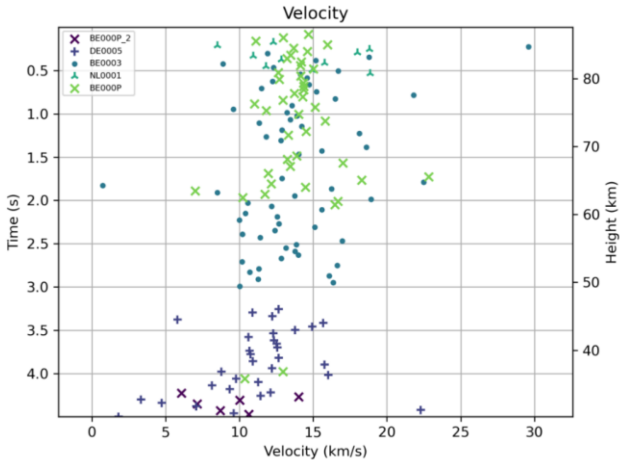

Figure 12 – Velocity as calculated by WMPL.

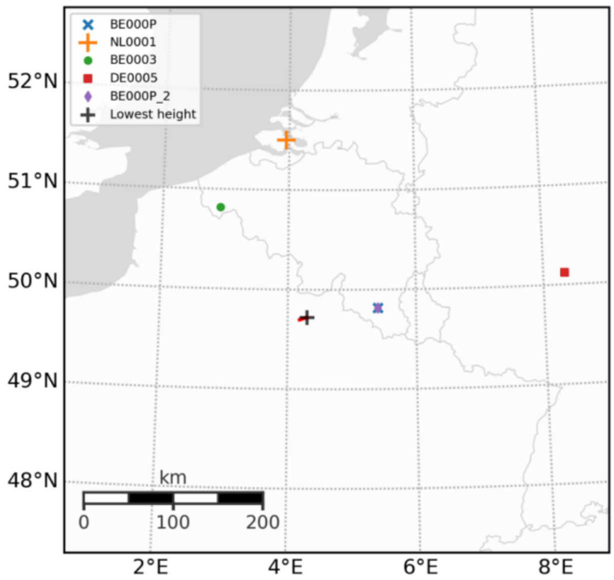

Figure 13 – The short ground track.

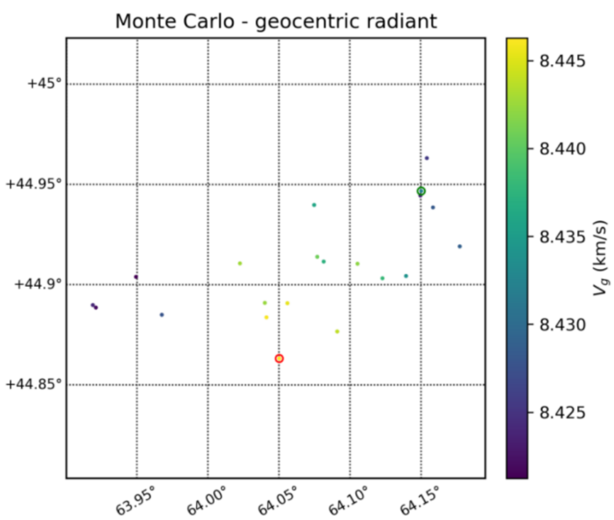

Figure 14 – Monte Carlo simulation for the geocentric radiant.

Table 1 – The orbital elements of the fireball of 9 January 2024 at $21^h45^m55.0^s$ UT as obtained with WMPL computation.

		±	95% CI	
α_g	64.05	0.08	[63.92, 64.17]	°
δ_g	44.86	0.02	[+44.87, +44.96]	°
H_b	87.55	0,03	[87.49, 87.58]	km
λ_b	4.1814	0.0004	[4.1809, 4.1821]	°E
φ_b	49.6957	0.0001	[49.6958, 49.6962]	°N
H_e	30.14	0.004	[30,14, 30,15]	km
λ_e	4.301	0.0005	[4.300, 4.302]	°E
φ_e	49.7203	0.0001	[49.7201, 49.7204]	°N
v_∞	13.96	0.005	[13.94, 13.96]	km/s
v_g	8.45	0.008	[8.42, 8.45]	km/s
a	1.70	0.002	[1.69, 1.70]	AU
q	0.9379	0.0001	[0.9378, 0.9382]	AU
e	0.447	0.0006	[0.445, 0.447]	–
ω	211.78	0.05	[211.69, 211.86]	°
Ω	288.78	0.00002	[288.78, 288.78]	°
i	5.41	0.005	[5.40, 5.42]	°
T_j	4.08	0.003	[4.08, 4.09]	

Figure 15 – Side view of the orbit of the object.

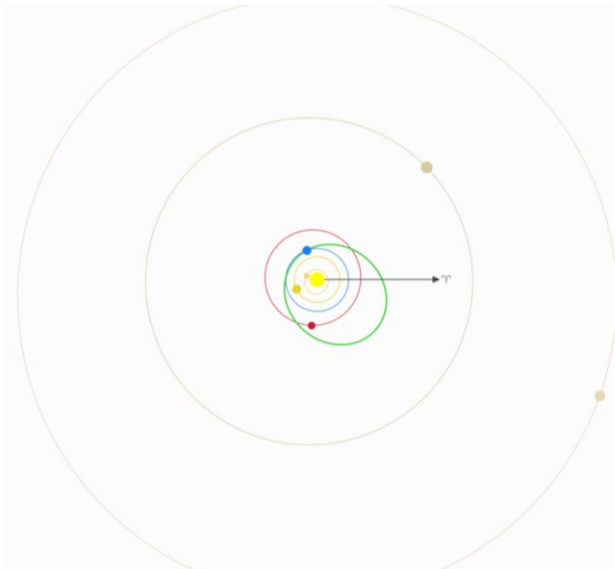

Figure 16 – Top view of the orbit of the object.

Acknowledgment

This report was possible thanks to the efforts of camera owners: *Jürgen Dörr*, *Kees Habraken*, *Steve Rau* and *Paul Roggemans* who quickly checked their observations, as well as Paul's knowledge of the camera network. And of course, to the programmers of the open source softwares RMS and WesternMeteorPyLib.

Bright bolide over the Moravian-Slovak border

Jakub Koukal[1,2] **and Libor Lenža**[1,2]

[1] **Valašské Meziříčí Observatory, Vsetínská 78, CZ75701 Valašské Meziříčí, Czech Republic**
jkoukal@astrovm.cz, libor.lenza@astrovm.cz

[2] **J. Heyrovský Institute of Physical Chemistry, Academy of Sciences of the Czech Republic**
Dolejškova 3, CZ18223 Prague 8, Czech Republic

Just a few days after three bright bolides, which were recorded on December 27, 2023, by instruments of the European Fireball Network, another bright bolide was recorded over the territory of the former Czechoslovakia. This bolide, which flew over the Moravian-Slovak border after two o'clock in the morning on January 9, 2024, was recorded by stations of the CEMeNt network (Central European MetEor NeTwork) as well as stations of the GMN network (Global Meteor Network), whose national component CSMON (Czech and Slovak Meteor Observation Network) operates within the Czech Republic and Slovakia. The bolide's flight was recorded by five cameras of the CEMeNt network, one of which was spectroscopic. Recording the spectrum of the bolide from spectrographs at the Valašské Meziříčí Observatory is very important because it provides us with a large amount of information about the chemical composition of the body. In the case of the CSMON network, the bolide's flight was recorded by eight cameras. From the available data from the cameras of the CEMeNt and CSMON networks, the bolide's trajectory in the atmosphere and the trajectory of the body in the Solar System were calculated.

1 Video observation – CEMENT

The bolide 20240109_011828 was recorded by cameras of the CEMeNt network on January 9, 2024, at $1^h18^m27.6^s \pm 0.1^s$ UT. Within the CEMeNt network (Central European MetEor NeTwork), the bolide was captured directly by four wide-angle stations (*Figure 1–4*). The flight record of the bolide is available from the Valašské Meziříčí SW and SE stations (Czech Republic, Valašské Meziříčí Observatory), Ždánice E station (Czech Republic, Ždánice Observatory), and Partizánske NW station (Slovakia, Partizánske Observatory). In addition to these stations, the spectrum of the bolide's flight was recorded by the spectrograph Valašské Meziříčí SPSW (Czech Republic, Valašské Meziříčí Observatory), which is crucial for determining the chemical properties of the body, namely the content of chemical elements. Unfortunately, it was negatively affected by weather conditions (quite heavy fog).

Figure 1 – Summary image of the bolide 20240109_011828 captured by the Valašské Meziříčí SW camera. Author: Valašské Meziříčí Observatory, p.o.

Figure 2 – Summary image of the bolide 20240109_011828 captured by the Valašské Meziříčí SE camera. Author: Valašské Meziříčí Observatory, p.o.

Figure 3 – Summary image of the bolide 20240109_011828 captured by the Ždánice E camera. Author: Ždánice Observatory.

Figure 4 – Summary image of the bolide 20240109_011828 captured by the Partizánske NW camera. Author: Partizánske Observatory.

2 Video observation – CSMON

The bolide 20240109_011828 was recorded by cameras of the CSMON network on January 9, 2024, at $1^h18^m27.7^s \pm 0.1^s$ UT. Within the CSMON network (Czech and Slovak Meteor Observation Network), the bolide was directly captured by eight wide-angle stations, of which data from five of them were used (*Figure 5–8*). The flight record of the bolide is available from stations CZ0003 (Czech Republic, Prague), CZ0007 (Czech Republic, Zlín), CZ000C and CZ000D (Czech Republic, Libňatov), and SK0002 (Slovakia, Sládkovičovo).

Figure 5 – Summary image of the bolide 20240109_011828 captured by the CZ0003 camera. Author: Milan Kalina.

Figure 6 – Summary image of the bolide 20240109_011828 captured by the CZ0007 camera. Author: Richard Káčerek.

Figure 7 – Summary image of the bolide 20240109_011828 captured by the CZ000C camera. Author: Luboš Morávek.

Figure 8 – Summary image of the bolide 20240109_011828 captured by the SK0002 camera. Author: Radim Stano.

3 Atmospheric trajectory, radiant and heliocentric orbit

The bright bolide 20240109_011828 is an ideal case for comparing the compatibility of data obtained by various systems and different processing techniques, as observations were recorded by both the CEMeNt and CSmon network systems.

For the CEMeNt network systems, the atmospheric trajectory and the orbit of the meteoroid in the Solar System were calculated using recordings from the Valašské Meziříčí SW and SE, Ždánice E, and Partizánske NW stations. Recordings from these stations were processed using the UFOCapture program, analyzed in the UFO Analyzer program, and the atmospheric trajectory and heliocentric orbit were calculated using the UFO Orbit program (SonotaCo, 2009). The projection of the beginning of the atmospheric trajectory was located at coordinates N48.7204° E17.1751° near the village of Petrova Ves (SK), with the meteor's altitude at that moment being 89.6 km above the Earth's surface. The projection of the end of the atmospheric trajectory was located at coordinates N48.9525° E17.8103° near the village of Paseky (CZ), with the meteor's altitude at that moment being 37.4 km above the Earth's surface (*Figures 9 and 10*). The bolide reached an absolute magnitude of –5.4m and traveled a distance of 75.0 km in the Earth's atmosphere during a flight time of 3.75 s (*Table 1*). Given the initial mass of the body and the final altitude of the atmospheric trajectory, it is highly probable that fragments of the body could not have impacted the Earth's surface as meteorites.

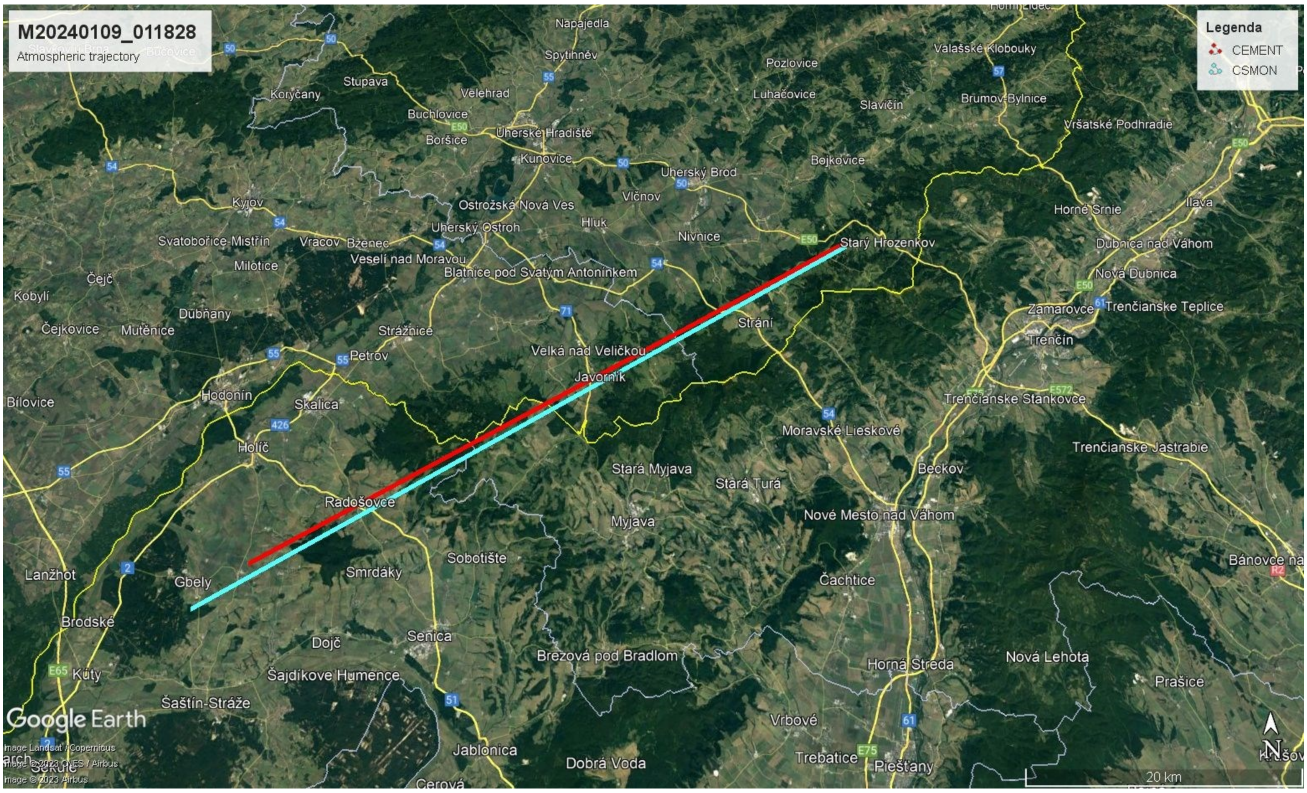

Figure 9 – 2D projection of the entire atmospheric trajectory of the bolide 20240109_011828 onto the surface of the Earth (source of map data: Google Earth, Google Inc.). Author: Jakub Koukal, Milan Kalina.

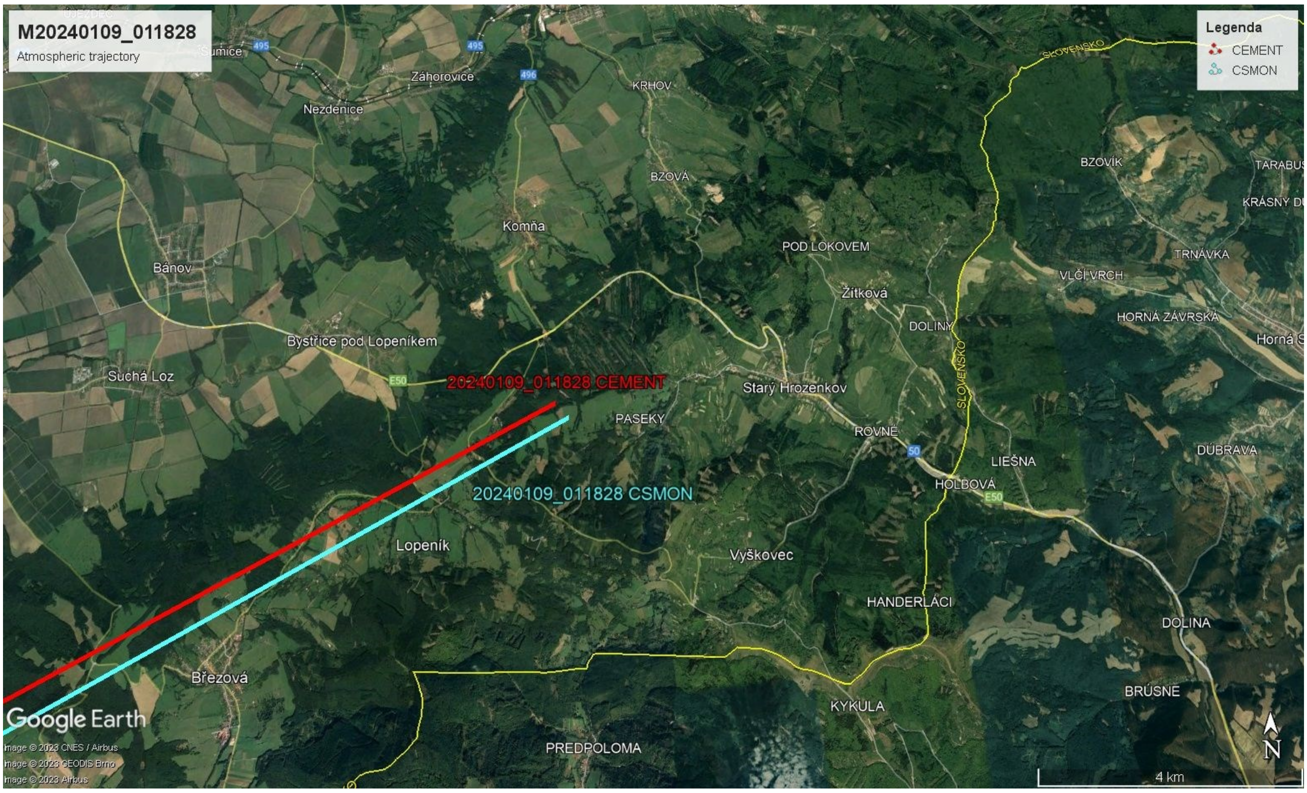

Figure 10 – 2D projection of the final part of the atmospheric trajectory of the bolide 20240109_011828 onto the surface of the Earth (source of map data: Google Earth, Google Inc.). Author: Jakub Koukal, Milan Kalina.

Therefore, the body's mass was most likely completely vaporized during the ablative phase of the bolide's flight.

The body entered the Earth's atmosphere at an angle of 44.42°, with a velocity of 22.41 km/s before entering the atmosphere. The velocity at the end of the observed atmospheric trajectory was 6.13 km/s. Therefore, it was a relatively slow bolide, with a geocentric velocity of the meteoroid being 19.65 km/s (*Table 1*). The body did not belong to any known meteor shower, so it is classified as a sporadic meteor. Before entering the atmosphere, the body moved along an elongated orbit (*Figure 11*) with a relatively high eccentricity (0.721), a low inclination to the plane of the ecliptic (5.35°), and a perihelion inside the orbit of Venus (0.6767 AU).

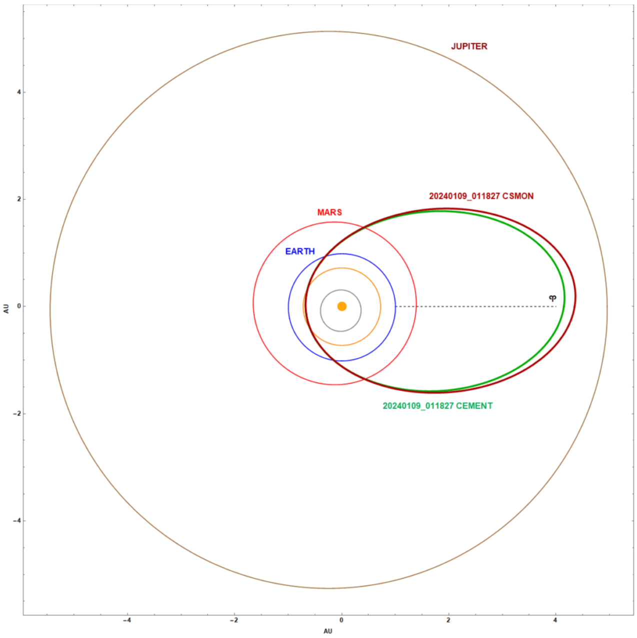

Figure 11 – Projection of the orbit of the bolide 20240109_011827 in the Solar System onto the plane of the ecliptic, including the effect of deceleration. Author: Jakub Koukal.

In the case of the CSMON network systems, the calculation of the bolide's atmospheric trajectory and its orbit in the Solar System utilized recordings from stations CZ0003, CZ0007, CZ000C, CZ000D and SK0002. The complete recording and processing were conducted using the open RMS system (Vida et al., 2020; 2021). The projection of the beginning of the atmospheric trajectory was located at coordinates N48.6986° E17.1225° near the town of Gbely (SK), with the meteor's altitude at that moment being 94.9 km above the Earth's surface. The projection of the end of the atmospheric trajectory was located at coordinates N48.9582° E17.8132° near the village of Paseky (CZ), with the meteor's altitude at that moment being 37.3 km above the Earth's surface (*Figures 9 and 10*). The body entered the Earth's atmosphere at an angle of 44.50°, with a velocity of 22.85 km/s before entering the atmosphere. Therefore, it was a relatively slow bolide, with a geocentric velocity of the meteoroid being 19.97 km/s (*Table 1*). The body was classified under the southern December delta Arietid meteor shower (IAU MDC 0288). Before entering the atmosphere, the body moved along an elongated orbit (*Figure 11*) with a relatively high eccentricity (0.733), a low inclination to the plane of the ecliptic (5.32°), and a perihelion inside the orbit of Venus (0.6729 AU).

The comparison of all orbital elements (heliocentric and geocentric) of the bolide's orbit, as well as the parameters of the atmospheric trajectory, shows that the data provided by the CEMeNt and CSMON network systems are compatible with each other and can be combined despite different recording systems and processing methods. The mutual deviations of the elements mostly fall within the measurement error range. The lower initial altitude of the bolide's atmospheric trajectory in the case of the CEMeNt network systems is caused by the lower sensitivity of the analog cameras used within this network.

Table 1 – Comparison of parameters of the atmospheric trajectory, heliocentric, and geocentric orbital elements of the bolide 20240109_011828, including the influence of deceleration on the bolide's trajectory. Author: Jakub Koukal, Milan Kalina.

Element	CEMeNt	CSMON
RA (°)	101.49 ± 0.14	101.54
DEC (°)	14.06 ± 0.16	14.25
v_g (km/s)	19.65 ± 0.42	19.97
a (AU)	2.421 ± 0.164	2.523
q (AU)	0.6767 ± 0.0060	0.6729
e (-)	0.721 ± 0.015	0.733
ω (°)	75.205 ± 0.279	75.296
Ω (°)	107.9183	107.937
i (°)	5.35 ± 0.04	5.32
H_B (km)	89.6 ± 0.1	94.9
H_E (km)	37.4 ± 0.1	37.3
Ev_{beg} (°)	44.42 ± 0.06	44.5
Az_{beg} (°)	240.07 ± 0.06	240.12
Lng_{beg} (°)	17.1751 ± 0.0008	17.1225
Lat_{beg} (°)	48.7204 ± 0.0019	48.6986
Lng_{end} (°)	17.8103 ± 0.0008	17.8132
Lat_{end} (°)	48.9525 ± 0.0019	48.9582
v_i (km/s)	22.41 ± 0.35	22.66

4 Physical properties

Figure 12 – Summary spectrum image of the bolide 20240109_011828 from the VM SPSW spectrograph. Author: Jakub Koukal.

In the case of the bolide 20240109_011828, the estimation of the initial mass of the body and its other physical properties can be based on the heliocentric orbit elements, the atmospheric trajectory and also the chemical properties (elemental analysis) obtained from the analysis of the spectrum of the bolide from the Valašské Meziříčí SPSW spectrograph (*Figure 12*).

For the initial determination of the parameters of the heliocentric orbit of the meteoroid, the Tisserand parameter with respect to Jupiter was calculated. Depending on the value of the Tisserand parameter, the inclination of the orbit, and the distance of the aphelion, the bodies can be divided into 4 groups. The bolide 20240109_011828 has a Tisserand parameter value of $T_J = 3.091$.

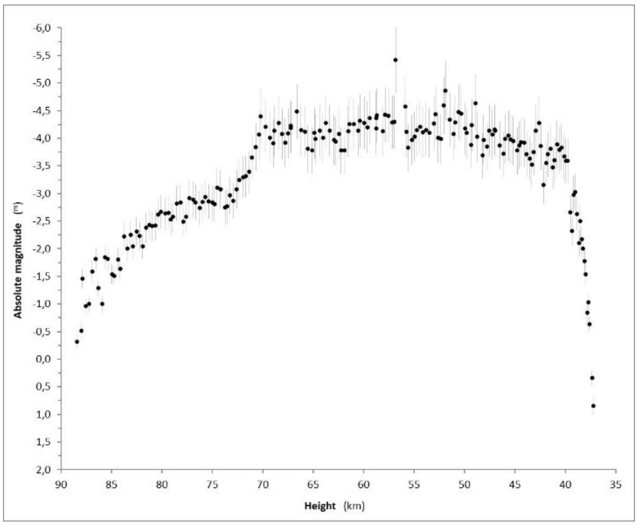

Figure 13 – Light curve (absolute brightness) progression from the Partizánske NW station. Author: Jakub Koukal.

According to this classification, the bolide belongs to the AST group, i.e., to the group of meteoroids with an asteroidal origin. However, according to the parameter K_B (7.555), which is a function of material properties and surface temperature (Ceplecha, 1968; Ceplecha and McCrosky, 1976; Ceplecha 1988), it belongs to the group of carbonaceous chondrites. According to the parameter P_E (-4.076), the bolide belongs to the group of ordinary chondrites. Using parameters that characterize the shape, velocity, and other properties of the body (*Table 1*), it was possible to calculate the initial mass of the body. Parallel to the calculation of the dynamic entry mass m_d, the calculation of the photometric entry mass m_f was performed. The initial dynamic mass of the meteoroid before entering the Earth's atmosphere was 0.92 kg (m_d), so it is unlikely that fragments of the original body could be found as meteorites on the Earth's surface. The calculation of the fragmentation strength of the meteoroid is based on the equality of dynamic pressure and the strength of the body as a whole at the moment of meteoroid breakup. The parameters of the atmosphere model at the given breakup altitude are calculated according to the NRLMSISE-00 model (Picone et al., 2002). The moment of breakup (fragmentation) of the body was determined from the course of the absolute brightness values of the bolide from the Partizánske NW station (*Figure 13*). The fragmentation strength of the main part of the body is 0.165 MPa (Popova et al., 2011), which places the body more in the group of ordinary chondrites (OC). The determined mineralogical density (Benyukh, 1974) of the body (2.72 g/cm^3) also suggests that the bolide 20190109_011828 was a body belonging to ordinary chondrites originating from the outer part of the main asteroid belt between Mars and Jupiter.

Acknowledgment

Thanks go to the coordinator of the CSMON network, *Milan Kalina*, for providing the data, as well as to all operators and owners of stations in the CEMeNt and CSMON networks. Thanks also go to all involved institutions for supporting the activities and growth of the network. The RPOS project (Cross-Border Observational Network Development) was co-financed from the Small Projects Fund of the Interreg V-A Program Slovakia – Czech Republic 2014 – 2020, call code 5/FMP/11b, reg. no. CZ/FMP/11b/05/058. The KOSOAP (Cooperating Network in the Field of Astronomical Observation Programs) and RPKS (Development of Cross-Border Cooperating Network for Professional Work and Education) projects were implemented by the Valašské Meziříčí Observatory (Czech Republic) and the Kysucké Nové Mesto Observatory (Slovakia) in cooperation with SMPH (Society for Interplanetary Matter). The projects were co-financed from the Micro-Projects Fund of the Operational Program for Cross-Border Cooperation Slovakia – Czech Republic 2007-2013. The purchase and operation of high-resolution spectroscopic cameras are partially funded by the Program for Regional Cooperation of the Czech Academy of Sciences, reg. no. R200402101 and grant APVV-0517-12 (FMFI UK). The purchase of instrument equipment located at the Valašské Meziříčí Observatory, p.o., was also supported by DEZA, a.s. and CS CABOT, spol. s r.o.

References

Benyukh V. V. (1974). "Mineralogical Density of Meteoroids in Several Streams". *Solar System Research*, **8**, 82.

Ceplecha Z. (1968). Discrete levels of meteor beginning height (No. NASA-CR-96295).

Ceplecha Z. and McCrosky R. E. (1976). "Fireball end heights: A diagnostic for the structure of meteoric material". *Journal of Geophysical Research*, **81**, 6257–6275.

Ceplecha Z. (1988). "Earth's influx of different populations of sporadic meteoroids from photographic and television data". *Astronomical Institutes of Czechoslovakia, Bulletin* (ISSN 0004-6248), **39**, 221–236.

Picone J. M., Hedin A. E., Drob D. P. and Aikin A. C. (2002). "NRLMSISE-00 empirical model of the atmosphere: Statistical comparisons and scientific issues”. *Journal of Geophysical Research: Space Physics*, **107**(A12), SIA-15.

Popova O., Borovička J., Hartmann W. K., Spurný P., Gnos E., Nemtchinov I. and Trigo-Rodríguez J. M. (2011). “Very low strengths of interplanetary meteoroids and small asteroids”. *Meteoritics & Planetary Science*, **46**(10), 1525–1550.

SonotaCo (2009). “A meteor shower catalog based on video observations in 2007-2008”. *WGN, Journal of the International Meteor Organization* **37**, 55–62.

Vida D., Gural P.S., Brown P.G., Campbell-Brown M. and Wiegert P. (2020). “Estimating trajectories of meteors: an observational Monte Carlo approach – I. Theory”. *Monthly Notices of the Royal Astronomical Society*, **491**, 2688–2705.

Vida D., Šegon D., Gural P. S., Brown P. G., McIntyre M. J. M., Dijkema T. J., Pavletić L., Kukić P., Mazur M. J., Eschman P., Roggemans P., Merlak A., Zubrović D. (2021). “The Global Meteor Network – Methodology and first results”. *Monthly Notices of the Royal Astronomical Society*, **506**, 5046–5074.

The mission of eMeteorNews is to offer fast meteor news to a global audience, a swift exchange of information in all fields of active amateur meteor work without editing constraints. eMeteorNews is freely available without any fees.

You are welcome to contribute to eMeteorNews on a regular or casual basis, if you wish to. Anyone can become an author or editor, send an email to us. See : https://www.emeteornews.net/writing-content-for-emeteornews/ for more information.

eMeteorNews webmaster: Radim Stano < radim.stano@outlook.com >.

Contributing to this issue:

- Bodakov V.
- Campbell-Burns P.
- Gulon T.
- Jenniskens P.
- Johannink C.
- Kalina M.
- Koukal J.
- Lenža L.
- Madiedo J.
- McIntyre M.
- Miskotte K.
- Ogawa H.
- Roggemans P.
- Scott J.M.
- Šegon D.
- Sergei I.
- Sicking W.
- Stano R.
- Sugimoto H.
- Van 't Leven J.
- Verbelen F.
- Vida D.

Online publication https://www.emeteornews.net
Listed and archived with ADS Abstract Service: https://ui.adsabs.harvard.edu/search/q=eMetN